Introduction to Nanoscience and Nanotechnology: A Workbook

M. Kuno

May 14, 2004

Contents

List of Figures

List of Tables

Preface

This set of lecture notes about nanoscience and nanotechnology was initially written over the spring and summer of 2003. After my initial appointment as an assistant professor in chemistry, I agreed to teach an introductory class on nanoscience and nanotechnology for incoming graduate students at the University of Notre Dame. However after accepting this task, it quickly became apparent to me that there were few resources available for teaching such a class, let alone any textbook. So while waiting for equipment to arrive, I undertook it upon myself to compile a series of lecture notes that would explain to the student some of the underlying concepts behind "nano". The motivation for this was to describe to the student the physics behind each concept or assumption commonly encountered in the nano literature rather than just providing a qualitative overview of developements in the field. I have also tried to illustrate and motivate these concepts with instances in the current literature where such concepts are applied or have been assumed. In this manner, the goal is to provide the student with a foundation by which they can critically analyze, and possibly in the future, contribute to the emerging nano field. It is also my hope that one day, these lecture notes can be converted into an introductory text so that others may benefit as well.

Masaru Kenneth Kuno
Notre Dame, IN
May 14, 2004

Chapter 1

Introduction

Preliminaries

What is "nano"? Well, without providing a definite answer to this question, nano is a popular (emerging) area of science and technology today. It has attracted the attention of researchers from all walks of life, from physics to chemistry to biology and engineering. Further impetus for this movement comes from the temendous increase in public and private funding for nano over the last ten years. A prime example of this is the new National Nanotechnology Initiative (NNI) created by former President Bill Clinton. The NNI increases funding in national nanoscience and nanotechnology research by hundreds of millions of dollars yearly. In addition, private sector contributions have jumped dramatically as evidenced by the plethora of small startup firms lining the tech corridors of the east and west.

Nano has even entered popular culture. It's used as a buzzword in contemporary books, movies and television commercials. For example, in the recent blockbuster, Spiderman, the Willem Dafoe character (the Green Goblin) is a famous (and wildly wealthy) nanotechnologist whose papers the Tobey McGuire character (Spiderman) has read and followed (see the scene outside of Columbia university). Likewise, in the movie "Minority Report" Tom Cruise's character undergoes eye surgery to avoid biometric fingerprinting. This scene involves a retinal eye transplant aided by so called "nano reconstructors". A scene in the DC metro shows him reading a newspaper with the headline "nanotechnology breakthrough". In television, a current GE commercial for washers and dryers features the storyline of: geeky nanotechnologist bumps into a supermodel at the laundromat resulting in love at first sight. We're therefore, implicitly, told to believe that their mix of

brains and beauty embody GE's new washer/dryer line. In books, the New York Times bestseller "Prey" by Michael Crighton features nanotechnology run amok with spawns of tiny nano bots escaping from the laboratory and hunting down people for food. (Sounds like the "Andromeda Strain" except recast with nano as opposed to an alien virus.).

The mantle of nano has also been adopted by various scientific visionaries. Perhaps the most prominent is Eric Drexler who has founded an institute, called the Foresight Institute, devoted to exploring his ideas. Concepts being discussed include developing tiny nano robots that will "live" inside us and repair our blood vessels when damaged, preventing heart attacks. They will also kill cancer, cure us when we are sick, mend bones when broken, make us smarter and even give us immortality. These nano robots will also serve as tiny factories, manufacturing anything and everything from food to antibiotics to energy. In turn, nanotechnology will provide a solution to all of mankind's problems whether it be hunger in developing countries or pollution in developed ones. Drexler therefore envisions a vast industrial revolution of unprecendented size and scale. At the same time, concurrent with his visions of a utopian future is a darker side, involving themes where such nano robots escape from the laboratory and evolve into sentient beings completely out of mankind's control. Such beings could then sow the seeds to mankind's own destruction in the spirit of recent movies and books such as The Terminator, The Matrix and Prey. Now, whether such predictions and visions of the future will ever become reality remains to be seen. However, any such developments will ultimately rely on the scientific research of today, which is, on a daily basis, laying down the foundation for tomorrow's nanoscience and nanotechnology.

In today's scientific realm, the word nano describes physical lengthscales that are on the order of a billionth of a meter long. Nanoscale materials therefore lie in a physical size regime between bulk, macroscale, materials (the realm of condensed matter physics) and molecular compounds (the realm of traditional chemistry). This mesoscopic size regime has previously been unexplored and beckons the researcher with images of a scientific wild wild west with opportunites abound for those willing to pack their wagons and head into the scientific and technological hinterland. In this respect, nanoscale physics, chemistry, biology and engineering asks basic, yet unanswered, questions such as how the optical and electrical properties of a given material evolve from those of individual atoms or molecules to those of the parent bulk. Other questions that nanoscience asks include:

- How does one make a nanometer sized object?

- How do you make many (identical) nanometer sized objects?
- How do the optical and electrical properties of this nanoscale object change with size?
- How does its optical and electrical properties change with its "dimensionality"?
- How do charges behave in nanoscale objects?
- How does charge transport occur in these materials?
- Do these nanoscale materials posess new and previously undiscovered properties?
- Are they useful?

The transition to nanoscience begins at this last point when we ask how these nanoscale materials might be exploited to improve our lives. Venture capital firms and mainstream industry have therefore taken up this challenge with many small startups trying to apply nanoscale materials in products ranging from better sunscreen lotions to fluorescent labels for biological imaging applications to next generation transistors that will one day store the entire content of the Library of Congress on the head of a pin. More established companies, such as GE, HP, Lucent and IBM, have also started their own in house nano programs to revolutionalize consumer lighting, personal computing, data storage and so forth. So whether it be for household lighting or consumer electronics, a nano solution exists and there is very likely a company or person pursuing this vision of a nano future.

So what is nano? This series of lecture notes tries to answer this question by explaining the physical concepts behind why such small, nanoscale, materials are so interesting and potentially useful.

Overview

The idea behind these lecture notes is as follows: First in Chapter 2, the composition of solids is discussed to introduce common crystal structures found in nanomaterials. Solids come in a number of forms, from amorphous (glass-like) to polycrystalline (multiple domains) to crystalline. Much of nanoscience and nanotechnology focuses on nanometer sized crystalline solids, hence the emphasis on crystal structure. In addition, the structure

section also illustrates the increase in surface to volume ratio for nanomaterials over bulk. This is because in nanometer sized systems up to 50% of the atoms lie at the surface of a nanostructure, in direct contrast to macroscopic solids where such numbers are typically much smaller. The surface is therefore potentially important in dictating a material's optical and electrical properties when nanometer sized. Furthermore, the increase in surface area is important to applications where the surface to volume ratio plays a critical role such as in catalysis as well as in photovoltaics. Developments in this area, using nanostructures, have led to increasingly efficient solar cells such as the Gratzel cell. Finally, the concept of crystal structure and the periodic potential due to the ordered arrangement of atoms is central to the concept of electronic bands, which we will discuss later on.

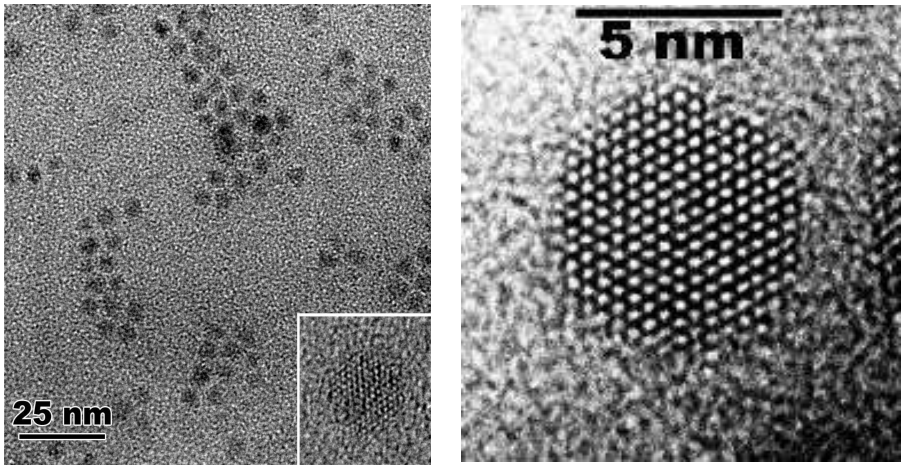

Figure 1.1: Transmission electron micrograph of individual CdSe quantum dots

Chapter 3 introducs the concept of length scales to put into perspective the actual physical lengths relevant to nano. Although being nanometer sized if often considered the essence of "nano", the relevant physical length scales are actually relative to the natural electron or hole length scales in the parent bulk material. These natural length scales can either be referred to by their deBroglie wavelength or by the exciton Bohr radius. Thus, while a given nanometer sized object of one material may qualify for nano, a similar sized object of another material may not.

Next the concept of quantum confinement is introduced in Chapter 4 through the simple quantum mechanical analogy of a particle in a 1 di-

mensional, 2 dimensional and 3 dimensional box. Quantum confinement is most commonly associated with nano in the sense that bulk materials generally exhibit continuous absorption and electronic spectra. However, upon reaching a physical length scale equivalent to or less than either the exciton Bohr radius or deBroglie wavelength both the optical and electronic spectra become discrete and more atomic-like. In the extreme case of quantum dots, confinement occurs along all three physical dimensions, x,y,and z such that the optical and electrical spectra become truly atomic-like. This is one reason why quantum dots or nanocrystals are often called artificial atoms.

Analogies comparing the particle in a one dimensional box to a quantum well, the particle in a two dimensional box to a quantum wire and the particle in a three dimensional box to a quantum dot provide only half the solution. If one considers that in a quantum well only one dimension is confined and that two others are "free", there are electronic states associated with these extra two degrees of freedom. Likewise in the case of a quantum wire, with two degrees of confinement, there exists one degree of freedom. So solving the particle in a two dimensional box problem models the electronic states along the two confined directions but does not address states associated with this remaining degree of freedom. To gain better insight into these additional states we introduce the concept of density of states (DOS) in Chapters 5,6,and 7. The density of states argument is subsequently applied to both the valence band and conduction band of a material. Putting together both valence and conduction band density of states introduces the concept of the joint density of states (JDOS) in Chapter 8 which, in turn, is related to the absorption coefficient of a material.

After describing the absorption spectra of 3D (bulk), 2D (quantum well), 1D (quantum wire), and 0D (quantum dot) systems we turn to the concept of photoluminescence. Generally speaking, in addition to absorbing light, systems will also emit light of certain frequencies. To describe this process, the Einstein A and B coefficients and their relationships are introduced and derived in Chapter 9. Finally, the emission spectrum of a bulk 3D material is calculated using the derived Einstein A and B coefficients. The concept of quantum yields and lifetimes, which describe the efficiency and timescale of the emission, completes this section.

Bands are introduced in Chapter 10. This topic is important because metals, semiconductors, and semi-metals all have bands due to the periodic potential experienced by the electron in a crystal. As mentioned earlier in the section on structure, this periodic potential occurs due to the ordered and repeating arrangement of atoms in a crystal. Furthermore, metals, semiconductors, insulators, and semi-metals can all be distinguished through

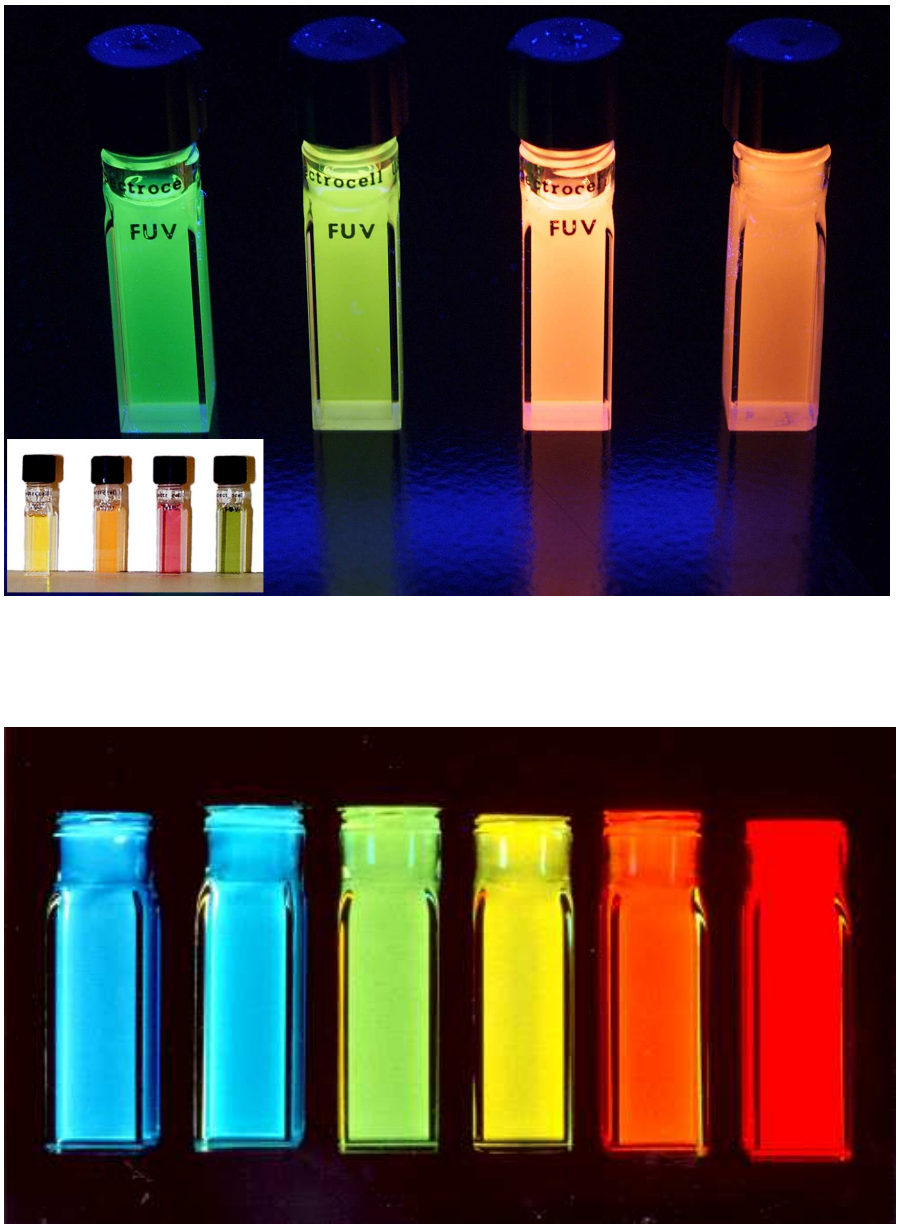

Figure 1.2: Photograph of the size dependent emission spectra of both HgS (top) and CdSe (bottom) quantum dots. Small quantum dots absorb and emit blue/green light, larger dots absorb and emit red light.

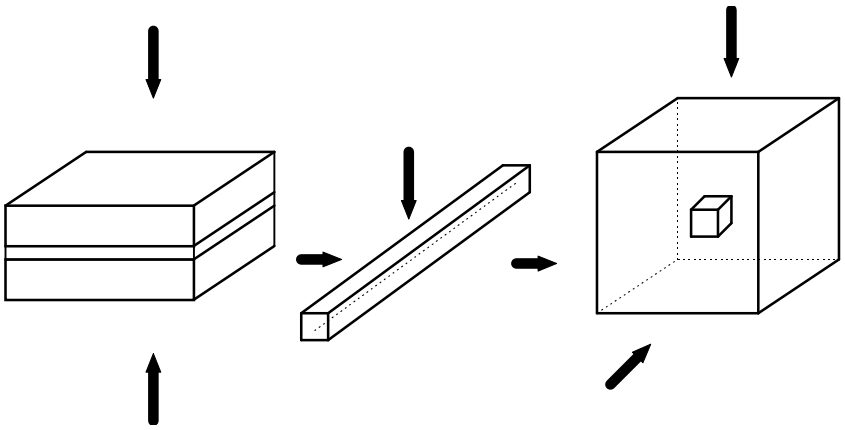

Figure 1.3: Cartoon of confinement along 1, 2 and 3 dimensions. Analogous to a quantum well, quantum wire and quantum dot.

the occupation of these bands by electrons. Metals have "full" conduction bands while semiconductors and insulators have "empty" conduction bands. At the same time, in the case of semiconductors and insulators there is a range of energies that cannot be populated by carriers separating the valence band from the conduction band. This forbidden range of energies (a no man's land for electrons) is referred to as the band gap. The band gap is extremely important for optoelectronic applications of semiconductors. For example, the band gap will generally determine what colors of light a given semiconductor material will absorb or emit and, in turn, will determine their usefulness in applications such as solar energy conversion, photodetectors, or lasing applications. An exploration of the band gap concept ultimately touches on the effects quantum confinement has on the optical and electrical properties of a material, which leads to the realization of a size dependent band gap.

Introducing the concept of bands is also important for another reason since researchers have envisioned that ordered arrays of quantum wells, or wires, or dots, much like the arrangement of atoms in a crystal, can ultimately lead to new "artificial" solids with artificial bands and corresponding band gaps. These bands and associated gaps are formed from the delocalization of carriers in this new periodic potential defined by the ordered arrangement of quantum dots, quantum wires, or quantum wells. Talk about designer materials. Imagine artificial elements or even artificial metals, semimetals, and semiconductors. No wonder visionaries such as Drexler envision

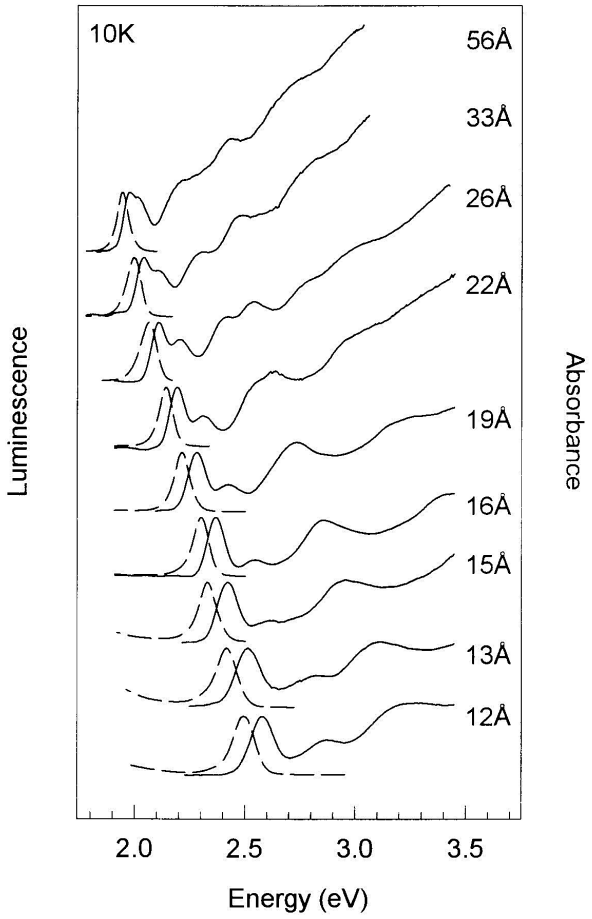

Figure 1.4: Size dependent absorption and emission spectra of colloidal CdSe quantum dots.

so much potential in nano. In the case of quantum wells, stacks of closely spaced wells have been grown leading to actual systems containing these minibands. In the case of quantum dots and wires, minibands have not been realized yet but this is not for lack of trying. The concept of creating artificial solids with tailor made bands from artificial atoms has been tantalizing to many.

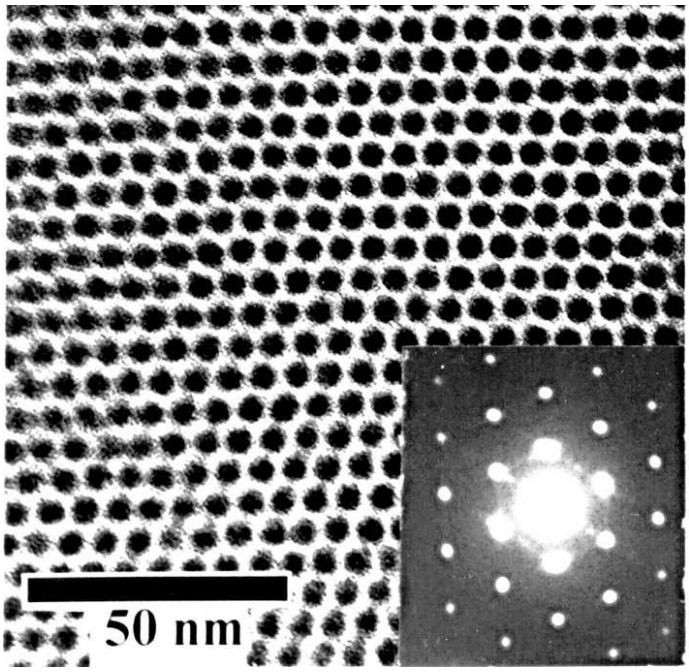

Figure 1.5: TEM micrograph of an array of colloidal CdSe quantum dots ordered into an artificial crystal. Each dark spot is an individual quantum dot. The white space in between dots is the organic ligands passivating the surface of the particle.

Not only do semiconductors, metals, insulators, and semi-metals absorb and emit light, but they also have electrical properties as well. These properties are greatly affected by quantum confinement and the discreteness of states just as with the aforementioned optical properties. Transport properties of these systems take center stage in the realm of devices where one desires to apply quantum dots, quantum wells, and quantum wires within opto-electronic devices such as single electron transistors. To this end, we introduce the concept of tunneling in Chapter 11 to motivate carrier trans-

port in nanometer-sized materials. Tunneling is a quantum mechanical effect where carriers can have non-zero probability of being located in energetically fobidden regions of a system. This becomes important when one considers that the discreteness of states in confined systems may mean that there are substantial "barriers" for carrier transport along certain physical directions of the material.

The WKB approximation is subsequently introduced in Chapter 12 to provide an approximate solution to Schrodinger's equation in situations where the potential or potential barrier for the carrier varies slowly. In this fashion, one can repeat the same tunneling calculations as in the previous section in a faster, more general, fashion. A common result for the form of the tunneling probablity through an arbitrary barrier is derived. This expression is commonly seen and assumed in much of the nano literature especially in scanning tunneling microscopy, as well as in another emerging field called molecular electronics.

After providing a gross overview of optical, electrical and transport properties of nanostructures, we turn to three topics that begin the transition from nanoscience to nanotechnology. Chapter 13 describes current methods for making nanoscale materials. Techniques such as molecular beam epitaxy (MBE), metal-organic chemical vapor deposition (MOCVD) and colloidal sysnthesis are described. A brief overview of each technique is given. Special emphasis is placed on better understanding colloidal growth models currently being used by chemists to make better, more uniform, quantum dots and nanorods. To this end, the classical LaMer and Dinegar growth model is derived and explained. Relations to the behavior of an ensemble size distribution are then discussed completing the section.

Once created, tools are needed to study as well as manipulate nanoscale objects. Chapter 14 describes some of the classical techniques used to characterize nanostructures such as transmission electron microscopy (TEM), secondary electron microscopy (SEM), atomic force microscopy (AFM) and scanning tunneling microscopy (STM). Newer techniques now coming into prominence are also discussed at the end of the section. In particular, the concepts behind dip-pen nanolithography and microcontact printing are illustrated.

Finally, Chapter 15 discusses applications of quantum dots, quantum wires, and quantum wells using examples from the current literature. Special emphasis is placed on the Coulomb blockade and Coulomb staircase problem, which is the basis of potential single electron transistors to be used in next generation electronics.

Chapter 2

Structure

Crystal structure of common materials

This section is not meant to be comprehensive. The interested reader may consult a number of excellent introductory references such as Kittel's introduction to solid state physics. The goal, however, is to illustrate the crystal structure of common materials often encountered in the nano literature. Solids generally appear in three forms, amorphous (no long range order, glass-like), polycrystalline (multiple domains) or crystalline (a single extended domain with long range order). Since nano typically concerns itself with crystalline metal nanoparticles and semiconductor nanocrystals, wires, and wells, having a basic picture of how the elements arrange themselves in these nanocrystalline systems is important. In this respect, crystal structure comes into play in many aspects of research, from a material's electronic spectra to its density and even to its powder x-ray diffraction pattern.

Atoms in a crystal are generally pictured as being arranged on an imaginary lattice. Individual atoms (or groups of atoms) are hung off of the lattice, much like Christmas ornaments. These individual (or groups of) atoms are referred to as the "basis" of the lattice. The endless repetition of basis atom(s) on a lattice makes up the crystal. In the simplest case, the basis consists of only a single atom and each atom is located directly over a lattice point. However, it is also very common to see a basis consisting of multiple atoms, which is the case when one deals with binary or even ternary semiconductors. Here the basis atoms do not necessarily sit at the same position as a lattice point, potentially causing some confusion when you first look at the crystal structures of these materials.

There are 14 three dimensional Bravais lattices shown in Figure 2.1.

These are also referred to as conventional unit cells (i.e. used in everyday life) as opposed to the primitive unit cell of which only the simple cubic (aka "primitive") lattice qualifies. That is, most of these unit cells are not the simplest repeating units of an extended lattice; one can find even simpler repeating units by looking harder. Rather, these conventional cells happen to be easy to visualize and interpret and hence are the ones most commonly used.

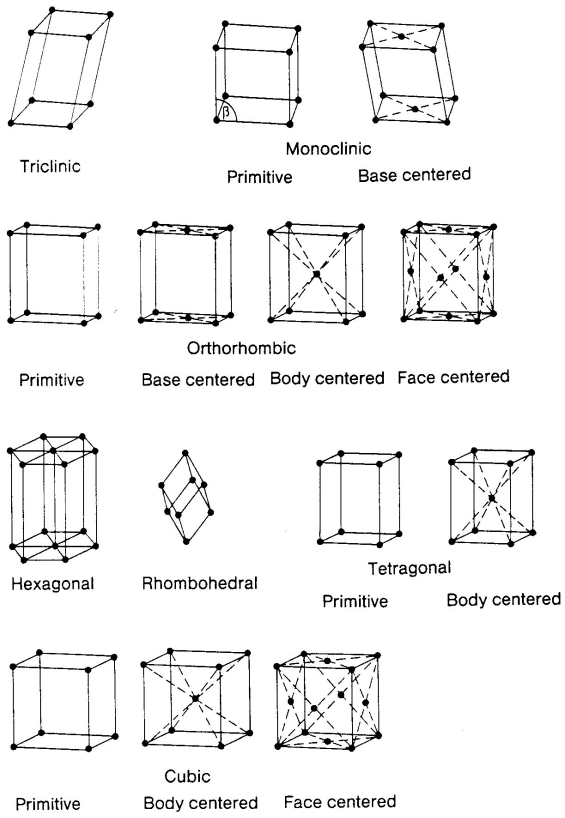

Figure 2.1: 14 3-dimensional Bravais lattices. From Ibach and Luth.

It is often useful to know the number of atoms in a unit cell. A general counting scheme for the number of atoms per unit cell follows.

- atoms entirely inside the unit cell: worth 1
- corner atoms: worth $\frac{1}{8}$

- face atoms: worth $\frac{1}{2}$
- edge atoms: worth $\frac{1}{4}$

Figure 2.2 illustrates the positions of an atom in the corner, face, edge and interior positions. The weighting scheme follows because each of these unit cells is surrounded by other unit cells, hence all atoms with the exception of interior ones are shared. The corner atoms are shared by 8 unit cells while the face atoms are shared by 2 cells and finally the edge atoms by four. Any atom in the interior of a unit cell is exclusive to that cell. This is illustrated in Figure 2.3. By counting atoms in this fashion, one can determine the number of atoms per unit cell.

Single element crystals

In the case of metals, the cubic lattices are important, with particular emphasis on the face centered cubic (FCC) and body centered cubic (BCC) structures. Both FCC and BCC structures have a single atom basis; thus, they strongly resemble the Bravais lattices or conventional unit cells seen in the previous diagram. The number of atoms per unit cell in the FCC case is 4 (8 corner atoms and 6 face atoms). Likewise, the number of atoms per BCC unit cell, using the above counting scheme, is 2 (1 interior atom and 8 corner atoms). Note that an alternative name exists for the FCC unit cell: cubic close packed (CCP), which should be remembered when reading the literature. Both unit cells are shown in Figures 2.4 and 2.5. Typical elements that crystallize in the FCC structure include: Cu, Ag, Au, Ni, Pd, Pt, and Al. Typical elements that crystallize in the BCC structure include: Fe, Cr, V, Nb, Ta, W and Mo. More complete tables can be found in Kittel.

Analogous to the FCC lattice is the hexagonal close packed (HCP) structure. A simple way to differentiate the two is the atomic packing order, which follows ABCABC in the case of FCC and ABABA in the case of HCP. The letters A, B, and C etc... represent different atom planes. The HCP structure has a conventional unit cell but also a primitive unit cell shown in Figure 2.6. It contains 2 atoms per unit cell (8 on the corners and 1 inside) as opposed to the conventional cell which has 12 per cell.

Another conventional unit cell that is often encountered is called the "diamond" structure. The diamond structure differs from its FCC and BCC counterparts because it has a multi atom basis. Therefore, it does not immediately resemble any of the 14 Bravais lattices. It is adopted by elements that have a tendency to form strong covalent bonds, resulting in tetrahedral bonding arrangements (Figure 2.7). The number of atoms per unit cell

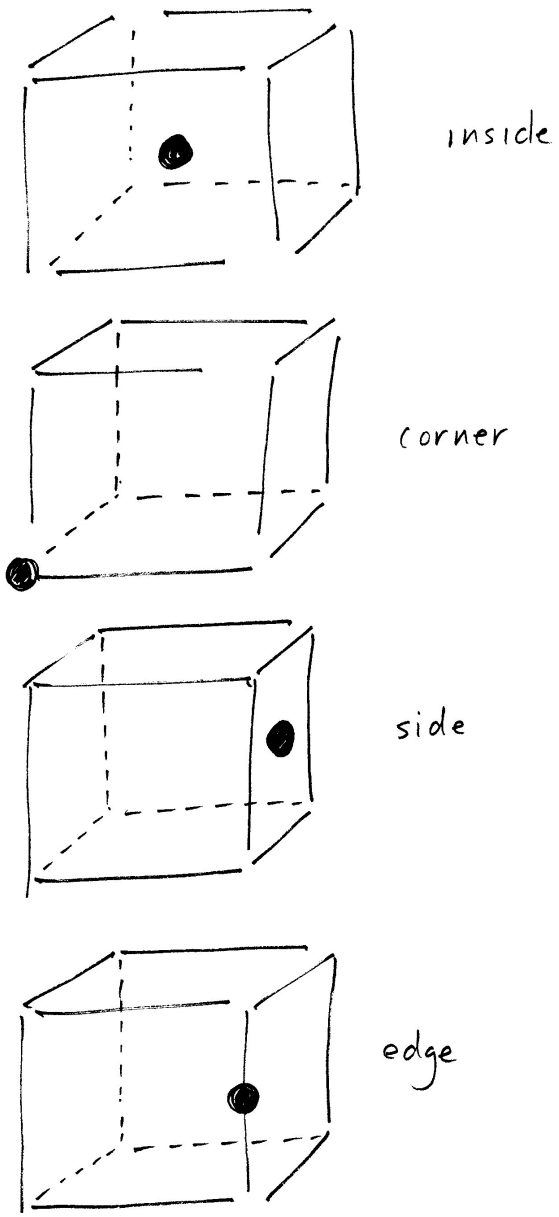

Figure 2.2: Number of atoms per unit cell. Counting scheme.

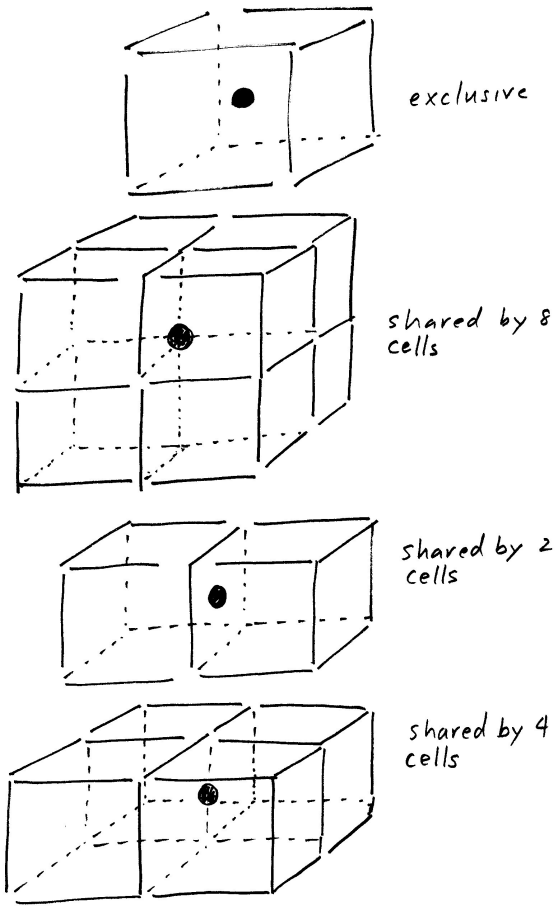

Figure 2.3: Cartoon showing sharing of atoms by multiple unit cells.

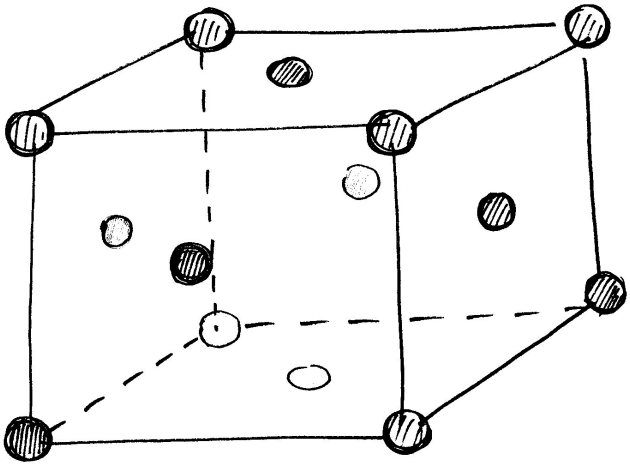

Figure 2.4: FCC unit cell

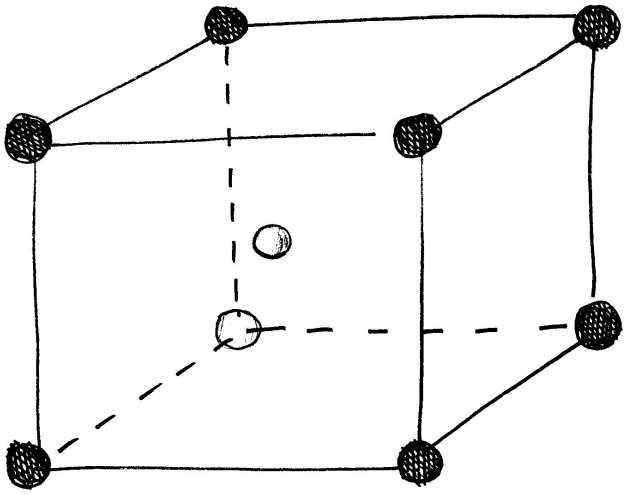

Figure 2.5: BCC unit cell

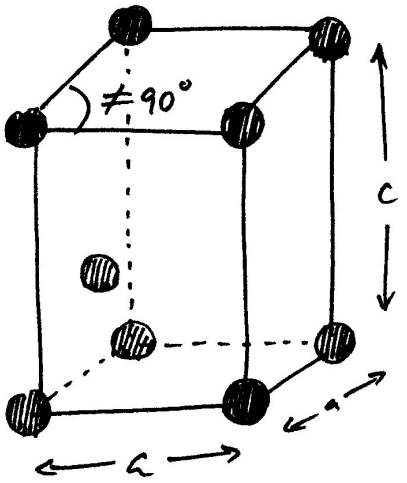

Figure 2.6: Primitive hexagonal unit cell.

in this case is 8 (8 corner atoms, 4 interior atoms, 6 face atoms). Some common elements that crystallize in the diamond structure include: C, Si, Ge and Sn. As a side note, one way to visualize the diamond unit cell is to picture two interpenetrating FCC lattices, offset from each other by a $(\frac{1}{4}, \frac{1}{4}, \frac{1}{4})$ displacement.

Compound crystals

In the case of binary compounds, such as III-V and II-V semiconductors, things get a little more complicated. One doesn't have the benefit of conventional unit cells that resemble any of the 14 standard Bravais lattices. Instead these conventional unit cells often have names such as the "NaCl" structure or the "ZnS" structure and so forth. This is because, unlike simple FCC or BCC metals, we no longer have a single atom basis, but rather a basis consisting of multiple atoms as well as a basis made up of different elements.

Common crystal lattices for semiconductors include the "ZnS", "NaCl" and "CsCl" lattices. The ZnS, also called zinc blende (ZB) or sphalerite, structure can be visualized as two interpenetrating FCC lattices offset by $(\frac{1}{4}, \frac{1}{4}, \frac{1}{4})$ in Figure 2.8. It is identical to the diamond structure we saw in the case of single element crystals. The only real difference is that now we

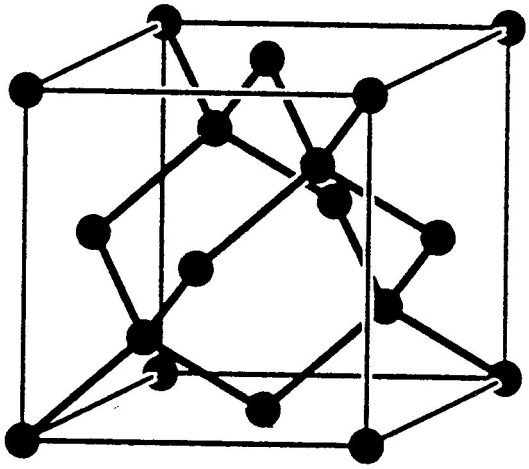

Figure 2.7: Diamond structure unit cell

have two elements making up the atom basis of the unit cell. Using the above counting scheme we find that there are 8 atoms per unit cell. This is further subdivided into 4 atoms of element 1, and 4 atoms of element 2. You will notice in the figure that the 4 atoms of one element are completely inside the unit cell and that the atoms of the other element are arranged as 8 corner and 6 face atoms.

The NaCl structure can be visualized as 2 interpenetrating FCC lattices offset by $(\frac{1}{2}, 0, 0)$ in Figure 2.9. It has 8 atoms per unit cell. This is broken up into 4 atoms from element 1 and 4 atoms from element 2. One can see in the figure that for element 1 there are 8 corner atoms and 6 face atoms. For element 2 there are 12 edge atoms and 1 interior atom.

The CsCl structure is the compound material version of the single element BCC unit cell. It is shown in Figure 2.10 where one can see that there are two elements present with one of them being the center atom. The atoms from the other element take up corner positions in the unit cell. The CsCl has two atoms per unit cell, 1 from each element.

The wurtzite crystal structure is the compound material version of the single element HCP structure. It has a multi atom basis. The primitive unit cell is shown in Figure 2.11 and contains 4 atoms per unit cell, 2 atoms from element 1 and 2 atoms from element 2.

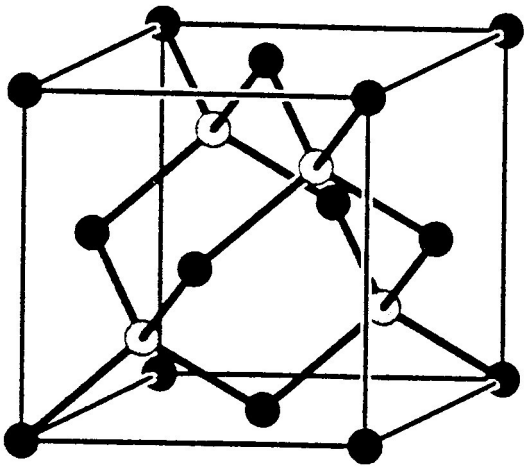

Figure 2.8: Zincblende or ZnS structure unit cell.

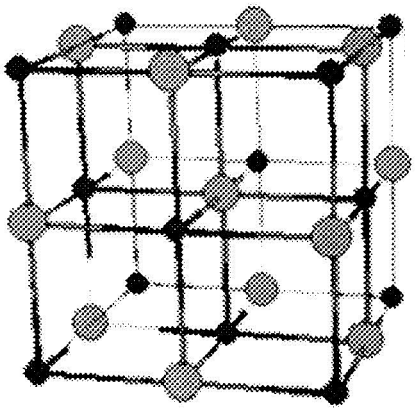

Figure 2.9: NaCl structure unit cell.

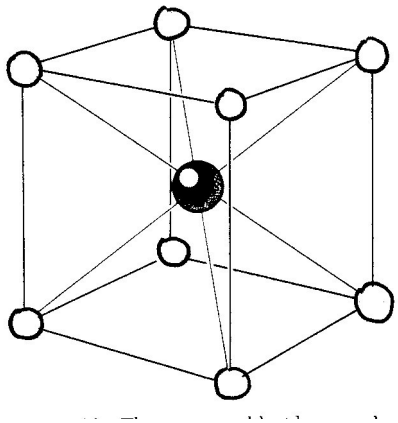

Figure 2.10: CsCl structure unit cell.

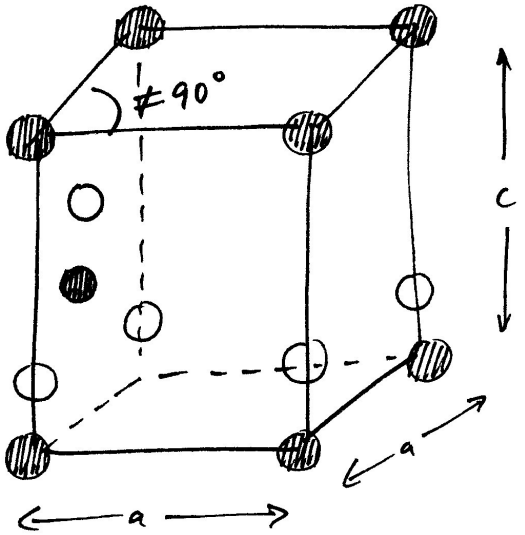

Figure 2.11: Primitive wurtzite unit cell.

Miller indices

Sometimes you will see the orientation of a crystal plane described by (001) and so forth. These numbers are referred to as Miller indices. They are generated using some simple rules described below.

- Take the desired plane and see where it intersects each x, y, z axis in multiples of the lattice constant. For the case of cubic lattices the lattice constant, a, is the same in all x, y, and z directions.
- Next take the reciprocal of each intersection point and reduce the three values to their lowest integer values. (i.e. divide out any common integer)
- Express the plane through these integers in parentheses as (abc)
- Should the plane not intersect an axis, say the z axis, just write a 0. For example $(ab0)$
- If the intercept is in the negative side of an axis, say the y axis, just put a bar over the number, for example $(a\bar{b}c)$.

Examples are illustrated in Figures 2.12 and 2.13.

Quick tables

Short tables of common metals and semiconductors are provided below with their standard crystal structure.

Common Metals

Table 2.1: Common metals

I	II	III	IV	V	VI
		B	C	N	
		Al	Si	P	S
Cu	Zn	Ga	Ge	As	Se
Ag	Cd	In	Sn	Sb	Te
Au	Hg	Tl	Pb	Bi	Po

- Ag=FCC [cubic] (alternatively called cubic closest packed)
- Au=FCC [cubic] (alternatively called cubic closest packed)

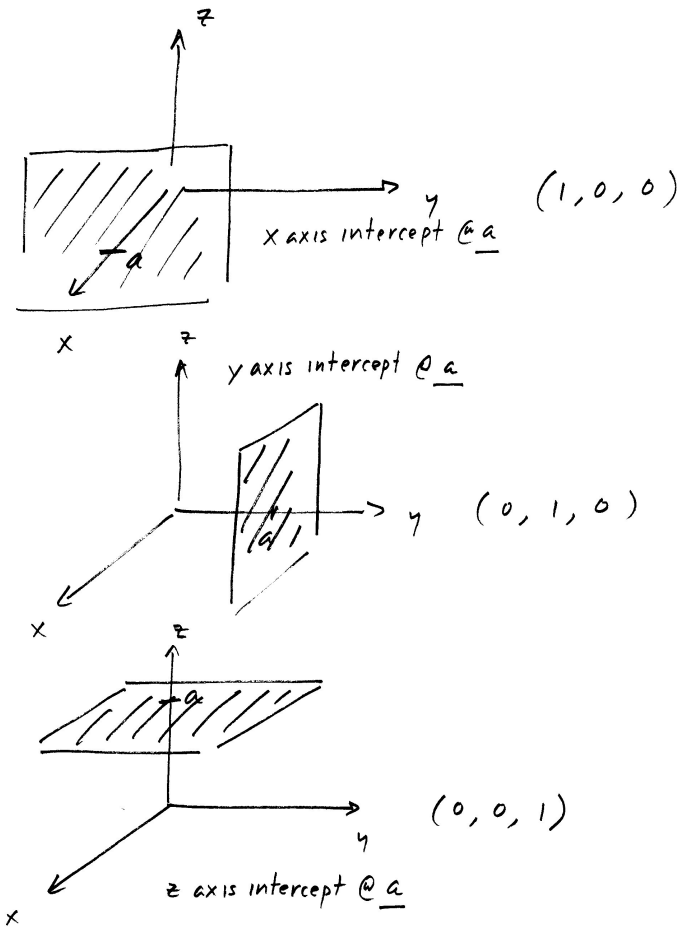

Figure 2.12: Examples of using Miller indices.

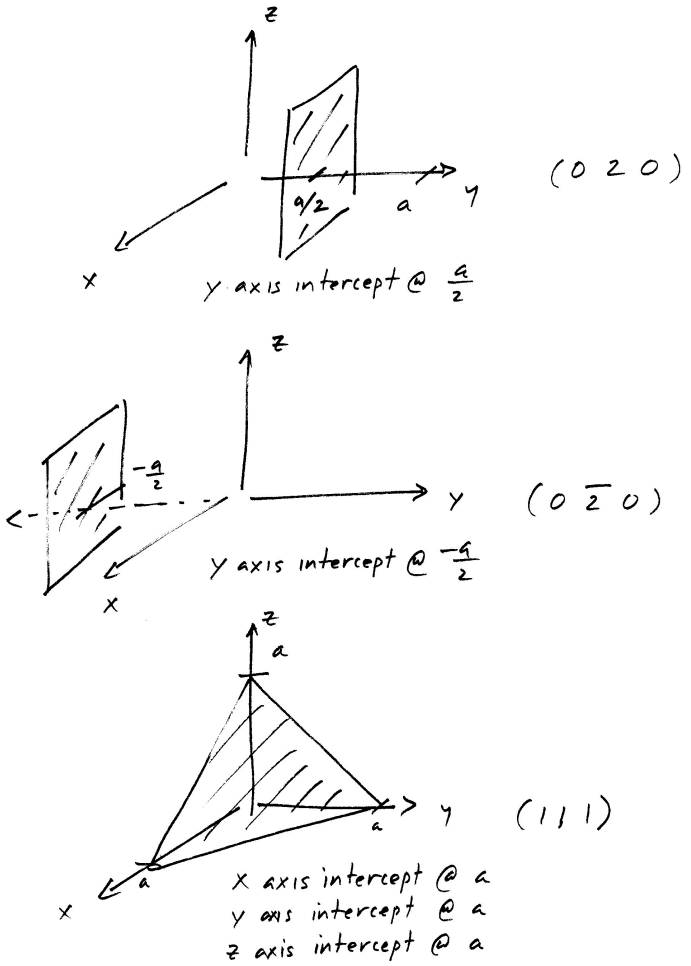

Figure 2.13: More examples of using Miller indices.

Common Semiconductors

Group IV

Table 2.2: Group IV semiconductors

I	II	III	IV	V	VI
		B	***C***	N	
		Al	***Si***	P	S
Cu	Zn	Ga	***Ge***	As	Se
Ag	Cd	In	Sn	Sb	Te
Au	Hg	Tl	Pb	Bi	Po

- Si=diamond structure
- Ge=diamond structure

III-V

Table 2.3: Group III-V semiconductors

I	II	III	IV	V	VI
		B	C	***N***	
		Al	Si	***P***	S
Cu	Zn	***Ga***	Ge	***As***	Se
Ag	Cd	***In***	Sn	***Sb***	Te
Au	Hg	Tl	Pb	Bi	Po

- GaN=ZB [cubic] (alternatively called ZnS structure)
- GaAs=ZB [cubic] (alternatively called ZnS structure)
- InP=ZB [cubic] (alternatively called ZnS structure)
- InAs=ZB [cubic] (alternatively called ZnS structure)

II-VI

- ZnS=ZB [cubic]
- ZnSe=ZB [cubic]

Table 2.4: Group II-VI semiconductors

I	II	III	IV	V	VI
		B	C	N	
		Al	Si	P	***S***
Cu	***Zn***	Ga	Ge	As	***Se***
Ag	***Cd***	In	Sn	Sb	***Te***
Au	Hg	Tl	Pb	Bi	Po

- CdS=ZB [cubic]
- CdSe=wurtzite [hexagonal]
- CdTe=ZB [cubic]

IV-VI

Table 2.5: Group IV-VI semiconductors

I	II	III	IV	V	VI
		B	C	N	
		Al	Si	P	***S***
Cu	Zn	Ga	Ge	As	***Se***
Ag	Cd	In	Sn	Sb	***Te***
Au	Hg	Tl	***Pb***	Bi	Po

- PbS=NaCl structure
- PbSe=NaCl structure
- PbTe=NaCl structure

Exercises

1. The lattice constant of Si is 5.43 $\mathring{A}$. Calculate the number of silicon atoms in a cubic centimeter.
2. Calculate the number of Ga atoms per cubic centimeter in a GaAs crystal. The lattice constant of GaAs is 5.65 $\mathring{A}$. Do the same for As atoms.

3. Consider an actual silicon device on a wafer with physical dimensions of 5 x 5 x 1 microns. Calculate the total number of atoms in the device.

4. Consider a slightly larger GaAs laser on the same wafer. Its dimensions are 100 x 100 x 20 microns. How many total atoms exist on this device.

5. Calculate the number of atoms in a 1.4 nm diameter Pt nanoparticle using the total number of unit cells present. Consider a FCC unit cell with a lattice constant of $a = 0.391$ nm.

6. Calculate the number of atoms in a 1.4 nm diameter Pt nanoparticle using the bulk density of Pt. Consider $\rho = 21.5 g/cm^3$.

7. Estimate the number of surface atoms and percentage of surface atoms in a 1.4 nm diameter Pt nanoparticle. One can calculate this through a unit cell approach but use whatever approach you like.

8. Cobalt is usually found with a hexagonal crystal structure. It was recently found to crystallize with a simple cubic structure, now called ϵ-cobalt. The lattice constant of ϵ-cobalt is $a = 6.097 \mathring{A}$. The density is $\rho = 8.635 g/cm^3$. The unit cell contains 20 atoms. Calculate the number of atoms in a 2 nm diameter nanocrystal through a unit cell argument.

9. Calculate the number of atoms in a 2 nm diamter ϵ-cobalt nanocrystal through a density argument. Use $\rho = 8.635 g/cm^3$.

10. Calculate the number of surface atoms and percentage of surface atoms in a 2 nm diameter ϵ-cobalt particle.

11. CdSe has a hexagonal unit cell. The lattice constants are $a = 4.3 \mathring{A}$ and $c = 7 \mathring{A}$. Calculate the total number of atoms in a CdSe quantum dot for a: 1, 2, 3, 4, 5, 6 nm diameter particle. How many atoms of each element are there?

12. For the same CdSe dots considered, calculate the fraction of surface atoms in each case and plot this on a graph.

13. Draw the surface of a Ag crystal cut along the (111) and (100) plane.

References

1. "Introduction to solid state physics"
   C. Kittel
   Wiley, New York, New York 1986.

2. "Solid state physics"
   N. W. Ashcroft and N. D. Mermin
   Holt, Rinehart and Winston, New York, New York 1976.

3. "Solid-state physics"
   H. Ibach and H. Luth
   Springer Verlag, Berlin 1990.

Relevant literature

1. "A solution-phase chemical approach to a new crystal structure of cobalt"
   D. P. Dinega and M. G. Bawendi
   Angew. Chem. Int. Ed. 38, 1788 (1999).

Chapter 3

Length scales

DeBroglie wavelength and exciton Bohr radius

Here we derive the relationship between the deBroglie wavelength and the exciton Bohr radius. The reason we do this is that often in the literature one sees a statement that a nanomaterial is in the "quantum confinement" regime because its size is smaller than the corresponding deBroglie wavelength of an electron or hole. At other times one sees the statement that a nanomaterial is quantum confined because its size is smaller than the corresponding exciton Bohr radius. We ask if these are the same statement.

In this section we show that the two are related and that, in fact, both statements essentially say the same thing.

Textbook Bohr radius

Here is the textbook equation for the Bohr radius of an electron

$$\boxed{a_0 = \frac{4\pi\epsilon_0\hbar^2}{mq^2}} \tag{3.1}$$

where $\epsilon_0 = 8.85\times10^{-12}$ F/m (permittivity), $\hbar = 1.054\times10^{-34}\ J\cdot s$ (Planck's constant over 2π), $m_e = 9.11\times10^{-31}$ kg (mass of a free electron) and $q = 1.602\times10^{-19}$ C (charge). If you plug all the numbers in and do the math you come up with the result

$$\begin{aligned} a_0 &= 5.28\times10^{-11}\text{meters} \\ &= 0.528 \text{ Angstroms} \end{aligned} \tag{3.2}$$

This is the standard Bohr radius one sees all the time.

Derivation

Basically we need to balance the centrifugal (outward) force of a carrier with the Coulomb attractive (inward) force.

$$\frac{mv^2}{r} = \frac{q^2}{4\pi\epsilon_0 r^2} \tag{3.3}$$

Here we make use of the relation

$$\boxed{2\pi r = n\lambda} \tag{3.4}$$

where n is an integer. The deBroglie relation comes in by relating the wavelength $\lambda = \frac{h}{p}$ where h is Planck's constant and p is the momentum of the particle ($p = mv$). Starting with the above equation we rearrange it to get

$$\lambda = \frac{2\pi r}{n} = \frac{h}{p} = \frac{h}{mv}$$

Solve for v to get

$$v = \frac{nh}{2\pi mr} = \frac{n\hbar}{mr}$$

Replace this into the main equation

$$\frac{n^2\hbar^2}{mr} = \frac{q^2}{4\pi\epsilon_0}$$

Rearrange this to get

$$r = \frac{4\pi\epsilon_0 n^2\hbar^2}{mq^2}$$

If $n = 1$ (the lowest orbit) this gives us the Bohr radius

$$a_0 = \frac{4\pi\epsilon_0\hbar^2}{mq^2}$$

which is the standard textbook equation we showed earlier.

At this point we note that if the electron or carrier is not in vacuum the equation should be modified to take into account the dielectric constant of the medium. (Instead of ϵ replace it with $\epsilon\epsilon_0$)

$$a_0 = \frac{4\pi\epsilon_0\epsilon\hbar^2}{mq^2} \tag{3.5}$$

Furthermore, for the case of an exciton (electron hole pair) in a semiconductor just replace the mass of the electron with the effective mass of the exciton.

$$\boxed{\frac{1}{m_{eff}} = \frac{1}{m_e} + \frac{1}{m_h}} \tag{3.6}$$

where m_e and m_h are the effective masses of electron and hole in the material.

Note that equation 3.4 basically gives the relation between the deBroglie wavelength and the exciton Bohr radius. So, in effect, our initial statements about confinement dealing with either the exciton Bohr radius or deBroglie wavelength are essentially one and the same. The deBroglie wavelength or exciton Bohr radius are therefore natural lenght scales by which to compare the physical size of a nanomaterial. In general objects with dimensions smaller than these natural length scales will exhibit quantum confinement effects. This will be discussed in more detail in subsequent chapters.

Examples

Here are some values for some common systems where I've taken values of the dielectric constant, electron and hole effective masses from the literature. One can derive the exciton Bohr radius of these systems, using the values below, in a straightforward fashion. This list is not meant to be comprehansive and the interested reader should consult the Landolt Bornstein tables for more complete values.

- GaAs:
  $m_e = 0.067m_0$
  $m_h = 0.45m_0$
  $\epsilon = 12.4$

- InAs:
  $m_e = 0.02m_0$

$m_h = 0.4m_0$
$\epsilon = 14.5$

- InP:
  $m_e = 0.07m_0$
  $m_h = 0.4m_0$
  $\epsilon = 14$

- CdS:
  $m_e = 0.2m_0$
  $m_h = 0.7m_0$
  $\epsilon = 8.6$

- CdSe:
  $m_e = 0.13m_0$
  $m_h = 0.45m_0$
  $\epsilon = 9.4$

Worked example

Case: (GaAs)

$$\begin{aligned} \frac{1}{m_{eff}} &= \frac{1}{m_e} + \frac{1}{m_h} \\ &= \frac{1}{0.067m_0} + \frac{1}{0.45m_0} \end{aligned}$$

leading to the effective mass

$$m_{eff} = 0.058m_0$$

$$\begin{aligned} a_b &= \frac{4\pi\epsilon_0\epsilon\hbar^2}{0.058m_0q^2} \\ &= \frac{4\pi(8.85\times10^{-12})(12.4)(1.054\times10^{-34})^2}{(0.058)(9.11\times10^{-31})(1.602\times10^{-19})^2} \\ &= 11.3 \text{ nm} \end{aligned}$$

Exciton Bohr radius for GaAs.

Case: (CdSe)

$$\begin{aligned}\frac{1}{m_{eff}} &= \frac{1}{m_e}+\frac{1}{m_h} \\ &= \frac{1}{0.013m_0}+\frac{1}{0.45m_0}\end{aligned}$$

leading to the effective mass

$$m_{eff} = 0.1m_0$$

$$\begin{aligned}a_b &= \frac{4\pi\epsilon_0\epsilon\hbar^2}{0.058m_0q^2} \\ &= \frac{4\pi(8.85\times10^{-12})(9.4)(1.054\times10^{-34})^2}{(0.1)(9.11\times10^{-31})(1.602\times10^{-19})^2} \\ &= 4.97 \text{ nm}\end{aligned}$$

Exciton Bohr radius for CdSe.

Exercises

1. What is the wavelength of a 1 eV photon?
2. What is the wavelength of a 2 eV photon?
3. What is the wavelength of a 3 eV photon?
4. What is your deBroglie wavelength (what's your weight in kg?) when moving at 10 m/s?
5. What is the deBroglie wavelength of a baseball (0.15 kg) moving at 50 m/s?
6. What is the deBroglie wavelength of C_{60} moving at 220 m/s? Read the corresponding article if you are interested. Arndt et. al. Nature 401, 680 (1999).

7. Calculate the exciton Bohr radius for the following semiconductors. If needed use values for what is called the heavy hole. Consult a good resource such as Landolt Bornstein.
   II-VI compounds
   CdS
   CdSe
   CdTe
   III-V compounds
   InP
   InAs
   IV-VI compounds
   PbS
   PbSe
   PbTe

8. Explain what the size of the exciton Bohr radius means for achieving quantum confinment. What systems are easiest for achieving confinement.

Chapter 4

Confinement

Quantum wells, wires and dots are often described using the analogy to a particle in a 1D box, a 2D box and a 3D box. This is because when the actual physical length scale of the system is smaller than the exciton Bohr radius or corresponding deBroglie wavelength (as we saw in the previous section), either or both the electron and hole experience confinment. In turn, the energies of the carrier along that dimension of the material are no longer continuous as in the case where there is no confinement. The appearance of discrete states is one of the fundamental signatures of nanomaterials. Since solving the Schrodinger equation of a carrier to find its eigenvalues and eigenfunctions involves using boundary conditions one can also immediately predict that the actual shape of a quantum well, wire or dot will also play a role in dictating the ordering and spacing of states. A nanowire will have a similar but different progression of states than a quantum dot (or nanocrystal). The same applies to quantum wells as well as more exotic shapes of nanostructures.

In this chapter we solve the simple analytical problems of a particle in a 1 dimensional rectangual box, a cylindrical wire and a sphere (particle in a spherical box) to illustrate the discreteness as well as progression of states in wells, wires and dots.

1 Dimension of confinement

Particle in a 1D infinite box

The potential is

$$V(x) = \begin{cases} \infty & \text{if } x <= 0 \\ 0 & \text{if } 0 < x < a \\ \infty & \text{if } x >= a \end{cases}$$

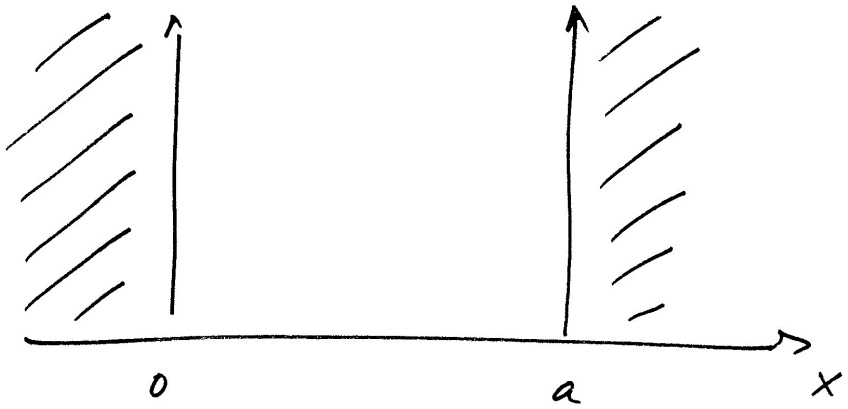

Figure 4.1: Cartoon of a one dimensional infinite barrier potential

The boundary conditions are

$$\Psi(0) = 0$$
$$\Psi(a) = 0$$

The Shrodinger equation to solve is

$$\boxed{-\frac{\hbar^2}{2m}\frac{d^2\Psi}{dx^2} + V\Psi = \varepsilon\Psi} \tag{4.1}$$

Rearrange to yield in the box region where $V = 0$

$$\frac{d^2\Psi}{dx^2} + k^2\Psi = 0 \tag{4.2}$$

where $k = \sqrt{\frac{2m\varepsilon}{\hbar^2}}$ General solutions are of the form

$$\Psi = Ae^{ikx} + Be^{-ikx} \tag{4.3}$$

Apply the boundary conditions now to simplify

$$\Psi(0) = A + B \rightarrow B = -A$$
$$\Psi(a) = Ae^{ikx} - Ae^{-ikx} = 0$$

This latter equation reduces to

$$2iA\frac{e^{ikx}-e^{-ikx}}{2i}=0$$

$$2iAsin(ka)=0$$

For this to be true and non-trivial ($A=0$), $ka=n\pi$. This leads to

$$\sqrt{\frac{2m\varepsilon}{\hbar^2}}a=n\pi$$

The energy can be solved for, to give

$$\boxed{\varepsilon=\frac{n^2h^2}{8ma^2}} \tag{4.4}$$

where n is an integer. Now by normalizing the wavefunction

$$\Psi^*\Psi=1$$

one basically gets the equation

$$N^2\int_0^a sin^2(kx)dx=1$$

The integral can be evaluated by recalling that $sin^2(kx)=\frac{1}{2}(1-cos(2kx))$. This is readily integrated to give $N=\sqrt{\frac{2}{a}}$ and the complete wavefunction as

$$\boxed{\Psi(x)=\sqrt{\frac{2}{a}}sin(kx)} \tag{4.5}$$

Exercises

1. Estimate the first few energies ($n=1,2,3$) for an electron in GaAs quantum wells of width 10 nm and 4 nm. Assume the mass is $0.067m_0$. Repeat the same calculation for a "heavy" hole ($m_{hh}=.5m_0$) and "light" hole ($m_{lh}=0.082m_0$). In all cases assume an infinite box model.

2. Use Mathcad, Matlab, Mathematica or your favorite mathematical modeling program and numerically determine the first 10 energies of the particle in an infinite box (previous problem). Draw the corresponding wavefunctions as well.

3. Consider the following potential in Figure 4.2. Find the energy levels and eigenfunctions. Assume knowledge of the harmonic oscillator wavefunctions and energies. (look them up if you need to) This problem does not require any extensive work.

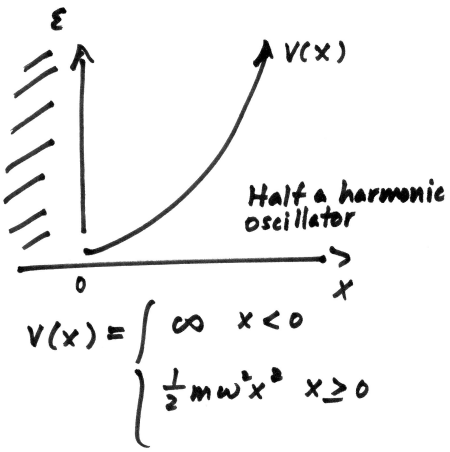

Figure 4.2: Half a harmonic oscillator

Particle in a 1D finite box

This problem is a little more complicated. From quantum mechnanics we know that the solution in the box region where the potential is zero will be wavelike. In the barrier region we also know that the solutions will be exponentially decaying.

The potential is

$$V(x) = \begin{cases} V & \text{if } x <= 0 \\ 0 & \text{if } 0 < x < a \\ V & \text{if } x >= a \end{cases}$$

The solutions are

$$\begin{aligned} \Psi_1(x) &= Ae^{\beta x} + Be^{-\beta x} \\ \Psi_2(x) &= Ce^{ikx} + De^{-ikx} \\ \Psi_3(x) &= Fe^{\beta x} + Ge^{-\beta x} \end{aligned}$$

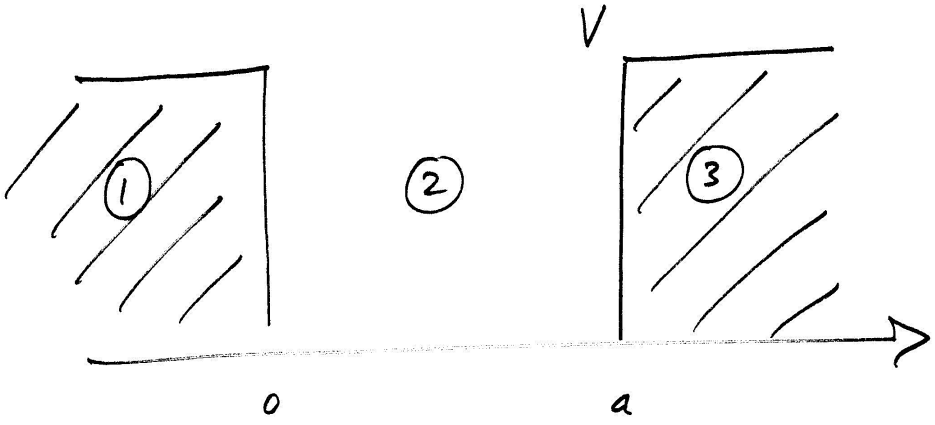

Figure 4.3: Cartoon of a one dimensional finite barrier potential

where $\beta = \sqrt{\frac{2m(V-\varepsilon)}{\hbar^2}}$ and $k = \sqrt{\frac{2m\varepsilon}{\hbar^2}}$. By finiteness of the wavefunction $B = 0$. In addition $F = 0$. The wavefunction must not blow up in the barrier region. Must be well behaved.

This leaves us with

$$\begin{aligned} \Psi_1(x) &= Ae^{\beta x} && (4.6)\\ \Psi_2(x) &= Ce^{ikx} + De^{-ikx} && (4.7)\\ \Psi_3(x) &= Ge^{-\beta x} && (4.8) \end{aligned}$$

Apply the boundary conditions and matching conditions as follows

$$\begin{aligned} \Psi_1(0) &= \Psi_2(0) \rightarrow A = C + D\\ \Psi_1^{'}(0) &= \Psi_2^{'}(0) \rightarrow A\beta = ikC - ikD\\ \Psi_2(a) &= \Psi_3(a) \rightarrow Ce^{ika} + De^{-ika} = Ge^{-\beta a}\\ \Psi_2^{'}(a) &= \Psi_3^{'}(a) \rightarrow ikCe^{ika} - ikDe^{-ika} = -\beta Ge^{-\beta a} \end{aligned}$$

This leads to a system of four equations and four unknowns (A,C,D,G). Arranged in matrix form it looks like

$$\begin{pmatrix} 1 & -1 & -1 & 0\\ \beta & -ik & ik & 0\\ 0 & e^{ika} & e^{-ika} & -e^{-\beta a}\\ 0 & ike^{ika} & -ike^{-ika} & \beta e^{-\beta a} \end{pmatrix} \begin{pmatrix} A\\ C\\ D\\ G \end{pmatrix} = 0$$

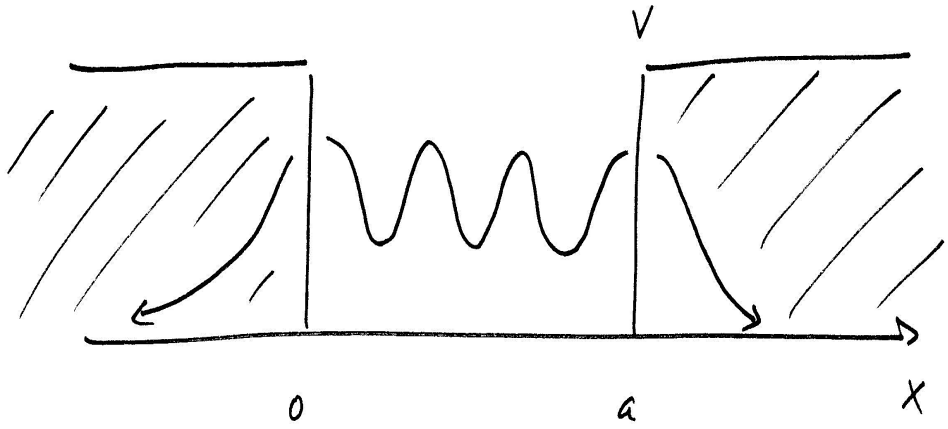

Figure 4.4: Sketch showing the behavior of the wavefunctions in the finite box model

Here either we get the trivial solution where A=C=D=G=0 or that the determinant of the large matrix is zero.

$$\begin{vmatrix} 1 & -1 & -1 & 0 \\ \beta & -ik & ik & 0 \\ 0 & e^{ika} & e^{-ika} & -e^{-\beta a} \\ 0 & ike^{ika} & -ike^{-ika} & \beta e^{-\beta a} \end{vmatrix} = 0 \tag{4.9}$$

Simplify this determinant. This can be done a number of ways. One possible path is shown.

$$-ik(\text{row 3}) + (\text{row 4}) \rightarrow (\text{row4})$$

The determinant becomes

$$\begin{vmatrix} 1 & -1 & -1 & 0 \\ 0 & (\beta - ik) & (\beta + ik) & 0 \\ 0 & e^{ika} & e^{-ika} & -e^{-\beta a} \\ 0 & 0 & -2ike^{-ika} & (\beta + ik)e^{-\beta a} \end{vmatrix} = 0$$

Followed by

$$-\frac{1}{\beta - ik}(\text{row 2}) \rightarrow (\text{row 2})$$
$$e^{-ika}(\text{row 3}) \rightarrow (\text{row 3})$$

yielding

$$\begin{vmatrix} 1 & -1 & -1 & 0 \\ 0 & -1 & -\frac{(\beta+ik)}{(\beta-ik)} & 0 \\ 0 & 1 & e^{-2ika} & -e^{-a(\beta+ik)} \\ 0 & 0 & -2ike^{-ika} & (\beta+ik)e^{-\beta a} \end{vmatrix} = 0$$

Additional steps

$$\begin{aligned} (\text{row } 2) + (\text{row } 3) &\rightarrow (\text{row } 3) \\ -(\text{row } 2) &\rightarrow (\text{row } 2) \end{aligned}$$

giving

$$\begin{vmatrix} 1 & -1 & -1 & 0 \\ 0 & 1 & \frac{(\beta+ik)}{(\beta-ik)} & 0 \\ 0 & 0 & e^{-2ika} - \frac{(\beta+ik)}{(\beta-ik)} & -e^{-a(\beta+ik)} \\ 0 & 0 & -2ike^{-ika} & (\beta+ik)e^{-\beta a} \end{vmatrix} = 0$$

Finding this determinant basically means finding the sub 2x2 determinant

$$\begin{vmatrix} e^{-2ika} - \frac{(\beta+ik)}{(\beta-ik)} & -e^{-a(\beta+ik)} \\ -2ike^{-ika} & (\beta+ik)e^{-\beta a} \end{vmatrix} = 0$$

This is the same as

$$\left(e^{-2ika} - \frac{(\beta+ik)}{(\beta-ik)}\right)(\beta+ik)e^{-\beta a} - 2ike^{-ika-a(\beta+ik)} = 0$$

$$(\beta+ik)e^{-2ika-\beta a} - \frac{(\beta+ik)^2}{(\beta-ik)}e^{-\beta a} - 2ike^{-2ika-\beta a} = 0$$

Drop the $e^{-\beta a}$ term to give

$$(\beta+ik)e^{-2ika} - \frac{(\beta+ik)^2}{(\beta-ik)} - 2ike^{-2ika} = 0$$

$$(\beta+ik-2ik)e^{-2ika} = \frac{(\beta+ik)^2}{(\beta-ik)}$$

$$(\beta-ik)^2e^{-2ika} = (\beta+ik)^2$$

Multiply both sides by e^{ika}

$$(\beta - ik)^2 e^{-ika} = (\beta + ik)^2 e^{ika}$$

$$(\beta + ik)^2 e^{ika} - (\beta - ik)^2 e^{-ika} = 0$$

Continue simplifying

$$(\beta^2 + 2i\beta k - k^2)e^{ika} - (\beta^2 - 2i\beta k - k^2)e^{-ika} = 0$$

$$(\beta^2 - k^2)(e^{ika} - e^{-ika}) + 2i\beta k(e^{ika} + e^{-ika}) = 0$$

$$2i(\beta^2 - k^2)sin(ka) + 4i\beta k cos(ka) = 0$$

$$(\beta^2 - k^2)sin(ka) + 2\beta k cos(ka) = 0$$

$$(\beta^2 - k^2)tank(ka) + 2\beta k = 0$$

Giving our final expression

$$\boxed{\tan(ka) = \frac{2\beta k}{(k^2 - \beta^2)}} \tag{4.10}$$

where $\beta = \sqrt{\frac{2m(V-\varepsilon)}{\hbar^2}}$ and $k = \sqrt{\frac{2m\varepsilon}{\hbar^2}}$. If we replace this into the above equation we get the equation

$$\boxed{\tan\left(\sqrt{\frac{2m\varepsilon}{\hbar^2}}a\right) = \frac{2\sqrt{\varepsilon(V-\varepsilon)}}{2\varepsilon - V}} \tag{4.11}$$

Solve this numerically to get all allowed values of the energy (i.e. find the roots).

Exercises

1. Consider the same GaAs quantum wells in the previous exercise (well widths of 4 nm and 10 nm). Assume the effective mass of the electron is $0.067m_o$. Also assume, now rather than an infinite box, we have a finite box with a 0.3 eV barrier. Calculate the energy of electron states trapped in the box. Increase the barrier to 1 eV. Calculate the energy

of electron states trapped in the box (also known as bound states). This can be done using your favorite mathematical modeling software such as Mathcad, Matlab, Mathematica etc. . ..

2 Dimensions of confinement

Paticle in an infinite circular box

The Schrodinger equation here is

$$\boxed{-\frac{\hbar^2}{2m}\nabla^2\Psi + V\Psi = \varepsilon\Psi}$$

The potential is

$$V(x) = \begin{cases} 0 & \text{if } r < a \\ \infty & \text{if } r >= a \end{cases}$$

In the region where the potential is zero

$$-\frac{\hbar^2}{2m}\nabla^2\Psi = \varepsilon\Psi$$

where ∇^2, the Laplacian in r, θ coordinates, is

$$\nabla^2 = \frac{1}{r}\frac{\partial}{\partial r}\left(r\frac{\partial}{\partial r}\right) + \frac{1}{r^2}\frac{\partial^2}{\partial\theta^2} \tag{4.12}$$

Insert this into the main equation to get

$$-\frac{\hbar^2}{2m}\left(\frac{1}{r}\frac{\partial}{\partial r}\left(r\frac{\partial\Psi}{\partial r}\right) + \frac{1}{r^2}\frac{\partial^2\Psi}{\partial\theta^2}\right) - \varepsilon\Psi = 0$$

$$\frac{1}{r}\frac{\partial}{\partial r}\left(r\frac{\partial\Psi}{\partial r}\right) + \frac{1}{r^2}\frac{\partial^2\Psi}{\partial\theta^2} + \frac{2m\varepsilon}{\hbar^2}\Psi = 0$$

$$\frac{1}{r}\frac{\partial}{\partial r}\left(r\frac{\partial\Psi}{\partial r}\right) + \frac{1}{r^2}\frac{\partial^2\Psi}{\partial\theta^2} + k^2\Psi = 0$$

Multiply through by r^2 to get

$$r\frac{\partial}{\partial r}\left(r\frac{\partial\Psi}{\partial r}\right) + (kr)^2\Psi + \frac{\partial^2\Psi}{\partial\theta^2} = 0$$

Note that you have part of this expression depends only on r and the other exclusively on θ. Assume a form of the wavefunction that is $\Psi = x(r)y(\theta)$. As shorthand just denote Ψ by xy. Let's evaluate the first two terms in the main equation above.

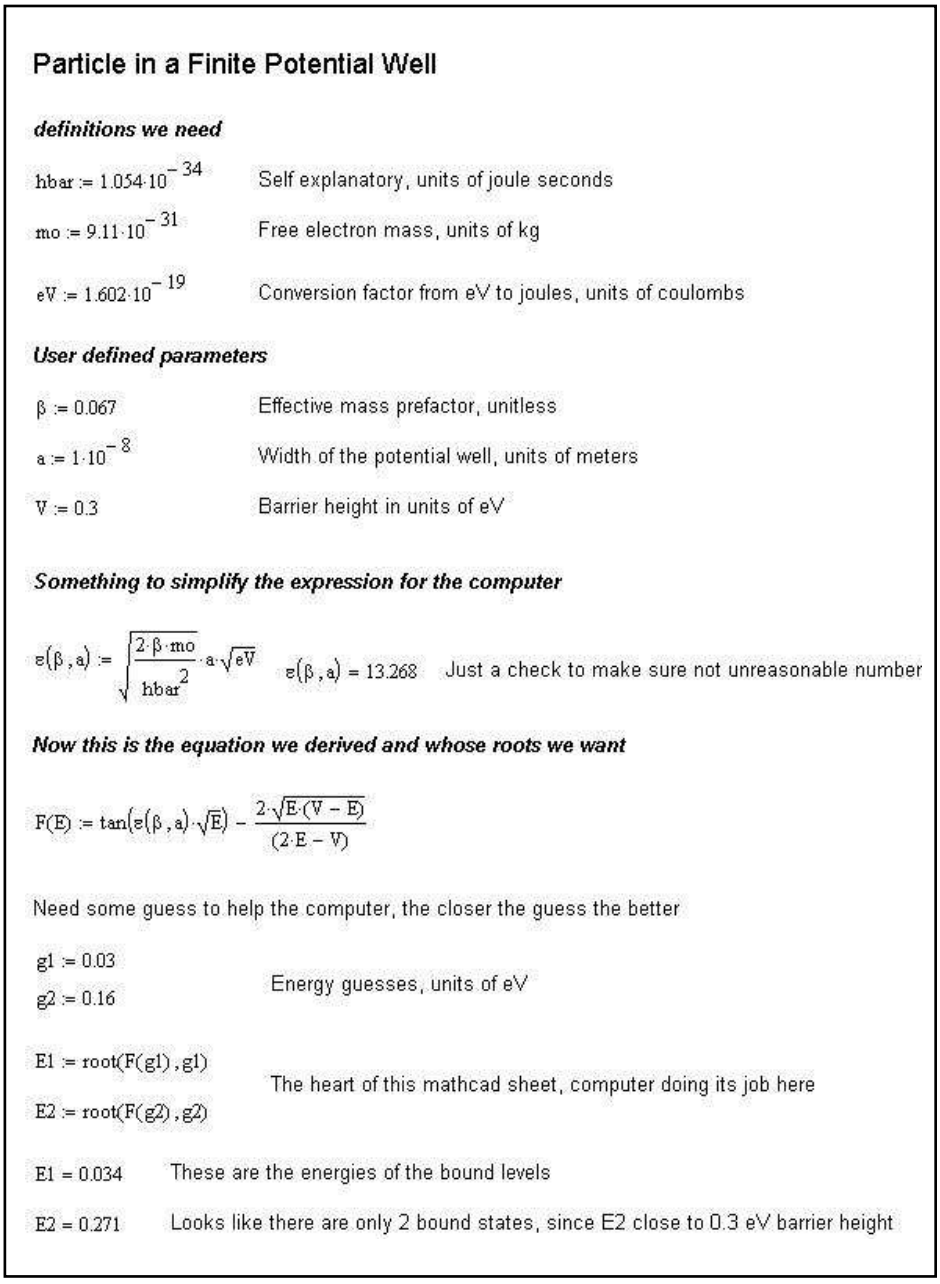

Particle in a Finite Potential Well

definitions we need

$hbar := 1.054 \cdot 10^{-34}$ Self explanatory, units of joule seconds

$mo := 9.11 \cdot 10^{-31}$ Free electron mass, units of kg

$eV := 1.602 \cdot 10^{-19}$ Conversion factor from eV to joules, units of coulombs

User defined parameters

$\beta := 0.067$ Effective mass prefactor, unitless

$a := 1 \cdot 10^{-8}$ Width of the potential well, units of meters

$V := 0.3$ Barrier height in units of eV

Something to simplify the expression for the computer

$$\varepsilon(\beta, a) := \sqrt{\frac{2 \cdot \beta \cdot mo}{hbar^2}} \cdot a \cdot \sqrt{eV} \qquad \varepsilon(\beta, a) = 13.268$$

Just a check to make sure not unreasonable number

Now this is the equation we derived and whose roots we want

$$F(E) := \tan\left(\varepsilon(\beta, a) \cdot \sqrt{E}\right) - \frac{2 \cdot \sqrt{E \cdot (V - E)}}{(2 \cdot E - V)}$$

Need some guess to help the computer, the closer the guess the better

$g1 := 0.03$
$g2 := 0.16$
Energy guesses, units of eV

$E1 := root(F(g1), g1)$
$E2 := root(F(g2), g2)$
The heart of this mathcad sheet, computer doing its job here

$E1 = 0.034$ These are the energies of the bound levels

$E2 = 0.271$ Looks like there are only 2 bound states, since E2 close to 0.3 eV barrier height

Figure 4.5: Mathcad sheet showing numerical solutions to the particle in a finite box problem

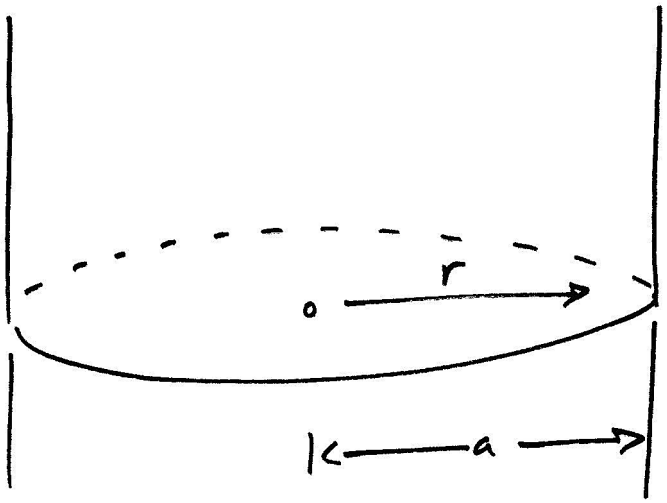

Figure 4.6: Cartoon of the infinite circular potential

- $\frac{\partial \Psi}{\partial r} = yx^{'}$
- $\left(r\frac{\partial \Psi}{\partial r}\right) = yrx^{'}$
- $\frac{\partial}{\partial r}\left(r\frac{\partial \Psi}{\partial r}\right) = yrx^{''} + yx^{'}$
- $r\frac{\partial}{\partial r}\left(r\frac{\partial \Psi}{\partial r}\right) = yr^2x^{''} + yrx^{'}$

Replace the last item into the above main equation to get

$$yr^2x^{''} + yrx^{'} + (kr)^2xy + xy^{''} = 0$$

Divide through by xy to get

$$\frac{r^2x^{''}}{x} + \frac{rx^{'}}{x} + (kr)^2 + \frac{y^{''}}{y} = 0 \tag{4.13}$$

Solve for y first.

$$\frac{y^{''}}{y} = -\left(\frac{r^2x^{''}}{x} + \frac{rx^{'}}{x} + (kr)^2\right)$$

let

$$m^2 = \left(\frac{r^2 x^{''}}{x} + \frac{r x^{'}}{x} + (kr)^2 \right)$$

which you notice is independent of θ and so to y appears as a constant. Replacing this into the above expression gives

$$y^{''} = -m^2 y \tag{4.14}$$

or

$$y^{''} + m^2 y = 0$$

leading to a general solution of the form

$$y(\theta) = Ae^{im\theta} + Be^{-im\theta} \tag{4.15}$$

Now given an explicit form for $y(\theta)$ (equation 14) replace this back into equation 13. This is because ultimately what we want is $x(r)$. Equation 13 becomes

$$\frac{r^2 x^{''}}{x} + \frac{r x^{'}}{x} + (kr)^2 - m^2 = 0$$
$$\frac{x^{''}}{x} + \frac{x^{'}}{rx} + \left(k^2 - \frac{m^2}{r^2} \right) = 0$$

leading to

$$\boxed{x^{''} + \tfrac{x^{'}}{r} + x\left(k^2 - \tfrac{m^2}{r^2}\right) = 0} \tag{4.16}$$

which is the normal Bessel equation. Alternatively, to make this look like something you look up in a book, let $z = kr$. This results in

$$\boxed{z^2 \tfrac{d^2 x}{dz^2} + z \tfrac{dx}{dz} + x(z^2 - m^2) = 0} \tag{4.17}$$

Solutions to this equation (for integer m) take the general form

$$\boxed{x(r) = AJ_m(z) + BY_m(z)} \tag{4.18}$$

which is a linear combination of $J_m(z)$ called Bessel functions of the first kind and $Y_m(z)$ called Bessel functions of the second kind. Note that Bessel functions of the first kind are well behaved at the origin but Bessel functions

of the second kind will diverge. Therefore, to obtain physically relevant solutions drop the Bessel functions of the second kind and only consider $J_m(z)$.

$$\boxed{x(r) = AJ_m(z)} \tag{4.19}$$

Finally, from our other boundary conditions, $J_m(ka) = 0$ Therefore $ka = \alpha$ which is the root of the Bessel function. Since $k = \sqrt{\frac{2m\varepsilon}{\hbar}}$ and $z = kr$, the eigenenergies that we desire are

$$\boxed{\varepsilon = \frac{\hbar^2\alpha^2}{2ma^2}} \tag{4.20}$$

where a is the radius of the circle, m is the mass of the particle and α are the roots (first, second, third etc...) of the Bessel function. (Please note that the m in the denominator is the mass of the particle, not the order of the Bessel function. Sorry for the notation glitch)

Exercises

1. Consider an InP nanowire of diameter 10, 15 and 20 nm (see the Lieber paper below). Assume $m_e = 0.078m_o$ and $m_h = 0.4m_o$. Calculate the energy of the first 3 optical transitions by adding these particle in a circular box energies to the bulk room temperature band gap of InP. Ignore the length of the wire for simplicity. What colors do you expect these wires to emit, UV, visible, IR?

2. Consider a quantum corral as described below in the Eigler paper. Assume the diameter of the corral is $71.3\mathring{A}$. Assume the effective mass of the electron is $m_e = 0.38m_o$. Calculate the first 3 electron energy levels of this corral.

3. For the same quantum corral above, draw the first three wavefunctions of the system. Use your favorite mathematical modeling program such as Mathcad, Matlab, Mathematica etc. . ..

Relevant reading

- "Size dependent photoluminescence from single indium phosphide nanowires" M. S. Gudiksen, J. Wang, C. M. Lieber J. Phys. Chem. B 106, 4036 (2002).

- "Confinement of electrons to quantum corrals on a metal surface" M. F. Crommie, C. P. Lutz, D. M. Eigler Science, 262, 218 (1993).

- "Quantum corrals" M. F. Crommie, C. P. Lutz, D. M. Eigler, E. J. Heller Physica D, 83, 98 (1995).

3 Dimensions of confinement

Particle in an infinite spherical box

This is a more complicated problem. Two approaches to a solution are illustrated with one leading to what are know as spherical Bessel function and the other to a solution involving regular Bessel functions of half integer order. The Schrodinger equation is

$$\boxed{-\frac{\hbar^2}{2m}\nabla^2\Psi + V\Psi = \varepsilon\Psi}$$

The potential is

$$V(x) = \begin{cases} 0 & \text{if } r < a \\ \infty & \text{if } r >= a \end{cases}$$

In the region inside the sphere where $V = 0$, this reduces to

$$-\frac{\hbar^2}{2m}\nabla^2\Psi = \varepsilon\Psi \tag{4.21}$$

where

$$\nabla^2 = \frac{1}{r^2}\frac{\partial}{\partial r}\left(r^2\frac{\partial}{\partial r}\right) + \frac{1}{r^2 sin(\theta)}\frac{\partial}{\partial\theta}\left(sin(\theta)\frac{\partial}{\partial\theta}\right) + \frac{1}{r^2\sin^2(\theta)}\frac{\partial^2}{\partial\phi^2} \tag{4.22}$$

If replaced into the above equation, multiply by $2mr^2$ on both sides to simplify giving

$$-\hbar^2 r^2\nabla^2\Psi = 2mr^2\varepsilon\Psi$$

Expanded out this looks like

$$-\hbar^2 r^2\left(\frac{1}{r^2}\frac{\partial}{\partial r}\left(r^2\frac{\partial\Psi}{\partial r}\right) + \frac{1}{r^2 sin(\theta)}\frac{\partial}{\partial\theta}\left(sin(\theta)\frac{\partial\Psi}{\partial\theta}\right) + \frac{1}{r^2\sin^2(\theta)}\frac{\partial^2\Psi}{\partial\phi^2}\right) = 2mr^2\varepsilon\Psi$$

$$-\hbar^2\left(\frac{\partial}{\partial r}\left(r^2\frac{\partial\Psi}{\partial r}\right) + \frac{1}{sin(\theta)}\frac{\partial}{\partial\theta}\left(sin(\theta)\frac{\partial\Psi}{\partial\theta}\right) + \frac{1}{sin^2(\theta)}\frac{\partial^2\Psi}{\partial\phi^2}\right) = 2mr^2\varepsilon\Psi$$

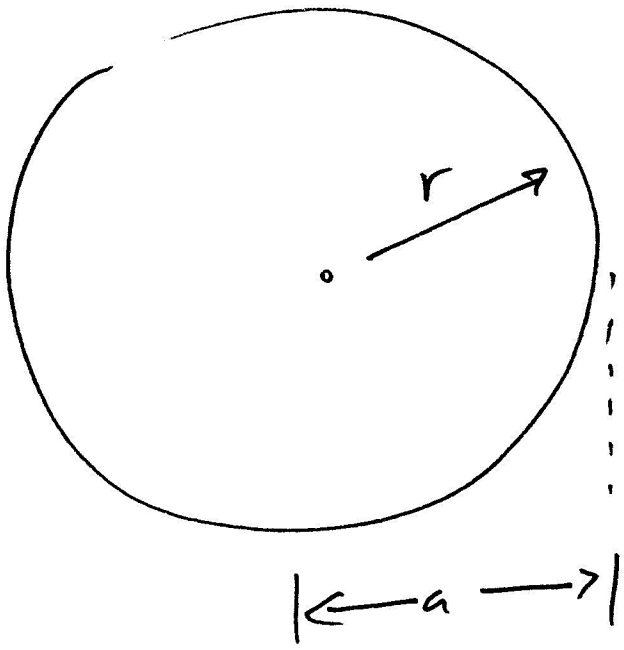

Figure 4.7: Cartoon of the infinite spherical potential

Rearrange to give

$$\begin{aligned} - \quad & \hbar^2 \frac{\partial}{\partial r}\left(r^2 \frac{\partial \Psi}{\partial r}\right) - 2mr^2\varepsilon\Psi \\ - \quad & \hbar^2 \left(\frac{1}{sin(\theta)}\frac{\partial}{\partial \theta}\left(sin(\theta)\frac{\partial}{\partial \theta}\right) - \frac{1}{sin^2(\theta)}\frac{\partial^2}{\partial \phi^2}\right)\Psi = 0 \end{aligned}$$

where recall that the third term looks familiar. Basically

$$\hat{L}^2 = -\hbar^2 \left(\frac{1}{sin(\theta)}\frac{\partial}{\partial \theta}\left(sin(\theta)\frac{\partial}{\partial \theta}\right) - \frac{1}{sin^2(\theta)}\frac{\partial^2}{\partial \phi^2}\right) \tag{4.23}$$

Our main equation then becomes

$$-\hbar^2 \frac{\partial}{\partial r}\left(r^2 \frac{\partial \Psi}{\partial r}\right) - 2mr^2\varepsilon\Psi + \hat{L}^2\Psi = 0$$

Furthermore, recall that $\hat{L}^2\Psi = \hbar^2 l(l+1)$ leading to

$$-\hbar^2 \frac{\partial}{\partial r}\left(r^2 \frac{\partial \Psi}{\partial r}\right) - 2mr^2\varepsilon\Psi + \hbar^2 l(l+1)\Psi = 0$$

Simplify this

$$\begin{aligned} -\hbar^2 \quad & \frac{\partial}{\partial r}\left(r^2 \frac{\partial \Psi}{\partial r}\right) - \Psi\left(2mr^2\varepsilon - \hbar^2 l(l+1)\right) = 0 \\ & \frac{\partial}{\partial r}\left(r^2 \frac{\partial \Psi}{\partial r}\right) + \Psi\left(\frac{2m\varepsilon}{\hbar^2}r^2 - l(l+1)\right) = 0 \end{aligned}$$

Let $k^2 = \frac{2m\varepsilon}{\hbar^2}$ giving

$$\frac{\partial}{\partial r}\left(r^2 \frac{\partial \Psi}{\partial r}\right) + \Psi\left(k^2 r^2 - l(l+1)\right) = 0 \tag{4.24}$$

At this point there are two ways to proceed from this equation. The first will lead to solutions involving so called "spherical" Bessel functions. The other will lead to solutions involving regular or normal Bessel functions of half integer order. Spherical and half integer order, normal, Bessel functions are proportional to each other so ultimately the solutions are the same.

Solution with spherical Bessel functions

Let $\Psi = x(r)y(\theta, \phi)$ The we can evaluate the following items using x and y as shorthand for $x(r)$ and $y(\theta, \phi)$

- $\frac{\partial \Psi}{\partial r} = yx^{'}$
- $r^2 \frac{\partial \Psi}{\partial r} = yr^2 x^{'}$
- $\frac{\partial}{\partial r}\left(r^2 \frac{\partial \Psi}{\partial r}\right) = y(r^2 x^{''} + 2rx^{'})$

Replace the last item into equation 23 giving

$$y(r^2 x^{''} + 2rx^{'}) + xy(k^2 r^2 - l(l+1)) = 0$$

Divide out y and continue simplifying.

$$r^2 x^{''} + 2rx^{'} + x(k^2 r^2 - l(l+1)) = 0$$

Let $z = kr$ (therefore $dr = \frac{dz}{k}$ and $dr^2 = \frac{dz^2}{k^2}$. these will be useful in a moment) and replace into the above expression

$$\begin{aligned} r^2 x^{''} + 2rx^{'} + x(z^2 - l(l+1)) &= 0 \\ r^2 \frac{d^2 x}{dr^2} + 2r\frac{dx}{dr} + x(z^2 - l(l+1)) &= 0 \\ k^2 r^2 \frac{d^2 x}{dz^2} + 2rk\frac{dx}{dz} + x(z^2 - l(l+1)) &= 0 \end{aligned}$$

or

$$\boxed{z^2 \frac{d^2 x}{dz^2} + 2z\frac{dx}{dz} + x(z^2 - l(l+1)) = 0} \tag{4.25}$$

This is the general spherical Bessel equation whose solutions take the form:

$$\boxed{x(r) = Aj_l(z) + By_l(z)} \tag{4.26}$$

where $j_l(z)$ are spherical Bessel functions of the first kind and $y_l(z)$ are spherical Bessel functions of the second kind (also known as spherical Neumann functions written as $n_l(z)$). Note that $j_l(z)$ is finite and well behaved at the origin while $y_l(z)$ diverges. So to get a physical solution, one must drop the spherical Bessel functions of the second kind leaving

$$\boxed{x(r) = Aj_l(z)} \tag{4.27}$$

The equation and its solutions can be looked up in a text like "Handbook of Mathematical Functions" Abramowitz and Stegun, pg 437. Note that these spherical Bessel functions are denoted by little $j_n(z)$ as opposed to big $J_n(z)$ which are normal Bessel functions (same with spherical Bessel functions of the second kind). Furthermore, spherical bessel functions are related to half integer Bessel functions, a subclass of normal Bessel functions as shown at the end of this chapter. Examples of the spherical Bessel function solutions are

- $j_0(z) = \frac{sin(z)}{z}$
- $j_1(z) = \frac{sin(z)}{z^2} - \frac{cos(z)}{z}$
- $j_2(z) = 3\frac{sin(z)}{z^3} - 3\frac{cos(z)}{z^2} - \frac{sin(z)}{z}$

and so forth.

Solution with half integer (normal) Bessel functions

Alternatively assume that the wavefunction has the form $\psi = \frac{x(r)}{r}y(\theta,\phi) = R(r)y(\theta,\phi)$ Replace this in equation 24 and start simplifying.

$$\frac{\partial}{\partial r}\left(r^2\frac{\partial \Psi}{\partial r}\right) + \Psi(k^2r^2 - l(l+1)) = 0$$

We need the following bits of information

- $\frac{\partial \Psi}{\partial r} = yx\left(-\frac{1}{r^2}\right) + \frac{y}{r}x^{'}$
- $r^2\frac{\partial \Psi}{\partial r} = -xy + ryx^{'}$
- $\frac{\partial}{\partial r}\left(r^2\frac{\partial \Psi}{\partial r}\right) = -x^{'}y + x^{''}ry + x^{'}y = x^{''}ry$

Replace the last item into our main equation

$$x^{''}ry + \frac{xy}{r}(k^2r^2 - l(l+1)) = 0$$

Get rid of y

$$rx^{''} + \frac{x}{r}(k^2r^2 - l(l+1)) = 0$$

$$x^{''} + x\left(k^2 - \frac{l(l+1)}{r^2}\right) = 0$$

Now let $z = kr$ and $x = \sqrt{z}\phi(z)$ $\left(dr = \frac{dz}{k}\right)$ giving

$$\frac{d^2x}{dr^2} + x\left(k^2 - \frac{l(l+1)}{r^2}\right) = 0$$

$$k^2\frac{d^2x}{dz^2} + \sqrt{z}\phi\left(k^2 - \frac{k^2l(l+1)}{z^2}\right) = 0$$

Use the following bits of information

- $\frac{dx}{dz} = \sqrt{z}\phi' + \phi\frac{1}{2}z^{-\frac{1}{2}}$
- $\frac{d^2x}{dz^2} = \sqrt{z}\phi'' + \phi'\frac{1}{2}z^{-\frac{1}{2}} + \frac{1}{2}\left(\phi\left(-\frac{1}{2}\right)z^{-\frac{3}{2}} + z^{-\frac{1}{2}}\phi'\right)$
- $\frac{d^2x}{dz^2} = \sqrt{z}\phi'' + \phi' z^{-\frac{1}{2}} - \frac{1}{4}\phi z^{-\frac{3}{2}}$

especially the last term to get

$$k^2\left(\sqrt{z}\phi'' + \phi' z^{-\frac{1}{2}} - \frac{\phi}{4}z^{-\frac{3}{2}}\right) + \sqrt{z}\phi\left(k^2 - \frac{k^2l(l+1)}{z^2}\right) = 0$$

Drop k^2 and continue simplifying

$$\sqrt{z}\phi'' + \phi' z^{-\frac{1}{2}} - \frac{\phi}{4}z^{-\frac{3}{2}} + \sqrt{z}\phi\left(1 - \frac{l(l+1)}{z^2}\right) = 0$$

$$z\phi'' + \phi' - \frac{\phi}{4z} + z\phi\left(1 - \frac{l(l+1)}{z^2}\right) = 0$$

$$z^2\phi'' + z\phi' - \frac{\phi}{4} + z^2\phi\left(1 - \frac{l(l+1)}{z^2}\right) = 0$$

$$z^2\phi'' + z\phi' + \phi\left(-\frac{1}{4} + z^2 - l(l+1)\right) = 0$$

$$z^2\phi'' + z\phi' + \phi\left(z^2 - \left(\frac{1}{4} + l(l+1)\right)\right) = 0$$

Note that the term in the inner parenthesis is equal to $\left(l + \frac{1}{2}\right)^2$ This simplifies the full expression to

$$z^2\phi'' + z\phi' + \phi\left(z^2 - \left(l + \frac{1}{2}\right)^2\right) = 0$$

Let $n = \left(l + \frac{1}{2}\right)$

$$\boxed{z^2\phi'' + z\phi' + \phi(z^2 - n^2) = 0} \tag{4.28}$$

This is the normal Bessel function equation. In this case where we have half-integer orders n then general solutions for ϕ are linear combinations of half integer Bessel functions. Furthermore, since $x(r) = \sqrt{z}\phi(z)$ and $R(r) = \frac{x(r)}{r}$ the general radial solution, $R(r)$, is

$$\begin{aligned} \phi(z) &= AJ_n(z) + BJ_n(z) \\ x(r) &= \sqrt{z}\left(A^{'}J_n(z) + B^{'}Y_n(z)\right) \end{aligned}$$

$$\boxed{R(r) = \tfrac{1}{\sqrt{z}}\left(A^{'}J_n(z) + B^{'}Y_n(z)\right)} \tag{4.29}$$

or more explicitly

$$\boxed{x(r) = \sqrt{z}\left(AJ_{\left(l+\frac{1}{2}\right)}(z) + BY_{\left(l+\frac{1}{2}\right)}(z)\right)} \tag{4.30}$$

We can look up the equation and its solution in a book like Abramowitz and Stegun but since Y_n diverges near the origin so it should be dropped immediately. This leaves

$$\boxed{R(r) = \tfrac{A^{'}}{\sqrt{z}}J_{\left(l+\frac{1}{2}\right)}(z)} \tag{4.31}$$

Summary

So in the end, regardless of how you came to the solution, to find the eigenvalues we need to find the roots, α, of either

$$\boxed{j_l(kr) = 0} \text{ spherical Bessel} \tag{4.32}$$

$$\boxed{J_{\left(l+\frac{1}{2}\right)}(kr) = 0} \text{ half integer Bessel} \tag{4.33}$$

So on finding the root one also has $\alpha = kr$ and from this the desired value of k. Note that for each value of l there are an infinite number of roots. The eigenvalues are then

$$\varepsilon = \frac{\hbar^2 k^2}{2m} \tag{4.34}$$

$$\boxed{\varepsilon = \tfrac{\hbar^2\alpha^2}{2mr^2}} \tag{4.35}$$

Finally, the relation between spherical Bessel functions and half integer Bessel functions are:

$$j_l(z) = \sqrt{\frac{\pi}{2z}} J_{(l+\frac{1}{2})}(z) \tag{4.36}$$

$$y_l = n_l(z) = \sqrt{\frac{\pi}{2z}} Y_{(l+\frac{1}{2})}(z) \tag{4.37}$$

So either approach to solving the problem is valid. Its your choice on what's most convenient.

Exercises

1. Calculate the eigenenergies of a free electron (mass m_o) in a 5 nm diameter sphere for $l = 0, 1, 2, 3$ using the lowest root of the Bessel function.

2. Calculate the eigenenergies of a free electron (mass m_o) in a 5 nm diameter sphere for $l = 0, 1, 2, 3$ using the second lowest root of the Bessel function.

3. Calculate the eigenenergies of a free electron (mass m_o) in a 5 nm diameter sphere for $l = 0, 1, 2, 3$ using the third lowest root of the Bessel function.

4. Summarize all these energies in ascending order of energy in one table.

5. Use Mathcad, Matlab, Mathematica or your favorite mathematical modeling program to draw the radial wavefunctions corresponding to the lowest three energies in your table. Don't forget to normalize the wavefunction.

6. Calculate the first 7 energy levels of a free electron in a 5 nm length three dimensional box. (All sides of the cube have length of 5 nm). Compare these results to the particle in a sphere case.

7. Qualitatively compare the size dependence of the energies for a particle in a 1D box (well), an infinite circular potential (wire) and a particle in an infinite spherical box (dot). Basically ask yourself how all these energies scale with r or a. Any similarities? Now take a look a Yu et. al., Nature Materials 2, 517 - 520 (01 Aug 2003) Letters and comment on it.

8. Often enough there is a Coulomb attraction between the electron and hole in a confined system. As a consequence the energies one calculates via particle in a box type expression are often corrected for this Coulomb attraction. Think back to the basic expression for the Coulomb energy and qualitatively explain why this term is important or not important. Hint: think of how these energies all scale with r or a.

Chapter 5

Density of states

The idea here is that while the confinement of an axis gives rise to discrete energies (as we saw in the previous section on confinement), in cases such as the quantum well and quantum wire, there are additional states along the unconfined axes (degrees of freedom). Here it is not practical to try and calculate the energies of each state since they are actually continuous bands or energies. As a consequence one way to get an idea of what the energies look like is to perform the following density of states argument. So when put together with the confined energies from the last section, these density of states calculations provide a more thorough description of what the electronic structure of 3D, 2D, 1D and 0D materials look like.

3 Dimensions (bulk)

Consider the volume in "k" space

$$V_k = \frac{4}{3}\pi k^3$$

where for a particle in this sphere

$$\begin{aligned} k_x &= \frac{2\pi}{L_x} \\ k_y &= \frac{2\pi}{L_y} \\ k_z &= \frac{2\pi}{L_z} \end{aligned}$$

Note that the 2π arises from the constraints of a periodic boundary condition as opposed to the more general $n\pi$ where $n = 0, 1, 2, 3 \ldots$. The volume of a

given mode is then $k_x k_y k_z$ The number of modes (N) in the sphere are then

$$N = \frac{V_k}{k_x k_y k_z} = \frac{\frac{4}{3}\pi k^3}{8\pi^3} L_x L_y L_z$$

Say the particle is an electron and we consider spin (up and down), then we multiply N by 2.

$$\begin{aligned} N^{'} &= 2N = 2\frac{\frac{4}{3}\pi k^3}{8\pi^3} L_x L_y L_z \\ &= \frac{k^3}{3\pi^2} L_x L_y L_z \text{ total number of states in sphere} \end{aligned}$$

Consider the density

$$\rho = \frac{N^{'}}{L_x L_y L_z} = \frac{k^3}{3\pi^2} \text{ number of states/unit volume}$$

Now consider the energy density defined as

$$\rho^{'} = \frac{d\rho}{d\varepsilon} = \frac{d\left(\frac{k^3}{3\pi^2}\right)}{d\varepsilon} = \frac{1}{3\pi^2}\frac{dk^3}{d\varepsilon} \tag{5.1}$$

where recall $k = \sqrt{\frac{2m\varepsilon}{\hbar^2}}$ for a free electron or alternatively $k^3 = \left(\frac{2m\varepsilon}{\hbar^2}\right)^{\frac{3}{2}}$. The expression becomes

$$\rho^{'} = \frac{1}{3\pi^2}\left(\frac{2m}{\hbar^2}\right)^{\frac{3}{2}} \frac{d\varepsilon^{\frac{3}{2}}}{d\varepsilon}$$

$$\rho^{'} = \frac{1}{3\pi^2}\left(\frac{2m}{\hbar^2}\right)^{\frac{3}{2}} \frac{3}{2}\varepsilon^{\frac{1}{2}}$$

$$\boxed{\rho^{'}_{3D} = \frac{1}{2\pi^2}\left(\frac{2m}{\hbar^2}\right)^{\frac{3}{2}} \sqrt{\varepsilon}} \tag{5.2}$$

This is the "density of states" in 3 dimensions. Note the square root dependence on energy

Exercises

1. Calculate the 3D density of states for free electrons with energy 0.1 eV. Express your answer in terms of eV and cm^3.

2. Assume the electron resides in a non-zero potential V. Express the 3D density of states in this situation. Hint, just alter the expression for k below equation 5.1.

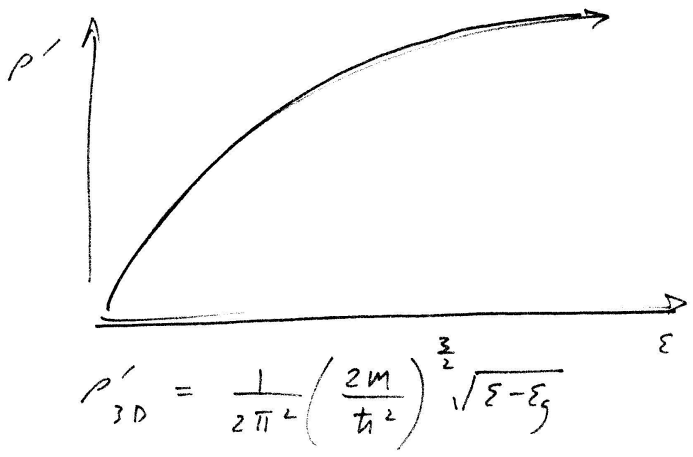

Figure 5.1: Density of states in a 3D material (bulk)

2 Dimensions (well)

Here we have 1 dimension that is quantized. Let's assume its the z direction. The total energy of this system is a sum of the energy along the quantized direction + the energy along the other 2 "free" directions. It is expressed as

$$\varepsilon_{tot} = \frac{\hbar^2 k_z^2}{2m} + \frac{\hbar^2 k^2}{2m} = \varepsilon_n + \varepsilon_{x,y} \tag{5.3}$$

where $k^2 = k_x^2 + k_y^2$ and $k_z = \frac{n\pi}{L_z}$ Consider now an area in k space

$$A_k = \pi k^2$$

where for the particle

$$\begin{aligned} k_x &= \frac{2\pi}{L_x} \\ k_y &= \frac{2\pi}{L_y} \end{aligned}$$

The area of a given mode is then $k_x k_y$ with the total number of modes (N) in the area being

$$N = \frac{\pi k^2}{4\pi^2} L_x L_y = \frac{k^2 L_x L_y}{4\pi}$$

Again if the particle is an electron and we consider spin, multiply by 2 to get

$$N^{'} = 2N = \frac{k^2 L_x L_y}{2\pi} \text{ total number of states in area}$$

Consider now a density

$$\rho = \frac{N^{'}}{L_x L_y} = \frac{k^2}{2\pi}$$

where recall that $k = \sqrt{\frac{2m\varepsilon}{\hbar^2}}$. Replacing this above gives

$$\rho = \frac{m\varepsilon}{\hbar^2 \pi} \text{ number of states per unit area}$$

Now consider the energy density

$$\rho^{'} = \frac{d\rho}{d\varepsilon} = \frac{m}{\hbar^2 \pi}$$

This is the energy density of the subband for a given k_z(or ε_n). For each successive k_z there will be an additional $\frac{m}{\hbar^2\pi}$ term and hence another subband. Therefore the density of states is written

$$\boxed{\rho^{'}_{2D} = \frac{m}{\hbar^2 \pi} \sum_n \Theta(\varepsilon - \varepsilon_n)} \tag{5.4}$$

where Θ is the Heavyside function.

Exercises

1. Calculate the 2D density of states for free electrons with energy 0.1 eV. Consider only the lowest subband. Express your answer in eV and cm^3 units.

1 Dimension (wire)

Consider now the situation where there are 2 dimensions confined and only 1 degree of freedom (say the x direction). The total energy of the system can be written as

$$\varepsilon_{tot} = \frac{\hbar^2 k_z^2}{2m} + \frac{\hbar^2 k_y^2}{2m} + \frac{\hbar^2 k^2}{2m} = \varepsilon_n + \varepsilon_m + \varepsilon_x \tag{5.5}$$

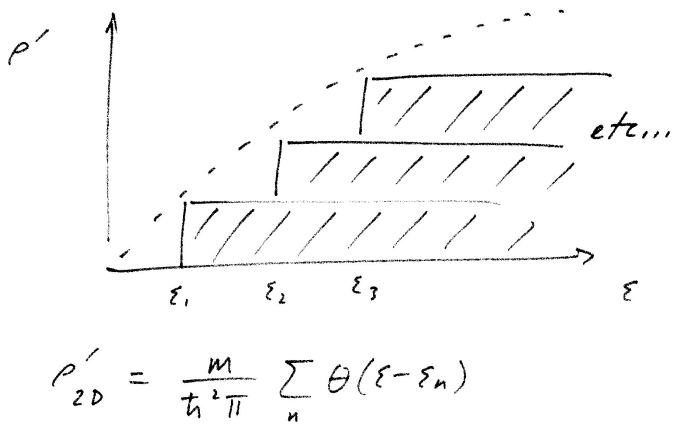

Figure 5.2: Density of states in a 2D material (quantum well)

where $k = k_x = \frac{2\pi}{L_x}$ Furthermore along the confined directions, $k_z = \frac{n\pi}{L_z}$, $k_y = \frac{m\pi}{L_y}$ and m, n are integers. Consider a length $2k$. The number of modes along this length is

$$N = \frac{2k}{k_x} = \frac{2k}{\left(\frac{2\pi}{L_x}\right)} = \frac{kL_x}{\pi} \text{ number of state along the line}$$

Now if we consider an electron again, ensure to take into account the spin degeneracy

$$N^{'} = 2N = \frac{2kL_x}{\pi}$$

Now a density is

$$\rho = \frac{N^{'}}{L_x} = \frac{2k}{\pi} = \frac{2}{\pi}\sqrt{\frac{2m\varepsilon}{\hbar^2}} \text{ number of states per unit length}$$

Consider the energy density

$$\begin{aligned} \rho^{'} &= \frac{d\rho}{d\varepsilon} = \frac{2}{\pi}\sqrt{\frac{2m}{\hbar^2}}\frac{d\sqrt{\varepsilon}}{d\varepsilon} = \frac{2}{\pi}\sqrt{\frac{2m}{\hbar^2}}\frac{1}{2}\varepsilon^{-\frac{1}{2}} \\ &= \frac{1}{\pi}\sqrt{\frac{2m}{\hbar^2}}\frac{1}{\sqrt{\varepsilon}} \end{aligned} \tag{5.6}$$

This is the energy density for a given n, m value or ($\varepsilon_n, \varepsilon_m$ combination). The complete expression taking into account all m, n combinations is

$$\boxed{\rho'_{1D} = \frac{1}{\pi}\sqrt{\frac{2m}{\hbar^2}}\sum_{n,m}\frac{1}{\sqrt{\varepsilon-\varepsilon_{n,m}}}\Theta(\varepsilon-\varepsilon_{n,m})} \tag{5.7}$$

where again, Θ is the Heavyside function. Notice the inverse square root dependence of the density of states with energy.

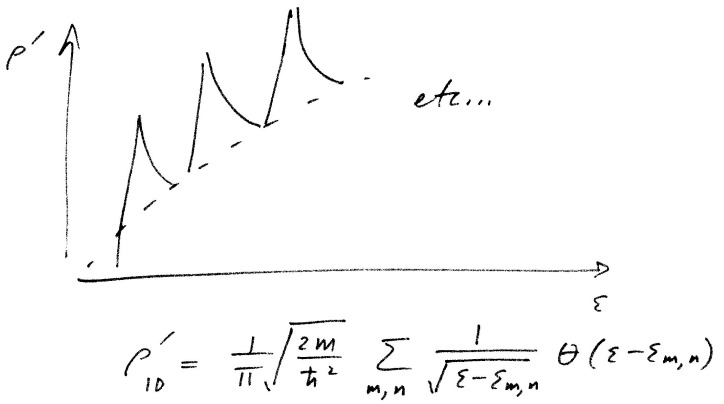

Figure 5.3: Density of states in a 1D material (quantum wire)

Exercises

1. Calculate the 1D density of states for free electrons with energy 0.1 eV above $\varepsilon_{n,m}$. Consider only the lowest subband. Express your result in units of eV and cm^3.

0 Dimension (dot)

Here since all three dimensions are confined the density of states is basically a series of delta functions. The total energy of the system is

$$\varepsilon_{tot} = \frac{\hbar^2 k_x^2}{2m} + \frac{\hbar^2 k_y^2}{2m} + \frac{\hbar^2 k_z^2}{2m} = \varepsilon_m + \varepsilon_n + \varepsilon_o \tag{5.8}$$

where m, n, o are integers and $k_x = \frac{m\pi}{L_x}$, $k_y = \frac{m\pi}{L_y}$, $k_z = \frac{m\pi}{L_z}$ The density of states is

$$\boxed{\rho'_{0D} = \delta\left(\varepsilon - \varepsilon_{m,n,o}\right)} \tag{5.9}$$

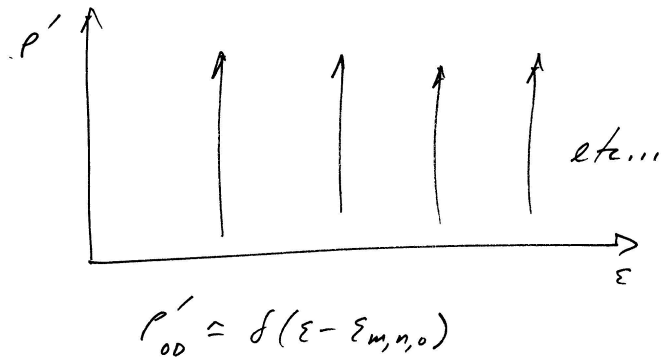

Figure 5.4: Density of states in a 0D material (quantum dot)

Exercises

1. Compare and contrast the density of states in the 0D case to the previous 3D, 2D and 1D cases.

Chapter 6

More density of states

Density of states in the conduction band

To do this calculation we need to know the probablility that an electron will occupy a given state of energy ε. This probability, $P_e(\varepsilon)$, is refered to as the Fermi Dirac distribution. In addition, we need to know the density of states ($\rho^{'}$) which we calculated in the last section. Recall that this density of states has units of number per unit volume per unit energy. Therefore $\rho^{'} d\varepsilon$ is the number of states per unit volume. The number of occupied states at a given energy per unit volume (or alternatively the concentration of electrons at a given energy) is therefore

$$n_e(\varepsilon) = P_e(\varepsilon)\rho^{'}(\varepsilon)d\varepsilon$$

where the Fermi Dirac distribution is

$$P_e(\varepsilon) = \frac{1}{1 + e^{\frac{\varepsilon - \varepsilon_F}{kT}}} \tag{6.1}$$

Here ε_F is the Fermi energy.

The total concentration of electrons in the conduction band is therefore the integral over all available energies

$$n_{tot} = \int_{\varepsilon_C}^{\infty} P_e(\varepsilon)\rho^{'}(\varepsilon)d\varepsilon \tag{6.2}$$

where ε_C is the energy where the conduction band starts. Consider the density of states we just derived for a 3D (bulk) material in the previous section, $\rho^{'}_{3D}$.

$$\rho^{'}_{3D} = \frac{1}{2\pi^2}\left(\frac{2m_e}{\hbar^2}\right)^{\frac{3}{2}}\sqrt{\varepsilon}$$

Now rather than have the origin of the energy start at 0, start it where the conduction band begins (ε_C). This expression can then be recast as

$$\rho_{3D}^{'} = \frac{1}{2\pi^2}\left(\frac{2m_e}{\hbar^2}\right)^{\frac{3}{2}}\sqrt{\varepsilon - \varepsilon_C} \tag{6.3}$$

Replace this and the Fermi Dirac distribution into the above expression for the total concentration of electrons in the conduction band to get

$$\begin{aligned} n_{tot} &= \int_{\varepsilon_C}^{\infty} \frac{1}{1+e^{\frac{\varepsilon-\varepsilon_F}{kT}}} \frac{1}{2\pi^2}\left(\frac{2m_e}{\hbar^2}\right)^{\frac{3}{2}}\sqrt{\varepsilon-\varepsilon_C}d\varepsilon \\ &= \frac{1}{2\pi^2}\left(\frac{2m_e}{\hbar^2}\right)^{\frac{3}{2}}\int_{\varepsilon_C}^{\infty}\frac{1}{1+e^{\frac{\varepsilon-\varepsilon_F}{kT}}}\sqrt{\varepsilon-\varepsilon_C}d\varepsilon \\ &= A\int_{\varepsilon_C}^{\infty}\frac{1}{1+e^{\frac{\varepsilon-\varepsilon_F}{kT}}}\sqrt{\varepsilon-\varepsilon_C}d\varepsilon \end{aligned}$$

where $A = \frac{1}{2\pi^2}\left(\frac{2m_e}{\hbar^2}\right)^{\frac{3}{2}}$. Note at this point that someone has already solved this integral and one can just look it up. The integral is called the Fermi integral or Fermi Dirac integral. It is defined as follows and its solutions labeled $F_{\frac{1}{2}}(\eta)$ can be looked up.

$$\boxed{F_{\frac{1}{2}}(\eta) = \int_0^{\infty}\frac{\sqrt{\eta}}{1+e^{\eta-\mu}}d\eta}$$

However, to stay instructive let's just consider the case where $\varepsilon - \varepsilon_F >> kT$. In this case the exponential in the denominator of the Fermi Dirac distribution will dominate and the expression basically becomes

$$\frac{1}{1+e^{\frac{\varepsilon-\varepsilon_F}{kT}}} \simeq \frac{1}{e^{\frac{\varepsilon-\varepsilon_F}{kT}}} = e^{-\frac{\varepsilon-\varepsilon_F}{kT}}$$

which has the Boltzman distribution form. Our expression for n_{tot} becomes

$$n_{tot} = A\int_{\varepsilon_C}^{\infty} e^{-\frac{\varepsilon-\varepsilon_C}{kT}}\sqrt{\varepsilon-\varepsilon_C}\,d\varepsilon \tag{6.4}$$

Now change variables and let $x = \frac{\varepsilon-\varepsilon_C}{kT}$ such that $\varepsilon = \varepsilon_C + xkT$ and $d\varepsilon = kTdx$. Note also that the limits of integration will change accordingly. This leads to

$$\begin{aligned} n_{tot} &= A\int_0^{\infty} e^{-\frac{1}{kT}[(\varepsilon-\varepsilon_C)+(\varepsilon_C-\varepsilon_F)]}(xkT)^{\frac{1}{2}}kTdx \\ &= A(kT)^{\frac{3}{2}}e^{-\frac{\varepsilon_C-\varepsilon_F}{kT}}\int_0^{\infty} e^{-x}x^{\frac{1}{2}}dx \end{aligned}$$

The last integral is a common function called the Gamma function. It is defined as follows

$$\Gamma(n) = \int_0^\infty e^{-x} x^{n-1} dx$$

and its values can be looked up in most reference books. In our case we have $\Gamma\left(\frac{3}{2}\right)$. Therefore n_{tot} can be expressed as

$$n_C \equiv n_{tot} = A(kT)^{\frac{3}{2}} e^{-\frac{\varepsilon_C - \varepsilon_F}{kT}} \Gamma\left(\frac{3}{2}\right)$$

To be consistent with other texts, we use n_C in lieu of n_{tot} at this point and also define $N_C = A(kT)^{\frac{3}{2}} \Gamma\left(\frac{3}{2}\right)$. This leads to the common textbook expression

$$\boxed{n_C = N_C e^{-\frac{\varepsilon_C - \varepsilon_F}{kT}}} \tag{6.5}$$

This is the expression for the effective density of states of the conduction band.

Density of states in the valence band

The way this is calculated mirrors the approach for the conduction band with a few minor changes. Again, we need the probability of finding a hole at a given energy $P_h(\varepsilon)$. Likewise we need the density of states calculated in the previous section. We will calculate the number of holes at a given energy per unit volume (or concentration of holes at a given energy)

$$n_h(\varepsilon) = P_h(\varepsilon) \rho^{'}(\varepsilon) d\varepsilon$$

where we use the relationship

$$P_e(\varepsilon) + P_h(\varepsilon) = 1$$

or

$$P_h(\varepsilon) = 1 - P_e(\varepsilon)$$

This lead to

$$P_h(\varepsilon) = 1 - \frac{1}{1 + e^{\frac{\varepsilon - \varepsilon_F}{kT}}} \tag{6.6}$$

The density of states is

$$\rho_{3D}^{'} = \frac{1}{2\pi^2}\left(\frac{2m_h}{\hbar^2}\right)^{\frac{3}{2}}\sqrt{\varepsilon_V - \varepsilon} \tag{6.7}$$

where ε_V is the energy where the valence band starts. Consequently the total concentration of holes in the valence band is the integral over all energies.

$$\begin{aligned} p_{tot} &= \int_{-\infty}^{\varepsilon_V} P_h(\varepsilon)\rho^{'}(\varepsilon)d\varepsilon \\ &= \int_{-\infty}^{\varepsilon_V}\left(1 - \frac{1}{1+e^{\frac{\varepsilon-\varepsilon_F}{kT}}}\right)\left(\frac{1}{2\pi^2}\right)\left(\frac{2m_h}{\hbar^2}\right)^{\frac{3}{2}}\sqrt{\varepsilon_V - \varepsilon}\, d\varepsilon \end{aligned}$$

For notational convenience let $B = \frac{1}{2\pi^2}\left(\frac{2m_h}{\hbar^2}\right)^{\frac{3}{2}}$. This leads to

$$p_{tot} = B\int_{-\infty}^{\varepsilon_V}\left(1 - \frac{1}{1+e^{\frac{\varepsilon-\varepsilon_F}{kT}}}\right)\sqrt{\varepsilon_V - \varepsilon}\, d\varepsilon$$

Since, generally speaking $\varepsilon < \varepsilon_F$

$$p_{tot} = B\int_{-\infty}^{\varepsilon_V}\left(1 - \frac{1}{1+e^{-\frac{\varepsilon_F-\varepsilon}{kT}}}\right)\sqrt{\varepsilon_V - \varepsilon}\, d\varepsilon$$

Approximate the stuff in parenthesis through the binomial expansion keeping only the first 2 terms.

$$\begin{aligned} \frac{1}{1+x} &\simeq 1 - x + x^2 - x^3 + x^4 + \ldots \\ \frac{1}{1+e^{-\frac{\varepsilon_F-\varepsilon}{kT}}} &\simeq 1 - e^{-\frac{\varepsilon_F-\varepsilon}{kT}} + \ldots \end{aligned}$$

Therefore

$$\left(1 - \frac{1}{1+e^{-\frac{\varepsilon_F-\varepsilon}{kT}}}\right) \simeq 1 - \left(1 - e^{-\frac{\varepsilon_F-\varepsilon}{kT}}\right) = e^{-\frac{\varepsilon_F-\varepsilon}{kT}}$$

Replacing this in the p_{tot} expression gives

$$p_{tot} = B\int_{-\infty}^{\varepsilon_V} e^{-\frac{\varepsilon_F-\varepsilon}{kT}}\sqrt{\varepsilon_V - \varepsilon}\, d\varepsilon$$

As with the conduction band case earlier, make a change of variables by letting $x = \frac{\varepsilon_V - \varepsilon}{kT}$ as well as $\varepsilon = \varepsilon_V - kTx$ and $d\varepsilon = -kTdx$. Note that the limits of integration change accordingly resulting in

$$\begin{aligned} p_{tot} &= B\int_{\infty}^{0} e^{-\frac{1}{kT}[(\varepsilon_F-\varepsilon_V)+(\varepsilon_V-\varepsilon)]}\sqrt{kTx}(-kT)dx \\ &= B\int_{0}^{\infty} e^{-\frac{\varepsilon_F-\varepsilon_V}{kT}} e^{-\frac{\varepsilon_V-\varepsilon}{kT}} (kT)^{\frac{3}{2}} x^{\frac{1}{2}} dx \\ &= B(kT)^{\frac{3}{2}} e^{-\frac{\varepsilon_F-\varepsilon}{kT}} \int_{0}^{\infty} e^{-x} x^{\frac{1}{2}} dx \end{aligned}$$

Recall that the last integral above is the Gamma function. We get the following expression upon recognizing this

$$p_{tot} = B(kT)^{\frac{3}{2}} e^{-\frac{\varepsilon_F-\varepsilon}{kT}} \Gamma\left(\frac{3}{2}\right)$$

To be consistent with common notation and other texts p_{tot} can be expressed as

$$\boxed{p_V \equiv p_{tot} = N_v e^{-\frac{\varepsilon_F-\varepsilon_V}{kT}}} \tag{6.8}$$

where $N_v = B(kT)^{\frac{3}{2}}\Gamma\left(\frac{3}{2}\right)$. The last expression gives the effective density of states for the valence band.

Summary

Fermi level of an intrinsic semiconductor

If the bulk semiconductor is intrinsic, there has been no doping of the material and hence no extra electrons or holes anwywhere. In this situation

$$n_C = p_V$$

where previously we found that

$$n_C = N_C e^{-\frac{\varepsilon_C-\varepsilon_F}{kT}} \text{ and } N_C = A(kT)^{\frac{3}{2}}\Gamma\left(\frac{3}{2}\right)$$
$$p_V = N_V e^{-\frac{\varepsilon_F-\varepsilon_V}{kT}} \text{ and } N_V = B(kT)^{\frac{3}{2}}\Gamma\left(\frac{3}{2}\right)$$

This leads to

$$N_C e^{-\frac{\varepsilon_C-\varepsilon_F}{kT}} = N_V e^{\frac{-\varepsilon_F-\varepsilon_V}{kT}}$$

or

$$Ae^{-\frac{\varepsilon_C-\varepsilon_F}{kT}} = Be^{-\frac{\varepsilon_F-\varepsilon_V}{kT}}$$

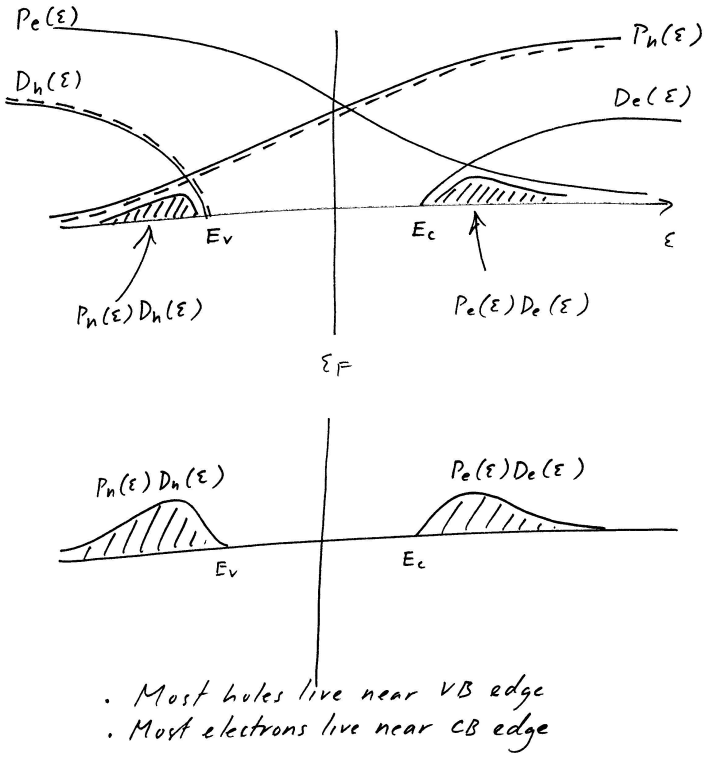

Figure 6.1: Sketch of the electron and hole distribution functions, their density of states and their population at the conduction and valence band edges.

where $A = \frac{1}{2\pi^2}\left(\frac{2m_e}{\hbar^2}\right)^{\frac{3}{2}}$ and $B = \frac{1}{2\pi^2}\left(\frac{2m_h}{\hbar^2}\right)^{\frac{3}{2}}$ and ultimately reduces to

$$\begin{aligned}
m_e^{\frac{3}{2}} e^{-\frac{\varepsilon_C-\varepsilon_F}{kT}} &= m_h^{\frac{3}{2}} e^{-\frac{\varepsilon_F-\varepsilon_V}{kT}} \\
e^{-\frac{\varepsilon_C-\varepsilon_F}{kT}} e^{\frac{\varepsilon_F-\varepsilon_V}{kT}} m_e^{\frac{3}{2}} &= m_h^{\frac{3}{2}} \\
e^{\frac{1}{kT}(-\varepsilon_C+\varepsilon_F+\varepsilon_F-\varepsilon_V)} &= \left(\frac{m_h}{m_e}\right)^{\frac{3}{2}} \\
e^{\frac{2\varepsilon_F}{kT}} e^{-\frac{\varepsilon_C+\varepsilon_V}{kT}} &= \left(\frac{m_h}{m_e}\right)^{\frac{3}{2}} \\
e^{\frac{2\varepsilon_F}{kT}} &= \left(\frac{m_h}{m_e}\right)^{\frac{3}{2}} e^{\frac{\varepsilon_C+\varepsilon_V}{kT}} \\
\ln\left(e^{\frac{2\varepsilon_F}{kT}}\right) &= \ln\left(\frac{m_h}{m_e}\right)^{\frac{3}{2}} + \ln\left(e^{\frac{\varepsilon_C+\varepsilon_V}{kT}}\right) \\
\frac{2\varepsilon_F}{kT} &= \ln\left(\frac{m_h}{m_e}\right)^{\frac{3}{2}} + \frac{\varepsilon_C+\varepsilon_V}{kT} \\
2\varepsilon_F &= kT\ln\left(\frac{m_h}{m_e}\right)^{\frac{3}{2}} + \varepsilon_C + \varepsilon_V \\
\varepsilon_F &= \frac{kT}{2}\ln\left(\frac{m_h}{m_e}\right)^{\frac{3}{2}} + \frac{\varepsilon_C+\varepsilon_C}{2}
\end{aligned}$$

This yields the final expression

$$\boxed{\varepsilon_F = \tfrac{\varepsilon_C+\varepsilon_C}{2} + \tfrac{3}{4}kT\ln\left(\tfrac{m_h}{m_e}\right)^{\frac{3}{2}}} \tag{6.9}$$

One can therefore see that at $T = 0$ the Fermi energy of an intrinsic semiconductor is at the halfway point between the top of the valence band and the bottom of the conduction band. Note also that since generally speaking $m_h > m_e$ the temperature dependent term is positive and slowly increases the Fermi level position with increasing temperature. To a good approximation however, the Fermi level is at the midway point between valence and conduction bands.

Exercises

- Calculate the intrinsic Fermi level of silicon at 0K, 10K, 77K, 300K and 600K. Note that $E_g = E_c + E_v$ and assume $m_e = 1.08m_o$ and $m_h = 0.55m_o$. Leave the answer in terms of E_g of if you desire look up the actual value of E_g and express the final answers in units of eV.

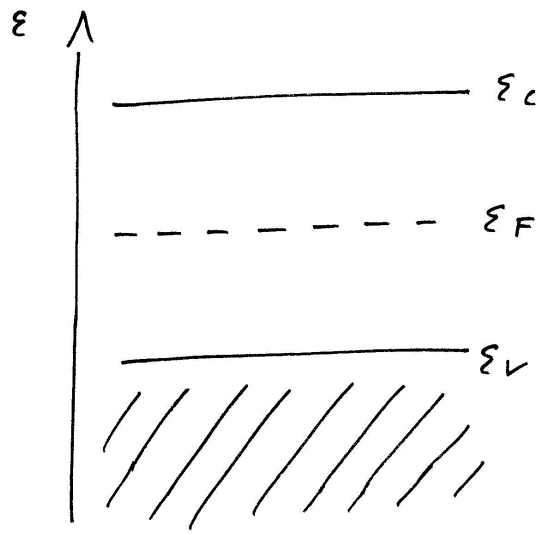

Figure 6.2: Sketch showing the Fermi level position at 0 degrees halfway between the conduction band and valence band positions.

Chapter 7

Even more density of states

In the previous section we ran through the calculation for the conduction and valence band density of states for a 3D (bulk) material. In this section we repeat the same calculations for materials with lower dimensions. In particular we do this for 2D and 1D materials that are representative of quantum wells and quantum wires respectively.

Density of states in the conduction band: 2D

We start with the Fermi Dirac distribution for electrons and also the density of states ($\rho_{2D}^{'}$) that we derived in an earlier section. Recall that

$$\rho_{2D}^{'} = \frac{m_e}{\hbar^2 \pi} \sum_n \Theta(\varepsilon - \varepsilon_n)$$

Consider only one of the subbands. For example, we could choose the first band.

In this case the density of states simplifies to

$$\rho_{2D}^{'} = \frac{m_e}{\hbar^2 \pi}$$

Now recall from the previous section that the number of states at a given energy per unit volume (or the concentration of electrons at a given energy) is

$$n_e(\varepsilon) = P_e(\varepsilon)\rho^{'}(\varepsilon)d\varepsilon$$

The total concentration of electrons in this first subband is the integral over all available energies. Rather than use n_{tot} as before let's just stick to n_c

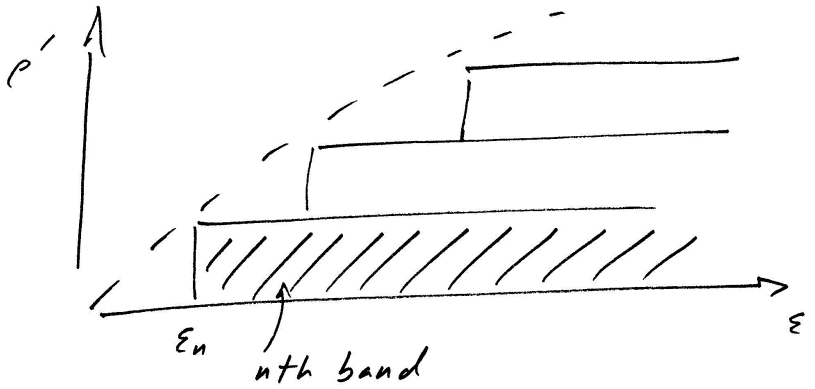

Figure 7.1: Conduction band density of states for a 2D material. The nth band is shaded to distinguish it from the other subbands.

from the start

$$n_c = \int_{\varepsilon_C}^{\infty} P_e(\varepsilon)\rho'(\varepsilon)d\varepsilon \tag{7.1}$$

where $P_e(\varepsilon) = \frac{1}{1+e^{\frac{\varepsilon-\varepsilon_F}{kT}}}$ is the Fermi Dirac distribution. Putting everything together we get

$$\begin{aligned} n_C &= \int_{\varepsilon_C}^{\infty} \left(\frac{1}{1+e^{\frac{\varepsilon-\varepsilon_F}{kT}}}\right) \frac{m_e}{\hbar^2\pi} d\varepsilon \\ &= \frac{m_e}{\hbar^2\pi} \int_{\varepsilon_C}^{\infty} \frac{1}{1+e^{\frac{\varepsilon-\varepsilon_F}{kT}}} d\varepsilon \end{aligned}$$

Since the band really begins at ε_n as opposed to ε_C like in the bulk the integral changes from

$$\int_{\varepsilon_C}^{\infty} \rightarrow \int_{\varepsilon_n}^{\infty}$$

leading to

$$n_C = \frac{m_e}{\hbar^2\pi} \int_{\varepsilon_n}^{\infty} \frac{d\varepsilon}{1+e^{\frac{\varepsilon-\varepsilon_F}{kT}}}$$

if now $\varepsilon - \varepsilon_F >> kT$

$$n_C = \frac{m_e}{\hbar^2\pi} \int_{\varepsilon_n}^{\infty} e^{-\frac{\varepsilon-\varepsilon_F}{kT}} d\varepsilon = -\frac{m_e kT}{\hbar^2\pi} e^{-\frac{\varepsilon-\varepsilon_F}{kT}} \Big|_{\varepsilon_n}^{\infty}$$

This leads to the final expression for the carrier density of the nth subband, which in our example we assumed was the lowest one. Hence this is the carrier density at the conduction band edge of a 2D material.

$$\boxed{n_C = \frac{m_e kT}{\hbar^2 \pi} e^{-\frac{\varepsilon_n - \varepsilon_F}{kT}}} \tag{7.2}$$

Density of states in the valence band:2D

As with the conduction band case we need the probability of occupying a given state in the valence band. This is denoted $P_h(\varepsilon)$ and is evaluated from

$$P_e(\varepsilon) + P_h(\varepsilon) = 1$$
$$P_h(\varepsilon) = 1 - P_e(\varepsilon)$$

where $P_e(\varepsilon)$ is the Fermi Dirac distribution leading to

$$P_h(\varepsilon) = 1 - \frac{1}{1 + e^{\frac{\varepsilon - \varepsilon_F}{kT}}}$$

The number of states at a given energy per unit volume (concentration at a given energy) is

$$n_h(\varepsilon) = P_h(\varepsilon)\rho^{'}(\varepsilon)d\varepsilon$$

If, as in the conduction band case, we consider only the nth subband $\rho^{'} = \frac{m_h}{\hbar^2 \pi}$ and for simplicity the first.

The total concentration of holes in this first subband is the integral over all energies. We get

$$\begin{aligned} p_V &= \int_{-\infty}^{\varepsilon_V} P_h(\varepsilon)\rho^{'}(\varepsilon)d\varepsilon \\ &= \int_{-\infty}^{\varepsilon_V} \left(1 - \frac{1}{1 + e^{\frac{\varepsilon - \varepsilon_F}{kT}}}\right)\left(\frac{m_h}{\hbar^2 \pi}\right) d\varepsilon \\ &= \frac{m_h}{\hbar^2 \pi} \int_{-\infty}^{\varepsilon_V} \left(1 - \frac{1}{1 + e^{\frac{\varepsilon - \varepsilon_F}{kT}}}\right) d\varepsilon \end{aligned} \tag{7.3}$$

Since the nth (in our case the first) subband begins at ε_n rather than ε_V as in the bulk, the limits of the integral change

$$\int_{-\infty}^{\varepsilon_V} \rightarrow \int_{-\infty}^{\varepsilon_n}$$

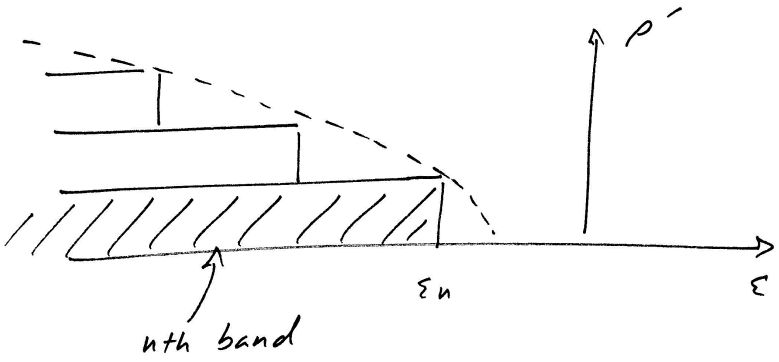

Figure 7.2: Valence band density of states for a 2D material. The nth band is shaded to distinguish it from the other subbands.

The expression becomes

$$p_V = \frac{m_h}{\hbar^2 \pi} \int_{-\infty}^{\varepsilon_n} \left(1 - \frac{1}{1 + e^{\frac{\varepsilon - \varepsilon_F}{kT}}} \right) d\varepsilon$$

Since for the valence band $\varepsilon < \varepsilon_F$

$$p_V = \frac{m_h}{\hbar^2 \pi} \int_{-\infty}^{\varepsilon_n} \left(1 - \frac{1}{1 + e^{-\frac{\varepsilon_F - \varepsilon}{kT}}} \right) d\varepsilon$$

Apply the binomial expansion of the term in parenthesis to simplify, keeping only the first two terms. Recall that

$$\frac{1}{1+x} = 1 - x + x^2 - x^3 + \ldots$$
$$\frac{1}{1 + e^{-\frac{\varepsilon_F - \varepsilon}{kT}}} = 1 - e^{-\frac{\varepsilon_F - \varepsilon}{kT}} + \ldots$$

such that

$$p_V = \frac{m_h}{\hbar^2 \pi} \int_{-\infty}^{\varepsilon_n} e^{-\frac{\varepsilon_F - \varepsilon}{kT}} d\varepsilon = \frac{m_h kT}{\hbar^2 \pi} e^{-\frac{\varepsilon_F - \varepsilon}{kT}} \Big|_{-\infty}^{\varepsilon_n}$$

This reduces to our desired final expression

$$\boxed{p_V = \frac{m_h kT}{\hbar^2 \pi} e^{-\frac{\varepsilon_F - \varepsilon_n}{kT}}} \tag{7.4}$$

Fermi level position:2D

The procedure for finding the Fermi level position is the same as in the 3D case. If we assume an intrinsic semiconductor with no doping such that there are no additional electrons or holes present

$$n_C = p_V$$

then

$$\frac{m_e kT}{\hbar^2 \pi} e^{-\frac{\varepsilon_{n1}-\varepsilon_F}{kT}} = \frac{m_h kT}{\hbar^2 \pi} e^{-\frac{\varepsilon_F-\varepsilon_{n2}}{kT}}$$

Note that n_1 and n_2 have been used to distinguish the start of the conduction band subband and the valence band subband respectively. The above expression reduces

$$\begin{aligned}
e^{\frac{1}{kT}(-\varepsilon_{n1}+\varepsilon_F+\varepsilon_F-\varepsilon_{n2})} &= \left(\frac{m_h}{m_e}\right) \\
e^{-\frac{1}{kT}(\varepsilon_{n1}+\varepsilon_{n2})+\frac{2\varepsilon_F}{kT}} &= \left(\frac{m_h}{m_e}\right) \\
e^{-\frac{\varepsilon_{n1}+\varepsilon_{n2}}{kT}} e^{\frac{2\varepsilon_F}{kT}} &= \left(\frac{m_h}{m_e}\right) \\
e^{\frac{2\varepsilon_F}{kT}} &= \left(\frac{m_h}{m_e}\right) e^{\frac{\varepsilon_{n1}+\varepsilon_{n2}}{kT}} \\
\ln\left(e^{\frac{2\varepsilon_F}{kT}}\right) &= \ln\left(\frac{m_h}{m_e}\right) + \ln\left(e^{\frac{\varepsilon_{n1}+\varepsilon_{n2}}{kT}}\right) \\
\frac{2\varepsilon_F}{kT} &= \ln\left(\frac{m_h}{m_e}\right) + \frac{\varepsilon_{n1}+\varepsilon_{n2}}{kT} \\
2\varepsilon_F &= kT \ln\left(\frac{m_h}{m_e}\right) + \varepsilon_{n1} + \varepsilon_{n2}
\end{aligned}$$

resulting in the final expression

$$\boxed{\varepsilon_F = \frac{\varepsilon_{n1}+\varepsilon_{n2}}{2} + \frac{kT}{2} \ln\left(\frac{m_h}{m_e}\right)} \tag{7.5}$$

As before, since $m_h > m_e$ the second term is positive and grows slowly with increasing temperature. To a first approximation however the Fermi level is midway between the valence band beginning and conduction band beginning.

Density of states in the conduction band:1D

We start with the Fermi Dirac distribution for electrons and the density of states ($\rho_{1D}^{'}$) that we derived earlier. Recall that

$$\rho_{1D}^{'} = \frac{1}{\pi}\sqrt{\frac{2m_e}{\hbar^2}}\sum_{m,n}\frac{1}{\sqrt{\varepsilon - \varepsilon_{m,n}}}\Theta(\varepsilon - \varepsilon_{m,n})$$

where Θ is the Heavyside function.

We consider only the (m,n)th subbband beginning at energy $\varepsilon_{m,n}$. For convenience we could say this is the first subband.

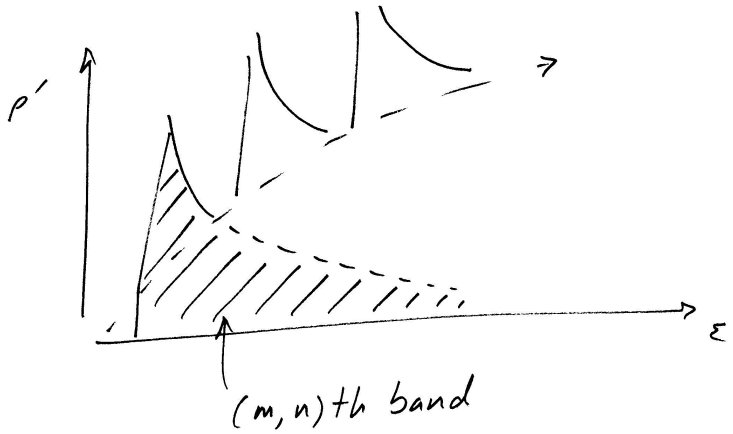

Figure 7.3: Conduction band density of states for a 1D material. The (m,n)th band is shaded to distinguish it from the other subbands.

The number of states at a given energy per unit volume (or the concentration at a given energy) is

$$n_e(\varepsilon) = P_e(\varepsilon)\rho^{'}(\varepsilon)d\varepsilon$$

The total concentration in the first subband is the integral over all possible energies

$$n_c = \int_{\varepsilon_C}^{\infty} P_e(\varepsilon)\rho^{'}(\varepsilon)d\varepsilon$$

where as before the Fermi Dirac distribution is

$$P_e(\varepsilon) = \frac{1}{1 + e^{\frac{\varepsilon - \varepsilon_F}{kT}}}$$

On introducing this, the total expression becomes

$$\begin{aligned} n_C &= \int_{\varepsilon_C}^{\infty} \frac{1}{1+e^{\frac{\varepsilon-\varepsilon_F}{kT}}} \frac{1}{\pi}\sqrt{\frac{2m_e}{\hbar^2}} \frac{1}{\sqrt{\varepsilon-\varepsilon_{m,n}}} d\varepsilon \\ &= \frac{1}{\pi}\sqrt{\frac{2m_e}{\hbar^2}} \int_{\varepsilon_C}^{\infty} \frac{1}{1+e^{\frac{\varepsilon-\varepsilon_F}{kT}}} \frac{1}{\sqrt{\varepsilon-\varepsilon_{m,n}}} d\varepsilon \end{aligned}$$

Since the band actually begins at $\varepsilon_{m,n}$ the limits of integration become

$$\int_{\varepsilon_C}^{\infty} \rightarrow \int_{\varepsilon_{m,n}}^{\infty}$$

Therefore

$$n_C = \frac{1}{\pi}\sqrt{\frac{2m_e}{\hbar^2}} \int_{\varepsilon_{m,n}}^{\infty} \left(\frac{1}{1+e^{\frac{\varepsilon-\varepsilon_F}{kT}}} \right) \frac{1}{\sqrt{\varepsilon-\varepsilon_{m,n}}} d\varepsilon$$

If $\varepsilon - \varepsilon_F >> kT$

$$\frac{1}{1+e^{\frac{\varepsilon-\varepsilon_F}{kT}}} \rightarrow e^{-\frac{\varepsilon-\varepsilon_F}{kT}}$$

leading to

$$\begin{aligned} n_C &= \frac{1}{\pi}\sqrt{\frac{2m_e}{\hbar^2}} \int_{\varepsilon_{m,n}}^{\infty} e^{-\frac{\varepsilon-\varepsilon_F}{kT}} \frac{1}{\sqrt{\varepsilon-\varepsilon_{m,n}}} d\varepsilon \\ &= \frac{1}{\pi}\sqrt{\frac{2m_e}{\hbar^2}} \int_{\varepsilon_{m,n}}^{\infty} e^{-\frac{\varepsilon-\varepsilon_{m,n}+\varepsilon_{m,n}-\varepsilon_F}{kT}} \frac{1}{\sqrt{\varepsilon-\varepsilon_{m,n}}} d\varepsilon \\ &= \frac{1}{\pi}\sqrt{\frac{2m_e}{\hbar^2}} \int_{\varepsilon_{m,n}}^{\infty} e^{-\frac{\varepsilon-\varepsilon_{m,n}}{kT}} e^{-\frac{\varepsilon_{m,n}-\varepsilon_F}{kT}} \frac{1}{\sqrt{\varepsilon-\varepsilon_{m,n}}} d\varepsilon \\ &= \frac{1}{\pi}\sqrt{\frac{2m_e}{\hbar^2}} e^{-\frac{\varepsilon_{m,n}-\varepsilon_F}{kT}} \int_{\varepsilon_{m,n}}^{\infty} e^{-\frac{\varepsilon-\varepsilon_{m,n}}{kT}} \frac{1}{\sqrt{\varepsilon-\varepsilon_{m,n}}} d\varepsilon \end{aligned}$$

Make a change of variables and let $x = \frac{\varepsilon-\varepsilon_{m,n}}{kT}$ such that $\varepsilon = \varepsilon_{m,n} + kTx$ and $d\varepsilon = kTdx$. Also make corresponding changes to the limits of integration resulting in

$$n_C = \frac{\sqrt{kT}}{\pi}\sqrt{\frac{2m_e}{\hbar^2}} e^{-\frac{\varepsilon_{m,n}-\varepsilon_F}{kT}} \int_0^{\infty} e^{-x} x^{-\frac{1}{2}} dx$$

Recall that the last integral is the Gamma function

$$n_C = \frac{\sqrt{kT}}{\pi}\sqrt{\frac{2m_e}{\hbar^2}}e^{-\frac{\varepsilon_{m,n}-\varepsilon_F}{kT}}\Gamma\left(\frac{1}{2}\right)$$

The final expression for the carrier concentration of a 1D material at the conduction band edge is

$$\boxed{n_C = \frac{1}{\pi}\sqrt{\frac{2m_e kT}{\hbar^2}}e^{-\frac{\varepsilon_{m,n}-\varepsilon_F}{kT}}\Gamma\left(\frac{1}{2}\right)} \tag{7.6}$$

Density of states in the valence band:1D

The way this is calculated is very similar to that for the conduction band. However, a few of the terms change slightly in appearance. As before we need the probability of occupying a given state in the valence band. We also need the density of states calculated in the previous section. The occupation probability is calculated from

$$P_e(\varepsilon) + P_h(\varepsilon) = 1$$
$$P_h(\varepsilon) = 1 - P_e(\varepsilon)$$

Here $P_e(\varepsilon)$ is the Fermi Dirac distribution leading to

$$P_h(\varepsilon) = 1 - \frac{1}{1 + e^{\frac{\varepsilon-\varepsilon_F}{kT}}}$$

The density of states is

$$\rho_{1D}^{'} = \frac{1}{\pi}\sqrt{\frac{2m_h}{\hbar^2}}\sum_{m,n}\frac{1}{\sqrt{\varepsilon_{m,n}-\varepsilon}}\Theta(\varepsilon_{m,n}-\varepsilon)$$

where Θ is the Heavyside function and the band explicitly starts at $\varepsilon_{m,n}$ causing its presence in the square root denominator. Now if we consider only the (m,n)th band, (and for convenience that could be the first one) the expression simplifies to

$$\rho_{1D}^{'} = \frac{1}{\pi}\sqrt{\frac{2m_h}{\hbar^2}}\frac{1}{\sqrt{\varepsilon_{m,n}-\varepsilon}}$$

The number of states at a given energy per unit volume (or concentration at a given energy) is

$$n_h(\varepsilon) = P_h(\varepsilon)\rho^{'}(\varepsilon)d\varepsilon$$

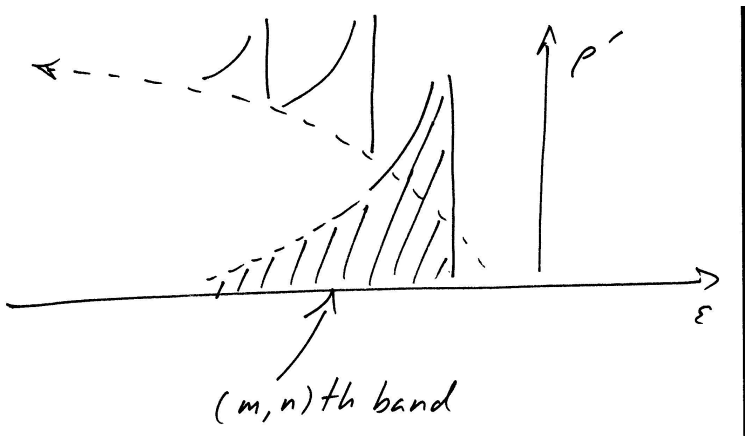

Figure 7.4: Valence band density of states for a 1D material. The (m,n)th band is shaded to distinguish it from the other subbands.

The total concentration in the subband is the integral over all energies

$$\begin{aligned} p_V &= \int_{-\infty}^{\varepsilon_V} P_h(\varepsilon)\rho'(\varepsilon)d\varepsilon \qquad (7.7)\\ &= \int_{-\infty}^{\varepsilon_V} \left(1 - \frac{1}{1+e^{\frac{\varepsilon-\varepsilon_F}{kT}}}\right) \frac{1}{\pi}\sqrt{\frac{2m_h}{\hbar^2}} \frac{1}{\sqrt{\varepsilon_{m,n}-\varepsilon}} d\varepsilon \\ &= \frac{1}{\pi}\sqrt{\frac{2m_h}{\hbar^2}} \int_{-\infty}^{\varepsilon_V} \left(1 - \frac{1}{1+e^{\frac{\varepsilon-\varepsilon_F}{kT}}}\right) \frac{1}{\sqrt{\varepsilon_{m,n}-\varepsilon}} d\varepsilon \end{aligned}$$

Since the band begins at $\varepsilon_{m,n}$ rather than at ε_V as in the bulk, the limits of integration change

$$\int_{-\infty}^{\varepsilon_V} \rightarrow \int_{-\infty}^{\varepsilon_{m,n}} \qquad (7.8)$$

The expression becomes

$$p_V = \frac{1}{\pi}\sqrt{\frac{2m_h}{\hbar^2}} \int_{-\infty}^{\varepsilon_{m,n}} \left(1 - \frac{1}{1+e^{\frac{\varepsilon-\varepsilon_F}{kT}}}\right) \frac{1}{\sqrt{\varepsilon_{m,n}-\varepsilon}} d\varepsilon$$

Furthermore, since $\varepsilon < \varepsilon_F$

$$p_V = \frac{1}{\pi}\sqrt{\frac{2m_h}{\hbar^2}} \int_{-\infty}^{\varepsilon_{m,n}} \left(1 - \frac{1}{1+e^{-\frac{\varepsilon_F-\varepsilon}{kT}}}\right) \frac{1}{\sqrt{\varepsilon_{m,n}-\varepsilon}} d\varepsilon$$

Using the binomial expansion and keeping only the first two terms

$$\begin{aligned}\frac{1}{1+x} &= 1-x+x^2-x^3+\ldots \\ \frac{1}{1+e^{-\frac{\varepsilon_F-\varepsilon}{kT}}} &= 1-e^{-\frac{\varepsilon_F-\varepsilon}{kT}}\end{aligned}$$

the term in parenthesis becomes

$$\left(1-\frac{1}{1+e^{-\frac{\varepsilon_F-\varepsilon}{kT}}}\right)=e^{-\frac{\varepsilon_F-\varepsilon}{kT}}$$

yielding

$$\begin{aligned}p_V &= \frac{1}{\pi}\sqrt{\frac{2m_h}{\hbar^2}}\int_{-\infty}^{\varepsilon_{m,n}} e^{-\frac{\varepsilon_F-\varepsilon}{kT}}\frac{1}{\sqrt{\varepsilon_{m,n}-\varepsilon}}d\varepsilon \\ &= \frac{1}{\pi}\sqrt{\frac{2m_h}{\hbar^2}}\int_{-\infty}^{\varepsilon_{m,n}} e^{-\frac{\varepsilon_F-\varepsilon_{m,n}+\varepsilon_{m,n}-\varepsilon}{kT}}\frac{1}{\sqrt{\varepsilon_{m,n}-\varepsilon}}d\varepsilon \\ &= \frac{1}{\pi}\sqrt{\frac{2m_h}{\hbar^2}}\int_{-\infty}^{\varepsilon_{m,n}} e^{-\frac{\varepsilon_F-\varepsilon_{m,n}}{kT}}e^{-\frac{\varepsilon_{m,n}-\varepsilon}{kT}}\frac{1}{\sqrt{\varepsilon_{m,n}-\varepsilon}}d\varepsilon \\ &= \frac{1}{\pi}\sqrt{\frac{2m_h}{\hbar^2}}e^{-\frac{\varepsilon_F-\varepsilon_{m,n}}{kT}}\int_{-\infty}^{\varepsilon_{m,n}} e^{-\frac{\varepsilon_{m,n}-\varepsilon}{kT}}\frac{1}{\sqrt{\varepsilon_{m,n}-\varepsilon}}d\varepsilon\end{aligned} \tag{7.9}$$

To simplify, make a change of variables. Let $x=\frac{\varepsilon_{m,n}-\varepsilon}{kT}$ or $\varepsilon=\varepsilon_{m,n}-kTx$ and $d\varepsilon=-kTdx$. Note also the corresponding changes in the limits of integration.

$$\begin{aligned}p_V &= \frac{1}{\pi}\sqrt{\frac{2m_h}{\hbar^2}}e^{-\frac{\varepsilon_F-\varepsilon_{m,n}}{kT}}\int_{\infty}^{0} e^{-x}\frac{1}{\sqrt{kT}\sqrt{x}}(-kT)dx \\ &= \frac{\sqrt{kT}}{\pi}\sqrt{\frac{2m_h}{\hbar^2}}e^{-\frac{\varepsilon_F-\varepsilon_{m,n}}{kT}}\int_{0}^{\infty} e^{-x}x^{-\frac{1}{2}}dx\end{aligned}$$

The resulting integral is the now familiar Gamma function. This lead to our final expression for the total concentration of holes in the valence band

$$\boxed{p_V=\frac{1}{\pi}\sqrt{\frac{2m_hkT}{\hbar^2}}e^{-\frac{\varepsilon_F-\varepsilon_{m,n}}{kT}}\Gamma\left(\frac{1}{2}\right)} \tag{7.10}$$

Fermi level position:1D

This evaluation goes the same was as for the 2D or 3D material. If we are dealing with intrinsic semiconductors with no additional doping

$$n_C = p_V$$

From what we have just evaluated

$$\frac{1}{\pi}\sqrt{\frac{2m_e kT}{\hbar^2}}\Gamma\left(\frac{1}{2}\right)e^{-\frac{\varepsilon_{m1,n1}-\varepsilon_F}{kT}} = \frac{1}{\pi}\sqrt{\frac{2m_h kT}{\hbar^2}}\Gamma\left(\frac{1}{2}\right)e^{-\frac{\varepsilon_F-\varepsilon_{m2,n2}}{kT}}$$

Here note that $\varepsilon_{m1,n1}$ and $\varepsilon_{m2,n2}$ are used to refer to the energies where the conduction and valence bands begin repsectively. This expression reduces as follows

$$\begin{aligned}
\sqrt{m_e}e^{-\frac{\varepsilon_{m1,n1}-\varepsilon_F}{kT}} &= \sqrt{m_h}e^{-\frac{\varepsilon_F-\varepsilon_{m2,n2}}{kT}} \\
e^{-\frac{(-\varepsilon_{m1,n1}+\varepsilon_F+\varepsilon_F-\varepsilon_{m2,n2})}{kT}} &= \sqrt{\frac{m_h}{m_e}} \\
e^{-\frac{\varepsilon_{m1,n1}+\varepsilon_{m2,n2}}{kT}}e^{\frac{2\varepsilon_F}{kT}} &= \sqrt{\frac{m_h}{m_e}} \\
e^{\frac{2\varepsilon_F}{kT}} &= \sqrt{\frac{m_h}{m_e}}e^{\frac{\varepsilon_{m1,n1}+\varepsilon_{m2,n2}}{kT}} \\
\ln\left(e^{\frac{2\varepsilon_F}{kT}}\right) &= \ln\left(\frac{m_h}{m_e}\right)^{\frac{1}{2}} + \ln\left(e^{\frac{\varepsilon_{m1,n1}+\varepsilon_{m2,n2}}{kT}}\right) \\
\frac{2\varepsilon_F}{kT} &= \ln\left(\frac{m_h}{m_e}\right)^{\frac{1}{2}} + \frac{\varepsilon_{m1,n1}+\varepsilon_{m2,n2}}{kT} \\
2\varepsilon_F &= \frac{kT}{2}\ln\left(\frac{m_h}{m_e}\right) + \varepsilon_{m1,n1} + \varepsilon_{m2,n2}
\end{aligned}$$

This leads to our final expression

$$\boxed{\varepsilon_F = \frac{\varepsilon_{m1,n1}+\varepsilon_{m2,n2}}{2} + \frac{kT}{4}\ln\left(\frac{m_h}{m_e}\right)} \tag{7.11}$$

Since $m_h > m_e$ the second term is positive and as a consequence the Fermi energy has a slight temperature dependence. However, as before, to a first approximation, it can be taken as the midpoint between the conduction band and valence band energies (the zero temperature limit).

Chapter 8

Joint density of states

In the previous sections we have calculated the "density of states" in both the conduction band and valence band separately. Interband transitions occur between both bands giving rise to optical transitions of the semiconductor. As a consequence it is instructive to calculate the "joint" density of states which is proportional to the absorption coefficient of the material.

3D bulk

We derive the density of states again as done previously. Consider a spherical volume of

$$V_k = \frac{4}{3}\pi k^3$$

The volume of a given mode was, recall $k_x k_y k_z$ where

$$\begin{aligned} k_x &= \frac{2\pi}{L_x} \\ k_y &= \frac{2\pi}{L_y} \\ k_z &= \frac{2\pi}{L_z} \end{aligned}$$

The number of modes or states in the given sphere is then

$$N = \frac{V_k}{k_x k_y k_z} = \frac{\frac{4}{3}\pi k^3}{8\pi^3} L_x L_y L_z$$

For an electron, multiply this by 2 to account for spin

$$\begin{aligned} N^{'} &= 2N = 2\frac{\frac{4}{3}\pi k^3}{8\pi^3}L_xL_yL_z \\ &= \frac{k^3}{3\pi^2}L_xL_yL_z \text{ total number of states in sphere} \end{aligned}$$

Consider as before, the density

$$\rho = \frac{N^{'}}{L_xL_yL_z} = \frac{k^3}{3\pi^2} \text{ number of states/unit volume}$$

Now consider the energy density

$$\rho^{'} = \frac{d\rho}{d\varepsilon} \text{ alternatively } \frac{d\rho}{dk}$$

Note that previously we solved for $\frac{d\rho}{d\varepsilon}$. This time however, let's solve for $\frac{d\rho}{dk}$.

$$\begin{aligned} \frac{d\rho}{d\varepsilon} &= \frac{1}{2\pi^2}\left(\frac{2m}{\hbar^2}\right)^{\frac{3}{2}}\sqrt{\varepsilon} \text{ (previously)} \\ \frac{d\rho}{dk} &= \frac{k^2}{\pi^2} \text{ (this time)} \end{aligned}$$

Starting with the energy density

$$\rho_2^{'} = \frac{d\rho}{dk} = \frac{k^2}{\pi^2} \tag{8.1}$$

divide by 2 to go back to only 1 spin orientation since in an optical transition spin flips are generally forbidden.

$$\rho_1^{'} = \frac{\rho_2^{'}}{2} = \frac{k^2}{2\pi^2} \tag{8.2}$$

This expression applies to either conduction band or valence band. Applying the following equivalence

$$\rho_j(\varepsilon)d\varepsilon = \rho_1^{'}(k)dk \tag{8.3}$$

we obtain

$$\begin{aligned} \rho_j(\varepsilon) &= \rho_2^{'}(k)\frac{dk}{d\varepsilon} \\ &= \frac{k^2}{2\pi^2}\frac{dk}{d\varepsilon} \end{aligned} \tag{8.4}$$

where ρ_j is the desired joint density of states. Now from the conservation of momentum, transitions in k are vertical such that the intitial k value in the valence band is the same k value as in the conduction band ($k_a = k_b = k$, where k_a is the k value in the valence band and k_b is the value in the conduction band).

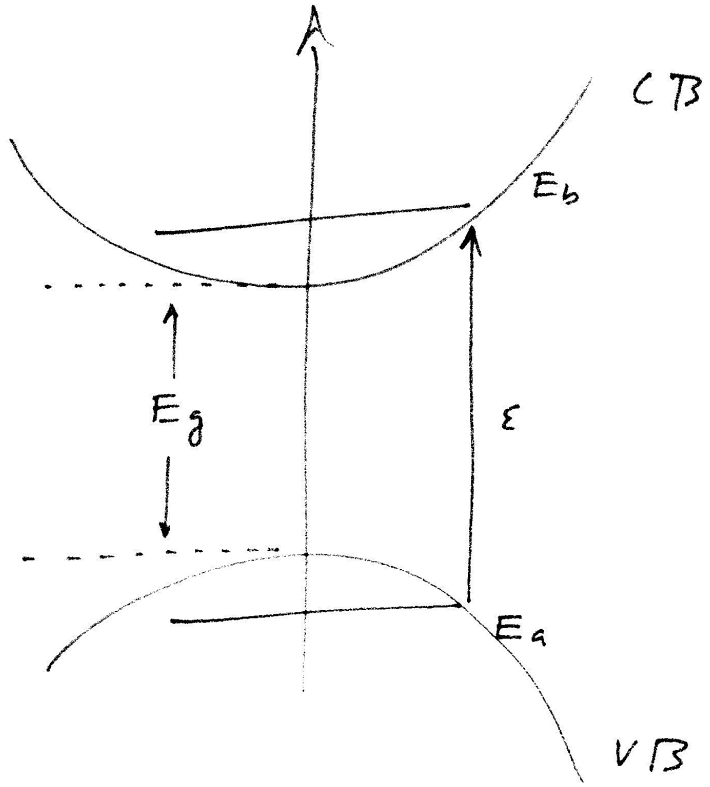

Figure 8.1: Cartoon showing momentum conserving vertical transition between the valence band and conduction band in k space

The energy of the initial state in the valence band is

$$\varepsilon_a = \varepsilon_v - \frac{\hbar^2 k_a}{2m_h}$$

Likewise the energy of the final state in the conduction band is

$$\varepsilon_b = \varepsilon_c + \frac{\hbar^2 k_b^2}{2m_e}$$

The energy of the transition is

$$\begin{aligned}\varepsilon &= \varepsilon_b - \varepsilon_a \\ &= \left(\varepsilon_c + \frac{\hbar^2 k^2}{2m_e}\right) - \left(\varepsilon_v - \frac{\hbar^2 k^2}{2m_h}\right) \\ &= (\varepsilon_c - \varepsilon_v) + \frac{\hbar^2 k^2}{2m_e} + \frac{\hbar^2 k^2}{2m_h} \\ &= \varepsilon_g + \frac{\hbar^2 k^2}{2}\left(\frac{1}{m_e} + \frac{1}{m_h}\right) \end{aligned} \tag{8.5}$$

where $\varepsilon_g = \varepsilon_c - \varepsilon_v$. Now from above

$$\frac{d\varepsilon}{dk} = \hbar^2 k \frac{m_e + m_e}{m_e m_h}$$

leading to the desired expression

$$\frac{dk}{d\varepsilon} = \frac{1}{\hbar^2 k}\left(\frac{m_e m_h}{m_e + m_h}\right) \tag{8.6}$$

Since $\rho_j(\varepsilon) = \frac{k^2}{2\pi^2}\left(\frac{dk}{d\varepsilon}\right)$

$$\begin{aligned}\rho_j(\varepsilon) &= \frac{k^2}{2\pi^2}\left(\frac{1}{\hbar^2 k}\right)\left(\frac{m_e m_h}{m_e + m_h}\right) = \frac{k}{2\pi^2\hbar^2}\left(\frac{m_e m_h}{m_e + m_h}\right) \\ &= \frac{k\mu}{2\pi^2\hbar^2} \end{aligned} \tag{8.7}$$

where for notational simplicity we have used the reduced mass $\mu = \frac{m_e m_h}{m_e + m_h}$
Now to continue towards our final expression, explicitly describe what k is

$$\begin{aligned}\varepsilon &= \varepsilon_g + \frac{\hbar^2 k^2}{2\mu} \\ &\downarrow \\ k^2 &= \frac{2\mu(\varepsilon - \varepsilon_g)}{\hbar^2}\end{aligned}$$

or

$$k = \frac{\sqrt{2\mu(\varepsilon - \varepsilon_g)}}{\hbar} \tag{8.8}$$

Replacing this into our main expression for ρ_j gives

$$\begin{aligned}\rho_j(\varepsilon) &= \frac{\mu}{2\pi^2\hbar^2}k \\ &= \left(\frac{\mu}{2\pi^2\hbar^2}\right)\sqrt{\frac{2\mu(\varepsilon - \varepsilon_g)}{\hbar^2}}\end{aligned}$$

which after some simplification gives

$$\boxed{\rho_j(\varepsilon) = \frac{1}{4\pi^2}\left(\frac{2\mu}{\hbar^2}\right)^{\frac{3}{2}}\sqrt{\varepsilon - \varepsilon_g}} \tag{8.9}$$

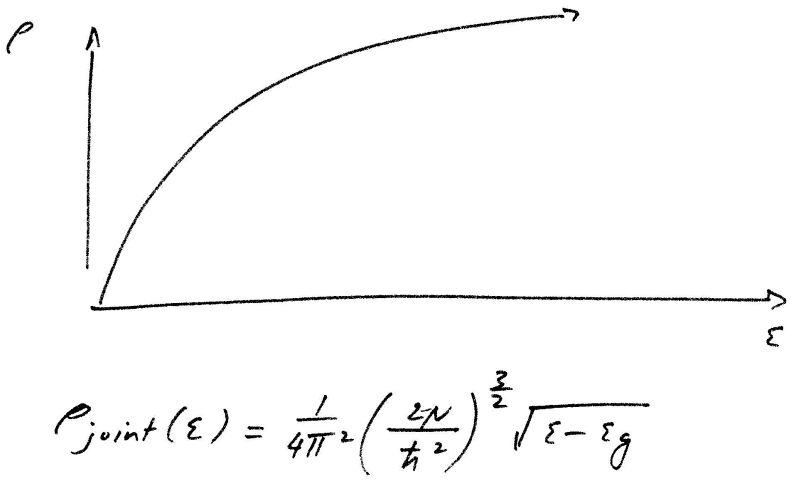

Figure 8.2: Joint density of states for a 3D material (bulk)

2D well

As we did before, consider an area in k-space of

$$A_k = 4\pi k^2$$

where the area occupied by a given mode or state is $k_y k_z$ (we implicitly assume that k_x represents the confined direction)

$$k_y = \frac{2\pi}{L_y}$$
$$k_z = \frac{2\pi}{L_z}$$

Together, the number of modes in the area is

$$N = \frac{A_k}{k_y k_z} = \frac{4\pi k^2}{4\pi^2} L_y L_z = \frac{k^2}{\pi} L_y L_z$$

Multiply by 2 to account for spin

$$N^{'} = 2N = \frac{2k^2}{\pi} L_y L_z$$

Now consider the density

$$\rho = \frac{N^{'}}{L_y L_z} = \frac{2k^2}{\pi} \tag{8.10}$$

with the energy density given by

$$\rho^{'} = \frac{d\rho}{d\varepsilon} \text{ or alternatively } \frac{d\rho}{dk}$$

Note that previously we solved for $\frac{d\rho}{d\varepsilon}$. This time, however, let's consider $\frac{d\rho}{dk}$.

$$\begin{aligned} \frac{d\rho}{d\varepsilon} &= \frac{m}{\pi\hbar^2} \text{ (previously)} \\ \frac{d\rho}{dk} &= \frac{4k}{\pi} \text{ (this time)} \end{aligned}$$

Starting with the energy density

$$\rho_2^{'} = \frac{d\rho}{dk} = \frac{4k}{\pi}$$

divide by 2 to get rid of the spin since formally speaking, spin flip optical transitions are forbidden.

$$\rho_1^{'} = \frac{\rho_2^{'}}{2} = \frac{2k}{\pi} \tag{8.11}$$

Now applying the following equivalence

$$\rho_j(\varepsilon) d\varepsilon = \rho_2^{'}(k) dk \tag{8.12}$$

one obtains

$$\begin{aligned} \rho_j(\varepsilon) &= \rho_1^{'}(k) \frac{dk}{d\varepsilon} \\ &= \frac{2k}{\pi} \frac{dk}{d\varepsilon} \end{aligned} \tag{8.13}$$

where ρ_j is the desired joint density of states. As before in the 3D case, the conservation of momentum means that transitions in k-space are "vertical".

That is, the initial k value in the valence band is the same as the final k value in the conduction band ($k_a = k_b = k$) where $k_a(k_b)$ is the valence (conduction) band k values.

The energy of the initial state in the valence band is

$$\varepsilon_a = \varepsilon_{n2} - \frac{\hbar^2 k^2}{2m_h}$$

Likewise the energy of the final state in the conduction band is

$$\varepsilon_b = \varepsilon_{n1} + \frac{\hbar^2 k^2}{2m_e}$$

The transition energy is

$$\begin{aligned} \varepsilon &= \varepsilon_b - \varepsilon_a \\ &= \varepsilon_{n1} - \varepsilon_{n2} + \frac{\hbar^2 k^2}{2}\left(\frac{1}{m_e} + \frac{1}{m_h}\right) \\ &= \varepsilon_g + \frac{\hbar^2 k^2}{2\mu} \end{aligned} \tag{8.14}$$

where ε_g (band gap) $= \varepsilon_{n1} - \varepsilon_{n2}$ and μ is the reduced mass $\mu = \frac{m_e m_h}{m_e + m_h}$ This leads to

$$\frac{d\varepsilon}{dk} = \frac{\hbar^2 k}{\mu}$$

or

$$\frac{dk}{d\varepsilon} = \frac{\mu}{\hbar^2 k} \tag{8.15}$$

such that when replaced into our main expression the desired expression for the joint density of states is

$$\boxed{\rho_j(\varepsilon) = \frac{2k}{\pi}\left(\frac{\mu}{\hbar^2 \pi}\right) = \frac{2\mu}{\hbar^2 \pi}} \tag{8.16}$$

1D wire

Consider the length in k-space

$$L_k = 2k$$

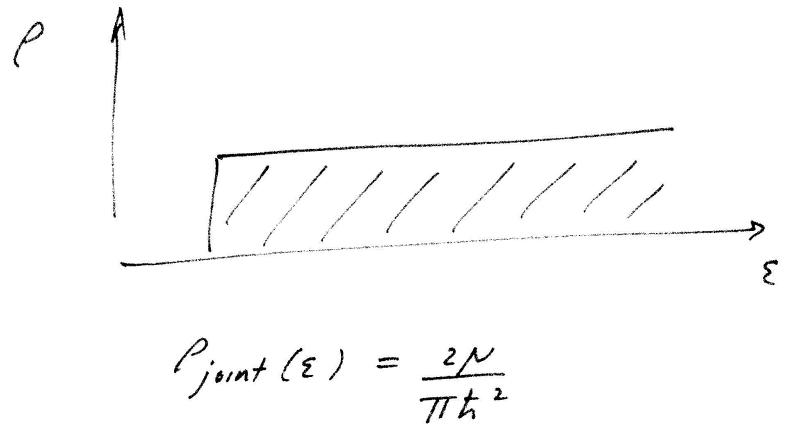

Figure 8.3: Joint density of states for a 2D material (quantum well)

The length occupied by a given mode or state is k_x where

$$k_x = \frac{2\pi}{L_x}$$

The number of states in the given length is

$$N = \frac{L_k}{k_x} = \frac{2k}{2\pi} L_x = \frac{kL_x}{\pi}$$

Multiply this by 2 to account for spin

$$N^{'} = 2\frac{kL_x}{\pi} \text{ total number of states}$$

Consider the density

$$\rho = \frac{N^{'}}{L_x} = \frac{2k}{\pi} \text{ number of states per unit length}$$

Then the energy density is

$$\rho^{'} = \frac{d\rho}{d\varepsilon} \text{ or alternatively } \frac{d\rho}{dk}$$

Previously we solved for $\frac{d\rho}{d\varepsilon}$

$$\begin{aligned} \frac{d\rho}{d\varepsilon} &= \frac{1}{\pi}\sqrt{\frac{2m}{\hbar^2}}\frac{1}{\sqrt{\varepsilon}} \text{ (previously)} \\ \frac{d\rho}{dk} &= \frac{2}{\pi} \text{ (this time)} \end{aligned}$$

Starting with the energy density

$$\rho_2^{'} = \frac{d\rho}{dk} = \frac{2}{\pi} \tag{8.17}$$

divide by 2 to consider only one spin orientation since spin flip transitions are generally forbidden.

$$\rho_1^{'} = \frac{\rho_2^{'}}{2} = \frac{1}{\pi}$$

Now apply the following equivalence

$$\rho_j(\varepsilon)d\varepsilon = \rho_1^{'}(k)dk$$

leading to

$$\begin{aligned} \rho_j(\varepsilon) &= \rho_1^{'}(k)\frac{dk}{d\varepsilon} \\ &= \frac{1}{\pi}\frac{dk}{d\varepsilon} \end{aligned} \tag{8.18}$$

where $\rho_j(\varepsilon)$ is the desired joint density of states. As in the other two cases, 3D and 2D, the conservation of momentum means that transitions in k-space are vertical so that $k_a = k_b = k$. Here k_a is the k value in the valence band and k_b is the k value in the conduction band.

The energy of the initial state in the valence band is

$$\varepsilon_a = \varepsilon_{m2,n2} - \frac{\hbar^2 k^2}{2m_h}$$

Likewise the energy of the final state in the conduction band is

$$\varepsilon_a = \varepsilon_{m1,n1} + \frac{\hbar^2 k^2}{2m_e}$$

The transition energy is

$$\begin{aligned} \varepsilon &= \varepsilon_b - \varepsilon_a \\ &= \varepsilon_{m1,n1} - \varepsilon_{m2,n2} + \frac{\hbar^2 k^2}{2}\left(\frac{1}{m_e} + \frac{1}{m_h}\right) \\ &= \varepsilon_g + \frac{\hbar^2 k^2}{2\mu} \end{aligned} \tag{8.19}$$

where $\varepsilon_g = \varepsilon_{m1,n1} - \varepsilon_{m2,n2}$ and the reduced mass $\mu = \frac{m_e m_h}{m_e + m_h}$. This leads to

$$\frac{d\varepsilon}{dk} = \frac{\hbar^2 k}{\mu}$$

or

$$\frac{dk}{d\varepsilon} = \frac{\mu}{\hbar^2 k} \tag{8.20}$$

Since $\rho_j(\varepsilon) = \frac{1}{\pi}\frac{dk}{d\varepsilon}$ the joint density becomes

$$\rho_j(\varepsilon) = \frac{\mu}{\pi\hbar^2}\frac{1}{k}$$

Now to continue towards our final expression we express k fully. Since $\varepsilon = \varepsilon_g + \frac{\hbar^2 k^2}{2\mu}$ we get

$$\begin{aligned} k^2 &= \frac{2\mu(\varepsilon - \varepsilon_g)}{\hbar^2} \\ &\downarrow \\ k &= \sqrt{\frac{2\mu}{\hbar^2}(\varepsilon - \varepsilon_g)} \\ &\downarrow \\ \frac{1}{k} &= \frac{\hbar}{\sqrt{2\mu}\sqrt{\varepsilon - \varepsilon_g}} \end{aligned}$$

This leads to the final expression for the joint density of states

$$\boxed{\rho_j(\varepsilon) = \frac{1}{\pi}\sqrt{\frac{\mu}{2\hbar^2}}\frac{1}{\sqrt{\varepsilon - \varepsilon_g}}} \tag{8.21}$$

Summary

Now that we have the explicit joint density of states for 3D, 2D and 1D materials we can summarize their implications for the absorption spectra of these materials. It can be shown that the absorption coefficient and joint density of states are proportional to each other. The calculation to achieve this involves Fermi's golden rule and will not be discussed at this point. To summarize

- 3D: $\rho_j \propto \sqrt{\varepsilon - \varepsilon_g}$

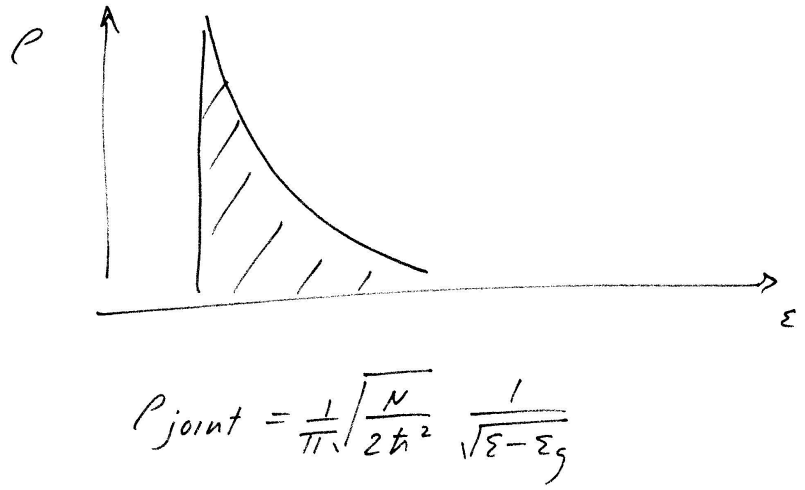

Figure 8.4: Joint density of states for a 1D material (quantum wire)

- 2D: $\rho_j \propto$ constant depending on the reduced mass
- 1D: $\rho_j \propto \frac{1}{\sqrt{\varepsilon - \varepsilon_g}}$
- 0D: $\rho_j \propto \delta(\varepsilon - \varepsilon_n)$

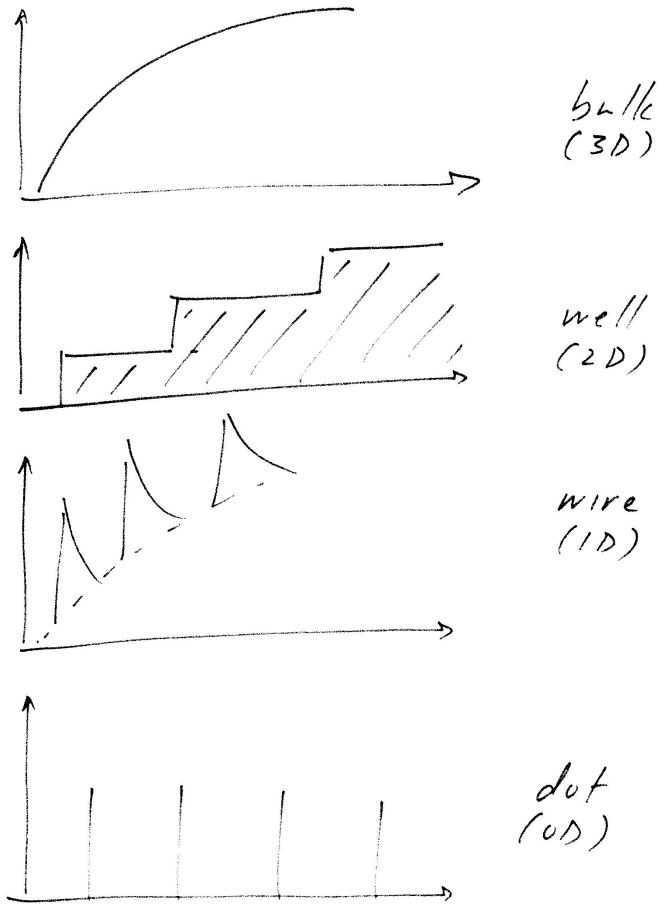

Figure 8.5: Summary of the joint density of states for 3D, 2D, 1D, and 0D materials

Chapter 9

Emission

In the last section, the absorption coefficient of materials with different dimensionality were shown to be proportional to the calculated joint density of states. In turn, one could predict that the absorption spectrum of these materials would look like. Here we work out the background behind spontaneous emission, a complementary process to absorption.

Preliminaries: Einstein A and B coefficients

Picture a two level system like that shown in the figure.

Here

- N_1 =population in the ground state or alternatively probability of being in the ground state
- N_2 =population in the excited state, alternatively probability of being in the excited state
- g_1 =degeneracy of ground state
- g_2 =degeneracy of excited state
- ρ =the energy density containing thermal and/or external contributions

Three processes were considered

1. absorption with total rate: $B_{12}\rho N_1$
2. stimulated emission with total rate: $B_{21}\rho N_2$

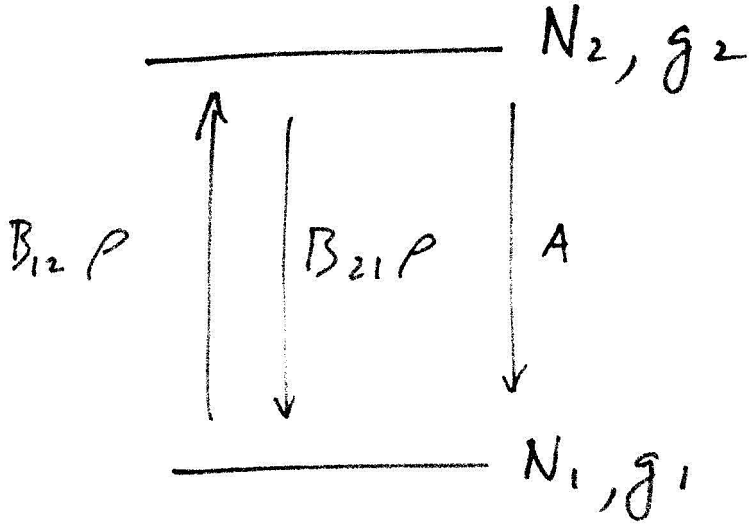

Figure 9.1: Two level system showing various transitions considered for Einstein A and B coefficients

3. spontaneous emission with total rate: AN_2

Putting everything together one obtains the following rate equations for populating either the ground or excited states

$$\begin{aligned}\frac{dN_1}{dt} &= -B_{12}\rho N_1 + B_{21}\rho N_2 + AN_2 \\ \frac{dN_2}{dt} &= B_{12}\rho N_1 - B_{21}\rho N_2 - AN_2\end{aligned}$$

In equilibrium, the upward and downward rates are equivalent ($\frac{dN_1}{dt} = \frac{dN_2}{dt} = 0$). So using either of the above expressions

$$B_{12}\rho N_1 - B_{21}\rho N_2 - AN_2 = 0$$

or

$$B_{12}\rho N_1 \text{ (upward)} = B_{21}\rho N_2 + AN_2 \text{ (downward)}$$

Solving for ρ gives

$$\begin{aligned}\rho &= \frac{AN_2}{B_{12}N_1 - B_{21}N_2} \\ &= \frac{A}{B_{12}\frac{N_1}{N_2} - B_{21}}\end{aligned}$$

where N_1 and N_2 are Boltzman distributed

$$\begin{aligned}N_1 &= \frac{1}{N}\sum_{i=1}^{g_1} e^{-\frac{\varepsilon_1-\varepsilon_F}{kT}} = \frac{g_1}{N}e^{-\frac{\varepsilon_1-\varepsilon_F}{kT}} \\ N_2 &= \frac{1}{N}\sum_{i=1}^{g_2} e^{-\frac{\varepsilon_2-\varepsilon_F}{kT}} = \frac{g_2}{N}e^{-\frac{\varepsilon_2-\varepsilon_F}{kT}}\end{aligned}$$

and N is a normalization constant. This leads to

$$\frac{N_1}{N_2} = \frac{g_1}{g_2}e^{-\frac{\varepsilon_1-\varepsilon_2}{kT}} = \frac{g_1}{g_2}e^{\frac{h\nu}{kT}}$$

where $h\nu = \varepsilon_2 - \varepsilon_1$ is the energy of the photon or transition. Replace this into the above expression for ρ giving

$$\rho(\nu) = \frac{A}{B_{12}\frac{g_1}{g_2}e^{\frac{h\nu}{kT}} - B_{21}} \tag{9.1}$$

This is the expression for the energy density derived by Einstein. Next he realized that this expression had to be equivalent to the Planck distribution for blackbody radiation. Expressed in terms of wavelength, the Planck distribution is (standard textbook expression)

$$\boxed{\rho_p(\lambda) = \frac{8\pi hc}{\lambda^5}\left(\frac{1}{e^{\frac{hc}{\lambda kT}}-1}\right)} \tag{9.2}$$

This expression is interesting from a historical point of view because when the derivative of this expression is set to zero one obtains the Wein displacement law for blackbody radiation. Likewise the integral of this expression gives what's called the Stefan Boltzman law for blackbody radiation. In a sense, knowing or unknowingly, Planck basically explained everything in one shot. Apparently he nearly suffered a nervous breakdown doing it.

Now back to the main discussion. Expressed in terms of ν rather than λ, the Planck energy density is (derived in the next section)

$$\boxed{\rho_p(\nu) = \frac{8\pi h\nu^3}{c^3}\left(\frac{1}{e^{\frac{h\nu}{kT}}-1}\right)} \tag{9.3}$$

Note that in general, in the absence of vacuum, the index of refraction must be taken into account when considering the speed of light.

Interlude: Derivation of Planck energy density

Just like in the density of states section, imagine a sphere of radius k with volume

$$V_k = \frac{4}{3}\pi k^3$$

where the volume of a given mode is $k_x k_y k_z$ and

$$\begin{aligned} k_x &= \frac{2\pi}{L_x} \\ k_y &= \frac{2\pi}{L_y} \\ k_z &= \frac{2\pi}{L_z} \end{aligned}$$

The number of modes in the given sphere is then (look familiar?)

$$N = \frac{V_k}{k_x k_y k_z} = \frac{\frac{4}{3}\pi k^3}{8\pi^3} L_x L_y L_z$$

For a photon now, multiply this by 2 to account for two possible polarizations

$$\begin{aligned} N^{'} &= 2N = 2\frac{\frac{4}{3}\pi k^3}{8\pi^3}L_xL_yL_z \\ &= \frac{k^3}{3\pi^2}L_xL_yL_z \text{ total number of modes} \end{aligned}$$

Consider the density

$$\rho = \frac{N^{'}}{L_xL_yL_z} = \frac{k^3}{3\pi^2} = \frac{k^3}{3\pi^2} \text{ number of modes/unit volume} \tag{9.4}$$

Here is where we diverge a little from the past. To get the frequency density, first let $k = \frac{2\pi}{\lambda}$ where $\lambda = \frac{c}{\nu}$. Therefore

$$k = \frac{2\pi\nu}{c}$$

alternatively $2\pi\nu\frac{n}{c}$ if the index of refraction is different from 1. Then ρ becomes

$$\rho = \frac{k^3}{3\pi^2} = \frac{8\pi}{3}\frac{\nu^3}{c^3}$$

Now like before, to get the frequency density (alternatively called the mode density)

$$\rho^{'} = \frac{d\rho}{d\nu} = \frac{8\pi\nu^2}{c^3} \text{ number per unit volume per unit frequency} \tag{9.5}$$

Planck next showed that the average energy per mode is

$$< \varepsilon >= \frac{h\nu}{e^{\frac{h\nu}{kT}} - 1}$$

leading to the Planck distribution

$$\begin{aligned} \rho_p(\nu) &= \rho^{'} < \varepsilon > \\ &= \frac{8\pi\nu^2}{c^3}\left(\frac{h\nu}{e^{\frac{h\nu}{kT}} - 1}\right) \\ &= \frac{8\pi h\nu^3}{c^3}\left(\frac{1}{e^{\frac{h\nu}{kT}} - 1}\right) \end{aligned}$$

Now back to where we left off. Equate the Einstein and Planck relations

$$\frac{A}{B_{12}\frac{g_1}{g_2}e^{\frac{h\nu}{kT}} - B_{21}} = \frac{8\pi h\nu^3}{c^3}\left(\frac{1}{e^{\frac{h\nu}{kT}} - 1}\right)$$

where note again that if the index is not 1 then replace c with $\frac{c}{n}$. Upon examination of the above equation, to achieve equivalence

$$B_{12}\frac{g_1}{g_2} = B_{21} \tag{9.6}$$

More usually you will see $g_1 = g_2$ such that the expression reduces to $B_{12} = B_{21}$. Furthermore

$$\frac{A}{B_{21}} = \frac{8\pi h\nu^3}{c^3}$$

yielding the standard textbook expression

$$\begin{aligned} A &= \frac{8\pi h\nu^3}{c^3}B_{21} \\ &= \frac{8\pi h\nu^3}{c^3}\frac{g_1}{g_2}B_{12} \end{aligned} \tag{9.7}$$

Again, note that if $g_1 = g_2$ you will commonly see written

$$\boxed{A = \tfrac{8\pi h\nu^3}{c^3}B_{12}} \tag{9.8}$$

Also if the index is not 1 (not vacuum) then replace c with $\frac{c}{n}$ in the above expressions. The above final expression are what are referred to as the relationship between Einstein A and B coefficients.

Word of caution

The Planck distribution is often written a number of ways. Different texts will have what on the surface appear to be completely different expressions. These difference actually arises because of differing definitions for the "density" being used by the various authors. Previously we saw two expression for the Planck distribution. The first, in terms of wavelength, has units of: number per unit volume per unit wavelength. The second, in terms of frequency, has units of: number per unit volume per unit frequency. Alternatively sometimes what people mean is the same expression but in units

of: number per unit volume per unit energy. This is potentially very confusing. One should look very carefully at what is meant by "density". Here we derive this third form of the Planck distribution with units: number per unit volume per unit energy.

Starting with

$$\rho = \frac{8\pi\nu^3}{3}\left(\frac{n}{c}\right)^3 \tag{9.9}$$

where this expression comes from the previous section where we derived the Planck distribution and where also the index of the medium has been explicitly considered (recall, replace c with $\frac{c}{n}$). Rearrange the expression to

$$\rho = \frac{8\pi n^3\nu^3}{3c^3}\left(\frac{h^3}{h^3}\right) = \frac{8\pi n^3(h\nu)^3}{3c^3h^3} = \frac{8\pi n^3\varepsilon^3}{3c^3h^3}$$

Now as before take the derivative with respect to energy to get the energy density

$$\begin{aligned}
\rho^{'} = \frac{d\rho}{d\varepsilon} &= \frac{8\pi n^3(3\varepsilon^2)}{3c^3h^3} \\
&= \frac{8\pi n^3\varepsilon^2}{c^3h^3} \\
&= \frac{8\pi n^3(h\nu)^2}{c^3h^3} \\
&= \frac{8\pi n^3\nu^2}{c^3h}
\end{aligned}$$

Some authors will leave it at the second step which is just $\rho^{'} = \frac{8\pi n^3\varepsilon^2}{c^3h^3}$. We will go with

$$\rho^{'} = \frac{8\pi n^3\nu^2}{c^3h} \tag{9.10}$$

Now earlier we had the Planck derived average energy to be

$$< \varepsilon >= \frac{h\nu}{e^{\frac{h\nu}{kT}} - 1}$$

This leads to an expression for the average number of photons which is

$$< p >= \frac{< \varepsilon >}{h\nu} = \frac{1}{e^{\frac{h\nu}{kT}} - 1} \tag{9.11}$$

The resulting Planck photon density is

$$\rho_p = \frac{8\pi n^3 \nu^2}{c^3 h} \left(\frac{1}{e^{\frac{h\nu}{kT}} - 1} \right) \text{ number per unit volume per unit energy} \tag{9.12}$$

This then leads to another set of relationships between Einstein A and B coefficients

$$\boxed{B_{12} = B_{21}} \tag{9.13}$$

$$\boxed{A = \frac{8\pi n^3 \nu^2}{c^3 h} B_{12} \text{ or } = \frac{8\pi n^3 \varepsilon^2}{c^3 h^3} B_{12}} \tag{9.14}$$

The only difference between these relations and the previous ones was how the Planck distribution was defined. Number per unit volume per unit energy (as done here) or number per unit volume per unit frequency (as done previously).

Einstein A and B coefficients revisited

In the last section we derived the relationships between the Einstein coefficients for absorption, stimulated emission and spontaneous emission. In this section, let's rederive the expression is a slightly different manner, but in a way that will be useful a little later on.

Let R_{12} be the unit transition rate from the ground state to the excited state (basically the rate constant)

$$\begin{aligned} R_{12} &= P_{abs} \rho d\varepsilon \\ &\equiv B_{12} \rho \end{aligned}$$

where

- ρ is the number of photons per unit volume per unit energy (note the units!)
- $\rho d\varepsilon$ is the number of photons per unit volume
- P_{abs} is the probability for absorption per unit time
- R_{12} is the absorptions per unit volume per unit time

and where $B_{12} = P_{abs} d\varepsilon$

As before set up the rate equations except now consider explicitly the probability of occupied and unoccupied states in the valence and conduction bands. Let

- f_1 =probability of occupied valence band state
- f_2 =probability of occupied conduction band state
- $1 - f_1$ =probability of unoccupied valence band state
- $1 - f_2$ =probability of unoccupied conduction band state

$1 \rightarrow 2$ **transition (absorption) requires**

- valence band state occupied (f_1)
- conduction band state empty ($1 - f_2$)

resulting in the joint probability being $f_1(1 - f_2)$ such that

$$R_{12,abs} = B_{12}\rho f_1(1 - f_2)$$

$2 \rightarrow 1$ **transition (stimulated emission) requires**

- valence band state empty ($1 - f_1$)
- conduction band state occupied (f_2)

resulting in the joint probability being $f_2(1 - f_1)$ such that

$$R_{21,stim} = B_{21}\rho f_2(1 - f_1)$$

$2 \rightarrow 1$ **transition (spontaneous emission) requires**

- valence band state empty ($1 - f_1$)
- conduction band state occupied (f_2)

resulting in the joint probability being $f_2(1 - f_1)$ such that

$$R_{21,spont} = Af_2(1 - f_1)$$

In all three cases f_1 and f_2 are Fermi Dirac distributions

$$\begin{aligned} f_1 &= \frac{1}{e^{\frac{\varepsilon_1 - \varepsilon_F}{kT}} + 1} \\ f_2 &= \frac{1}{e^{\frac{\varepsilon_2 - \varepsilon_F}{kT}} + 1} \end{aligned}$$

At this point, for simplicity, assume that $g_1 = g_2$. At equilibrium the upward and downward rates equal resulting in

$$\begin{aligned} R_{12,abs} &= R_{21,stim} + R_{21,spont} \\ B_{12}\rho f_1(1-f_2) &= B_{21}\rho f_2(1-f_1) + Af_2(1-f_1) \end{aligned}$$

Rearrange this to solve for ρ

$$\rho[B_{12}f_1(1-f_2) - B_{21}f_2(1-f_1)] = Af_2(1-f_1)$$

which gives

$$\begin{aligned} \rho &= \frac{Af_2(1-f_1)}{B_{12}f_1(1-f_2) - B_{21}f_2(1-f_1)} \\ &= \frac{A}{B_{12}\frac{f_1(1-f_2)}{f_2(1-f_1)} - B_{21}} \end{aligned}$$

Now introduce the explicit expression for f_1 and f_2. To simplify

$$\begin{aligned} \frac{f_1(1-f_2)}{f_2(1-f_1)} &= \frac{\left(\frac{1}{e^{\frac{\varepsilon_1-\varepsilon_F}{kT}}+1}\right)\left(1-\frac{1}{e^{\frac{\varepsilon_2-\varepsilon_F}{kT}}+1}\right)}{\left(\frac{1}{e^{\frac{\varepsilon_2-\varepsilon_F}{kT}}+1}\right)\left(1-\frac{1}{e^{\frac{\varepsilon_1-\varepsilon_F}{kT}}+1}\right)} \\ &= e^{\frac{\varepsilon_2-\varepsilon_1}{kT}} \\ &= e^{\frac{h\nu}{kT}} \end{aligned}$$

Replace this into the main expression for ρ to get

$$\rho = \frac{A}{B_{12}\frac{f_1(1-f_2)}{f_2(1-f_1)} - B_{21}} = \frac{A}{B_{12}e^{\frac{h\nu}{kT}} - B_{21}}$$

But ρ equals the Planck distribution

$$\rho = \frac{A}{B_{12}e^{\frac{h\nu}{kT}} - B_{21}} = \frac{8\pi n^3\nu^2}{c^3h}\left(\frac{1}{e^{\frac{h\nu}{kT}}-1}\right)$$

meaning that for this to be true

$$B_{12} = B_{21}$$

and

$$A = \frac{8\pi n^3\nu^2}{c^3h}B_{12}$$

which are exactly the same Einstein A and B relations we found before.

Emission spectrum

Here we will calculate the emission spectrum of a 3D material using the Einstein A and B coefficients. Define the (net) unit transition rate from the ground state to the excited state.

$$R_{net} = P_{abs}\rho d\varepsilon \tag{9.15}$$

where as before

- ρ is the number of photons per unit volume per unit energy
- $\rho d\varepsilon$ is the number of photons per unit volume
- P_{abs} is the probability for absorption per unit volume
- R_{net} is the absorptions per unit volume per unit time

Now consider the net rate upwards from 1 to 2 including stimulated emission

$$\begin{aligned} R_{12,abs} &= B_{12}\rho f_1(1-f_2) \text{ (transition rate per unit volume)} \\ R_{21,stim} &= B_{21}\rho f_2(1-f_1) \text{ (transition rate per unit volume)} \end{aligned}$$

such that the net upwards rate is

$$\begin{aligned} R_{net} &= R_{12,abs} - R_{21,stim} \text{ (transition rate per unit volume)} \\ &= B_{12}\rho f_1(1-f_2) - B_{21}\rho f_2(1-f_1) \end{aligned}$$

Since we have already shown that $B_{12} = B_{21}$

$$R_{net} = B_{12}\rho[f_1(1-f_2) - f_2(1-f_1)] \tag{9.16}$$

Equating the two expressions for ρ gives

$$\begin{aligned} P_{abs}\rho d\varepsilon &= B_{12}\rho[f_1(1-f_2) - f_2(1-f_1)] \\ P_{abs}d\varepsilon &= B_{12}[f_1(1-f_2) - f_2(1-f_1)] \end{aligned}$$

Here we relate P_{abs} to the absorption coefficient as follows

$$P_{abs} = \frac{c}{n}\alpha$$

How? If P is the absolute probability for an absorption event and $\frac{dP}{dt} \equiv P_{abs}$

$$\begin{aligned} \frac{dP}{dt} &= \frac{dP}{dz}\left(\frac{dz}{dt}\right) \\ P_{abs} &= \alpha\left(\frac{c}{n}\right) \end{aligned}$$

Insert this P_{abs} expression into the above equivalence to get

$$\alpha\left(\frac{d}{n}\right)d\varepsilon = B_{12}[f_1(1-f_2) - f_2(1-f_1)]$$

Rearrange this to solve for B_{12}

$$B_{12} = \alpha\left(\frac{c}{n}\right)\frac{d\varepsilon}{[f_1(1-f_2) - f_2(1-f_1)]}$$

Relate B_{12} to A using our derived Einstein A and B coefficients.

$$\begin{aligned} A &= \frac{8\pi n^3\nu^2}{c^3h}B_{12} = \frac{8\pi\nu^2}{h}\left(\frac{n}{c}\right)^3\alpha\left(\frac{c}{n}\right)\frac{d\varepsilon}{[f_1(1-f_2) - f_2(1-f_1)]} \\ &= \frac{8\pi\nu^2}{h}\left(\frac{n}{c}\right)^2\alpha\frac{d\varepsilon}{[f_1(1-f_2) - f_2(1-f_1)]} \end{aligned}$$

Now recall that

$$R_{21,spont} = Af_2(1-f_1)$$

such that

$$\begin{aligned} R_{21,spont} &= \alpha\frac{8\pi\nu^2}{h}\left(\frac{n}{c}\right)^2\frac{f_2(1-f_1)d\varepsilon}{[f_1(1-f_2) - f_2(1-f_1)]} \\ &= \alpha\frac{8\pi\nu^2}{h}\left(\frac{n}{c}\right)^2\frac{d\varepsilon}{\frac{f_1(1-f_2)}{f_2(1-f_1)} - 1} \end{aligned}$$

Now for convenience define

$$r_{spont}(\varepsilon)d\varepsilon = R_{21}$$

where $r_{spont}(\varepsilon)$ is the transition rate per unit volume per unit energy. By inspection

$$r_{spont}(\varepsilon) = \alpha\frac{8\pi\nu^2}{h}\left(\frac{n}{c}\right)^2\frac{1}{\frac{f_1(1-f_2)}{f_2(1-f_1)} - 1}$$

and

$$\begin{aligned} f_1 &= \frac{1}{e^{\frac{\varepsilon_1-\varepsilon_F}{kT}} + 1} \\ f_2 &= \frac{1}{e^{\frac{\varepsilon_2-\varepsilon_F}{kT}} + 1} \end{aligned}$$

We've solved the ratio in the denominator before giving

$$\frac{f_1(1-f_2)}{f_2(1-f_1)} = e^{\frac{h\nu}{kT}}$$

Putting everything together

$$r_{spont}(\varepsilon) = \alpha\left(\frac{8\pi\nu^2}{h}\right)\left(\frac{n}{c}\right)^2\left(\frac{1}{e^{\frac{h\nu}{kT}}+1}\right)$$

If $h\nu > kT$ the term in parenthesis $\sim e^{-\frac{h\nu}{kT}}$ and the main expression becomes

$$r_{spont}(\varepsilon) = \alpha\left(\frac{8\pi\nu^2}{h}\right)\left(\frac{n}{c}\right)^2 e^{-\frac{h\nu}{kT}} \tag{9.17}$$

We can stop here or continue to express this as an intensity.

$$I_{3D}(\varepsilon) = \varepsilon\frac{r_{spont}(\varepsilon)}{\alpha_{exc}(\varepsilon)}$$

where $\alpha_{exc}(\varepsilon)$ is the absorption coefficient at the particular excitation position. This value is a constant.

$$\begin{aligned} I_{3D}(\varepsilon) &= (h\nu)\frac{\alpha\left(\frac{8\pi\nu^2}{h}\right)\left(\frac{n}{c}\right)^2 e^{-\frac{h\nu}{kT}}}{\alpha_{exc}(\varepsilon)} \\ &= \frac{\alpha}{\alpha_{exc}}(8\pi\nu^3)\left(\frac{n}{c}\right)^2 e^{-\frac{h\nu}{kT}} \end{aligned} \tag{9.18}$$

Finally, for a 3D material the absorption coefficient is proportional to the joint density of states

$$\alpha \propto A\sqrt{\varepsilon-\varepsilon_g}$$

where A is a constant. This leads to our final expression for the emission spectrum

$$I_{3D} = \frac{A\sqrt{\varepsilon-\varepsilon_g}}{\alpha_{exc}}(8\pi\nu^3)\left(\frac{n}{c}\right)^2 e^{-\frac{h\nu}{kT}} \tag{9.19}$$

$$\boxed{I_{3D} = A'\sqrt{\varepsilon-\varepsilon_g}e^{-\frac{h\nu}{kT}}} \tag{9.20}$$

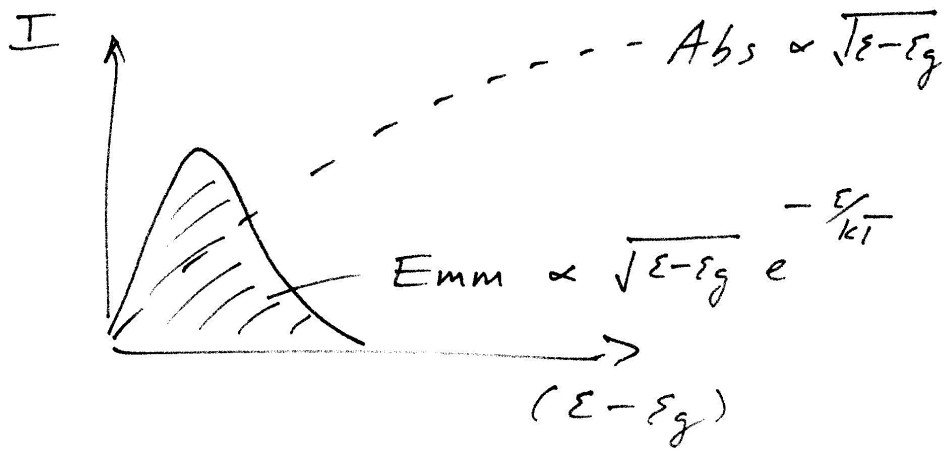

Figure 9.2: Derived emission spectrum for a 3D material using Einstein A and B coefficients

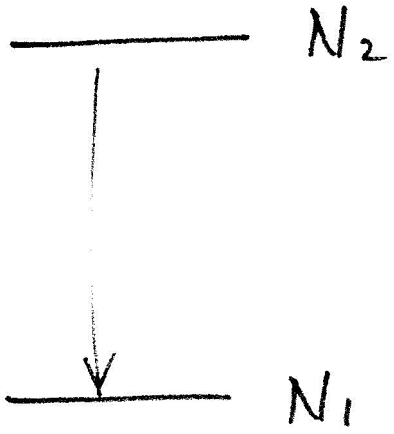

Figure 9.3: Two level system considered in pulsed experiment. Only the (downward) radiative transition is considered.

Quantum yields and lifetimes

Here we discuss some complementary aspects to the emission. Imagine populating the excited state of the system and immediately (i.e. instantaneously) turning off the light. Basically this is a pulsed experiment.

The depopulation of the excited state occurs by spontaneous emission since stimulated emission only occurs in the presence of the excitation. The relevant rate equation is

$$\frac{dN_2}{dt} = -AN_2$$

or if $A = k_{rad}$

$$\begin{aligned} \frac{dN_2}{dt} &= k_{rad}N_2 \\ \frac{dN_2}{N_2} &= -k_{rad}dt \\ \ln N_2 &= -k_{rad}t + \text{ (const)} \\ N_2 &= Ce^{-k_{rad}t} \end{aligned}$$

At $t = 0$ $C = N_2(0)$ resulting in

$$N_2(t) = N_2(0)e^{-k_{rad}t} \tag{9.21}$$

The decay will be exponential and $\tau = \frac{1}{k_{rad}}$ is called the lifetime of the excited state.

In general, however, since we dont live in a perfect world, there are other de-excitation pathways. These include energy transfer or non-radiative decay through defect states. So in general the total decay rate out of the excited state is the sum of all rates

$$k_{tot} = k_{rad} + k_1 + k_2 + k_3 + \ldots$$

giving

$$\begin{aligned} \frac{dN_2}{dt} &= -(k_{rad} + k_1 + k_2 + k_3 + \ldots)N_2 \\ &= -\left(k_{rad} + \sum_i^n k_i\right) N_2 \\ &= -k_{tot}N_2 \end{aligned}$$

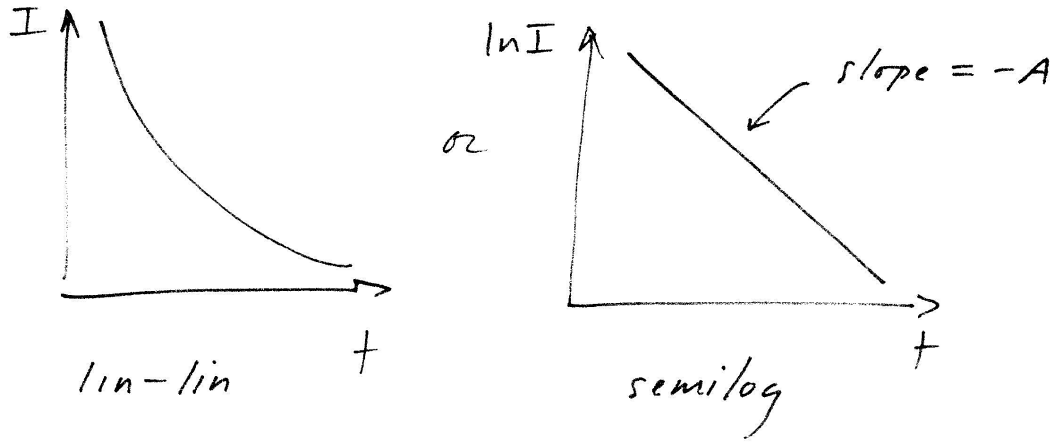

Figure 9.4: Linear and semilogarithmic plots of the excited state decay profile.

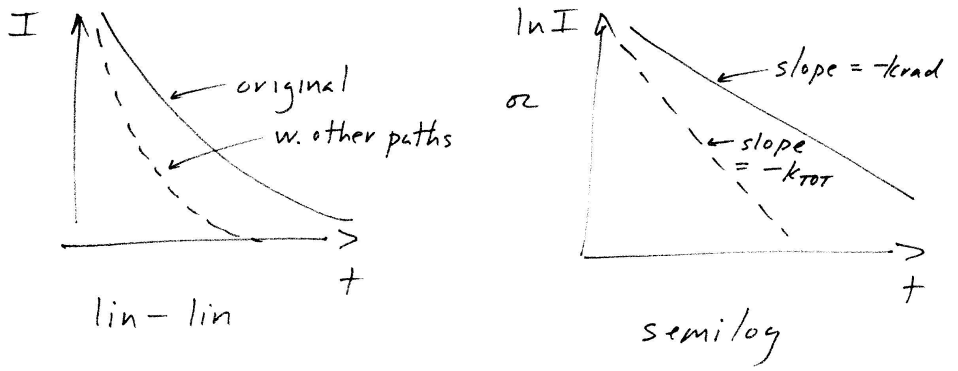

Figure 9.5: Linear and semilogarithmic plots of the excited state decay in the absence and presence of multiple decay pathways.

Only the k_{rad} pathway gives you emission. Therefore, the efficiency of emission is called the quantum yield (QY) and is defined by

$$\boxed{QY = \frac{k_{rad}}{k_{tot}} \text{ or } \frac{\frac{1}{\tau_{rad}}}{\frac{1}{\tau_{tot}}} = \frac{\tau_{tot}}{\tau_{rad}}} \tag{9.22}$$

For most applications, one desires a QY that is as close to unity as possible ($QY = 1$). For example, such applications could involve lasers, light emitting diodes, fluorescent tags and so forth.

Exercises

1. The first part of this chapter described three processes: (stimulated) absorption, stimulated emission, and spontaneous emission. Rationalize why there isn't a fourth process called spontaneous absorption.

2. Spontaneous emission competes with thermally stimulated emission (Planck radiation is the source). Show that at 300 K, thermal stimulation dominates for frequencies well below $5x10^{12}$ Hz whereas spontaneous emission dominates for frequencies well above $5x10^{12}$ Hz. Which mechanism dominates for visible light.

3. Come up with an alternative means of measuring the quantum yield of a system based on its fluorecence decay profile. See Figure 9.5. Assume an exponential decay and consider its pure radiative decay as well as its radiative decay in the presence of other non-radiative recombination pathways.

4. Show mathematically how one extracts the average decay time of an exponential process. Compare this to the 1/e lifetime.

5. Derive a relation between the half life (50% mark) and the lifetime of the state.

6. Explain how one measures the quantum yield of something in real life.

7. Show how the Plank expression reduces to both the Wein displacement law and the Stefan Boltzman law for blackbody radiation. What are the Wein and Stefan Boltzman laws anyway?

Chapter 10

Bands

Kronig Penney Approximation with Rectangular Barriers

An approximation to a crystalline solid is a periodic potential consisting of rectangular barriers. This is called the Kronig-Penny model and has analytical solutions. Although this is a crude approximation to the true potential experienced by the electron, the importance of the model lies in the idea that the periodicity of the potential is the root cause for the emergence of what are called band gaps. There are discontinuities in the energies that an electron can have. This ultimately leads to the distinction between metals, semiconductors and insulators.

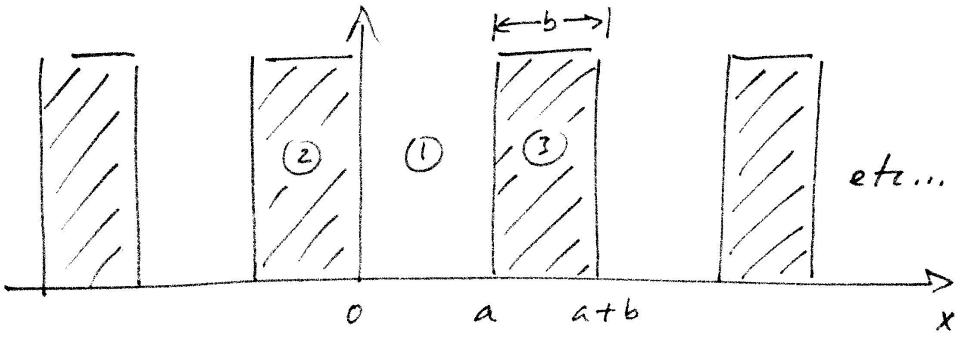

Figure 10.1: Periodic potential of rectangular barriers

Region 1:

$$-\frac{\hbar^2}{2m}\frac{d^2\Psi}{x^2} = \varepsilon\Psi \tag{10.1}$$
$$\frac{d^2\Psi}{dx^2} = -\frac{2m\varepsilon}{\hbar^2}\Psi$$
$$\frac{d^2\Psi}{dx^2} + \frac{2m\varepsilon}{\hbar^2}\Psi = 0$$

Therefore

$$\frac{d^2\Psi}{dx^2} + k^2\Psi = 0 \tag{10.2}$$

where

$$k^2 = \frac{2m\varepsilon}{\hbar^2}$$

Region 2:

$$-\frac{\hbar^2}{2m}\frac{d^2\Psi}{dx^2} + V\Psi = \varepsilon\Psi$$
$$-\frac{\hbar^2}{2m}\frac{d^2\Psi}{dx^2} = (\varepsilon - V)\,\Psi$$
$$\frac{d^2\Psi}{dx^2} = \frac{2m\,(V-\varepsilon)}{\hbar^2}\Psi$$
$$\frac{d^2\Psi}{dx^2} - \frac{2m\,(V-\varepsilon)}{\hbar^2}\Psi = 0$$

Therefore

$$\frac{d^2\Psi}{dx^2} - \phi^2\Psi = 0 \tag{10.3}$$

where

$$\phi^2 = \frac{2m\,(V-\varepsilon)}{\hbar^2}$$

The wavefunctions in regions 1 and 2 are:

$$\Psi_1 = Ae^{ikx} + Be^{-ikx}{}_{\text{region 1}} \tag{10.4}$$
$$\Psi_2 = Ce^{\phi x} + De^{-\phi x}{}_{\text{region 2}} \tag{10.5}$$

Now apply Bloch's theorem where

$$\Psi(x+a) = \Psi(x)e^{ilx}_{\text{for delta function potential with period a}}$$

or alternatively

$$\Psi(x+(a+b)) = \Psi(x)e^{il(a+b)}_{\text{for periodic potential with period a+b}}$$

leading to

Region 3:

$$\begin{aligned} \Psi_3 &= \Psi_2 e^{il(a+b)} && (10.6) \\ \text{or} & \\ \Psi_3 &= \left(Ce^{\phi x} + De^{-\phi x}\right) e^{il(a+b)} && (10.7) \end{aligned}$$

Now apply the matching conditions for wavefunctions

$$\begin{aligned} \Psi_1(0) &= \Psi_2(0) \rightarrow A + B = C + D \\ \Psi_1^{'}(0) &= \Psi_2^{'}(0) \rightarrow ik(A+B) = \phi(C-D) \\ \Psi_1(a) &= \Psi_3(a) \rightarrow Ae^{ika} + Be^{-ika} = (Ce^{-\phi b} + De^{\phi b})e^{il(a+b)} \\ \Psi_1^{'}(a) &= \Psi_3^{'}(a) \rightarrow ikAe^{ika} - ikBe^{-ika} = (\phi Ce^{-\phi b} - D\phi e^{\phi b})e^{il(a+b)} \end{aligned}$$

where we used the fact that

$$\begin{aligned} \Psi_3(a) &= \Psi_2(-b)e^{il(a+b)} \\ \Psi_3^{'}(a) &= \Psi_2^{'}(-b)e^{il(a+b)} \end{aligned}$$

This leads to a system of four equations with four unknowns (A, B, C, D). The system can be recast into matrix form. However, to give a non-trivial solution (A=B=C=D=0) one must have the determinant of prefactors equal zero. This means solving the following equation.

$$\begin{vmatrix} 1 & 1 & -1 & -1 \\ ik & -ik & -\phi & \phi \\ e^{ika} & e^{-ika} & -e^{-\phi b+il(a+b)} & -e^{\phi b+il(a+b)} \\ ike^{ika} & -ike^{-ika} & -\phi e^{-\phi b+il(a+b)} & \phi e^{\phi b+il(a+b)} \end{vmatrix} = 0 \qquad (10.8)$$

Most texts will skip the tedious steps to the final expression. Here we outline what needs to be done. The solution can be approached a number

of ways. This is just one. Apply the following steps to generate successively simpler determinants.

$$-ik(\text{row1}) + (\text{row2}) \rightarrow (\text{row2})$$
$$-ik(\text{row2}) + (\text{row4}) \rightarrow (\text{row4})$$

yeilding

$$\begin{vmatrix} 1 & 1 & -1 & -1 \\ 0 & -2ik & (ik-\phi) & (ik+\phi) \\ e^{ika} & e^{-ika} & -e^{-\phi b+il(a+b)} & -e^{\phi b+il(a+b)} \\ 0 & -2ike^{-ika} & (ik-\phi)e^{-\phi b+il(a+b)} & (ik+\phi)e^{\phi b+il(a+b)} \end{vmatrix} = 0$$

$$-e^{ika}(\text{row1}) + (\text{row3}) \rightarrow (\text{row3})$$

yielding

$$\begin{vmatrix} 1 & 1 & -1 & -1 \\ 0 & -2ik & (ik-\phi) & (ik+\phi) \\ 0 & e^{-ika}-e^{ika} & e^{ika}-e^{-\phi b+il(a+b)} & e^{ika}-e^{\phi b+il(a+b)} \\ 0 & -2ike^{-ika} & (ik-\phi)e^{-\phi b+il(a+b)} & (ik+\phi)e^{\phi b+il(a+b)} \end{vmatrix} = 0$$

then

$$-e^{-ika}(\text{row2}) + (\text{row4}) \rightarrow (\text{row4})$$

yielding

$$\begin{vmatrix} 1 & 1 & -1 & -1 \\ 0 & -2ik & (ik-\phi) & (ik+\phi) \\ 0 & e^{-ika}-e^{ika} & e^{ika}-e^{-\phi b+il(a+b)} & e^{ika}-e^{\phi b+il(a+b)} \\ 0 & 0 & (ik-\phi)\left[-e^{-ika}+e^{-\phi b+il(a+b)}\right] & (ik+\phi)\left[-e^{-ika}+e^{\phi b+il(a+b)}\right] \end{vmatrix} = 0$$

At this point the finding the 4x4 determinant becomes the same as finding the sub 3x3 determinant. To simplify our notation let

$$\begin{aligned} (1) &= (ik-\phi)\left[-e^{-ika}+e^{-\phi b+il(a+b)}\right] \\ (2) &= (ik+\phi)\left[-e^{-ika}+e^{\phi b+il(a+b)}\right] \end{aligned}$$

then the 3x3 becomes

$$\begin{vmatrix} -2ik & (ik-\phi) & (ik+\phi) \\ e^{-ika}-e^{ika} & e^{ika}-e^{-\phi b+il(a+b)} & e^{ika}-e^{\phi b+il(a+b)} \\ 0 & (ik-\phi)(1) & (ik+\phi)(2) \end{vmatrix} = 0$$

which is equivalent to

$$\begin{aligned} &- \quad 2ik \begin{vmatrix} e^{ika}-e^{-\phi b+il(a+b)} & e^{ika}-e^{\phi b+il(a+b)} \\ (ik-\phi)(1) & (ik+\phi)(2) \end{vmatrix} \\ &+ \quad 2i\sin(ka) \begin{vmatrix} (ik-\phi) & (ik+\phi) \\ (ik-\phi)(1) & (ik+\phi)(2) \end{vmatrix} = 0 \end{aligned}$$

$$\begin{aligned} &- \quad 2ik \begin{vmatrix} e^{ika}-e^{-\phi b+il(a+b)} & e^{ika}-e^{\phi b+il(a+b)} \\ (ik-\phi)(1) & (ik+\phi)(2) \end{vmatrix} \\ &+ \quad 2i\sin(ka)\left[(-k^2-\phi^2)(2)-(-k^2-\phi^2)(1)\right] = 0 \end{aligned}$$

$$\begin{aligned} &- \quad 2ik \begin{vmatrix} e^{ika}-e^{-\phi b+il(a+b)} & e^{ika}-e^{\phi b+il(a+b)} \\ (ik-\phi)(1) & (ik+\phi)(2) \end{vmatrix} \\ &+ \quad 2i(-k^2-\phi^2)\sin(ka)\left[(2)-(1)\right] = 0 \end{aligned}$$

$$\begin{aligned} &- \quad 2ik \begin{vmatrix} e^{ika}-e^{-\phi b+il(a+b)} & e^{ika}-e^{\phi b+il(a+b)} \\ (ik-\phi)(1) & (ik+\phi)(2) \end{vmatrix} \\ &+ \quad 4i(-k^2-\phi^2)\sin(ka)sinh(\phi b)e^{il(a+b)} = 0 \end{aligned}$$

The top determinant is a little tedious but can be evaluate to give

$$\begin{aligned} &- \quad 4ik\left[-\phi-\phi e^{2il(a+b)}+2e^{il(a+b)}\left(-k\sinh(\phi b)\sin(ka)+\phi\cosh(\phi b)\cos(ka)\right)\right] \\ &+ \quad 4i(-k^2-\phi^2)\sin(ka)\sinh(\phi b)e^{il(a+b)} = 0 \end{aligned}$$

This expands to

$$4ik\phi + 4ik\phi e^{2il(a+b)} - 8ike^{il(a+b)}\left(-k\sinh(\phi b)\sin(ka) + \phi\cosh(\phi b)\cos(ka)\right) \\ +4i(-k^2-\phi^2)e^{il(a+b)}\sin(ka)\sinh(\phi b) = 0$$

Multiply by $e^{-il(a+b)}$ to get

$$4ik\phi e^{-il(a+b)} + 4ik\phi e^{il(a+b)} - 8ik\left(-k\sinh(\phi b)\sin(ka) + \phi\cosh(\phi b)\cos(ka)\right) \\ +4i(-k^2-\phi^2)\sinh(\phi b)\sin(ka) = 0$$

Divide by $4i$ to get

$$2k\phi\cos(l(a+b)) + 2k^2\sinh(\phi b)\sin(ka) - 2k\phi\cosh(\phi b)\cos(ka) \\ +(-k^2-\phi^2)\sinh(\phi b)\sin(ka) = 0$$

This leads to the following textbook expression after some simplification

$$\boxed{\left(\tfrac{\phi^2-k^2}{2k\phi}\right)\sinh(\phi b)\sin(ka) + \cosh(\phi b)\cos(ka) = \cos(l(a+b)} \tag{10.9}$$

Kronig Penney V=0 Limit

Starting with our Kronig Penney expression derived above

$$\left(\frac{\phi^2-k^2}{2k\phi}\right)\sinh(\phi b)\sin(ka) + \cosh(\phi b)\cos(ka) = \cos(l(a+b)$$

recall that

$$\begin{aligned} \phi^2 &= \frac{2m(V-\varepsilon)}{\hbar^2} \rightarrow \phi = \sqrt{\frac{2m(V-\varepsilon)}{\hbar^2}} \\ k^2 &= \frac{2m\varepsilon}{\hbar^2} \rightarrow k = \sqrt{\frac{2m\varepsilon}{\hbar^2}} \end{aligned}$$

if V=0

$$\phi^2 = -\frac{2m\varepsilon}{\hbar^2} \rightarrow \phi = i\sqrt{\frac{2m\varepsilon}{\hbar^2}} = ik$$

the Kronig Penney expression becomes

$$\left(\frac{-k^2-k^2}{2ik^2}\right)\sinh(ikb)\sin(ka)+\cosh(ikb)\cos(ka)=\cos(l(a+b))$$

where

$$\begin{aligned}\sinh(iu) &= i\sin(u)\\ \cosh(iu) &= \cos(u)\end{aligned}$$

leading to

$$-\sin(kb)\sin(ka)+\cos(kb)\cos(ka)=\cos(l(a+b))$$

For this to be true

$$l=k$$

or

$$l=\sqrt{\frac{2m\varepsilon}{\hbar^2}} \tag{10.10}$$

This gives the energies of a free particle

$$\boxed{\varepsilon=\tfrac{\hbar^2 l^2}{2m}}$$

Kronig Penney V$=\infty$ Limit

Starting with our original Kronig Penney expression

$$\left(\frac{\phi^2-k^2}{2k\phi}\right)\sinh(\phi b)\sin(ka)+\cosh(\phi b)\cos(ka)=\cos(l(a+b))$$

where

$$\begin{aligned}k^2 &= \frac{2m\varepsilon}{\hbar^2}\\ \phi^2 &= \frac{2m\left(V-\varepsilon\right)}{\hbar^2}\end{aligned}$$

Let's rearrange everything in terms of unitless variables if possible

$$\begin{aligned} k^2 &= \frac{2m\varepsilon}{\hbar^2}\left(\frac{V}{V}\right) = \frac{2mV}{\hbar^2}\left(\frac{\varepsilon}{V}\right) = \frac{2mV}{\hbar^2}\delta \\ \phi^2 &= \frac{2m}{\hbar^2}\left(V - \varepsilon\frac{V}{V}\right) = \frac{2mV}{\hbar^2}(1-\delta) \end{aligned}$$

where in both cases $\delta = \varepsilon/V$. Therefore

$$\begin{aligned} \left(\frac{\phi^2 - k^2}{2k\phi}\right) &= \frac{\left[\frac{2mV}{\hbar^2}(1-\delta)\right] - \left[\frac{2mV}{\hbar^2}\delta\right]}{2\sqrt{\frac{2mV}{\hbar^2}\delta}\sqrt{\frac{2mV}{\hbar^2}(1-\delta)}} \\ &= \frac{(1-2\delta)}{2\sqrt{\delta(1-\delta)}} \end{aligned}$$

Consider also how ϕb and ka simplify.

$$\begin{aligned} \phi b &= \sqrt{\frac{2mV}{\hbar^2}(1-\delta)}b = \sqrt{\frac{2mV}{\hbar^2}(1-\delta)}b\left(\frac{a}{a}\right) \\ &= \left[\sqrt{\frac{2mV}{\hbar^2}}a\right]\left(\frac{b}{a}\right)\sqrt{1-\delta} \\ &= Ar\sqrt{1-\delta} \end{aligned}$$

where $A = \sqrt{\frac{2mV}{\hbar^2}}a$ and $r = b/a$ are constants. Likewise

$$\begin{aligned} ka &= \sqrt{\frac{2mV\delta}{\hbar^2}}a \\ &= A\sqrt{\delta} \end{aligned}$$

Replace both into our previous equation to get

Case ($\delta < 1$)

$$\frac{(1-2\delta)}{2\sqrt{\delta(1-\delta)}}\sinh(Ar\sqrt{1-\delta})\sin(A\sqrt{\delta} + \cosh(Ar\sqrt{1-\delta})\cos(A\sqrt{\delta}) = \cos(la(1+r)) \quad (10.11)$$

where $\delta < 1$ implicitly.

Case $(\delta > 1)$

In this case

$$\begin{aligned}\sqrt{1-\delta} &= i\sqrt{\delta-1}\\ \sinh(iu) &= i\sin(u)\\ \cosh(iu) &= \cos(u)\end{aligned}$$

Replace into our previous equation to get

$$\frac{(1-2\delta)}{2i\sqrt{\delta(\delta-1)}} i\sin(Ar\sqrt{\delta-1})\sin(A\sqrt{\delta}) + \cos(Ar\sqrt{\delta-1})\cos(A\sqrt{\delta}) = \cos(la(1+r))$$

which reduces to

$$\frac{(1-2\delta)}{2\sqrt{\delta(\delta-1)}} \sin(Ar\sqrt{\delta-1})\sin(A\sqrt{\delta}) + \cos(Ar\sqrt{\delta-1})\cos(A\sqrt{\delta}) = \cos(la(1+r)) \quad (10.12)$$

Case $(\delta = 1)$

Here note that

$$\begin{aligned}\sinh(0) &= 0\\ \cosh(0) &= 1\end{aligned}$$

and that

$$lim_{t\to 0}\frac{\sin(t)}{t} = 1$$

Rearrange the original expression as follows

$$\frac{(1-2\delta)}{2\sqrt{\delta}}\left(\frac{Ar}{Ar}\right)\frac{\sin(Ar\sqrt{\delta-1})}{\sqrt{\delta-1}}\sin(A\sqrt{\delta}) + \cos(Ar\sqrt{\delta-1})\cos(A\sqrt{\delta}) = \cos(la(1+r))$$

Let $\delta = 1$ and recall the limit of $\sin(t)/t$ as $t \to 0$.

$$-\frac{1}{2}Ar\frac{\sin(Ar)}{Ar}\sin(A)+\cos(A)=\cos(la(1+r))$$

continue reducing the expression to get

$$-\frac{Ar}{2}\sin(A)+\cos(A)=\cos(la(1+r)) \tag{10.13}$$

All cases ($\delta<1$), ($\delta>1$) and ($\delta=1$)

In all three cases above the resulting relationship can be expressed crudely as some function of δ equals the right hand side.

$$F(\delta)=\cos(la(1+r)) \tag{10.14}$$

This relation cannot exactly be solved analytically but is done numerically. However one notes at this point that the right hand side of the expression $\cos(la(1+r))$ will cycle periodically between +1 and -1.

Let $V\to\infty$

Continuing our simplification of the this expression, we let $V\to\infty$. As a consequence $\delta=\frac{\varepsilon}{V}\to 0$ and $A\to\infty$.

$$\frac{(1-2\delta)}{2\sqrt{\delta(1-\delta)}}\sinh(Ar\sqrt{1-\delta})\sin(A\sqrt{\delta})+\cosh(Ar\sqrt{1-\delta})\cos(A\sqrt{\delta})$$
$$=\cos(la(1+r))$$

approximately becomes

$$\frac{1}{2\sqrt{\delta}}\sinh(Ar)\sin(A\sqrt{\delta})+\cosh(Ar)=\cos(la(1+r))$$

Here in the approximation, the first term on the left hand side will dominate the second ($\cosh(Ar)$) because of the $\frac{1}{\sqrt{\delta}}$ term. We then get something like

$$\frac{1}{2\sqrt{\delta}}\left(\frac{e^{Ar}-e^{-Ar}}{2}\right)\sin(A\sqrt{\delta})\approx\cos(la(1+r))$$

or

$$\frac{e^{Ar}}{4\sqrt{\delta}}\sin(A\sqrt{\delta}) \approx \cos(la(1+r))$$

Since $\frac{e^{Ar}}{4\sqrt{\delta}}$ diverges, $\sin(A\sqrt{\delta})$ must approach zero to make the left hand side fall between +1 and -1 which are the limits of the right hand side $(\cos(la(1+r)))$.

In the limit that $\sin(A\sqrt{\delta}) = 0$,

$A\sqrt{\delta} = n\pi$

where recall that $A = \sqrt{\frac{2mV}{\hbar^2}}a$ and $\sqrt{\delta} = \sqrt{\frac{\varepsilon}{V}}$ This then leads to the familiar expression for the energies of a particle in a box.

$$\boxed{\varepsilon = \frac{n^2h^2}{8ma^2}} \tag{10.15}$$

Kronig Penney Approximation with Delta Function Barriers

Sometimes the Kronig Penney relation is deived assuming a Delta function potential rather than using rectangular barriers with finite width.

We run through this derivation for completeness. So starting with our original Kronig Penney relation

$$\frac{\phi^2 - k^2}{2k\phi}\sinh(\phi b)\sin(ka) + \cosh(\phi b)\cos(ka) = \cos(l(a+b))$$

One generally makes the following substitution. Let

$$P = \frac{\phi^2 ab}{2} \tag{10.16}$$

where P is basically a dimensionless number. As a consequence $b = \frac{2P}{\phi^2 a}$. Replace into the original expression and make the following simplifications

$$\frac{\phi^2 - k^2}{2k\phi} \approx \frac{\phi^2}{2k\phi} = \frac{\phi}{2k} \tag{10.17}$$

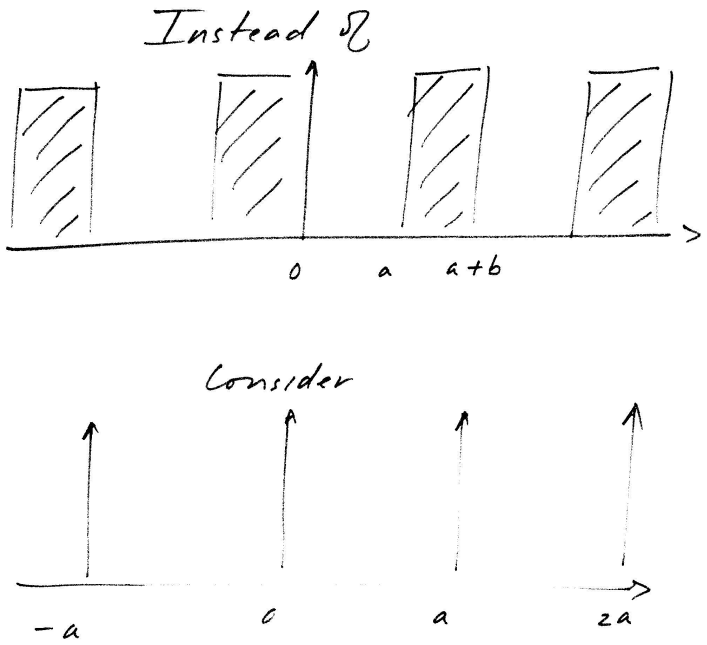

Figure 10.2: Above: original periodic potential of rectangular barriers. Below: approximation using a periodic array of delta functions.

Recall that $\phi = \sqrt{\frac{2m(V-\varepsilon)}{\hbar^2}}$ and $k = \sqrt{\frac{2me}{\hbar^2}}$ with $\phi \to \infty$ since $V \to \infty$. as well as

$$\sinh(\phi b) = lim_{\left(\frac{2P}{\phi a}\right)\to 0} \sinh\left(\frac{2P}{\phi a}\right) = \frac{2P}{\phi a}$$
$$\cosh(\phi b) = lim_{\left(\frac{2P}{\phi a}\right)\to 0} \cosh\left(\frac{2P}{\phi a}\right) = 1$$

where we have made use of a Taylor series as follows.

$$\cosh(x) = \frac{e^x + e^{-x}}{2} \approx \frac{(1+x)+(1-x)}{2} = 1$$
$$\sinh(x) = \frac{e^x - e^{-x}}{2} \approx \frac{(1+x)-(1-x)}{2} = x$$

Then our main equation becomes

$$P\frac{\sin(ka)}{ka} + \cos(ka) = \cos(la) \tag{10.18}$$

At this point we can take our limits of $V = 0 (P = 0)$ or $V = \infty (P = \infty)$ and see what happens.

Case $(P = 0)$

Here we get

$$\cos(ka) = \cos(la)$$

Therefore $k = l$ or that $l = \sqrt{\frac{2m\varepsilon}{\hbar^2}}$ leading to

$$\boxed{\varepsilon = \frac{\hbar^2 l^2}{2m}} \tag{10.19}$$

which again is the energy of a free electron.

Case ($P = \infty$)

Here to allow the left hand side of the expression to have finite values $\frac{\sin(ka)}{ka}$ must be very small. In the limit that $\frac{\sin(ka)}{ka} = 0$, $ka = n\pi$ This immediately leads to

$$\boxed{\varepsilon = \frac{n^2h^2}{8ma^2}} \tag{10.20}$$

which are the energies of a particle in a box.

Summary

One can therefore see that the Kronig Penney model lies in between the two limiting cases for the behavior of an electron in a potential. At one end there is the free electron limit and at the other is the particle in a box limit. In between is the regime giving existence to the notion of bands separated by energy gaps. So as usually mentioned in textbooks, at this point we point out that metals are those materials that have their conduction band half full, semiconductors are those materials where the valence band is full but where the band gap is not humongous (let's say < 4 eV) and insulators are those materials where the valence band is full and where the band gap is huge (say > 4 eV).

Exercises

1. Consider the rectangular barrier Kronig Penney model discussed early on. Use Mathcad, Matlab, Mathematica or your favorite mathematical modeling program to visualize the actual bands. Choose a potential well width of your own choosing, a barrier width, again defined by you, and a nominally high barrier height. Plot the free electron energies on top of the bands you have drawn. Show the plot in both the periodic zone scheme and the reduced zone scheme.

2. Consider the delta function modification of the Kronig Penney model. Again use a mathematical modeling program to draw the bands in the periodic and reduced zone schemes. Choose whatever barrier height, well and barrier width you desire.

Kronig Penney Model

some definitions we will need

$hbar \equiv 1.0546 \cdot 10^{-34}$ self explanatory, units of Joule * seconds

$mo \equiv 9.11 \cdot 10^{-31}$ free electron mass, units of kg

$eV \equiv 1.602 \cdot 10^{-19}$ conversion factor from eV to joule, units of coulomb

initial user defined values

$a := 2 \cdot 10^{-10}$ potential well width, units of meters

$\zeta := 0.1$ user defined multiplicative constant for barrier width, see below

$Vo := 100$ this is the barrier height, units of eV

****

$b(\zeta) := \zeta \cdot a$ barrier width as multiple of well width, units of meters

$P(\zeta) := a + b(\zeta)$ this is the period of the potential, made function of b since we change later

$x := 0, 0.01 \cdot P(\zeta) .. 3 \cdot P(\zeta)$ this is the range in real space to be evaluated

$n := 1$ first zone only

$kmax := n \cdot \left(\frac{\pi}{P(\zeta)} \right)$

$k := -kmax, -0.95 \cdot kmax .. kmax$ this is the range of k space to be evaluated

$\alpha(E) := \sqrt{\frac{2 \cdot mo \cdot (E \cdot eV)}{hbar^2}}$ this is part of the exponent to wavefunction in zero potential well

$\beta(E, Vo) := \sqrt{\frac{2 \cdot mo \cdot (Vo - E) \cdot eV}{hbar^2}}$ this is part of the exponent to wavefunction in barrier

$C(E, k, \zeta, Vo) := \cosh(\beta(E, Vo) \cdot b(\zeta)) \cdot \cos(\alpha(E) \cdot a) - \cos(k \cdot P(\zeta))$ C is part of full expression which we are breaking up for printing purposes, otherwise overruns right margin

$F(E, k, \zeta, Vo) := \frac{\beta(E, Vo)^2 - \alpha(E)^2}{2 \cdot \alpha(E) \cdot \beta(E, Vo)} \cdot \sinh(\beta(E, Vo) \cdot b(\zeta)) \cdot \sin(\alpha(E) \cdot a) + C(E, k, \zeta, Vo)$

this is that large equation whose roots we desire

$V1(x, \zeta, Vo) := Vo \cdot [\Phi(x - a) \cdot \Phi(P(\zeta) - x) + \Phi[x - (P(\zeta) + a)] \cdot \Phi(2 \cdot P(\zeta) - x)]$

Breaking up the potential for printing purposes, otherwise overruns right margin

Figure 10.3: Mathcad numerical solutions to the general Kronig Penney model

$V(x,\zeta,Vo) := V1(x,\zeta,Vo) + Vo\cdot[\Phi[x-(2\cdot P(\zeta)+a)]\cdot\Phi(3\cdot P(\zeta)-x)]$

this is the total rectangular periodic potential, good only for 3 periods

Note, Phi here is just a step function and we are manipulating them to reproduce true potential
this is just for graphing purposes, Phi is a built in mathcad function

****

Some more work on the user part, initial guesses for root

$g1 := 5$ your initial guess to help the computer with band 1

$g2 := 20$ your initial guess to help the computer with band 2

$g3 := 55$ your initial guess to help the computer with band 3

(Note, play with values get "reasonable" bands)

$E1(k,\zeta,Vo) := root(F(g1,k,\zeta,Vo),g1)$ these are the energies of band 1

$E2(k,\zeta,Vo) := root(F(g2,k,\zeta,Vo),g2)$ these are the energies of band 2

$E3(k,\zeta,Vo) := root(F(g3,k,\zeta,Vo),g3)$ these are the energies of band 3

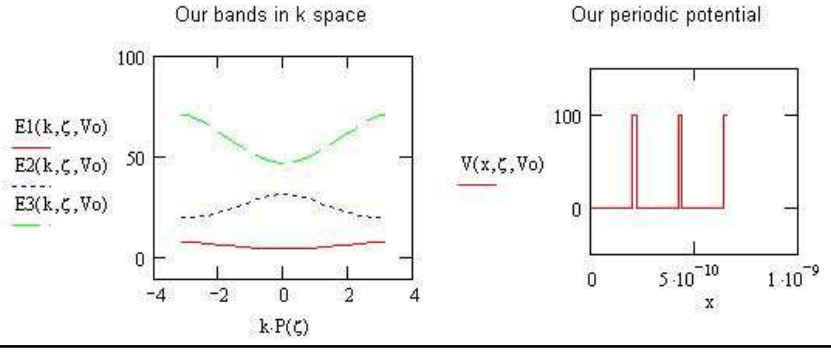

Figure 10.4: Mathcad numerical solutions to the general Kronig Penney model continued

Kronig-Penney Revisited

$$F(\delta, A, r) := \frac{(1-2\cdot\delta)}{2\cdot\sqrt{\delta\cdot(1-\delta)}}\cdot\sinh\left(A\cdot r\cdot\sqrt{1-\delta}\right)\cdot\sin\left(A\cdot\sqrt{\delta}\right) + \cosh\left(A\cdot r\cdot\sqrt{1-\delta}\right)\cdot\cos\left(A\cdot\sqrt{\delta}\right)$$

this is the function we derived

some definitions we will need

$hbar \equiv 1.0546\cdot10^{-34}$ self explanatory, units of Joule * seconds

$mo \equiv 9.11\cdot10^{-31}$ free electron mass, units of kg

$eV \equiv 1.602\cdot10^{-19}$ conversion factor from eV to joule, units of coulomb

Initial user defined values here

$V := 100$ Barrier height, units of eV

$a := 2\cdot10^{-10}$ Well width, units of meters

$\beta := 0.1$ Barrier width prefactor

$b := \beta\cdot a$ Barrier width, units of meters

$r := \frac{b}{a}$ Recall that r = b/a

$A := \sqrt{\frac{2\cdot mo\cdot V\cdot eV}{hbar^2}}\cdot a$ $A = 10.246$ This is our definition for A

$Marker1(\delta) := 1$ These are just markers to show region of valid solutions

$Marker2(\delta) := -1$ These are just markers to show region of valid solutions

$\delta := 0.01, 0.02 .. 4$ The range of δ to evaluate over. Recall δ = E/V

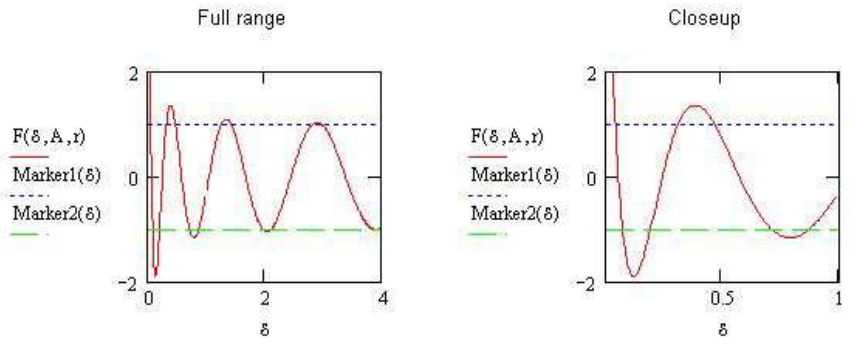

Figure 10.5: Mathcad numerical solutions to approximations of the Kronig Penney model

Kronig Penney Delta Function Approximation

User defined values

$Vo := 100$ barrier potential in units of eV

$a := 2 \cdot 10^{-10}$ potential well width, units of meters

$\zeta := 0.2$ user defined multiplicative constant for barrier width, see below

$b(\zeta) := \zeta \cdot a$ barrier width as multiple of well width, units of meters

$P(\zeta) := a + b(\zeta)$ this is the period of the potential, made function of b since we change later

$hbar := 1.054 \cdot 10^{-34}$ hbar in units of joule second

$mo := 9.11 \cdot 10^{-31}$ free electron mass, units of kg

$eV := 1.602 \cdot 10^{-19}$ conversion factor from eV to joule, units of Coulomb

$$\alpha(E) := \sqrt{\frac{2 \cdot mo \cdot E \cdot eV}{hbar^2}}$$ Exponent of the potential well solutions

$$\phi(E) := \sqrt{\frac{2 \cdot mo \cdot (Vo - E) \cdot eV}{hbar^2}}$$ Exponent of the barrier solutions

$$Pconst(\zeta) := \frac{mo \cdot a \cdot b(\zeta) \cdot Vo \cdot eV}{hbar^2}$$ $Pconst(\zeta) = 10.51$ This is the constant prefactor P in the delta function approximation of Kronig Penney where V >>> E and ϕ basically loses E dep

$n := 1$ First zone only

$$kmax := n \cdot \left(\frac{\pi}{P(\zeta)}\right)$$ $kmax = 1.309 \times 10^{10}$ $k := -kmax, -0.95 \cdot kmax .. kmax$

this is the function whose roots we will determine this is the range of k space to be evaluated

$$F(E,k,\zeta) := Pconst(\zeta) \cdot \left(\frac{\sin(\alpha(E) \cdot P(\zeta))}{\alpha(E) \cdot P(\zeta)}\right) + \cos(\alpha(E) \cdot P(\zeta)) - \cos(k \cdot P(\zeta))$$

$g1 := 1$ initial guess for root finding routine, band 1

$g2 := 15$ initial guess for root finding routine, band 2

$g3 := 40$ initial guess for root finding routine, band 3

$E1(k,\zeta) := root(F(g1,k,\zeta), g1)$ $E2(k,\zeta) := root(F(g2,k,\zeta), g2)$ $E3(k,\zeta) := root(F(g3,k,\zeta), g3)$

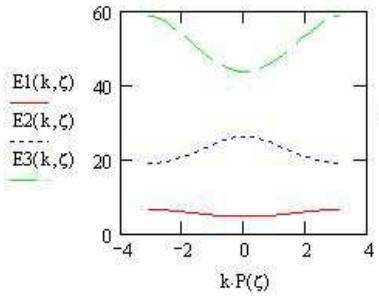

reduced zone scheme

Figure 10.6: Mathcad numerical solutions to the delta function Kronig Penney model

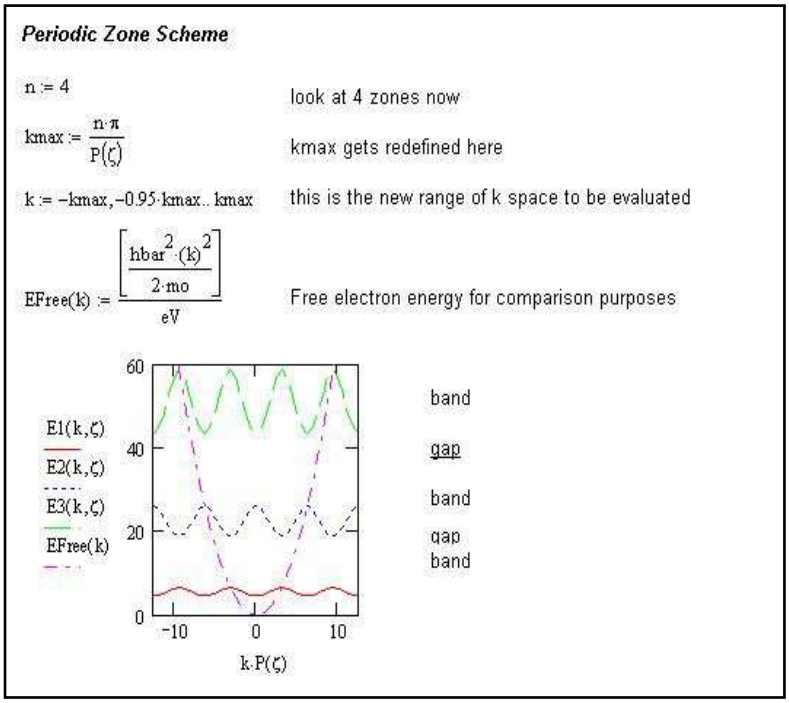

Figure 10.7: Mathcad numerical solutions to the delta function Kronig Penney model continued

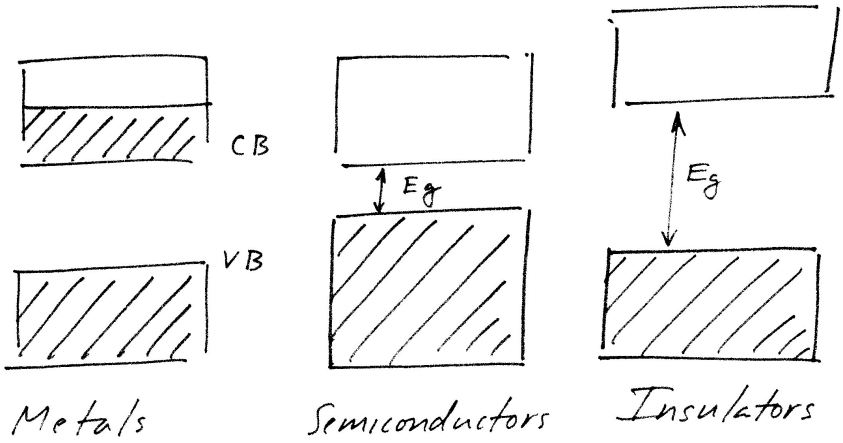

Figure 10.8: Cartoon of the differences between metals, semiconductors and insulators.

Examples from the literature

Here are selected papers from the literature dealing with one area of nanoscience or nanotechnology which is the creation of artifical solids with tailored properties. Crudely one version of this is to use quantum dots as artificial atoms. When arranged in a periodic manner (basically a crystal) the overlap of the electron wavefunctions will create user defined optical and electrical properties as well as the formation of artificial bands as we just described. These go by the name minibands and have already been achieved in the case of arrays of stacked quantum wells.

The papers below are listed in no particular order

1. "Architechtonic quantum dot solids"
   G. Markovich, C. P. Collier, S. E. Henrichs, F. Remacle, R. D. Levine, J. R. Heath
   Accounts of Chemical Research, 32, 415 (1999).

2. "Nanocrystal superlattices"
   C. P. Collier, T. Vossmeyer, J. R. Heath
   Annual Review of Physical Chemistry, 49, 371 (1998).

3. "Highly oriented molecular Ag nanocrystal arrays"
S. A. Harfenist, Z. L. Wang, M. M. Alvarez, I. Vezmar, R. L. Whetten
Journal of Physical Chemistry, 100, 13904 (1996).

4. "Synthesis of a quantum dot superlattice using molecularly linked metal clusters
R. G. Osifchin, W. J. Mahoney, J. D. Bielefeld, R. P. Andres, J. I. Henderson, C. P. Kubiak
Superlattices and Microstructures, 18, 283 (1995).

5. "Architecture with designer atoms: Simple theoretical consideration"
F. Remacle and R. D. Levine
Proceedings of the National Academy of Science, 97, 553 (2000).

6. "Preparation and characterisation of silver quantum dot superlattice using self-assembled monolayers of pentanedithiol"
S. Pethkar, M. Aslam, I. S. Mulla, P. Ganeshan, K. Vijayamohanan
Journal of Materials Chemistry, 11, 1710 (2001).

7. "Miniband formation in a quantum dot crystal"
O. L. Lazarenkova and A. A. Balandin
Journal of Applied Physics, 89, 5509 (2001).

8. "Reversible tuning of silver quantum dot monolayers through the metal-insulator transition"
C. P. Collier, R. J. Saykally, J. J. Shiang, S. E. Henrichs, J. R. Heath
Science, 277, 1978 (1997).

9. "Optical properties of thin films of Au@SiO2 Particles"
T. Ung, L. M. Liz-Marzan, P. Mulvaney
Journal of Physical Chemistry B, 105, 3441 (2001).

Chapter 11

Tunneling

Potential step

This is the simplest example of tunneling. Picture the following potential step.

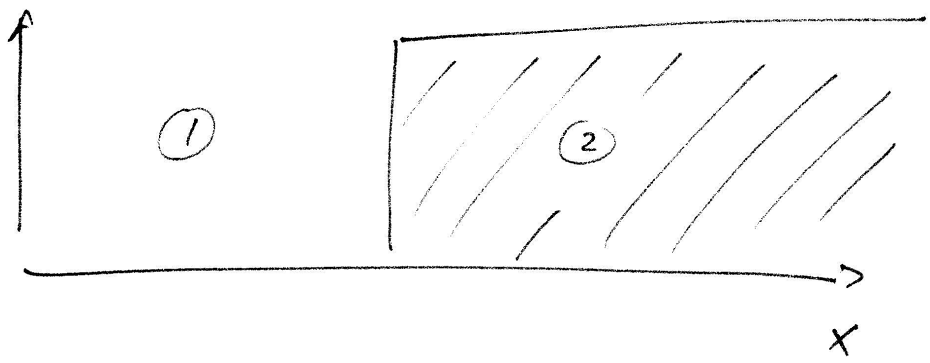

Figure 11.1: Cartoon of the potential step

The Schrodinger equation is

$$-\frac{\hbar^2}{2m}\frac{d^2\Psi}{dx^2} + V\Psi = \varepsilon\Psi$$

This can be rearranged as follows.

In region 1 where $V = 0$

$$-\frac{\hbar^2}{2m}\frac{d^2\Psi}{dx^2} = (\varepsilon - V)\Psi$$

$$\begin{aligned} \frac{d^2\Psi}{dx^2} &= -\frac{2m}{\hbar^2}\varepsilon\Psi \\ \frac{d^2\Psi}{dx^2} + k^2\Psi &= 0 \end{aligned}$$

where $k^2 = \frac{2m\varepsilon}{\hbar^2}$. Solutions to the wavefunction are

$$\Psi_1 = Ae^{ikx} + Be^{-ikx} \tag{11.1}$$

In region 2 where V is finite, there are two cases.

- Case 1: $\varepsilon > V$
- Case 2: $\varepsilon < V$

Case 1: $(\varepsilon > V)$

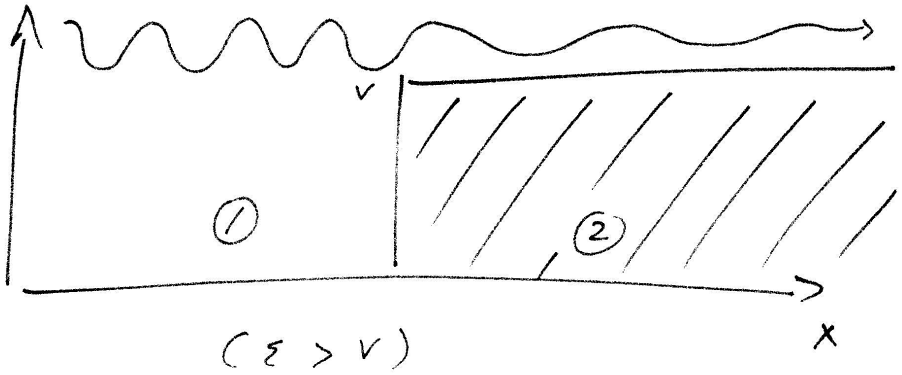

Figure 11.2: Behavior of the wavefunction in the potential step case where $\varepsilon > V$

$$\begin{aligned} -\frac{\hbar^2}{2m}\frac{d^2\Psi}{dx^2} + V\Psi &= \varepsilon\Psi \\ -\frac{\hbar^2}{2m}\frac{d^2\Psi}{dx^2} &= (\varepsilon - V)\Psi \\ \frac{d^2\Psi}{dx^2} &= -\frac{2m}{\hbar^2}(\varepsilon - V)\Psi \\ \frac{d^2\Psi}{dx^2} + \phi^2\Psi &= 0 \end{aligned}$$

where $\phi^2 = \frac{2m(\varepsilon - V)}{\hbar^2}$. Solutions to the wavefunction for this case, in this region, are

$$\Psi_2 = Ce^{i\phi x} + De^{-i\phi x} \tag{11.2}$$

Case 2: $(\varepsilon < V)$

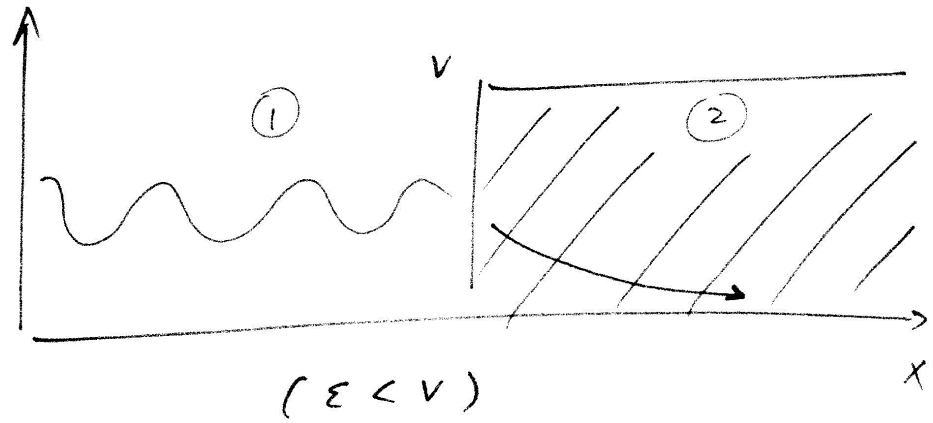

Figure 11.3: Behavior of the wavefunction in the potential step case where $\varepsilon < V$

$$\begin{aligned}
-\frac{\hbar^2}{2m}\frac{d^2\Psi}{dx^2} + V\Psi &= \varepsilon\Psi \\
-\frac{\hbar^2}{2m}\frac{d^2\Psi}{dx^2} &= (\varepsilon - V)\Psi \\
\frac{d^2\Psi}{dx^2} &= -\frac{2m}{\hbar^2}(\varepsilon - V)\Psi \\
\frac{d^2\Psi}{dx^2} &= \frac{2m}{\hbar^2}(V - \varepsilon)\Psi \\
\frac{d^2\Psi}{dx^2} - \beta^2\Psi &= 0
\end{aligned}$$

where $\beta^2 = \frac{2m(V - \varepsilon)}{\hbar^2}$. Solutions to the wavefunction for this case, in this region, are

$$\Psi_2 = Ce^{\beta x} + De^{-\beta x} \tag{11.3}$$

Now in order to proceed, we need to employ the matching conditions for the wavefunctions. The matching conditions are:

1. $\Psi_1(0) = \Psi_2(0)$
2. $\Psi_1'(0) = \Psi_2'(0)$

Furthermore, the wavefunction must be finite valued. That is, the wavefunction can't blow up or do strange things.

Transmission and reflection coefficients; $\varepsilon > V$

The wavefunctions in this case are

$$\begin{aligned} \Psi_1 &= Ae^{ikx} + Be^{-ikx} \\ \Psi_2 &= Ce^{i\phi x} + De^{-i\phi x} \end{aligned}$$

Since there are no sources of particles on the right to support a left going wave, $D = 0$. The wavefunctions become

$$\begin{aligned} \Psi_1 &= Ae^{ikx} + Be^{-ikx} \\ \Psi_2 &= Ce^{i\phi x} \end{aligned}$$

Apply the matching conditions. First one

$$\begin{aligned} \Psi_1(0) &= \Psi_2(0) \\ A + B &= C \end{aligned}$$

Second matching condition

$$\begin{aligned} \Psi_1'(0) &= \Psi_2'(0) \\ Aike^{ikx} - Bike^{-ikx} &= Ci\phi e^{i\phi x} \\ Aik - Bik &= Ci\phi \\ k(A - B) &= \phi C \end{aligned}$$

Now take the resulting equations and solve for A and B

$$\begin{aligned} A + B &= C \\ A - B &= \frac{\phi}{k} C \\ &\downarrow \\ 2A &= C\left(1 + \frac{\phi}{k}\right) \\ A &= \frac{C}{2}\left(1 + \frac{\phi}{k}\right) \end{aligned} \tag{11.4}$$

Next B

$$\begin{aligned} A+B &= C \\ -A+B &= -\frac{\phi}{k}C \\ &\downarrow \\ 2B &= C\left(1-\frac{\phi}{k}\right) \\ B &= \frac{C}{2}\left(1-\frac{\phi}{k}\right) \end{aligned} \tag{11.5}$$

Now the incident "flux" of particles from the left onto the potential step is

$$v_1|A|^2 \tag{11.6}$$

where v_1 is the velocity in region 1 and $|A|^2$ is the relative probability of a right going wave in region 1. Similarly

$$v_1|B|^2 \tag{11.7}$$

is the reflected flux at the potential step where again v_1 is the velocity in region 1 and $|B|^2$ is the relative probability of a left going wave. Finally

$$v_2|C|^2 \tag{11.8}$$

is the transmitted flux where v_2 is the velocity in region 2 and $|C|^2$ is the relative probability of a right going wave in region 2.

The fraction of particles reflected is therefore

$$\begin{aligned} R &\equiv \frac{v_1|B|^2}{v_1|A|^2} = \left|\frac{B}{A}\right|^2 = \frac{B^*B}{A^*A} \\ R &= \frac{\frac{C^2}{4}\left(1-\frac{\phi}{k}\right)^2}{\frac{C^2}{4}\left(1+\frac{\phi}{k}\right)^2} \end{aligned}$$

$$\boxed{R = \frac{(k-\phi_2)^2}{(k+\phi_2)^2} > 0} \tag{11.9}$$

So oddly enough, this is non-classical. Some reflection occurs even though $\varepsilon > V$.

Next, the fraction of particles transmitted is

$$\begin{aligned} T &\equiv \frac{v_2|C|^2}{v_1|A|^2} = \frac{\phi|C|^2}{k|A|^2} = \frac{\phi C^2}{k\frac{C^2}{4}\left(1+\frac{\phi}{k}\right)^2} \\ &= \frac{4\phi}{k\left(1+\frac{\phi}{k}\right)^2} = \frac{4k^2\phi}{k(k+\phi)^2} \end{aligned}$$

resulting in

$$\boxed{T = \frac{4k\phi}{(k+\phi)^2} \neq 0} \tag{11.10}$$

Transmission and reflection coefficients; $\varepsilon < V$

Recall that the wavefunctions in this case are

$$\begin{aligned} \Psi_1 &= Ae^{ikx} + Be^{-ikx} \\ \Psi_2 &= Ce^{\beta x} + De^{-\beta x} \end{aligned}$$

where $k = \sqrt{\frac{2m\varepsilon}{\hbar}}$ and $\beta = \sqrt{\frac{2m(V-\varepsilon)}{\hbar}}$. Now recall that the wavefunction in region 1 and 2 must be finite valued. This means that $C = 0$. Can't have something blow up here. Therefore

$$\begin{aligned} \Psi_1 &= Ae^{ikx} + Be^{-ikx} \\ \Psi_2 &= De^{-\beta x} \end{aligned}$$

Apply the matching conditions now. First one

$$\begin{aligned} \Psi_1(0) &= \Psi_2(0) \\ A + B &= D \end{aligned}$$

Second one

$$\begin{aligned} \Psi_1'(0) &= \Psi_2'(0) \\ ikA - ikB &= -\beta D \\ ik(A-B) &= -\beta D \end{aligned}$$

Now take the resulting equations and solve for A and B. First let's solve for the A coefficient.

$$A + B = D$$

$$\begin{aligned} A - B &= -\frac{\beta}{ik} D \\ &\downarrow \\ 2A &= D\left(1 - \frac{\beta}{ik}\right) \\ A &= \frac{D}{2}\left(1 - \frac{\beta}{ik}\right) \end{aligned} \tag{11.11}$$

Now let's solve for B

$$\begin{aligned} A + B &= D \\ -A + B &= \frac{\beta}{ik} D \\ 2B &= D\left(1 + \frac{\beta}{ik}\right) \\ B &= \frac{D}{2}\left(1 + \frac{\beta}{ik}\right) \end{aligned} \tag{11.12}$$

From before, the relevant fluxes are

$$\begin{aligned} &v_1|A|^2 \text{ (leftgoing)} \\ &v_1|B|^2 \text{ (rightgoing)} \\ &v_2|C|^2 \text{ (transmitted)} \end{aligned}$$

The fraction of particles reflected is

$$\begin{aligned} R &= \frac{v_1|B|^2}{v_1|A|^2} = \left|\frac{B}{A}\right|^2 = \frac{B^* B}{A^* A} \\ &= \frac{\frac{D^2}{4}\left(1 + \frac{\beta}{ik}\right)\left(1 - \frac{\beta}{ik}\right)}{\frac{D^2}{4}\left(1 - \frac{\beta}{ik}\right)\left(1 + \frac{\beta}{ik}\right)} \\ &= \frac{\frac{D^2}{4}\left(1 + \frac{\beta^2}{k^2}\right)}{\frac{D^2}{4}\left(1 + \frac{\beta^2}{k^2}\right)} \\ &= 1 \end{aligned}$$

However the fraction transmitted is

$$\begin{aligned} T &= \frac{v_2|D|^2}{v_1|A|^2} = \frac{\beta|D|^2}{k|A|^2} \\ &= \frac{\beta D^2}{k\frac{D^2}{4}\left(1 + \frac{\beta^2}{k^2}\right)} \end{aligned}$$

$$= \frac{4\beta}{k\left(1+\frac{\beta^2}{k^2}\right)}$$

giving

$$\boxed{T = \frac{4\beta k}{(k^2+\beta^2)} \neq 0} \tag{11.13}$$

This gives a non-classical result. There is some probability of finding soemething in region 2.

Potential barrier

From the last section we know that the wavefunctions have the following form.

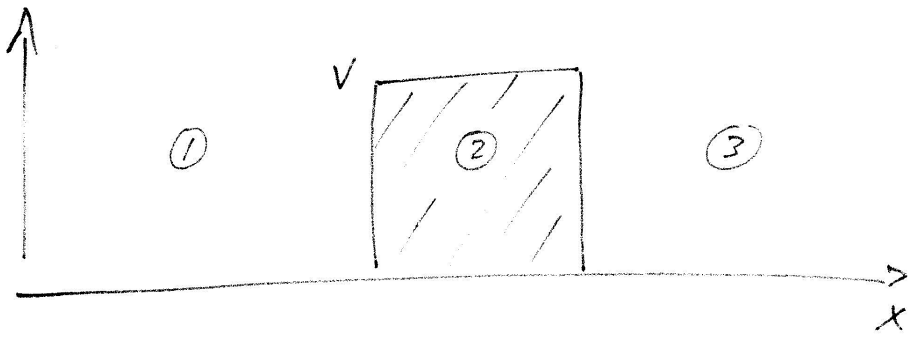

Figure 11.4: Cartoon of the potential barrier

$$\begin{aligned}
\Psi_1 &= Ae^{ikx} + Be^{-ikx} \\
\Psi_2 &= Ce^{i\phi x} + De^{-i\phi x} \ (\varepsilon > V) \\
\Psi_2 &= Ce^{\beta x} + De^{-\beta x} \ (\varepsilon < V) \\
\Psi_3 &= Fe^{ikx} + Ge^{-ikx}
\end{aligned}$$

where $k^2 = \frac{2m\varepsilon}{\hbar^2}$, $\phi^2 = \frac{2m(\varepsilon - V)}{\hbar^2}$, and $\beta^2 = \frac{2m(V-\varepsilon)}{\hbar^2}$. Now as before we apply the matching conditions to the wavefunctions to solve for the coefficients and in turn for the transmission (T) and reflection (R) coefficients.

Case 1: $(\varepsilon > V)$

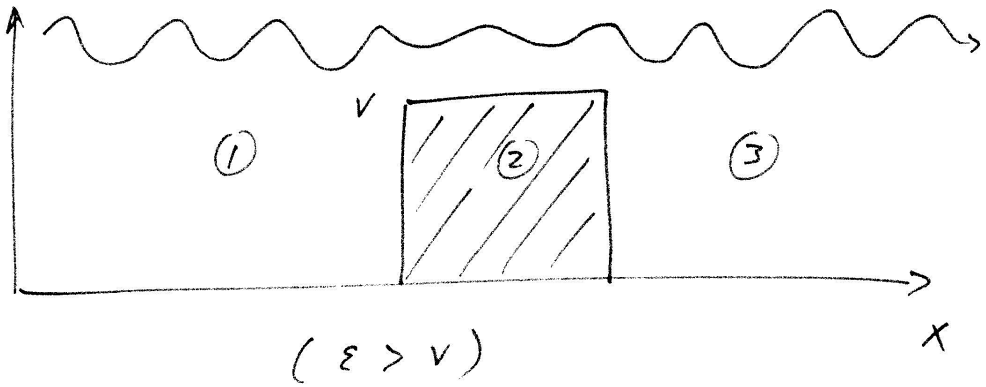

Figure 11.5: Behavior of the wavefunction in the potential barrier case where $\varepsilon > V$

Assuming that there is no source of particles on the right then $G = 0$. The wavefunctions in the three regions become

$$\begin{aligned} \Psi_1 &= Ae^{ikx} + Be^{-ikx} \\ \Psi_2 &= Ce^{i\phi x} + De^{-i\phi x} \\ \Psi_3 &= Fe^{ikx} \end{aligned}$$

Apply the matching conditions at $x = 0$. First one

$$\begin{aligned} \Psi_1(0) &= \Psi_2(0) \\ A + B &= C + D \end{aligned} \tag{11.14}$$

Second one

$$\begin{aligned} \Psi_1^{'}(0) &= \Psi_2^{'}(0) \\ Aik - Bik &= Ci\phi - Di\phi \\ A - B &= \frac{\phi}{k}(C - D) \end{aligned} \tag{11.15}$$

Apply the matching conditions at $x = a$. First one

$$\begin{aligned} \Psi_2(a) &= \Psi_3(a) \\ Ce^{i\phi a} + De^{-i\phi a} &= Fe^{ika} \end{aligned} \tag{11.16}$$

Second one

$$\begin{aligned} \Psi_2^{'}(a) &= \Psi_3^{'}(a) \\ Ci\phi e^{i\phi a} - Di\phi e^{-i\phi a} &= Fike^{ika} \\ C\phi e^{i\phi a} - D\phi e^{-i\phi a} &= Fke^{ika} \end{aligned} \tag{11.17}$$

Solve for A.

$$\begin{aligned} A + B &= C + D \\ A - B &= \frac{\phi}{k}C - \frac{\phi}{k}D \\ &\downarrow \\ 2A &= C\left(1 + \frac{\phi}{k}\right) + D\left(1 - \frac{\phi}{k}\right) \\ A &= \frac{C}{2}\left(1 + \frac{\phi}{k}\right) + \frac{D}{2}\left(1 - \frac{\phi}{k}\right) \end{aligned} \tag{11.18}$$

Solve for B.

$$\begin{aligned} A + B &= C + D \\ -A + B &= -\frac{\phi}{k}C + \frac{\phi}{k}D \\ &\downarrow \\ 2B &= C\left(1 - \frac{\phi}{k}\right) + D\left(1 + \frac{\phi}{k}\right) \\ B &= \frac{C}{2}\left(1 - \frac{\phi}{k}\right) + \frac{D}{2}\left(1 + \frac{\phi}{k}\right) \end{aligned} \tag{11.19}$$

Solve for C.

$$\begin{aligned} Ce^{i\phi a} + De^{-i\phi a} &= Fe^{ika} \\ C\phi e^{i\phi a} - D\phi e^{-i\phi a} &= Fke^{ika} \\ &\downarrow \\ C\phi e^{i\phi a} + D\phi e^{-i\phi a} &= F\phi e^{ika} \\ C\phi e^{i\phi a} - D\phi e^{-i\phi a} &= Fke^{ika} \\ &\downarrow \\ 2C\phi e^{i\phi a} &= F(k+\phi)e^{ika} \\ C &= F\frac{k+\phi}{2\phi}e^{ia(k-\phi)} \end{aligned} \tag{11.20}$$

Solve for D.

$$\begin{aligned} Ce^{i\phi a} + De^{-i\phi a} &= Fe^{ika} \\ -C\phi e^{i\phi a} + D\phi e^{-i\phi a} &= -Fke^{ika} \\ &\downarrow \\ C\phi e^{i\phi a} + D\phi e^{-i\phi a} &= F\phi e^{ika} \\ -C\phi e^{i\phi a} + D\phi e^{-i\phi a} &= -Fke^{ika} \\ &\downarrow \\ 2D\phi e^{-i\phi a} &= F(\phi - k)e^{ika} \\ D &= F\frac{\phi - k}{2\phi}e^{ia(k+\phi)} \end{aligned} \tag{11.21}$$

Now that we have expressions for A,B,C,D all in terms of F, let's re-express everything in terms of F. From before

$$\begin{aligned} A &= \frac{1}{2}C\left(1+\frac{\phi}{k}\right) + \frac{1}{2}D\left(1-\frac{\phi}{k}\right) \\ &= \frac{1}{2}F\frac{k+\phi}{2\phi}e^{ia(k-\phi)}\left(1+\frac{\phi}{k}\right) + \frac{1}{2}F\frac{\phi-k}{2\phi}e^{ia(k+\phi)}\left(1-\frac{\phi}{k}\right) \\ &= \frac{F}{4\phi}\left((k+\phi)\left(1+\frac{\phi}{k}\right)e^{ia(k-\phi)} + (\phi-k)\left(1-\frac{\phi}{k}\right)e^{ia(k+\phi)}\right) \\ &= \frac{F}{4\phi}\left(\frac{(k+\phi)(k+\phi)}{k}e^{ia(k-\phi)} - \frac{(k-\phi)(k-\phi)}{k}e^{ia(k+\phi)}\right) \\ &= \frac{Fe^{ika}}{4k\phi}\left((k+\phi)^2e^{-ia\phi} - (k-\phi)^2e^{ia\phi}\right) \\ &= \frac{Fe^{ika}}{4k\phi}\left(k^2e^{-ia\phi} + 2k\phi e^{-ia\phi} + \phi^2e^{-ia\phi} - k^2e^{ia\phi} + 2k\phi e^{ia\phi} - \phi^2e^{ia\phi}\right) \\ &= \frac{Fe^{ika}}{4k\phi}\left(-k^2\left(e^{ia\phi} - e^{-ia\phi}\right) - \phi^2\left(e^{ia\phi} - e^{-ia\phi}\right) + 2k\phi\left(e^{ia\phi} + e^{-ia\phi}\right)\right) \\ &= \frac{Fe^{ika}}{4k\phi}\left(4k\phi\frac{e^{ia\phi} + e^{-ia\phi}}{2} - 2i(k^2+\phi^2)\frac{e^{ia\phi} - e^{-ia\phi}}{2i}\right) \end{aligned}$$

This gives our desired expression for A

$$A = \frac{Fe^{ika}}{4k\phi}\left(4k\phi cos(\phi a) - 2i(k^2+\phi^2)sin(\phi a)\right) \tag{11.22}$$

Next we do B

$$B = \frac{1}{2}C\left(1-\frac{\phi}{k}\right) + \frac{1}{2}D\left(1+\frac{\phi}{k}\right)$$

$$
\begin{aligned}
&= \frac{1}{2}F\frac{k+\phi}{2\phi}e^{ia(k-\phi)}\left(1-\frac{\phi}{k}\right)+\frac{1}{2}F\frac{\phi-k}{2\phi}e^{ia(k+\phi)}\left(1+\frac{\phi}{k}\right)\\
&= \frac{F}{4\phi}\left((k+\phi)\left(1-\frac{\phi}{k}\right)e^{ia(k-\phi)}+(\phi-k)\left(1+\frac{\phi}{k}\right)e^{ia(k+\phi)}\right)\\
&= \frac{F}{4\phi}\left(\frac{(k+\phi)(k-\phi)}{k}e^{ia(k-\phi)}-\frac{(k-\phi)(k+\phi)}{k}e^{ia(k+\phi)}\right)\\
&= \frac{F}{4k\phi}\left((k^2-\phi^2)e^{ia(k-\phi)}-(k^2-\phi^2)e^{ia(k+\phi)}\right)\\
&= \frac{2iF(k^2-\phi^2)}{4k\phi}e^{ika}\left(\frac{e^{-ia\phi}-e^{ia\phi}}{2i}\right)\\
&= \frac{2iF(-k^2+\phi^2)}{4k\phi}e^{ika}\left(\frac{-e^{-ia\phi}+e^{ia\phi}}{2i}\right)
\end{aligned}
$$

giving us our desired expression for B

$$B = \frac{iF(\phi^2-k^2)}{2k\phi}e^{ika}sin(\phi a) \tag{11.23}$$

Now (finally!) we can evaluate what the reflection and transmission coefficients are. From before the relevant fluxes are

$$
\begin{aligned}
&v_1|A|^2 \text{ (leftgoing)}\\
&v_1|B|^2 \text{ (rightgoing)}\\
&v_3|F|^2 \text{ (transmitted)}
\end{aligned}
$$

The fraction of particles reflected is

$$
\begin{aligned}
R &= \frac{v_1|B|^2}{v_1|A|^2} = \left|\frac{B}{A}\right|^2 = \frac{B^*B}{A^*A}\\
&= \frac{\frac{F^2(\phi^2-k^2)^2}{4(k\phi)^2}sin^2(\phi a)}{\frac{F^2}{16(k\phi)^2}\left(16(k\phi)^2cos^2(\phi a)+4(k^2+\phi^2)sin^2(\phi a)\right)}
\end{aligned}
$$

$$\boxed{R = \frac{(\phi^2-k^2)^2sin^2(\phi a)}{4(k\phi)^2cos^2(\phi a)+(k^2+\phi^2)sin^2(\phi a)}} \tag{11.24}$$

The fraction transmitted is

$$T = \frac{v_3|F|^2}{v_1|A|^2}$$

where note that $v_3 = v_1$. Therefore

$$\begin{aligned} T &= \frac{|F|^2}{|A|^2} = \frac{F^*F}{A^*A} \\ &= \frac{16(k\phi)^2}{16(k\phi)^2 cos^2(\phi a) + 4(k^2+\phi^2)^2 sin^2(\phi a)} \\ &= \frac{1}{cos^2(\phi a) + \frac{(k^2+\phi^2)^2}{4(k\phi)^2} sin^2(\phi a)} \end{aligned} \tag{11.25}$$

Now we could stop here, but usually in many textbooks they expand this out a little further. Recall that

$$\begin{aligned} k^2 &= \frac{2m\varepsilon}{\hbar^2} \\ \phi^2 &= \frac{2m(\varepsilon - V)}{\hbar^2} \\ (k\phi)^2 &= \frac{4m^2}{\hbar^4}\varepsilon(\varepsilon - V) \end{aligned}$$

This leads to

$$\begin{aligned} T &= \frac{1}{cos^2(\phi a) + \frac{(2m\varepsilon + 2m(\varepsilon - V))^2}{16m^2\varepsilon(\varepsilon - V)} sin^2(\phi a)} \\ &= \frac{1}{cos^2(\phi a) + \frac{4m^2(2\varepsilon - V)^2}{16m^2\varepsilon(\varepsilon - V)} sin^2(\phi a)} \\ &= \frac{1}{cos^2(\phi a) + \frac{(2\varepsilon - V)^2}{4\varepsilon(\varepsilon - V)} sin^2(\phi a)} \\ &= \frac{4\varepsilon(\varepsilon - V)}{4\varepsilon(\varepsilon - V)cos^2(\phi a) + (4\varepsilon^2 - 4\varepsilon V + V^2)sin^2(\phi a)} \\ &= \frac{4\varepsilon(\varepsilon - V)}{4\varepsilon^2 cos^2(\phi a) - 4\varepsilon V cos^2(\phi a) + 4\varepsilon^2 sin^2(\phi a) - 4\varepsilon V sin^2(\phi a) + V^2 sin^2(\phi a)} \\ &= \frac{4\varepsilon(\varepsilon - V)}{(4\varepsilon^2 - 4\varepsilon V) + V^2 sin^2(\phi a)} \\ &= \frac{4\varepsilon(\varepsilon - V)}{4\varepsilon(\varepsilon - V) + V^2 sin^2(\phi a)} \end{aligned}$$

This leads to the standard textbook expression

$$\boxed{T = \frac{1}{1 + \frac{V^2}{4\varepsilon(\varepsilon - V)} sin^2(\phi a)}} \tag{11.26}$$

Case 2: $(\varepsilon < V)$

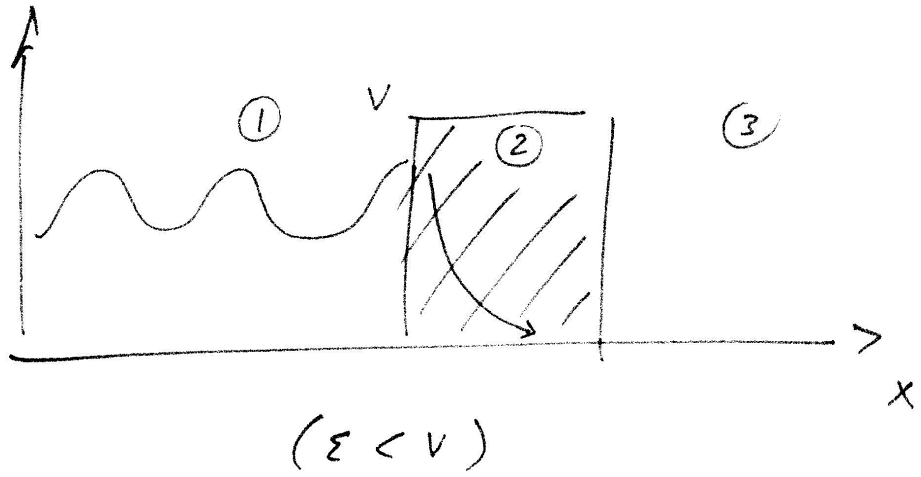

Figure 11.6: Behavior of the wavefunction in the potential barrier case where $\varepsilon < V$

Now rather than doing all this math again, one can be smart about this. Just note that $\beta = i\phi$. So take our previous results from case 1 and just replace ϕ with $i\phi$. (We just analyze the transmission coefficient since this is what we really care about). Another tortuous math workout. Starting with the assumption of no sources on the right ($G = 0$), the wavefunctions are

$$\begin{aligned} \Psi_1 &= Ae^{ikx} + Be^{-ikx} \\ \Psi_2 &= Ce^{\beta x} + De^{-\beta x} \\ \Psi_3 &= Fe^{ikx} \end{aligned}$$

Apply the matching conditions at $x = a$. First one

$$\begin{aligned} \Psi_1(0) &= \Psi_2(0) \\ A + B &= C + D \end{aligned} \tag{11.27}$$

Second one

$$\begin{aligned} \Psi_1^{'}(0) &= \Psi_2^{'}(0) \\ A - B &= \frac{\beta}{ik}(C - D) \end{aligned} \tag{11.28}$$

Apply the matching conditions at $x = a$. First one

$$\begin{aligned} \Psi_2(a) &= \Psi_3(a) \\ Ce^{\beta a} + De^{-\beta a} &= Fe^{ika} \end{aligned} \tag{11.29}$$

Second one

$$\begin{aligned} \Psi_2^{'}(a) &= \Psi_3^{'}(a) \\ Ce^{\beta a} - De^{-\beta a} &= \frac{ik}{\beta} Fe^{ika} \end{aligned} \tag{11.30}$$

Solve for A

$$\begin{aligned} A + B &= C + D \\ A - B &= \frac{\beta}{ik}(C - D) \\ &\downarrow \\ 2A &= C\left(1 + \frac{\beta}{ik}\right) + D\left(1 - \frac{\beta}{ik}\right) \\ A &= \frac{C}{2}\left(1 + \frac{\beta}{ik}\right) + \frac{D}{2}\left(1 - \frac{\beta}{ik}\right) \end{aligned} \tag{11.31}$$

Solve for B

$$\begin{aligned} A + B &= C + D \\ -A + B &= \frac{\beta}{ik}(-C + D) \\ &\downarrow \\ 2B &= C\left(1 - \frac{\beta}{ik}\right) + D\left(1 + \frac{\beta}{ik}\right) \\ B &= \frac{C}{2}\left(1 - \frac{\beta}{ik}\right) + \frac{D}{2}\left(1 + \frac{\beta}{ik}\right) \end{aligned} \tag{11.32}$$

Solve for C

$$\begin{aligned} Ce^{\beta a} + De^{-\beta a} &= Fe^{ika} \\ Ce^{\beta a} - De^{-\beta a} &= \frac{ik}{\beta} Fe^{ika} \\ &\downarrow \\ 2Ce^{\beta a} &= F\left(1 + \frac{ik}{\beta}\right) e^{ika} \\ C &= \frac{F}{2}\left(1 + \frac{ik}{\beta}\right) e^{ika - \beta a} \end{aligned} \tag{11.33}$$

Solve for D

$$\begin{aligned} Ce^{\beta a} + De^{-\beta a} &= Fe^{ika} \\ -Ce^{\beta a} + De^{-\beta a} &= -\frac{ik}{\beta} Fe^{ika} \\ &\downarrow \\ 2De^{-\beta a} &= F\left(1 - \frac{ik}{\beta}\right) e^{ika} \\ D &= \frac{F}{2}\left(1 - \frac{ik}{\beta}\right) e^{ika+\beta a} \end{aligned} \tag{11.34}$$

Now we have a relation for A in terms of C and D. Replace the above C and D expressions into A to obtain A as a function of F (we did B just for the sake of completeness).

$$\begin{aligned} A &= \frac{F}{4}\left(1 + \frac{ik}{\beta}\right)\left(1 + \frac{\beta}{ik}\right) e^{ika-\beta a} + \frac{F}{4}\left(1 - \frac{ik}{\beta}\right)\left(1 - \frac{\beta}{ik}\right) e^{ika+\beta a} \\ &= \frac{F}{4}\left(2 + \frac{\beta}{ik} + \frac{ik}{\beta}\right) e^{ika-\beta a} + \frac{F}{4}\left(2 - \frac{\beta}{ik} - \frac{ik}{\beta}\right) e^{ika+\beta a} \\ &= \frac{F}{4} e^{ika}\left(\left(2 + \frac{\beta}{ik} + \frac{ik}{\beta}\right) e^{-\beta a} + \left(2 - \frac{\beta}{ik} - \frac{ik}{\beta}\right) e^{\beta a}\right) \end{aligned} \tag{11.35}$$

Now from before we know that the transmission coefficient is

$$\begin{aligned} T &= \left|\frac{F}{A}\right|^2 = \frac{F^* F}{A^* A} \\ &= \frac{16}{\left(2 + \frac{\beta}{ik} + \frac{ik}{\beta}\right)^2 + \left(2 - \frac{\beta}{ik} - \frac{ik}{\beta}\right)^2 + 2\left(2 + \frac{\beta}{ik} + \frac{ik}{\beta}\right)\left(2 - \frac{\beta}{ik} - \frac{ik}{\beta}\right) cosh(2\beta a)} \\ &= \frac{16}{\left(2 + \frac{\beta^2 - k^2}{\beta ik}\right)^2 + \left(2 - \frac{\beta^2 - k^2}{\beta ik}\right)^2 + 2\left(2 + \frac{\beta}{ik} + \frac{ik}{\beta}\right)\left(2 - \frac{\beta}{ik} - \frac{ik}{\beta}\right) cosh(2\beta a)} \\ &= \frac{16}{8 - 2\frac{(\beta^2 - k^2)^2}{(\beta k)^2} + 2\left(4 + \frac{\beta^2 - k^2}{(\beta k)^2}\right) cosh(2\beta a)} \\ &= \frac{16}{\left(8 - \frac{2(\beta^2 - k^2)^2}{(\beta k)^2}\right) + \left(8 + \frac{2(\beta^2 - k^2)^2}{(\beta k)^2}\right) cosh(2\beta a)} \end{aligned}$$

it gets ugly here but can be simplified to give

$$= \frac{16(\beta k)^2}{8(\beta k)^2(1 + cosh(2\beta a)) - 2(\beta^2 - k^2)^2(1 - cosh(2\beta a))}$$

Now use the relation $cosh(2x) = 1 + 2sinh^2(x)$ to get

$$= \frac{1}{1+\frac{(\beta^2+k^2)^2}{4(\beta k)^2}sinh^2(\beta a)}$$

where $\beta^2 = \frac{2m(V-\varepsilon)}{\hbar^2}$, $k^2 = \frac{2m\varepsilon}{\hbar^2}$, and $(\beta k)^2 = \frac{4m^2\varepsilon(V-\varepsilon)}{\hbar^4}$. This leads us to our final textbook expression

$$\boxed{T = \frac{1}{1+\frac{V^2}{4\varepsilon(V-\varepsilon)}sinh^2(\beta a)}} \tag{11.36}$$

Again $T \neq 0$ and we obtain a non-classical result.

Exercises

1. A conduction electron in a semiconductor can be described as a free particle in a constant potential with an effective mass m_e. Both the constant potential and the effective mass are material dependent. Consider the following idealized one dimensional system where semi-infinite slabs of semiconductors A and B are joined together. (See Figure 11.7) Assume that one of the matching conditions is $\frac{1}{m_A}\Psi_A(0) = \frac{1}{m_B}\Psi_B(0)$. Also assume $V_o > 0$. (A) Find the transmission coefficient T for $E > V_o$ for a right going wave. (B) Now assume that $m_B < m_A$. Show that an appropriate choice of incoming energy E yields complete transmission ($T = 1$). Is there such an energy if $m_B > m_A$. (C) Show that for $V_o = 0$ and $m_A \neq m_B$, T is always less than unity.

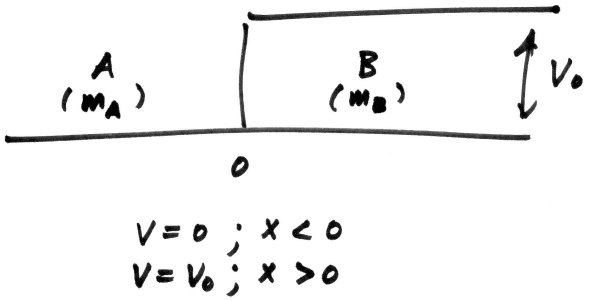

Figure 11.7: Semiconductor junction

Chapter 12

The WKB approximation

Preliminaries

Here we derive the WKB form of the wavefunction. Starting with the Schrodinger equation in the regime where $\varepsilon > V$

$$\begin{aligned} -\frac{\hbar^2}{2m}\frac{d^2\Psi}{dx^2} + V\Psi &= \varepsilon\Psi \\ -\frac{\hbar^2}{2m}\frac{d^2\Psi}{dx^2} &= (\varepsilon - V)\Psi \\ \frac{d^2\Psi}{dx^2} &= -\frac{2m}{\hbar^2}(\varepsilon - V)\Psi \\ \frac{d^2\Psi}{dx^2} + \frac{2m}{\hbar^2}(\varepsilon - V)\Psi &= 0 \end{aligned} \tag{12.1}$$

Let $k^2 = \frac{2m}{\hbar^2}(\varepsilon - V)$ so that we get

$$\frac{d^2\Psi}{dx^2} + k^2\Psi = 0$$

Now in general, if the potential is slowly varying, then both the amplitude and the phase of the wavefunction will change. The general form of the wavefunction is

$$\Psi(x) = A(x)e^{i\phi(x)} = Ae^{i\phi} \text{ (shorthand)} \tag{12.2}$$

So we insert this form of the wavefunction into Schrodinger's equation above. To begin we evaluate some derivatives that we will need. First derivative

$$\begin{aligned} \frac{d\Psi}{dx} &= Aie^{i\phi}\phi^{'} + e^{i\phi}A^{'} \\ &= (A^{'} + iA\phi^{'})e^{i\phi} \end{aligned} \tag{12.3}$$

Next we do the second derivative

$$\begin{aligned}\frac{d^2\Psi}{dx^2} &= i(A^{'}+iA\phi^{'})e^{i\phi}\phi^{'}+e^{i\phi}(A^{''}+iA\phi^{''}+i\phi^{'}A^{'}) \\ &= (iA^{'}\phi^{'}-A\phi^{'2})e^{i\phi}+(A^{''}+iA\phi^{''}+i\phi^{'}A^{'})e^{i\phi} \\ &= (2iA^{'}\phi^{'}-A\phi^{'2}+A^{''}+iA\phi^{''})e^{i\phi} \\ &= (A^{''}+2iA^{'}\phi^{'}+iA\phi^{''}-A\phi^{'2})e^{i\phi} \qquad (12.4)\end{aligned}$$

Replace this into the above Schrodinger equation; $\frac{d^2\Psi}{dx^2}+k^2\Psi=0$

$$\begin{aligned}(A^{''}+2iA^{'}\phi^{'}+iA\phi^{''}-A\phi^{'2})e^{i\phi}+k^2Ae^{i\phi} &= 0 \\ A^{''}+2iA^{'}\phi^{'}+iA\phi^{''}-A\phi^{'2}+k^2A &= 0 \qquad (12.5)\end{aligned}$$

Group the real and imaginary terms. First the real terms

$$\begin{aligned}A^{''}-A\phi^{'2}+k^2A &= 0 \\ A^{''}-A\phi^{'2} &= -k^2A \qquad (12.6)\end{aligned}$$

Next the imaginary terms

$$\begin{aligned}2iA^{'}\phi^{'}+iA\phi^{''} &= 0 \\ 2A^{'}\phi^{'}+A\phi^{''} &= 0 \\ (A^2\phi^{'})^{'} &= 0 \qquad (12.7)\end{aligned}$$

Now we want to solve for A,ϕ so we can have an explicit wavefunction. Solve the imaginary equation first

$$\begin{aligned}(A^2\phi^{'})^{'} &= 0 \\ A^2\phi^{'} &= C^2 \text{ (a constant)} \\ A^2 &= \frac{C^2}{\phi^{'}} \\ A &= \frac{C}{\sqrt{\phi^{'}}} \qquad (12.8)\end{aligned}$$

The real part cannot be solve exactly. However, if A varies very slowly then $A^{''}$ is very small and can be ignored.

$$\begin{aligned}A^{''}-A\phi^{'2} &= -k^2A \\ -A\phi^{'2} &= -k^2A \\ -\phi^{'2} &= -k^2 \\ \phi^{'} &= \pm k \\ \phi &= \pm\int k\,dx \qquad (12.9)\end{aligned}$$

Put these two expressions for A and ϕ back into our wavefunction

$$\begin{aligned} \Psi &= Ae^{i\phi} \\ &= \frac{C_\pm}{\sqrt{k}} e^{\pm i \int k dx} \end{aligned} \tag{12.10}$$

This is the desired form of the WKB wavefunction in the case where $\varepsilon > V$. In the case where $\varepsilon < V$ the WKB form of the wavefunction is

$$\Psi = \frac{C_\pm}{\sqrt{\beta}} e^{\pm \int \beta dx} \tag{12.11}$$

which is basicall the same as the first case but where we just replace k with $i\beta$.

Arbitrary potential step

Using our just derived WKB wavefunctions we evaluate the following arbitrary potential step.

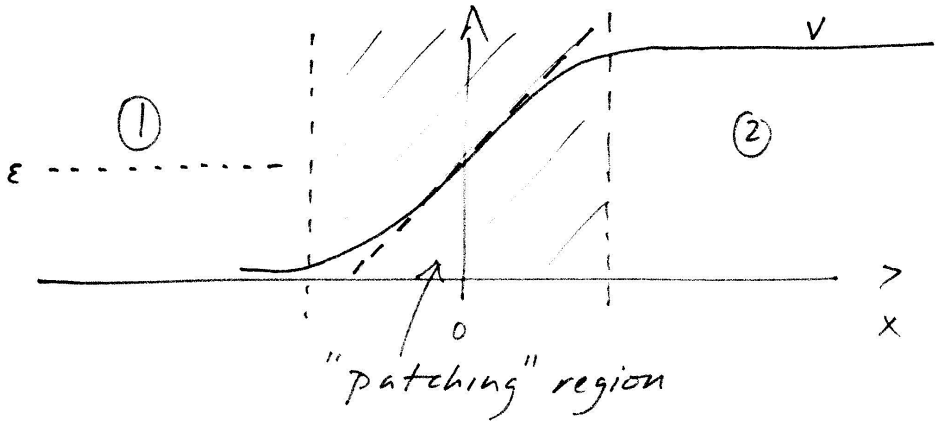

Figure 12.1: Cartoon of the arbitrary potential step

The wavefunctions in region 1 and region 2 are, in general

$$\begin{aligned} \Psi_1 &= \frac{A}{\sqrt{k}} e^{i \int_x^0 k dx} + \frac{B}{\sqrt{k}} e^{-i \int_x^0 k dx} \text{ where } (x < 0) \\ \Psi_2 &= \frac{C}{\sqrt{\beta}} e^{\int_0^x \beta dx} + \frac{D}{\sqrt{\beta}} e^{- \int_0^x \beta dx} \text{ where } (x > 0) \end{aligned}$$

Because we can't have the wavefunction blow up in region 2 ($C = 0$). The wavefunctions are therefore

$$\Psi_1 = \frac{A}{\sqrt{k}} e^{i\int_x^0 k dx} + \frac{B}{\sqrt{k}} e^{-i\int_x^0 k dx} \text{ where } (x < 0) \tag{12.12}$$

$$\Psi_2 = \frac{D}{\sqrt{\beta}} e^{-\int_0^x \beta dx} \text{ where } (x > 0) \tag{12.13}$$

Now consider a linear approximation to the potential between region 1 and region 2

$$V = \varepsilon + V^{'} x \tag{12.14}$$

First we determine the patching wavefunction in the boundary, no man's land, between region 1 and region 2. Starting with the Schrodinger equation

$$\frac{-\hbar^2}{2m}\frac{d^2\Psi_p}{dx^2} + V\Psi_p = \varepsilon\Psi_p$$

where $V = \varepsilon + V^{'} x$. This reduces as follows

$$\begin{aligned} -\frac{\hbar^2}{2m}\frac{d^2\Psi_p}{dx^2} + (\varepsilon + V^{'} x)\Psi_p &= \varepsilon\Psi_p \\ -\frac{\hbar^2}{2m}\frac{d^2\Psi_p}{dx^2} + V^{'} x\Psi_p &= 0 \\ \frac{d^2\Psi_p}{dx^2} - \frac{2mV^{'}}{\hbar^2} x\Psi_p &= 0 \\ \frac{d^2\Psi_p}{dx^2} &= \frac{2mV^{'}}{\hbar^2} x\Psi_p \end{aligned}$$

Let $\alpha^3 = \frac{2mV^{'}}{\hbar^2}$ leading to

$$\frac{d^2\Psi_p}{dx^2} = \alpha^3 x\Psi_p$$

Now let $z = \alpha x$ leading to

$$\frac{d^2\Psi_p}{dz^2} = z\Psi_p \tag{12.15}$$

This is Airy's equation whose solutions are called Airy functions. General solution is a linear combination of Airy functions, $A_i(z)$ and $B_i(z)$. The

asymptotic forms of Airy functions are for ($z < 0$)

$$\begin{aligned} A_i(z) &= \frac{1}{\sqrt{\pi}(-z)^{\frac{1}{4}}} sin(\frac{2}{3}(-z)^{\frac{3}{2}} + \frac{\pi}{4}) \\ B_i(z) &= \frac{1}{\sqrt{\pi}(-z)^{\frac{1}{4}}} cos(\frac{2}{3}(-z)^{\frac{3}{2}} + \frac{\pi}{4}) \end{aligned}$$

and for ($z > 0$)

$$\begin{aligned} A_i(z) &= \frac{1}{2\sqrt{\pi}z^{\frac{1}{4}}} e^{-\frac{2}{3}z^{\frac{3}{2}}} \\ B_i(z) &= \frac{1}{\sqrt{\pi}z^{\frac{1}{4}}} e^{\frac{2}{3}z^{\frac{3}{2}}} \end{aligned}$$

Now

$$\Psi_p = aA_i(z) + bB_i(z) \tag{12.16}$$

where a and b are constants. Now in region 1

$$k = \sqrt{\frac{2m(\varepsilon - V)}{\hbar^2}}$$

where $V = (\varepsilon + V^{'}x)$

$$\begin{aligned} k &= \sqrt{\frac{2mV^{'}}{\hbar^2}}\sqrt{-x} \\ &= \alpha^{\frac{3}{2}}\sqrt{-x} \end{aligned} \tag{12.17}$$

where recall that $\alpha = \left(\frac{2mV^{'}}{\hbar^2}\right)^{\frac{1}{3}}$.

In region 2

$$\begin{aligned} \beta &= \sqrt{\frac{2m(V - \varepsilon)}{\hbar^2}} \\ &= \sqrt{\frac{2mV^{'}}{\hbar^2}}\sqrt{x} \\ &= \alpha^{\frac{3}{2}}\sqrt{x} \end{aligned} \tag{12.18}$$

Now go back to the wavefunctions in region 1 and region 2 and make them more explicit.

Region 1

$$\Psi_1 = \frac{A}{\sqrt{k}} e^{i\int_x^0 k dx} + \frac{B}{\sqrt{k}} e^{-i\int_x^0 k dx}$$

and $k = \alpha^{\frac{3}{2}}\sqrt{-x}$

$$\begin{aligned}\Psi_1 &= \frac{A}{\alpha^{\frac{3}{4}}(-x)^{\frac{1}{4}}} e^{i\int_x^0 \alpha^{\frac{3}{2}}\sqrt{-x}dx} + \frac{B}{\alpha^{\frac{3}{4}}(-x)^{\frac{1}{4}}} e^{-i\int_x^0 \alpha^{\frac{3}{2}}\sqrt{-x}dx}\end{aligned}$$

evaluate integral by letting y=-x, doing the integral and then renaming y as x

$$\begin{aligned}&= \frac{A}{\alpha^{\frac{3}{4}}(-x)^{\frac{1}{4}}} e^{\frac{2i}{3}(-\alpha x)^{\frac{3}{2}}} + \frac{B}{\alpha^{\frac{3}{4}}(-x)^{\frac{1}{4}}} e^{-\frac{2i}{3}(-\alpha x)^{\frac{3}{2}}} \\ &= \frac{A}{\sqrt{\alpha}(-\alpha x)^{\frac{1}{4}}} e^{\frac{2i}{3}(-\alpha x)^{\frac{3}{2}}} + \frac{B}{\sqrt{\alpha}(-\alpha x)^{\frac{1}{4}}} e^{-\frac{2i}{3}(-\alpha x)^{\frac{3}{2}}} \qquad (12.19)\end{aligned}$$

Region 2

$$\Psi_2 = \frac{D}{\sqrt{\beta}} e^{-\int_0^x \beta dx}$$

where $\beta = \alpha^{\frac{3}{2}}\sqrt{x}$

$$\begin{aligned}\Psi_2 &= \frac{D}{\alpha^{\frac{3}{4}}x^{\frac{1}{4}}} e^{-\int_0^x \sqrt{x}dx} \\ &= \frac{D}{\sqrt{x}(\alpha x)^{\frac{1}{4}}} e^{-\frac{2}{3}(\alpha x)^{\frac{3}{2}}} \qquad (12.20)\end{aligned}$$

Now at this point, compare these explicit wavefunctions to the patching wavefunctions in regions 1 and 2.

Region 2 $(x > 0)(z > 0)$

$$\begin{aligned}\Psi_p &= aA_i(z) + bB_i(z) \\ &= \frac{a}{2\sqrt{\pi}z^{\frac{1}{4}}} e^{-\frac{2}{3}z^{\frac{3}{2}}} + \frac{b}{\sqrt{\pi}z^{\frac{1}{4}}} e^{\frac{2}{3}z^{\frac{3}{2}}}\end{aligned}$$

compared to

$$\Psi_2 = \frac{D}{\sqrt{\alpha}(\alpha x)^{\frac{1}{4}}} e^{-\frac{2}{3}(\alpha x)^{\frac{3}{2}}}$$

By inspection, one can tell immediately that

$$b = 0 \qquad (12.21)$$

$$a = 2D\sqrt{\frac{\pi}{\alpha}} \qquad (12.22)$$

Now go back and do the same comparison in region 1

Region 1 $(x < 0)(z < 0)$

$$\begin{aligned} \Psi_p &= aA_i(z) \\ \Psi_p &= 2D\sqrt{\frac{\pi}{a}}A_i(z) \end{aligned}$$

where

$$\begin{aligned} A_i(z) &= \frac{1}{\sqrt{\pi}(-z)^{\frac{1}{4}}} sin(\frac{2}{3}(-z)^{\frac{3}{2}} + \frac{\pi}{4}) \\ &= \frac{1}{\sqrt{\pi}(-z)^{\frac{1}{4}}} \left(\frac{e^{i(\frac{2}{3}(-z)^{\frac{3}{2}} + \frac{\pi}{4})} - e^{-i(\frac{2}{3}(-z)^{\frac{3}{2}} + \frac{\pi}{4})}}{2i} \right) \\ &= \frac{1}{(-z)^{\frac{1}{4}}} \left(\frac{e^{i\frac{\pi}{4}}}{2i\sqrt{\pi}} e^{i\frac{2}{3}(-z)^{\frac{3}{2}}} - \frac{e^{-i\frac{\pi}{4}}}{2i\sqrt{\pi}} e^{-i\frac{2}{3}(-z)^{\frac{3}{2}}} \right) \end{aligned}$$

yielding

$$\Psi_p = \frac{1}{(-z)^{\frac{1}{4}}} \left(\frac{De^{i\frac{\pi}{4}}}{i\sqrt{\alpha}} e^{\frac{2i}{3}(-z)^{\frac{3}{2}}} - \frac{De^{-i\frac{\pi}{4}}}{i\sqrt{\alpha}} e^{-\frac{2i}{3}(-z)^{\frac{3}{2}}} \right)$$

versus

$$\Psi_1 = \frac{1}{(-\alpha x)^{\frac{1}{4}}} \left(\frac{A}{\sqrt{\alpha}} e^{\frac{2i}{3}(-\alpha x)^{\frac{3}{2}}} + \frac{B}{\sqrt{\alpha}} e^{-\frac{2i}{3}(-\alpha x)^{\frac{3}{2}}} \right)$$

Now by inspection

$$A = -iDe^{i\frac{\pi}{4}} \tag{12.23}$$

$$B = iDe^{-i\frac{\pi}{4}} \tag{12.24}$$

Now put everything together for the WKB wavefunctions we showed at the beginning of the section

$$\begin{aligned} \Psi_1 &= \frac{A}{\sqrt{k}} e^{i\int_x^0 kdx} + \frac{B}{\sqrt{k}} e^{-i\int_x^0 kdx} \text{ where } (x < 0) \\ \Psi_2 &= \frac{D}{\sqrt{\beta}} e^{-\int_0^x \beta dx} \text{ where } (x > 0) \end{aligned}$$

where now $A = -iDe^{i\frac{\pi}{4}}$ and $B = iDe^{-i\frac{\pi}{4}}$ to get

$$\Psi_1 = \frac{2D}{\sqrt{k}} sin(\frac{\pi}{4} + \int_x^0 kdx) \tag{12.25}$$

$$\Psi_2 = \frac{D}{\sqrt{\beta}} e^{-\int_0^x \beta dx} \tag{12.26}$$

Arbitrary potential drop

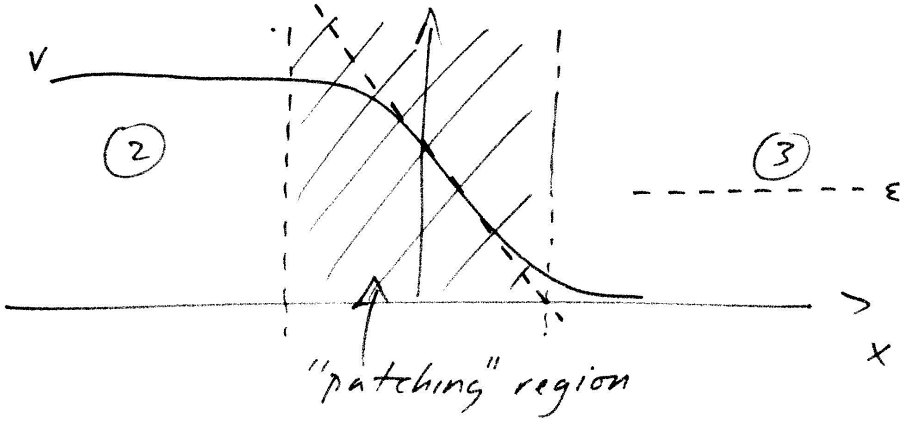

Figure 12.2: Cartoon of the arbitrary potential drop

Using our derived WKB wavefunctions we have the general form in regions 2 and 3

$$\begin{aligned}\Psi_2 &= \frac{C}{\sqrt{\beta}}e^{\int_x^0 \beta dx} + \frac{D}{\sqrt{\beta}}e^{-\int_x^0 \beta dx} \text{ where } (x<0)\\ \Psi_3 &= \frac{F}{\sqrt{k}}e^{i\int_0^x k dx} + \frac{G}{\sqrt{k}}e^{-i\int_0^x k dx} \text{ where } (x>0)\end{aligned}$$

Since we can't have the wavefunctions behave badly, $C = 0$ to prevent it from blowing up in region 2. This leaves us with t wavfunction forms

$$\begin{aligned}\Psi_2 &= \frac{D}{\sqrt{\beta}}e^{-\int_x^0 \beta dx} \\ \Psi_3 &= \frac{F}{\sqrt{k}}e^{i\int_0^x k dx} + \frac{G}{\sqrt{k}}e^{-i\int_0^x k dx}\end{aligned} \tag{12.27}$$

Now consider an approximation to the potential in the region between 2 and 3 of the linear form

$$V = (\varepsilon - V^{'}x) \tag{12.28}$$

First we determine the patching wavefunctions in the region between 2 and 3. Starting with Schrodinger's equation (if you went thorough the last section

all of what follows will be familiar)

$$\begin{aligned} -\frac{\hbar^2}{2m}\frac{d^2\Psi_p}{dx^2} + V\Psi_p &= \varepsilon\Psi_p \\ -\frac{\hbar^2}{2m}\frac{d^2\Psi_p}{dx^2} + (\varepsilon - V^{'}x)\Psi_p &= \varepsilon\Psi_p \\ -\frac{\hbar^2}{2m}\frac{d^2\Psi_p}{dx^2} - V^{'}x\Psi_p &= 0 \\ \frac{d^2\Psi_p}{dx^2} + \frac{2mV^{'}x}{\hbar^2}\Psi_p &= 0 \end{aligned}$$

Let $\alpha^3 = \frac{2mV^{'}}{\hbar^2}$ leading to

$$\frac{d^2\Psi_p}{dx^2} + \alpha^3 x\Psi_p = 0$$

Now let $z = -\alpha x$

$$\frac{d^2\Psi_p}{dz^2} = z\Psi_p \tag{12.29}$$

Again, this is the Airy equation with accompanying Airy functions. The general solution is a linear combination of the form

$$\Psi_p = aA_i(z) + bB_i(z) \tag{12.30}$$

where a and b are constants.

In region 2

$$\beta = \sqrt{\frac{2m(V-\varepsilon)}{\hbar^2}}$$

where $V = \varepsilon - V^{'}x$

$$\begin{aligned} &= \sqrt{\frac{2mV^{'}}{\hbar^2}}\sqrt{-x} \\ &= \alpha^{\frac{3}{2}}\sqrt{-x} \end{aligned} \tag{12.31}$$

In region 3

$$\begin{aligned} k &= \sqrt{\frac{2m(\varepsilon - V)}{\hbar^2}} \\ &= \sqrt{\frac{2mV^{'}}{\hbar^2}}\sqrt{x} \\ &= \alpha^{\frac{3}{2}}\sqrt{x} \end{aligned} \tag{12.32}$$

Now with β and k go back and make more explicit our wavefunctions in regions 2 and 3.

Region 2

$$\begin{aligned}\Psi_2 &= \frac{D}{\sqrt{\beta}}e^{-\int_x^0 \beta dx} \\ &= \frac{D}{\alpha^{\frac{3}{4}}(-x)^{\frac{1}{4}}}e^{-\alpha^{\frac{3}{2}}\int_x^0 (-x)^{\frac{1}{2}}dx}\end{aligned}$$

solve the integral by letting y=-x, integrating and then renaming y=x

$$= \frac{D}{\sqrt{\alpha}(-\alpha x)^{\frac{1}{4}}}e^{-\frac{2}{3}(-\alpha x)^{\frac{3}{2}}} \tag{12.33}$$

Region 3

$$\begin{aligned}\Psi_3 &= \frac{F}{\sqrt{k}}e^{i\int_0^x kdx} + \frac{G}{\sqrt{k}}e^{-i\int_0^x kdx} \\ &= \frac{F}{\sqrt{\alpha}(\alpha x)^{\frac{1}{4}}}e^{\int_0^x \alpha^{\frac{3}{2}}x^{\frac{1}{2}}dx} + \frac{G}{\sqrt{\alpha}(\alpha x)^{\frac{1}{4}}}e^{-\int_0^x \alpha^{\frac{3}{2}}x^{\frac{1}{2}}dx} \\ &= \frac{F}{\sqrt{\alpha}(\alpha x)^{\frac{1}{4}}}e^{\frac{2i}{3}(\alpha x)^{\frac{3}{2}}} + \frac{G}{\sqrt{\alpha}(\alpha x)^{\frac{1}{4}}}e^{-\frac{2i}{3}(\alpha x)^{\frac{3}{2}}} \qquad (12.34)\end{aligned}$$

Now compare these explicit wavefunctions to the patching wavefunctions in regions 2 and 3

Region 2 $(x < 0)$ $(z > 0)$ since $(z = -\alpha x)$

$$\begin{aligned}\Psi_p &= aA_i(z) + bB_i(z) \\ &= \frac{a}{2\sqrt{\pi}z^{\frac{1}{4}}}e^{-\frac{2}{3}z^{\frac{3}{2}}} + \frac{b}{\sqrt{\pi}z^{\frac{1}{4}}}e^{\frac{2}{3}z^{\frac{3}{2}}}\end{aligned}$$

versus

$$\Psi_2 = \frac{D}{\sqrt{\alpha}(-\alpha x)^{\frac{1}{4}}}e^{-\frac{2}{3}(-\alpha x)^{\frac{3}{2}}}$$

By insepction

$$b = 0 \tag{12.35}$$

$$a = 2D\sqrt{\frac{\pi}{\alpha}} \tag{12.36}$$

Region 1 $(x > 0)$ $(z < 0)$ since $(z = -\alpha x)$

$$\begin{aligned}
\Psi_p &= aA_i(z) \\
&= 2D\sqrt{\frac{\pi}{\alpha}}A_i(z) \\
&= \frac{a}{\sqrt{\pi}(-z)^{\frac{1}{4}}}sin(\frac{2}{3}(-z)^{\frac{3}{2}} + \frac{\pi}{4}) \\
&= \frac{a}{\sqrt{\pi}(-z)^{\frac{1}{4}}}\left(\frac{e^{i\frac{\pi}{4}}e^{\frac{2i}{3}(-z)^{\frac{3}{2}}} - e^{-i\frac{\pi}{4}}e^{-\frac{2i}{3}(-z)^{\frac{3}{2}}}}{2i}\right) \\
&= \frac{1}{(-z)^{\frac{1}{4}}}\left(\frac{ae^{i\frac{\pi}{4}}}{\sqrt{\pi}2i}e^{\frac{2i}{3}(-z)^{\frac{3}{2}}} - \frac{ae^{-i\frac{\pi}{4}}}{\sqrt{\pi}2i}e^{-\frac{2i}{3}(-z)^{\frac{3}{2}}}\right)
\end{aligned}$$

versus

$$\Psi_3 = \frac{1}{(\alpha x)^{\frac{1}{4}}}\left(\frac{F}{\sqrt{\alpha}}e^{\frac{2i}{3}(\alpha x)^{\frac{3}{2}}} + \frac{G}{\sqrt{\alpha}}e^{-\frac{2i}{3}(\alpha x)^{\frac{3}{2}}}\right)$$

By inspection

$$F = -iDe^{i\frac{\pi}{4}} \tag{12.37}$$

$$G = iDe^{-i\frac{\pi}{4}} \tag{12.38}$$

Now put everything together for the WKB wavefunctions we saw at the beginning of the section

$$\begin{aligned}
\Psi_2 &= \frac{D}{\sqrt{\beta}}e^{-\int_x^0 \beta dx} \\
\Psi_3 &= \frac{F}{\sqrt{k}}e^{i\int_0^x kdx} + \frac{G}{\sqrt{k}}e^{-i\int_0^x kdx}
\end{aligned}$$

where now $F = -iDe^{i\frac{\pi}{4}}$ and $G = iDe^{-i\frac{\pi}{4}}$ leading to

$$\Psi_2 = \frac{D}{\sqrt{\beta}}e^{-\int_x^0 \beta dx} \tag{12.39}$$

$$\Psi_3 = \frac{2D}{\sqrt{k}}sin(\frac{\pi}{4} + \int_0^x kdx) \tag{12.40}$$

Arbitrary potential barrier

This next section basically puts together all the work we did in the previous two sections for the arbitrary potential step and potential drop. The combination of both is the potential barrier.

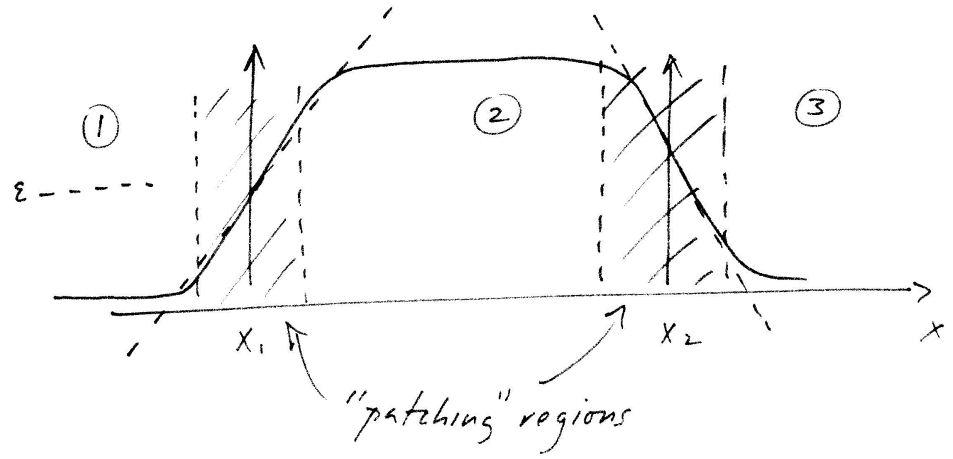

Figure 12.3: Cartoon of the arbitrary potential barrier

The solution for the transmission coefficient will lead to the general form of the tunneling probability that is ubiquitous in textbooks, in the literature and in experiments like scanning tunneling microscopy. The derivation involves a lot of tortuous math but follows the same train of thought as used in the earlier two sections.

Picture an arbitrary barrier of the form shown below. Now the general form of the WKB wavefunctions as derived earlier is

$$\Psi_1 = \frac{A}{\sqrt{k}} e^{i\int_x^{x_1} k dx} + \frac{B}{\sqrt{k}} e^{-i\int_x^{x_1} k dx} \text{ where } (x < x_1) \tag{12.41}$$

$$\Psi_2 = \frac{C}{\sqrt{\beta}} e^{\int_{x_1}^{x} \beta dx} + \frac{D}{\sqrt{\beta}} e^{-\int_{x_1}^{x} \beta dx} \text{ where } (x_1 < x < x_2) \tag{12.42}$$

$$\Psi_3 = \frac{F}{\sqrt{k}} e^{i\int_{x_2}^{x} k dx} \text{ where } (x > x_2) \tag{12.43}$$

Since there are no sources of particles on the right everything moves in a left to right direction and hence Ψ_3 has only one component above.

Remember in what follows that ultimately what we want to solve for is

$$T = \frac{v_3|F|^2}{v_1|A|^2} = \frac{k|F|^2}{k|A|^2} = \frac{|F|^2}{|A|^2}$$

You will find that our strategy is to express A in terms of F.

First we determine the patching wavefunction in the boundary region between 1 and 2. Starting with the Schrodinger equation

$$\begin{aligned} -\frac{\hbar^2}{2m}\frac{d^2\Psi_p}{dx^2} + V\Psi_p &= \varepsilon\Psi_p \\ -\frac{\hbar^2}{2m}\frac{d^2\Psi_p}{dx^2} + (\varepsilon + V^{'}x)\Psi_p &= \varepsilon\Psi_p \\ -\frac{\hbar^2}{2m}\frac{d^2\Psi_p}{dx^2} + V^{'}x\Psi_p &= 0 \\ \frac{d^2\Psi_p}{dx^2} - \frac{2mV^{'}x}{\hbar^2}\Psi_p &= 0 \end{aligned}$$

Let $\alpha^3 = \frac{2mV^{'}}{\hbar^2}$ resulting in

$$\frac{d^2\Psi_p}{dx^2} = \alpha^3 x\Psi_p$$

Now let $z = \alpha x$

$$\frac{d^2\Psi_p}{dz^2} = z\Psi_p$$

As before, this is the Airy equation whose general solution is a linear combination of Airy functions

$$\Psi_p = aA_i(z) + bB_i(z)$$

Now in the left part of region 2 (bordering region 1)

$$\begin{aligned} \beta &= \sqrt{\frac{2m(V-\varepsilon)}{\hbar^2}} \\ &= \sqrt{\frac{2mV^{'}}{\hbar^2}}\sqrt{x} \\ &= \alpha^{\frac{3}{2}}\sqrt{x} \end{aligned} \tag{12.44}$$

In the right part of region 1 (bordering region 2)

$$\begin{aligned} k &= \sqrt{\frac{2m(\varepsilon-V)}{\hbar^2}} \\ &= \sqrt{\frac{2mV^{'}}{\hbar^2}}\sqrt{-x} \\ &= \alpha^{\frac{3}{2}}\sqrt{-x} \end{aligned} \tag{12.45}$$

Now go back to the wavefunctions in regions 1 and 2 and make them more explicit using the above. Starting with

$$\begin{aligned}\Psi_1 &= \frac{A}{\sqrt{k}}e^{i\int_x^{x_1} k dx} + \frac{B}{\sqrt{k}}e^{-i\int_x^{x_1} k dx} \\ \Psi_2 &= \frac{C}{\sqrt{\beta}}e^{\int_{x_1}^{x} \beta dx} + \frac{D}{\sqrt{\beta}}e^{-\int_{x_1}^{x} \beta dx}\end{aligned}$$

temporarily shift the origin to x_1 (i.e. $x_1 = 0$). Then this basically becomes the same problem that we solved earlier. After we are done we can shift back the origin to where it used to be. First wavefunction

$$\Psi_1 = \frac{A}{\alpha^{\frac{3}{4}}(-x)^{\frac{1}{4}}}e^{i\int_x^0 \alpha^{\frac{3}{2}}\sqrt{-x}dx} + \frac{B}{\alpha^{\frac{3}{4}}(-x)^{\frac{1}{4}}}e^{-i\int_x^0 \alpha^{\frac{3}{2}}\sqrt{-x}dx}$$

solve integral by letting y=-x, integrate then rename y=x

$$= \frac{A}{\sqrt{\alpha}(-\alpha x)^{\frac{1}{4}}}e^{\frac{2i}{3}(-\alpha x)^{\frac{3}{2}}} + \frac{B}{\sqrt{\alpha}(-\alpha x)^{\frac{1}{4}}}e^{-\frac{2i}{3}(-\alpha x)^{\frac{3}{2}}} \tag{12.46}$$

Second wavefunction

$$\begin{aligned}\Psi_2 &= \frac{C}{\sqrt{\alpha}(\alpha x)^{\frac{1}{4}}}e^{\int_0^x \alpha^{\frac{3}{2}}\sqrt{x}dx} + \frac{D}{\sqrt{\alpha}(\alpha x)^{\frac{1}{4}}}e^{-\int_0^x \alpha^{\frac{3}{2}}\sqrt{x}dx} \\ &= \frac{C}{\sqrt{\alpha}(\alpha x)^{\frac{1}{4}}}e^{\frac{2}{3}(\alpha x)^{\frac{3}{2}}} + \frac{D}{\sqrt{\alpha}(\alpha x)^{\frac{1}{4}}}e^{-\frac{2}{3}(\alpha x)^{\frac{3}{2}}} \qquad (12.47)\end{aligned}$$

Now compare these explicit wavefunctions with the patching wavefunction.

Left part of region 2 (bordering region 1) $(x > 0)$ $(z > 0)$

$$\begin{aligned}\Psi_p &= aA_i(z) + bB_i(z) \\ &= \frac{a}{2\sqrt{\pi}z^{\frac{1}{4}}}e^{-\frac{2}{3}z^{\frac{3}{2}}} + \frac{b}{\sqrt{\pi}z^{\frac{1}{4}}}e^{\frac{2}{3}z^{\frac{3}{2}}}\end{aligned}$$

versus

$$\Psi_2 = \frac{C}{\sqrt{\alpha}(\alpha x)^{\frac{1}{4}}}e^{\frac{2}{3}(\alpha x)^{\frac{3}{2}}} + \frac{D}{\sqrt{\alpha}(\alpha x)^{\frac{1}{4}}}e^{-\frac{2}{3}(\alpha x)^{\frac{3}{2}}}$$

By inspection

$$b = C\sqrt{\frac{\pi}{\alpha}} \tag{12.48}$$

$$a = 2D\sqrt{\frac{\pi}{\alpha}} \tag{12.49}$$

Right part of region 1 (bordering region 2) $(x < 0)$ $(z < 0)$

$$\begin{aligned}
\Psi_p &= aA_i(z) + bB_i(z) \\
&= 2D\sqrt{\frac{\pi}{\alpha}}A_i(z) + C\sqrt{\frac{\pi}{\alpha}}B_i(z) \\
&= 2D\sqrt{\frac{\pi}{\alpha}}\frac{1}{\sqrt{\pi}(-z)^{\frac{1}{4}}}sin(\frac{2}{3}(-z)^{\frac{3}{2}} + \frac{\pi}{4}) + C\sqrt{\frac{\pi}{\alpha}}\frac{1}{\sqrt{\pi}(-z)^{\frac{1}{4}}}cos(\frac{2}{3}(-z)^{\frac{3}{2}} + \frac{\pi}{4}) \\
&= \frac{2D}{\sqrt{\alpha}(-z)^{\frac{1}{4}}}sin(\frac{2}{3}(-z)^{\frac{3}{2}} + \frac{\pi}{4}) + \frac{C}{\sqrt{\alpha}(-z)^{\frac{1}{4}}}cos(\frac{2}{3}(-z)^{\frac{3}{2}} + \frac{\pi}{4})
\end{aligned}$$

skipping some steps

$$\begin{aligned}
&= \frac{1}{\sqrt{\alpha}(-z)^{\frac{1}{4}}}\left(\frac{1}{2}\left(\frac{2D}{i} + C\right)\right)e^{i(\frac{\pi}{4}+\frac{2}{3}(-z)^{\frac{3}{2}})} \\
&+ \frac{1}{\sqrt{\alpha}(-z)^{\frac{1}{4}}}\left(\frac{1}{2}\left(-\frac{2D}{i} + C\right)\right)e^{-i(\frac{\pi}{4}+\frac{2}{3}(-z)^{\frac{3}{2}})} \\
&= \frac{1}{\sqrt{\alpha}(-z)^{\frac{1}{4}}}\left(\frac{e^{i\frac{\pi}{4}}}{2}\left(\frac{2D}{i} + C\right)\right)e^{\frac{2i}{3}(-z)^{\frac{3}{2}}} \\
&+ \frac{1}{\sqrt{\alpha}(-z)^{\frac{1}{4}}}\left(\frac{e^{-i\frac{\pi}{4}}}{2}\left(-\frac{2D}{i} + C\right)\right)e^{-\frac{2i}{3}(-z)^{\frac{3}{2}}}
\end{aligned}$$

compared to

$$\Psi_1 = \frac{A}{\sqrt{\alpha}(-\alpha x)^{\frac{1}{4}}}e^{\frac{2i}{3}(\alpha x)^{\frac{3}{2}}} + \frac{B}{\sqrt{\alpha}(-\alpha x)^{\frac{1}{4}}}e^{-\frac{2i}{3}(\alpha x)^{\frac{3}{2}}}$$

By inspection

$$A = \frac{e^{i\frac{\pi}{4}}}{2}\left(\frac{2D}{i} + C\right) \tag{12.50}$$

$$B = \frac{e^{-i\frac{\pi}{4}}}{2}\left(-\frac{2D}{i} + C\right) \tag{12.51}$$

Now consider the interface between regions 2 and 3. The potential here can be modeled in a linear fashion

$$V = (\varepsilon - V^{'}x) \tag{12.52}$$

First determine the patching wavefucntion in the boundary region. Start with Schrodinger's equation again

$$-\frac{\hbar^2}{2m}\frac{d^2\Psi_p}{dx^2} + V\Psi_p = \varepsilon\Psi_p$$

$$\begin{aligned} -\frac{\hbar^2}{2m}\frac{d^2\Psi_p}{dx^2} + (\varepsilon - V^{'}x\Psi_p) &= \varepsilon\Psi_p \\ -\frac{\hbar^2}{2m}\frac{d^2\Psi_p}{dx^2} - V^{'}x\Psi_p &= 0 \\ \frac{d^2\Psi_p}{dx^2} + \frac{2mV^{'}x}{\hbar^2}x\Psi_p &= 0 \end{aligned}$$

Let $\alpha^3 = \frac{2mV^{'}}{\hbar^2}$ giving

$$\frac{d^2\Psi_p}{dx^2} + \alpha^3 x\Psi_p = 0$$

Now let $z = -\alpha x$ resulting in

$$\frac{d^2\Psi_p}{dz^2} = z\Psi_p$$

This is the Airy equation again with the general solution being a combination of Airy functions.

$$\Psi_p = aA_i(z) + bB_i(z)$$

Now in the right part of region 2 (bordering region 3)

$$\begin{aligned} \beta &= \sqrt{\frac{2m(V-\varepsilon)}{\hbar^2}} \\ &= \sqrt{\frac{2mV^{'}}{\hbar^2}}\sqrt{-x} \\ &= \alpha^{\frac{3}{2}}\sqrt{-x} \end{aligned} \tag{12.53}$$

were recall $V = \varepsilon - V^{'}x$

Now in the left part of region 3 (bordering region 2)

$$\begin{aligned} k &= \sqrt{\frac{2m(\varepsilon-V)}{\hbar^2}} \\ &= \sqrt{\frac{2mV^{'}}{\hbar^2}}\sqrt{x} \\ &= \alpha^{\frac{3}{2}}\sqrt{x} \end{aligned} \tag{12.54}$$

Now go back to the wavefunctions in regions 2 and 3 and make them explicit.

$$\begin{aligned}\Psi_2 &= \frac{C}{\sqrt{\beta}}e^{\int_{x_1}^{x}\beta dx} + \frac{D}{\sqrt{\beta}}e^{-\int_{x_1}^{x}\beta dx} \\ \Psi_3 &= \frac{F}{\sqrt{k}}e^{i\int_{x_2}^{x}k dx}\end{aligned}$$

rearrange wavefunctions to get

$$\begin{aligned}\Psi_2 &= \frac{C}{\sqrt{\beta}}e^{\int_{x_1}^{x_2}\beta dx+\int_{x_2}^{x}\beta dx} + \frac{D}{\sqrt{\beta}}e^{-\int_{x_1}^{x_2}\beta dx-\int_{x_2}^{x}\beta dx} \\ \Psi_3 &= \frac{F}{\sqrt{k}}e^{i\int_{x_2}^{x}k dx}\end{aligned}$$

now let $\gamma = \int_{x_1}^{x_2}\beta dx$

$$\Psi_2 = \frac{C}{\sqrt{\beta}}e^{\gamma}e^{\int_{x_2}^{x}\beta dx} + \frac{D}{\sqrt{\beta}}e^{-\gamma}e^{\int_{x_2}^{x}\beta dx} \tag{12.55}$$

$$\Psi_3 = \frac{F}{\sqrt{k}}e^{i\int_{x_2}^{x}k dx} \tag{12.56}$$

Now temporarily translate the origin to x_2 (i.e. $x_2 = 0$). This leads to

$$\begin{aligned}\Psi_2 &= \frac{C}{\sqrt{\beta}}e^{\gamma}e^{\int_{0}^{x}\beta dx} + \frac{D}{\sqrt{\beta}}e^{-\gamma}e^{\int_{0}^{x}\beta dx} \\ \Psi_3 &= \frac{F}{\sqrt{k}}e^{i\int_{0}^{x}k dx}\end{aligned}$$

Now we use the derived explicit forms for β and k to get explicit forms for the wavefunctions. First wavefunction

$$\Psi_2 = \frac{C}{\sqrt{\alpha}(-\alpha x)^{\frac{1}{4}}}e^{\gamma}e^{\int_0^x \alpha^{\frac{3}{2}}\sqrt{-x}dx} + \frac{D}{\sqrt{\alpha}(-\alpha x)^{\frac{1}{4}}}e^{-\gamma}e^{-\int_0^x \alpha^{\frac{3}{2}}\sqrt{-x}dx}$$

solve the integral by letting y=-x, integrating, then rename y=x

$$= \frac{Ce^{\gamma}}{\sqrt{\alpha}(-\alpha x)^{\frac{1}{4}}}e^{-\frac{2}{3}(-\alpha x)^{\frac{3}{2}}} + \frac{De^{-\gamma}}{\sqrt{\alpha}(-\alpha x)^{\frac{1}{4}}}e^{\frac{2}{3}(-\alpha x)^{\frac{3}{2}}} \tag{12.57}$$

Second wavefunction

$$\begin{aligned}\Psi_3 &= \frac{F}{\sqrt{\alpha}(\alpha x)^{\frac{1}{4}}}e^{i\int_0^x \alpha^{\frac{3}{2}}\sqrt{x}dx} \\ &= \frac{F}{\sqrt{\alpha}(\alpha x)^{\frac{1}{4}}}e^{\frac{2i}{3}(\alpha x)^{\frac{3}{2}}}\end{aligned} \tag{12.58}$$

Now compare these explicit wavefunctions to the patching wavefunction
Right side of region 2 (bordering region 3) $(x < 0)$ $(z > 0)$

$$\begin{aligned}\Psi_p &= aA_i(z) + bB_i(z) \\ &= \frac{a}{2\sqrt{\pi}z^{\frac{1}{4}}}e^{-\frac{2}{3}z^{\frac{3}{2}}} + \frac{b}{\sqrt{\pi}z^{\frac{1}{4}}}e^{\frac{2}{3}z^{\frac{3}{2}}}\end{aligned}$$

compared to

$$\Psi_2 = \frac{Ce^{\gamma}}{\sqrt{\alpha}(-\alpha x)^{\frac{1}{4}}}e^{-\frac{2}{3}(-\alpha x)^{\frac{3}{2}}} + \frac{De^{-\gamma}}{\sqrt{\alpha}(-\alpha x)^{\frac{1}{4}}}e^{\frac{2}{3}(-\alpha x)^{\frac{3}{2}}}$$

By inspection

$$a = 2C\sqrt{\frac{\pi}{\alpha}}e^{\gamma} \tag{12.59}$$

$$b = D\sqrt{\frac{\pi}{\alpha}}e^{-\gamma} \tag{12.60}$$

Left side of region 3 (bordering region 2) $(x > 0)$ $(z < 0)$

$$\begin{aligned}\Psi_p &= aA_i(z) + bB_i(z) \\ &= 2C\sqrt{\frac{\pi}{\alpha}}e^{\gamma}A_i(z) + D\sqrt{\frac{\pi}{\alpha}}e^{-\gamma}B_i(z) \\ &= \frac{2Ce^{\gamma}}{\sqrt{\alpha}(-z)^{\frac{1}{4}}}sin(\frac{2}{3}(-z)^{\frac{3}{2}} + \frac{\pi}{4}) + \frac{De^{-\gamma}}{\sqrt{\alpha}(-z)^{\frac{1}{4}}}cos(\frac{2}{3}(-z)^{\frac{3}{2}} + \frac{\pi}{4})\end{aligned}$$

$$\begin{aligned}&= \frac{2Ce^{\gamma}}{\sqrt{\alpha}(-z)^{\frac{1}{4}}}\left(\frac{e^{i\frac{\pi}{4}}e^{\frac{2i}{3}(-z)^{\frac{3}{2}}} - e^{-i\frac{\pi}{4}}e^{-\frac{2i}{3}(-z)^{\frac{3}{2}}}}{2i}\right) \\ &+ \frac{De^{-\gamma}}{\sqrt{\alpha}(-z)^{\frac{1}{4}}}\left(\frac{e^{i\frac{\pi}{4}}e^{\frac{2i}{3}(-z)^{\frac{3}{2}}} + e^{-i\frac{\pi}{4}}e^{-\frac{2i}{3}(-z)^{\frac{3}{2}}}}{2}\right)\end{aligned}$$

$$\begin{aligned}&= \frac{1}{\sqrt{\alpha}(-z)^{\frac{1}{4}}}\left(\frac{1}{2}\left(\frac{2Ce^{\gamma}}{i} + De^{-\gamma}\right)e^{i\frac{\pi}{4}}\right)e^{\frac{2i}{3}(-z)^{\frac{3}{2}}} \\ &+ \frac{1}{\sqrt{\alpha}(-z)^{\frac{1}{4}}}\left(\frac{1}{2}\left(\frac{-2Ce^{\gamma}}{i} + De^{-\gamma}\right)e^{-i\frac{\pi}{4}}\right)e^{-\frac{2i}{3}(-z)^{\frac{3}{2}}}\end{aligned}$$

compare this to

$$\Psi_3 = \frac{F}{\sqrt{\alpha}(\alpha x)^{\frac{1}{4}}} e^{\frac{2i}{3}(\alpha x)^{\frac{3}{2}}}$$

By inspection

$$F = \frac{e^{i\frac{\pi}{4}}}{2}\left(\frac{2Ce^{\gamma}}{i} + De^{-\gamma}\right) \tag{12.61}$$

or more importantly

$$\frac{1}{2}\left(\frac{-2Ce^{\gamma}}{i} + De^{-\gamma}\right) e^{-i\frac{\pi}{4}} = 0$$

yielding

$$C = \frac{iF}{2} e^{-i\frac{\pi}{4}} e^{-\gamma} \tag{12.62}$$

$$D = Fe^{-i\frac{\pi}{4}} e^{\gamma} \tag{12.63}$$

Finally these expression can be inserted into our expression for A derived earlier.

$$\begin{aligned} A &= \frac{e^{i\frac{\pi}{4}}}{2}\left(\frac{2D}{i} + C\right) \\ &= iF\left(\frac{e^{-\gamma}}{4} - e^{\gamma}\right) \end{aligned} \tag{12.64}$$

Now the transmission coefficient is

$$\begin{aligned} T &= \frac{v_3|F|^2}{v_1|A|^2} = \frac{k|F|^2}{k|A|^2} = \frac{|F|^2}{|A|^2} = \frac{F^*F}{A^*A} \\ &= \frac{F^2}{F^2\left(\frac{e^{-\gamma}}{4} - e^{\gamma}\right)^2} = \frac{1}{\left(\frac{e^{-\gamma}}{4} - e^{\gamma}\right)^2} \\ &= \frac{1}{e^{2\gamma}\left(\frac{e^{-2\gamma}}{4} - 1\right)^2} = \frac{e^{-2\gamma}}{\left(\frac{e^{-2\gamma}}{4} - 1\right)^2} \\ &= \frac{e^{-2\gamma}}{\left(1 - \frac{e^{-2\gamma}}{4}\right)^2} \end{aligned}$$

So after all this effort, the transmission coefficient has the form

$$T = \frac{e^{-2\gamma}}{\left(1 - \frac{e^{-2\gamma}}{4}\right)^2} \tag{12.65}$$

which in the case of large γ reduces to the ubiquitous textbook and literature expression

$$\boxed{T \approx e^{-2\gamma}} \tag{12.66}$$

where $\gamma = \int_{x_1}^{x_2} \beta dx$ and $\beta = \sqrt{\frac{2m(V-\varepsilon)}{\hbar^2}}$. No mas!

Example: Field emission

Also known as Fowler Nordheim tunneling. Assume a triangular form of the barrier where

$$(V - \varepsilon) = \phi\left(1 - \frac{x}{a}\right) \tag{12.67}$$

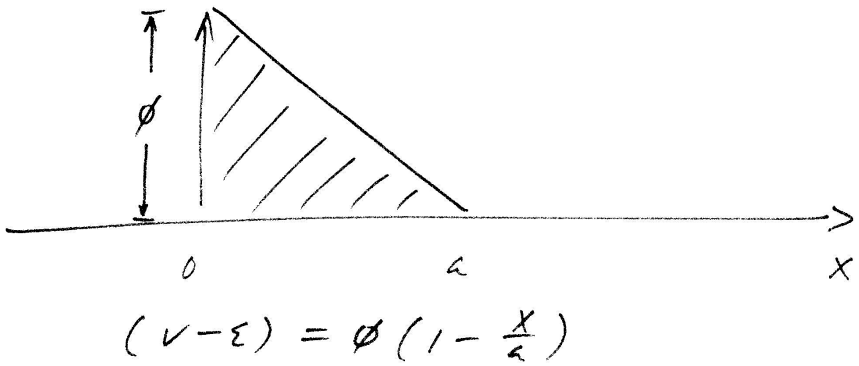

Figure 12.4: Sketch of the triangular barrier considered in field emission or Fowler Nordheim tunneling.

From the WKB approximation derived above

$$T \sim e^{-2\gamma}$$

where $\gamma = \int_0^a \sqrt{\frac{2m(V-\varepsilon)}{\hbar}} dx$. This leads to

$$\begin{aligned} T &= e^{-\frac{2}{\hbar}\sqrt{2m}\int_0^a \sqrt{V-\varepsilon}\ dx} \\ &= e^{-\frac{2}{\hbar}\sqrt{2m}\int_0^a \sqrt{\phi\left(1-\frac{x}{a}\right)} dx} \\ &= e^{-\frac{2}{\hbar}\sqrt{2m}\int_0^a \sqrt{\phi-\frac{\phi x}{a}} dx} \end{aligned}$$

Integrate the exponent to get

$$\begin{aligned} -\frac{2}{\hbar}\sqrt{2m}\int_0^a \sqrt{\phi - \frac{\phi x}{a}} &= \frac{2}{\hbar}\sqrt{2m}\left(\frac{a}{\phi}\right)\left(\phi - \frac{\phi x}{a}\right)^{\frac{3}{2}}\frac{2}{3}\Bigg|_0^a \\ &= \frac{4}{3}\frac{\sqrt{2m}}{\hbar}\frac{a}{\phi}\phi^{\frac{3}{2}} \\ &= \frac{4}{3}\frac{\sqrt{2m}}{\hbar}\frac{1}{\vec{E}}\phi^{\frac{3}{2}} \end{aligned}$$

where $\vec{E} = \frac{\phi}{a}$ is the electric field. This leads to our final expression

$$\boxed{T = e^{-\frac{4}{3}\frac{\sqrt{2m}}{\hbar}\frac{\phi^{\frac{3}{2}}}{\vec{E}}}} \tag{12.68}$$

You can see that the tunneling probability depends to the 3/2 power of the barrier height. This is the underlying relation behind the Fowler Nordheim tunneling model.

Example: Schottky barrier

This problem arises when one has a metal-semiconductor junction. Here

$$(V - \varepsilon) \approx \phi\left(1 - \left(\frac{x}{a}\right)^2\right) \tag{12.69}$$

From the WKB approximation

$$T = e^{-2\gamma}$$

where $\gamma = \int_0^a \sqrt{\frac{2m(V-\varepsilon)}{\hbar}}dx$. This leads to

$$\begin{aligned} T &= e^{-\frac{2}{\hbar}\int_0^a \sqrt{2m\phi\left(1-\left(\frac{x}{a}\right)^2\right)}dx} \\ &= e^{-\frac{2}{\hbar}\sqrt{2m\phi}\int_0^a \sqrt{1-(\frac{x}{a})^2}dx} \end{aligned}$$

Let $y = \frac{x}{a}$ where also $dx = ady$. Don't forget the limits of integration change as well.

$$\begin{aligned} T &= e^{-\frac{2}{\hbar}\sqrt{2m\phi}\int_0^1 \sqrt{1-y^2}ady} \\ &= e^{-\frac{2}{\hbar}a\sqrt{2m\phi}\int_0^1 \sqrt{1-y^2}dy} \end{aligned}$$

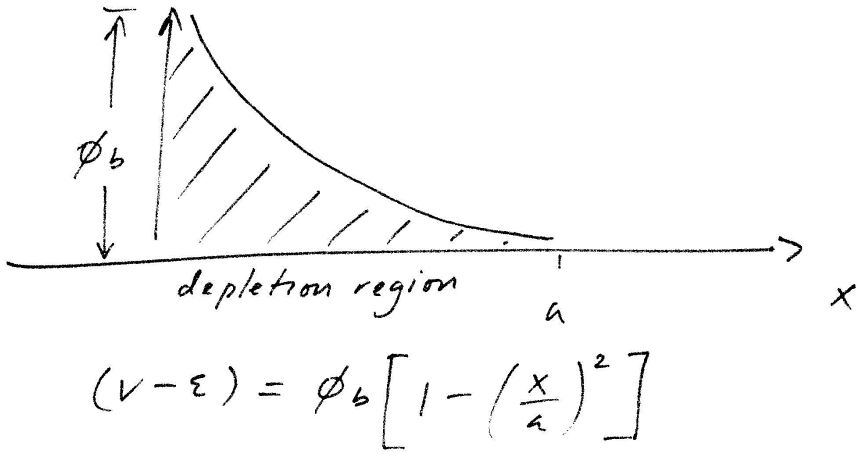

Figure 12.5: Sketch of the Shottky barrier

To integrate, make another change of variables. Let $y = sin(\theta)$; $dy = cos(\theta)d\theta$

$$T = e^{-\frac{2}{\hbar}a\sqrt{2m\phi}\int_0^{\frac{\pi}{2}} cos^2(\theta)d\theta}$$

where $cos^2(\theta) = \frac{1}{2}(1 + cos(2\theta))$

$$T = e^{-\frac{2}{\hbar}a\sqrt{2m\phi}\frac{1}{2}\int_0^{\frac{\pi}{2}}(1+cos(2\theta))d\theta}$$

giving our final expression

$$\boxed{T = e^{-a\frac{\pi}{2}\sqrt{\frac{2m\phi}{\hbar^2}}}} \tag{12.70}$$

Here one notices that the tunneling probability varies as the square root of the barrier height, $\phi^{\frac{1}{2}}$.

Example: Symmetric parabolic barrier

Here

$$(V - \varepsilon) = C\left(\frac{a^2}{4} - x^2\right) \tag{12.71}$$

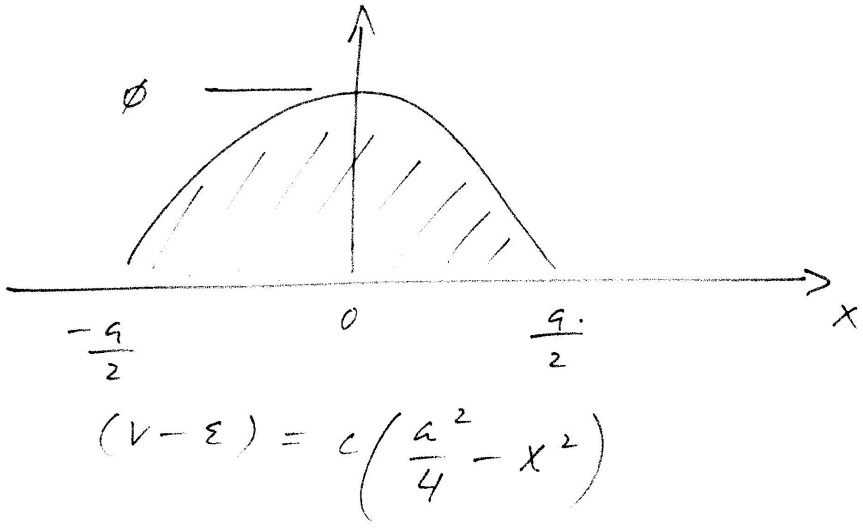

Figure 12.6: Sketch of an arbitrary symmetric parabolic barrier

where C is a constant with appropriate units.

From the WKB approximation, the tunneling probability through this barrier is

$$T = e^{-2\gamma}$$

where $\gamma = \int_0^a \sqrt{\frac{2m(V-\varepsilon)}{\hbar}}dx$. This leads to

$$T = e^{-\frac{2}{\hbar}\int_{\frac{-a}{2}}^{\frac{a}{2}} \sqrt{2mC\left(\frac{a^2}{4}-x^2\right)}dx}$$

Evaluate the exponent

$$-\frac{2\sqrt{2mC}}{\hbar}\int_{\frac{-a}{2}}^{\frac{a}{2}} \sqrt{\frac{a^2}{4} - x^2}dx$$

Let $x = \frac{a}{2}sin\theta$, $dx = \frac{a}{2}cos\theta d\theta$. Also change the limits. The expoenent becomes

$$-\frac{2\sqrt{2mC}}{\hbar}\int_{\frac{-\pi}{2}}^{\frac{\pi}{2}} \sqrt{\frac{a^2}{4} - \frac{a^2}{4}sin^2\theta}\left(\frac{a}{2}cos\theta\right)d\theta$$

$$
\begin{aligned}
&= -\frac{2\sqrt{2mC}}{\hbar}\int_{\frac{-\pi}{2}}^{\frac{\pi}{2}}\left(\frac{a}{2}\right)^2\sqrt{1-sin^2\theta}(cos\theta)d\theta \\
&= -\frac{2\sqrt{2mC}}{\hbar}\frac{a^2}{4}\int_{\frac{-\pi}{2}}^{\frac{\pi}{2}}cos^2\theta d\theta \\
&= -\frac{\sqrt{2mC}a^2}{2\hbar}\int_{\frac{-\pi}{2}}^{\frac{\pi}{2}}cos^2\theta d\theta
\end{aligned}
$$

where $cos^2\theta = \frac{1}{2}(1+cos2\theta)$

$$
\begin{aligned}
&= -\frac{\sqrt{2mC}a^2}{4\hbar}\int_{\frac{-\pi}{2}}^{\frac{\pi}{2}}1+cos2\theta d\theta \\
&= -\frac{\sqrt{2mC}a^2\pi}{4\hbar} \\
&= -\frac{\sqrt{2m}\pi}{\hbar\sqrt{C}}\phi
\end{aligned}
$$

where ϕ the barrier height is $\phi = C\left(\frac{a^2}{4}\right)$. This leads to our final expression

$$\boxed{T = e^{-\sqrt{\frac{2m}{C}}\frac{\pi}{\hbar}\phi}} \tag{12.72}$$

where the tunneling probability depends upon ϕ alone rather than to some power of it.

Exercises

1. Derive the transmission probability of a particle through a rectangular barrier of height V_o and width l.

2. Assume a rectangular barrier of height 4 eV and width 2 nm. For a free electron what is the tunneling probability through this barrier using a WKB formalism.

3. For the same 4 eV barrier and electron mass, what is the tunneling probability when the barrier width is increased by 50%. What is the probablity when the barrier width is decreased by 50%.

4. For the same 2 nm wide barrier and electron mass, what is the tunneling probability when the barrier height is increased by 50%. What is the probability when the barrier height is decreased by 50%.

5. Use the WKB approximation to find the transimssion coefficient for the potential $V(x) = 0$ if $x < 0$ and $V(x) = V_o - kx$ when $x > 0$. Here V_o and k are constants. Refer to figure 12.7. Hint: Find the turning points of the system where $V(x) = \epsilon$ to find the limits of integration.

6. Calculate the transmission coefficient of the following potential barrier using the WKB approximation. The potential is: $V(x) = V_o\left(1 - \frac{x^2}{a^2}\right)$ when $-a <= x <= a$. Also $V(x) = 0$ elsewhere. See figure 12.8. Use the same hint about the turning points and the integration limits as described in the previous problem.

7. Consider the classic alpha decay problem using the just derived WKB approximation. The potential is $V(r) = \frac{2Ze^2}{4\pi\epsilon_o r}$ for $r > r_1$ where r_1 is the radius of the nuclei. Carry the WKB integral (Equation 12.66) from r_1 to r_2 where $r_2 = \frac{2Ze^2}{4\pi\epsilon_o E}$ and determine the tunneling probability. Make suitable approximations to simplify things as much as possible.

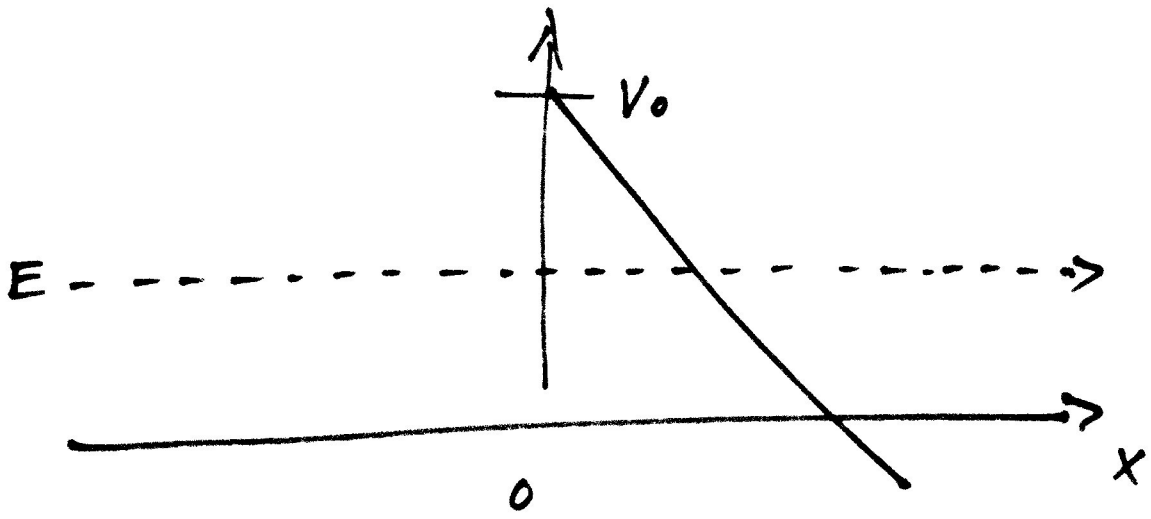

Figure 12.7: Sketch of a linearly decaying barrier

Relevant literature

These references are listed in no particular order

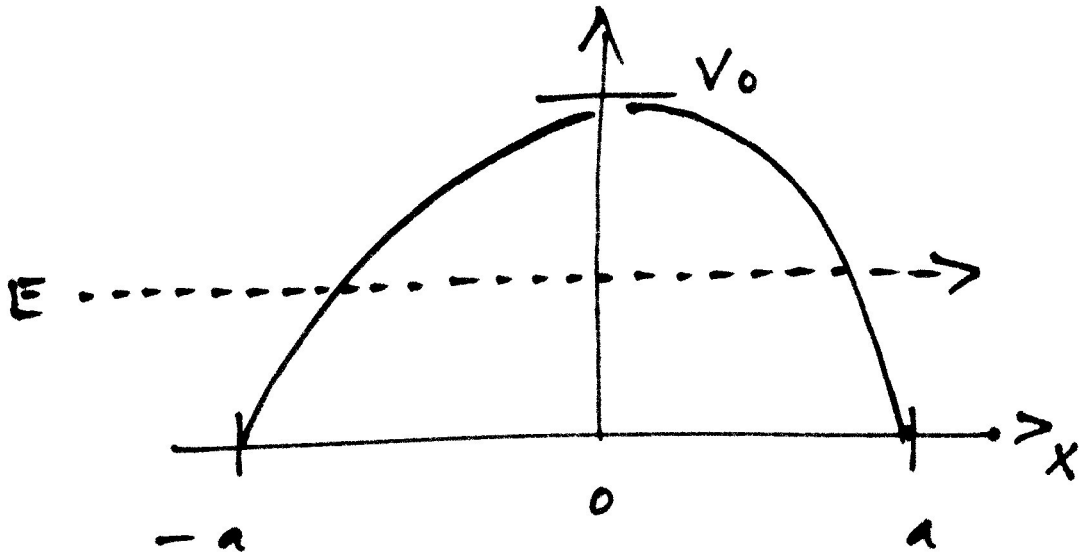

Figure 12.8: Sketch of a symmetric parabolic barrier

- "A carbon nanotube field-emission electron source"
  W. A deHeer, A. Chatelain, D. Ugarte
  Science, 270, 1179 (1995).

- "Field emission from carbon nanotubes: the first five years"
  J-M Bonard, H. Kind, T. Stockli, L-O Nilsson
  Solid-State Electronics, 45, 893 (2001).

- "Stripping voltammetry of Cu overlayers deposited on self-assembled monolayers: field emission of electrons through a phenylene ethylene oligomer"
  M. S. Doescher, J. M. Tour, A. M. Rawlett, M. L. Myrick
  J. Phys. Chem. B, 105, 105 (2001).

- "Time resolved photoelectrochemistry with size-quantized PbS adsorbed on gold"
  E.P.A.M. Bakkers, J.J. Kelly, D. Vanmaekelbergh
  Journal of Electronanalytical Chemistry, 482, 48 (2000).

- "Fluorescence intermittency in single InP quantum dots"

M. Kuno, D. P. Fromm, A. Gallagher, D. J. Nesbitt, O. I. Micic, A. J. Nozik
Nano Lett. 1, 557 (2001).

- "On/off fluorescence intermittency of single semiconductor quantum dots"
M. Kuno, D. P. Fromm, H. F. Hamann, A. Gallagher, D. J. Nesbitt
J. Chem. Phys. 115, 1028 (2001).

Chapter 13

Synthesis

Molecular Beam Epitaxy (MBE)

The basic idea behind this technique is fairly simple. In practice, however, its realization is more involved (and more expensive). MBE essentially consists of an ultrahigh vacuum chamber into which a substrate is loaded onto a heated sample holder. Precursors of desired elements (Ga, As, Al, P, In etc...) are then loaded into heated crucibles or furnaces (called Knudsen cells) outfitted with computer controlled shutters on their exits. The precursors are then heated such that when the shutters are opened one obtains a beam of atoms directed towards the substrate. Under such low pressures, the atomic species have very long mean free paths allowing them to reach the substrate without collisions with other gas phase species in the chamber. By controlling the temperature as well as the sequence/timing of opening and closing the shutters one can deposit very uniform films of semiconductor materials. In this fashion one can obtain precise nanometer lengthscale quantum well structures.

Under certain conditions where one deposits distinct semiconductor layers with different lattice constants, its also possible to grow islands of a semiconductor on top of another effectively allowing the synthesis of semiconductor quantum dots. The basic idea is that after a few layers of the new lattice mismatched semiconductor has been deposited, the strain at the interface changes the mode of growth from within the plane to out of the plane. Small islands are therefore formed which are the desired quantum dots. This technique is refered to as Stranski Krastanow growth.

A crude sketch of a MBE apparatus is shown below.

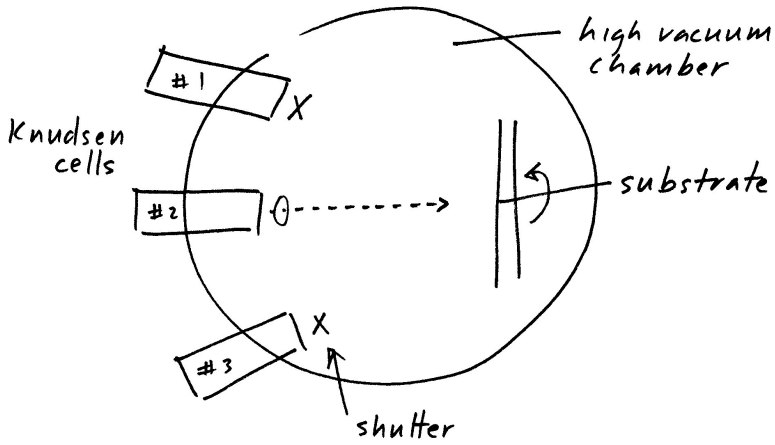

Figure 13.1: Cartoon of a MBE apparatus

Metal Organic Chemical Vapor Deposition (MOCVD)

MOCVD operates on a similar principle to MBE. However the apparatus differs greatly. MOCVD is generally conducted using a quartz tube furnace with a heated substrate. Clearly this is a much less expensive setup. One doesn't need turbo pumps, vacuum chambers, load locks, EELS guns and other MBE accoutrements. Organometallic or metal-organic compounds such as trimethylaluminum, trimethygallium, trimethylindium as well as gases such as phosphine or arsine can be introduced into the heated reactor and allowed to decompose giving the desired elemental species. In the case of liquid organometallic precursors such as trimethylaluminum (above), the compound is brought into the gas phase by bubbling a carrier gas such as helium through the compound and allowing the gas to carry small amounts of the precursor into the reaction chamber. Like MBE, MOCVD can be used to grow thin films of materials. This technique has also been used, more recently, in the synthesis of semiconductor nanowires in the presence of gold nanoparticle catalysts. One potential disadvantage of the technique is the uniformity of the resulting films or deposition of materials. This is because the flow of gasses above the substrate may not be completely uniform. As a consequence one should consider ways to better control the flow and subsequent distribution of precursors over the substrate.

A sketch of the apparatus is shown below.

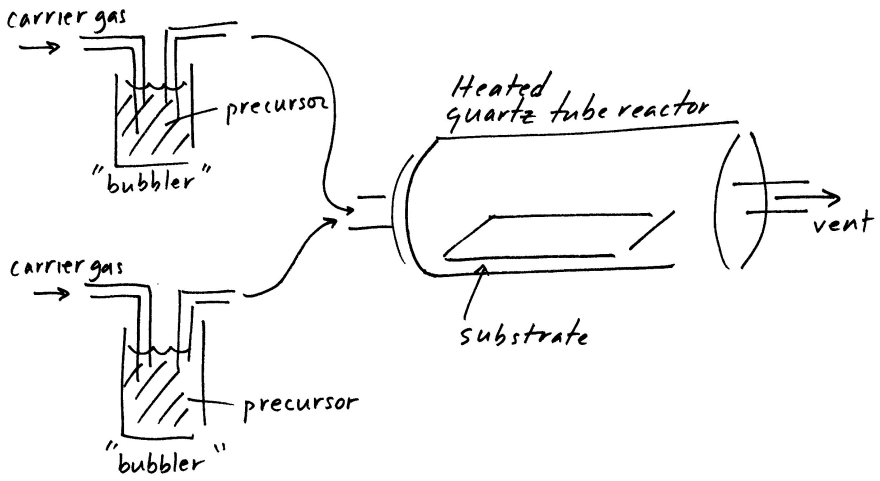

Figure 13.2: Cartoon of a MOCVD apparatus

Colloidal growth

Description

Colloidal growth is a chemist's approach to making nanostructures. There are different variations of this approach so no general description can fit all techniques. However a few are highlighted here. Some of the original quantum dots were created in supersaturated solutions within a glass matrix. Basically, molten silicate glasses were doped to the point of supersaturation with metal salts of the desired semiconducting material. The melt is then rapidly quenched, resulting in a precipitation of the desired semiconducting material into tiny seed nuclei (or alternatively the rapid quench can be thought of as a discrete temporal nucleation of seed particles). The glass solution then undergoes a secondary heat treatment with temperatures ranging from 400 to 1000 degrees Celcius. By varying the temperature and duration of the secondary heat treatment one can vary the average size of the nanocrystals.

Alternatively, others have employed inverse micelles as a means of quantum dot or even nanowire synthesis. In this preparation, surfactants such as bis(2-ethylhexyl)phosphate (also called AOT) are used to create small inverse micelles consisting of a hydrophilic interior and a hydrophobic exterior. Aqueous solutions of metal salts are then introduced into these compart-

mentalized water pools. Subsequent reactions are conducted in the aqueous phase (whether it be reduction of the metal precursor using sodium borohydride or reaction with a second chalcogen source such as S, Se or Te) to create metal or semiconductor nanoparticles. After the reaction, the nanocrystallites are sometimes extracted by adding a surface passivating agent which drops them out of solution. The recovered powder is then redissolved in a suitable solvent. To a first approximation, the average size of the nanocrystallies is determined by the initial ratio of water to surfactant, often called the "W" or "Ω" value.

One of the most successful approaches to the colloidal synthesis of nanocrystal and nanorods involves using coordinating as well as non coordinating solvents. In this approach organometallic precursors such as dimethylcadmium and trioctylphosphine selenide are injected into hot (temperatures on the order of 300 degrees Celcius) trioctylphosphine oxide. Upon injection, the precursors decompose to give desired elements of the final semiconductor. The rapid injection is analogous to the rapid quench in glasses and results in a discrete temporal nucleation of seed particles. The temperature of the solution is then slowly raised to allow the controlled growth of particles in the coordinating (or non-coordinating) solvent. This, again, is analogous to the secondary heat treatment with glasses with the main difference being lower overall temperatures (300 degrees versus 400 to 1000 degrees C). The average size of the nanomaterial is determined by the temperature and the duration of the heating and can be monitored spectroscopically.

A figure of such an apparatus is shown below.

LaMer and Dinegar growth model

Start with Fick's first law.

$$\boxed{Q(t) = -4\pi r^2 D \frac{dc}{dr}} \tag{13.1}$$

where Q(t) is the "flux" of stuff going to make the particle, D is the diffusion coefficent and r is a radial length from the center of the growing particle. We should point out that this "flux" has units of stuff/time as opposed to the more usual definition of flux. Now with this let's manipulate the first expression a little bit to get.

$$\frac{Q(t)}{-4\pi r^2 D} = \frac{dc}{dr}$$

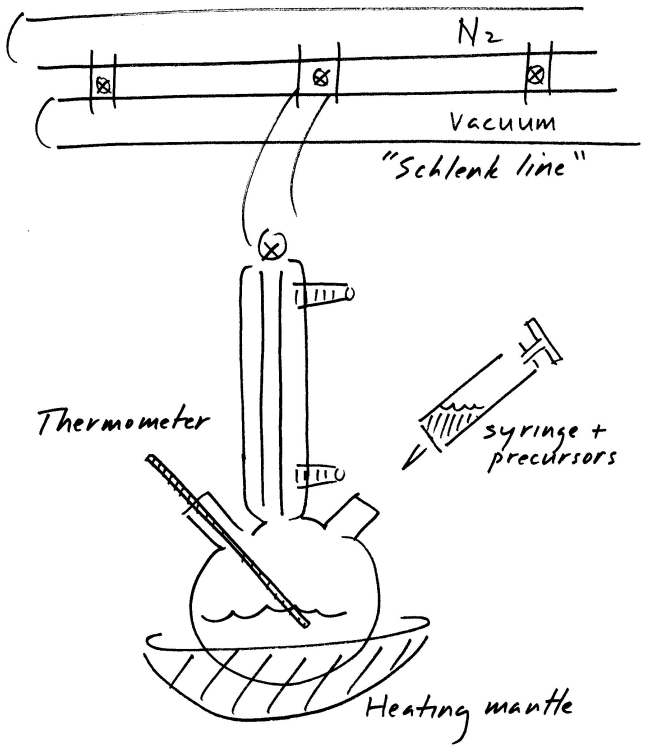

Figure 13.3: Cartoon of an apparatus commonly used for colloidal synthesis

$$\frac{Q(t)dr}{-4\pi r^2 D} = dc$$

Integrate the last expression

$$\frac{Q(t)}{-4\pi D}\int \frac{dr}{r^2} = \int dc$$

to get

$$\frac{Q(t)}{4\pi Dr} + Const = C(r,t)$$

This constant is a constant with respect to r. However it could, in general, depend on time. So more generally we get

$$\frac{Q(t)}{4\pi Dr} + f(t) = C(r,t) \tag{13.2}$$

Apply boundary conditions now to make more explicit the expression. There are four to consider.

- When $r = a$, where a is the radius of the growing particle, $C(a,t) = C_s$. C_s is the saturation concentration of the stuff being deposited, called "monomer".
- $C(r, t = 0) = C_{ss}$. Here C_{ss} is the supersaturation concentration of the solution at $t = 0$.
- $\frac{\partial C}{\partial t}|_{r=h} = \frac{Q(t)}{\frac{4}{3}\pi h^3}$
- $Q(0) = 0$ Flux is zero at zero time as expected.

Apply boundary condition 2

$$\begin{aligned} C(r, t=0) &= C_{ss} \\ C(r,0) &= \frac{Q(0)}{4\pi Dr} + f(0) \end{aligned}$$

Since $Q(0) = 0$ (boundary condition 4)

$$C(r,0) = f(0) = C_{ss} \tag{13.3}$$

Apply boundary condition 3

Start with the original expression

$$C(r,t) = \frac{Q(t)}{4\pi r D} + f(t)$$

take its time derivative

$$\left.\frac{\partial C(r,t)}{\partial t}\right|_{r=h} = \left.\frac{1}{4\pi r D}\frac{dQ(t)}{dt}\right|_{r=h} + \frac{df(t)}{dt} = \frac{Q(t)}{\frac{4}{3}\pi h^3}$$

or on rearranging

$$\frac{df(t)}{dt} = \frac{Q(t)}{\frac{4}{3}\pi h^3} - \frac{1}{4\pi h D}\frac{dQ(t)}{dt}$$

Now integrate this to get

$$f(t)|_0^t = \frac{1}{\frac{4}{3}\pi h^3}\int_0^t Q(t)dt - \left.\frac{1}{4\pi h D}Q(t)\right|_0^t$$

This becomes

$$f(t) - f(0) = \frac{1}{\frac{4}{3}\pi h^3}\int_0^t Q(t)dt - \frac{1}{4\pi h D}(Q(t) - Q(0))$$

where $f(0) = C_{ss}$ and $Q(0) = 0$. The reduces to

$$f(t) = C_{ss} + \frac{1}{\frac{4}{3}\pi h^3}\int_0^t Q(t)dt - \frac{Q(t)}{4\pi h D}$$

Since $C(r,t) = \frac{Q(t)}{4\pi r D} + f(t)$ we can use the above expression for $f(t)$ to get

$$\begin{aligned} C(r,t) &= \frac{Q(t)}{4\pi r D} + C_{ss} + \frac{1}{\frac{4}{3}\pi h^3}\int_0^t Q(t)dt - \frac{Q(t)}{4\pi h D} \\ &= \frac{Q(t)}{4\pi D}\left(\frac{1}{r} - \frac{1}{h}\right) + C_{ss} + \frac{1}{\frac{4}{3}\pi h^3}\int_0^t Q(t)dt \end{aligned}$$

Since in general $h >> r$ we get

$$C(r,t) \approx \frac{Q(t)}{4\pi D}\left(\frac{1}{r}\right) + C_{ss} + \frac{1}{\frac{4}{3}\pi h^3}\int_0^t Q(t)dt$$

Now if

$$-Q(t) = 4\pi\rho a^2 \frac{da}{dt} \tag{13.4}$$

(a reasonable thought given that the flux in the opposite direction is reflected by the growth of the particle) one gets after replacing this in the previous expression, where ρ is the density of the material being deposited

$$C(r=a,t) \approx -\frac{4\pi\rho a^2 \frac{da}{dt}}{4\pi D a} + C_{ss} - \frac{4\pi\rho}{\frac{4}{3}\pi h^3}\int_0^t a^2 \frac{da}{dt} dt$$

or

$$C(r=a,t) \approx -\frac{\rho a \frac{da}{dt}}{D} + C_{ss} - \frac{3\rho}{h^3}\int_0^t a^2 \frac{da}{dt} dt$$

Integrate the last integral by parts. Let $u = a^2$, $du = 2ada$, $dv = \frac{da}{dt}$ and $v = a$. We get

$$\begin{aligned} C(r=a,t) &\approx -\frac{\rho a \frac{da}{dt}}{D} + C_{ss} - \frac{3\rho}{h^3}\left(a^3\Big|_0^t - \int_0^t 2a^2 da\right) \\ &\approx -\frac{\rho a}{D}\left(\frac{da}{dt}\right) + C_{ss} - \frac{3\rho}{h^3}\left(a^3(t) - a^3(0) - \frac{2}{3}a^3\Big|_0^t\right) \end{aligned}$$

Recall that at $t = 0$, $a(0) = 0$ Particle has not grown yet. This allows us to simplify the above expression to

$$\begin{aligned} &\approx -\frac{\rho a}{D}\left(\frac{da}{dt}\right) + C_{ss} - \frac{3\rho}{h^3}\left(a^3(t) - \frac{2}{3}\left(a^3(t) - a^3(0)\right)\right) \\ &\approx -\frac{\rho a}{D}\left(\frac{da}{dt}\right) + C_{ss} - \frac{3\rho}{h^3}\left(\frac{a^3(t)}{3}\right) \\ &\approx -\frac{\rho a}{D}\left(\frac{da}{dt}\right) + C_{ss} - \frac{\rho a^3}{h^3} \end{aligned}$$

Leading to our final expression

$$C(r=a,t) \approx C_{ss} - \frac{\rho a}{D}\left(\frac{da}{dt}\right) - \frac{\rho a^3}{h^3} \tag{13.5}$$

Apply boundary condition 1

Here apply it to the final expression we just derived above.

$$C(r=a,t) \approx C_{ss} - \frac{\rho a}{D}\left(\frac{da}{dt}\right) - \frac{\rho a^3}{h^3} = C_s$$

Rearrange to give

$$\frac{\rho a}{D}\left(\frac{da}{dt}\right) = (C_{ss} - C_s) - \frac{\rho a^3}{h^3}$$

or

$$a\frac{da}{dt} = \frac{D}{\rho}(C_{ss} - C_s) - \frac{Da^3}{h^3}$$

At this point note that $\frac{d(a^2)}{dt} = 2a\frac{da}{dt}$ so that $a\frac{da}{dt} = \frac{1}{2}\frac{d(a^2)}{dt}$. Insert this into the above expression to get

$$\frac{d(a^2)}{dt} = \frac{2D}{\rho}(C_{ss} - C_s) - \frac{2Da^3}{h^3} \tag{13.6}$$

This last last expression gives you the behavior for the size of the particle as a function of time, which is what we were ultimately after. We can proceed to solve this equation by either looking this up in a table of integrals, which is what LaMer and Dinegar ultimately did, or we could solve it numerically. Another option is to note that in general $\frac{a}{h} << 1$ so basically the last term in the expression drops out. We get the approximation

$$\frac{d(a^2)}{dt} \approx \frac{2D}{\rho}(C_{ss} - C_s) \tag{13.7}$$

You will notice that the radius of the particle with essentially grow as the square root of time ($a \propto \sqrt{t}$). Now following Sugimoto we invoke the Gibbs Thomson equation as follows

$$C_{ss} = C_\infty e^{\frac{2\sigma V_m}{r^* RT}}$$
$$C_s = C_\infty e^{\frac{2\sigma V_m}{aRT}}$$

Here a is the radius of the particle at a given time. r^* is the radius of the particle that would make its ensemble concentration equivalent to the initial "monomer" concentration (think about this point, its will be important in a bit). To simplify the notation, let $r_o = \frac{2\sigma V_m}{RT}$

$$C_{ss} = C_\infty e^{\frac{r_o}{r^*}} \tag{13.8}$$
$$C_s = C_\infty e^{\frac{r_o}{a}} \tag{13.9}$$

If the exponent is small (and it doesn't have to be) then we can do a Taylor series expansion of the above to get (keeping only 1st 2 terms)

$$C_{ss} \approx C_\infty(1 + \frac{r_0}{r} + \ldots)$$
$$C_S \approx C_\infty(1 + \frac{r_0}{a} + \ldots)$$

Replace into our main equation to get

$$\frac{d(a^2)}{dt} \approx \frac{2D}{\rho}\left(C_\infty r_0\left(\frac{1}{r^*} - \frac{1}{a}\right)\right) \tag{13.10}$$

or alternatively

$$2a\frac{da}{dt} = \frac{2D}{\rho}C_\infty r_0\left(\frac{1}{r^*} - \frac{1}{a}\right)$$
$$\frac{da}{dt} = \frac{D}{\rho}C_\infty\left(\frac{r_0}{a}\right)\left(\frac{1}{r^*} - \frac{1}{a}\right)$$

Let

$$K = \frac{DC_\infty r_0}{\rho}$$

leading to

$$\boxed{\frac{da}{dt} = \frac{K}{a}\left(\frac{1}{r^*} - \frac{1}{a}\right)} \tag{13.11}$$

Now qualitatively speaking, just look at the sign of the right hand side, basically determined but the stuff in the parenthesis. You see if $a = r^*$ no growth occurs ($\frac{da}{dt} = 0$). If $a < r^*$ then $\frac{da}{dt}$ is negative and basically your

particles dissolve (negative growth). Now if $a > r^*$ then $\frac{da}{dt}$ is positive and your particles grow.

A graph of this equation is shown below. You will see that small particles have a steeper slope or faster rate of growth. Larger particles have a flatter slope so they grow slower.

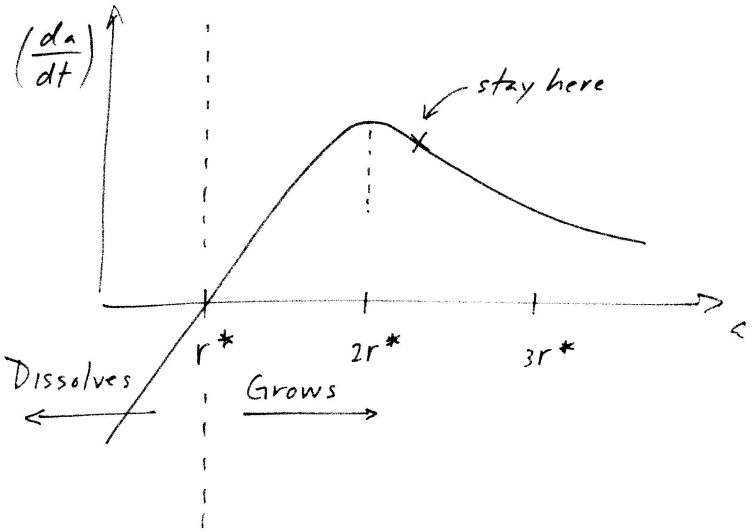

Figure 13.4: Sketch of the LaMer growth rate as a function of the critical radius r^*

Now one underlying point of this whole picture is that C_∞ is constant (i.e. r^* is constant). In reality though, since this is a closed system, the monomer concentration decreases as it gets consumed. So r^* is actually changing in time. If we think in dynamic terms as $t \to \infty$, $r^* \to \infty$ and one actually falls at different places on the above curve as a function of time. Basically your particle size will correspond to a steadily decreasing factor of r^* and you move to the left on the curve. If you have a situation where $\frac{da}{dt}$ becomes negative then your particles will start to dissolve. The worst case is that you have sizes that straddle r^* at any given time so that some particles grow, others dissolve and you end up with a very poor size distribution of your sample.

Size distribution

This section follows the work of Sugimoto who argued that the size distribution of the ensemble is proportional to

$$\text{size dist} \propto \frac{d\left(\frac{da}{dt}\right)}{da} \tag{13.12}$$

Using the relation derived earlier

$$\begin{aligned}\frac{d\left(\frac{da}{dt}\right)}{da} &= K\left(-\frac{1}{r^*a^2}+\frac{2}{a^3}\right)\left(\frac{da}{da}\right)\\ &= \frac{K}{a^2}\left(\frac{2}{a}-\frac{1}{r^*}\right)\left(\frac{da}{da}\right)\end{aligned}$$

where

$$\left(\frac{da}{da}\right)=\left(\frac{da}{dt}\right)\left(\frac{dt}{da}\right)$$

Divide both sides by $\frac{dt}{da}$ to get

$$\begin{aligned}\left(\frac{da}{dt}\right)\frac{d\left(\frac{da}{dt}\right)}{da} &= \frac{K}{a^2}\left(\frac{2}{a}-\frac{1}{r^*}\right)\left(\frac{da}{dt}\right)\\ \frac{d\left(\frac{da}{dt}\right)}{dt} &= \frac{K}{a^2}\left(\frac{2}{a}-\frac{1}{r^*}\right)\left(\frac{da}{dt}\right)\end{aligned}$$

Let $\sigma=\frac{da}{dt}$ giving

$$\frac{d\sigma}{dt}=\frac{K}{a^2}\left(\frac{2}{a}-\frac{1}{r^*}\right)\sigma \tag{13.13}$$

Alternatively

$$\boxed{\frac{d\sigma}{dt}=\frac{K}{a^2}\left(\frac{2r^*-a}{r^*a}\right)\sigma} \tag{13.14}$$

Now its clear to see that if $a > 2r^*$, $\left(\frac{d\sigma}{dt}\right)$ is negative valued. The size distribution of the sample will narrow. This is called the "focusing" regime.

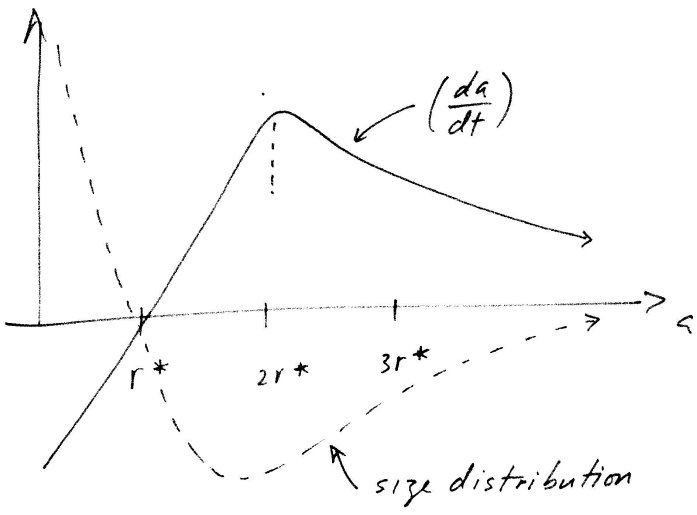

Figure 13.5: Sketch of both the LaMer growth rate and size distribution as a function of the critical radius r^*

However, if $a < 2r^* \left(\frac{d\sigma}{dt}\right)$ is positive valued and the size distribution will increase. This is called the "defocusing" regime.

Recall our discussion earlier about the dynamic nature of r^*. It goes without saying that in a closed system as time increases r^* will also increase. The actual size of the particle will in absolute terms become a smaller fraction of r^* causing you to progressively move left on our diagram. As you move left the distribution will broaden. To keep the size distribution or even narrow it you need to fight the depletion or monomers causing r^* to increase. This means as the reaction progresses you add more precursor to the reaction. The extra addition can be accomplished a number of ways. Peng for example just adds subsequent injection of precursors into the reaction mixture. Sugimoto and others however build in a resevoir of precursors that slowly get released to the reaction as time increases.

Reaction controlled growth

The previous discussion has assumed diffusion limited growth. However it's possible to have the reaction controlled situation. LaMer, Sugimoto and others have shown that in this case the relevant growth equation can be

expressed as

$$\frac{da}{dt} = K_r \left(\frac{1}{r^*} - \frac{1}{a} \right) \tag{13.15}$$

where K_r is a constant. To see how the size distribution behaves in this situation repeat the analysis done earlier for the diffusion controlled growth case.

$$\text{size dist} \propto \frac{d\left(\frac{da}{dt}\right)}{da}$$

When explicitly evaluated this leads to

$$\frac{d\left(\frac{da}{dt}\right)}{da} = \frac{K_r}{a^2}\left(\frac{da}{da}\right)$$

where recall that

$$\left(\frac{da}{da}\right) = \left(\frac{da}{dt}\right)\left(\frac{dt}{da}\right)$$

Replace into our expression and divide by $\left(\frac{dt}{da}\right)$ on both sides. This gives

$$\frac{da}{dt}\frac{d\left(\frac{da}{dt}\right)}{da} = \frac{K_r}{a^2}\left(\frac{da}{dt}\right)$$

$$\frac{d\left(\frac{da}{dt}\right)}{dt} = \frac{K_r}{a^2}\left(\frac{da}{dt}\right)$$

Let $\sigma = \frac{da}{dt}$ giving

$$\frac{d\sigma}{dt} = \frac{K_r}{a^2}\sigma \tag{13.16}$$

You will notice here that this expression is always positive. In effect it tells us that there will always be some broadening of the size distribution during the particle growth.

Exercises

1. Read any of the papers listed below or select a paper from the current literature and discuss it.

Relevant reading

1. "Theory, production and mechanism of formation of monodispersed hydrosols" V. K. LaMer, R. H. Dinegar J. Am. Chem. Soc. 72, 4847 (1950).

2. "Preparation of monodispersed colloidal particles" T. Sugimoto Advances in colloid and interface science, 28, 65 (1987).

3. "The kinetics of precipitation from supersaturated solid solutions" I. M. Lifshitz, V. V. Slyozov J. Phys. Chem. Solids, 19, 35 (1961).

References directly related to LaMer and Sugimoto models

These are some papers from the literature that deal with the LaMer/Dinegar and Sugimoto models discussed above. The papers are in no particular order.

1. "Formation of high quality CdS and other II-IV semiconductor nanocrystals in noncoordinating solvents:Tunable reactivity of monomers"
W. W. Yu and X. Peng
Angew. Chem. Int. Ed. 41, 2368 (2002).

2. "Kinetics of II-VI and III-V colloidal semiconductor nanocrystal growth: Focusing of size distributions"
X. Peng, J. Wickham and A. P. Alivisatos
J. Am. Chem. Soc. 120, 5343 (1998).

3. "Nearly monodisperse and shap-controlled CdSe nanocrystals via alternative routes: Nucleation and growth"
Z. A. Peng and X. Peng
J. Am. Chem. Soc. 124, 3343 (2002).

4. "Formation of high quality CdTe, CdSe, and CdS nanocrystals using CdO as precursor"
Z. A. Peng and X. Peng

J. Am. Chem. Soc. 123, 183 (2001).

5. "Formation of high quality InP and InAs nanocrystals in a noncoordinating solvent"
D. Battaglia and X. Peng
Nano Letters, 2, 1027 (2002).

6. "The kinetics of growth of semiconductor nanocrystals in a hot amphiphile matrix"
C. D. Dushkin, S. Saita, Y. Yoshie, Y. Yamaguchi
Advances in Colloid and Interface Science, 88, 37 (2000).

7. "Evolution of an ensemble of nanoparticles in a colloidal solution: Theoretical study" D. V. Talapin, A. L. Rogach, M. Haase, H. Weller J. Phys. Chem. B 105, 12278 (2001).

Relevant literature

The following papers describe some of the syntheses for nanoscale materials. They are listed in no particular order.

- "Large-scale production of single-walled carbon nanotubes by the electric-arc technique"
C. Journet et al.
Nature 388, 756 (1997).

- "Large scale CVD synthesis of single-walled carbon nanotubes"
A. M. Cassell, J. A. Raymakers, J. Kong, H. Dai
J. Phys. Chem. B 103, 6484 (1999).

- "Chemical vapor deposition of methane for single-walled carbon nanotubes"
J. Kong, A. M. Cassell, H. Dai
Chem. Phys. Lett. 292, 567 (1998).

- "General synthesis of compound semiconductor nanowires"
X. Duan, C. M. Lieber
Advanced Materials, 12, 298 (2000).

- "A laser ablation metode for the synthesis of crystalline semiconductor nanowires"
  A. M. Morales, C. M. Lieber
  Science, 279, 208 (1998).

- "Epitaxial core-shell and core-multishell nanowire heterostructures"
  L. J. Lauhon, M. S. Gudiksen, D. Wang, C. M. Lieber
  Nature, 420, 57 (2002).

- "Inorganic semiconductor nanowires"
  Y. Wu, H. Yan, M. Huang, B. Messer, J. H. Song, P. Yang
  Chem. Eur. J. 8, 1261 (2002).

- "Direct observation of vapor-liquid-solid nanowire growth"
  Y. Wu, P. Yang
  J. Am. Chem. Soc. 123, 3165 (2001).

- "High quality gaN nanowires synthesized using a CVD approach"
  J. C. Wang, S. Q. Feng, D. P. Yu
  Appl. Phys. A 75, 691 (2002).

- "Antimony nanowire arrays fabricated by pulsed electrodeposition in anodic alumina membranes"
  Y. Zhang, G. Li, Y. Wu, B. Zhang, W. Song. L. Zhang
  Adv. Mater. 14, 1227 (2002).

- "Silicon nanotubes"
  J. Sha, J. Niu, X. Ma, J. Xu, X. Zhang, Q. Yang, D. Yang
  Adv. Mater. 14, 1219 (2002).

- "Silicon nanowires: preparation, device fabrication, and transport properties"
  J-Y Yu, S-W Chung, J. R. Heath
  J. Phys. Chem. B 104, 11864 (2000).

- "Diameter-controlled synthesis of carbon nanotubes"
  C. L. Cheung, A. Kurtz, H. Park, C. M. Lieber
  J. Phys. Chem. B 106, 2429 (2002).

- "Superlattices of platinum and palladium nanoparticles"
  J. E. Martin, J. P. Wilcoxon, J. Odinek, P. Provencio
  J. Phys. Chem. B 106, 971 (2002).

- "Some recent advances in nanostructure preparation from gold and silver particles: a short topical review"
  M. Brust, C. J. Kiely
  Colloids and Surfaces A: Physicochemical and Engineering Aspects, 202, 175 (2002).

- "X-ray photoelectron spectroscopy of CdSe nanocrystals with applications to studies of the nanocrystal surface"
  J. E. Bowen Katari, V. L. Colvin, A. P. Alivisatos
  J. Phys. Chem. B 98, 4109 (1994).

- "Colloidal nanocrystal shape and size control: the case of cobalt"
  V. F. Puentes, K. M. Krishnan, A. P. Alivisatos
  Science, 291, 2115 (2001).

- "Synthesis, self-assembly and magneticbehavior of a two dimensional superlattice of single-crystal ϵ-Co nanoparticles"
  V. F. Puentes, K. M. Krishnan, A. P. Alivisatos
  Appl. Phys. Lett. 78, 2187 (2001).

- "Monodisperse FePt nanoparticles and ferromagnetic FePt nanocrystal superlattices"
  S. Sun, C. B. Murray, D. Weller, L. Folks, A. Moser
  Science, 287, 1989 (2000).

- "Water-in-oil microemulsion synthesis of platinum-ruthenium nanoparticles, their characterization and electrocatalytic properties"
  X. Zhang, K-Y Chan
  Chem. Mater. 15, 451 (2003).

- "Synthesis and characterization of monodisperse nanocrystals and close-packed nanocrystal assemblies"
  C. B. Murray, C. R. Kagan, M. G. Bawendi
  Annu. Rev. Mater. Sci. 30, 545 (2000).

Chapter 14

Tools

Electron microscopies

Transmission electron microscopy

In the TEM experiment, a thin or diluted sample is bombarded under high vacuum with a focused beam of electrons. Electrons that are transmitted through the material form contrast patterns that reproduce the image of the sample. This pattern arises from the scattering of electrons off of atoms coposing the sample. In addition, diffracted electrons give information about the lattice structure of the material. In the case of nanocrystallites, analysis of TEM images is partially responsible for the sizing curves of colloidal quantum dots. The shape of the sample can also be determined from the image.

Secondary electron microscopy

In the SEM experiment, an electron beam is focused and raster scanned over the sample. When the incident electrons interact with the sample a number of effects take place, such as the emission of secondary electrons. These effects are highly localized to the region directly under the electron beam and can be used to create an image of the sample. In addition, elemental analysis through energy dispersive or wavelength dispersive techniques can be done using other detectors.

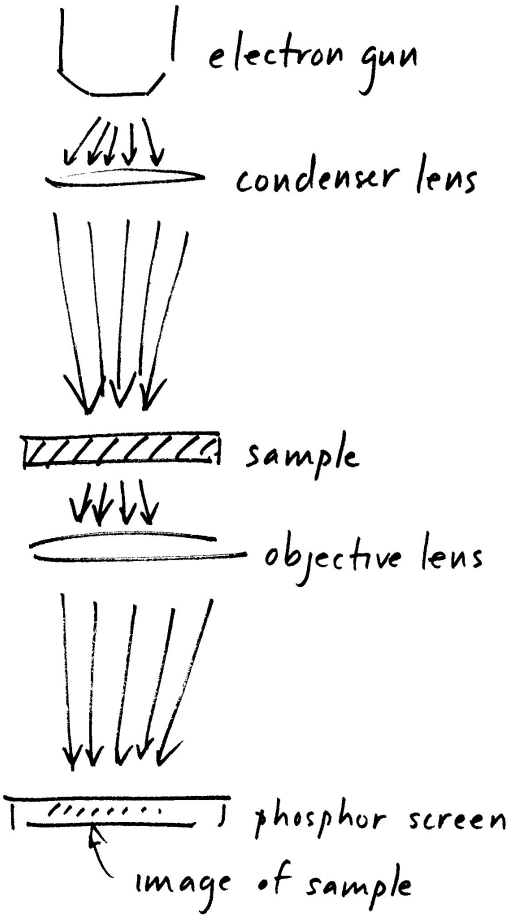

Figure 14.1: Cartoon showing the TEM technique

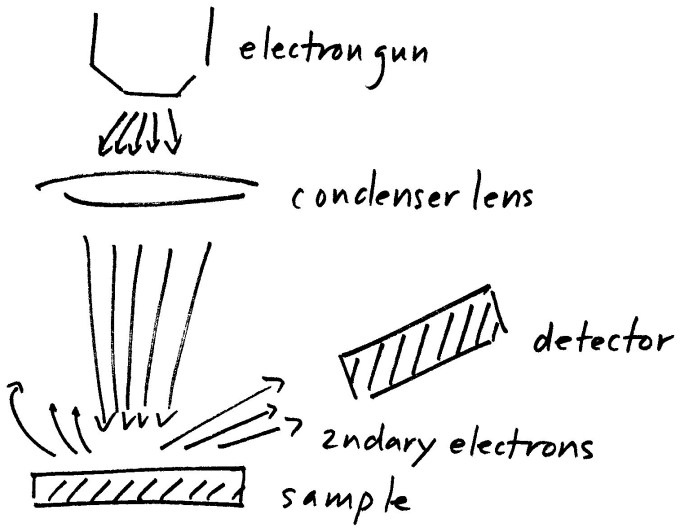

Figure 14.2: Cartoon showing the SEM technique

Probe microscopies

Atomic force microscopy

The atomic force experiment works by using a sharp silicon or silicon nitride cantilever. This tip is brought close to the surface of the sample in question, close enought that atomic forces occur between tip and sample. These forces can be either repulsive or attractive. In the repulsive mode or contact/intermittent contact (tapping mode) mode of operation, the tip position over the surface of the sample is kept constant through a feedback mechanism. In the attractive regime or non contact mode, attractive forces bend the tip bringing it closer to the sample which in turn is detected through a number of means. In any of the modes, the attractive or repulsive forces plus response of the system to counteract them are used as a means of generating a topographic image of the sample. The AFM has been used to move individual nanostructures. It has also been used as a tool to "scratch" surfaces and make nanoscale patterns. There are other variations of this probe technique such as magnetic force microscopy (MFM) and electrostatic force microscopy (EFM).

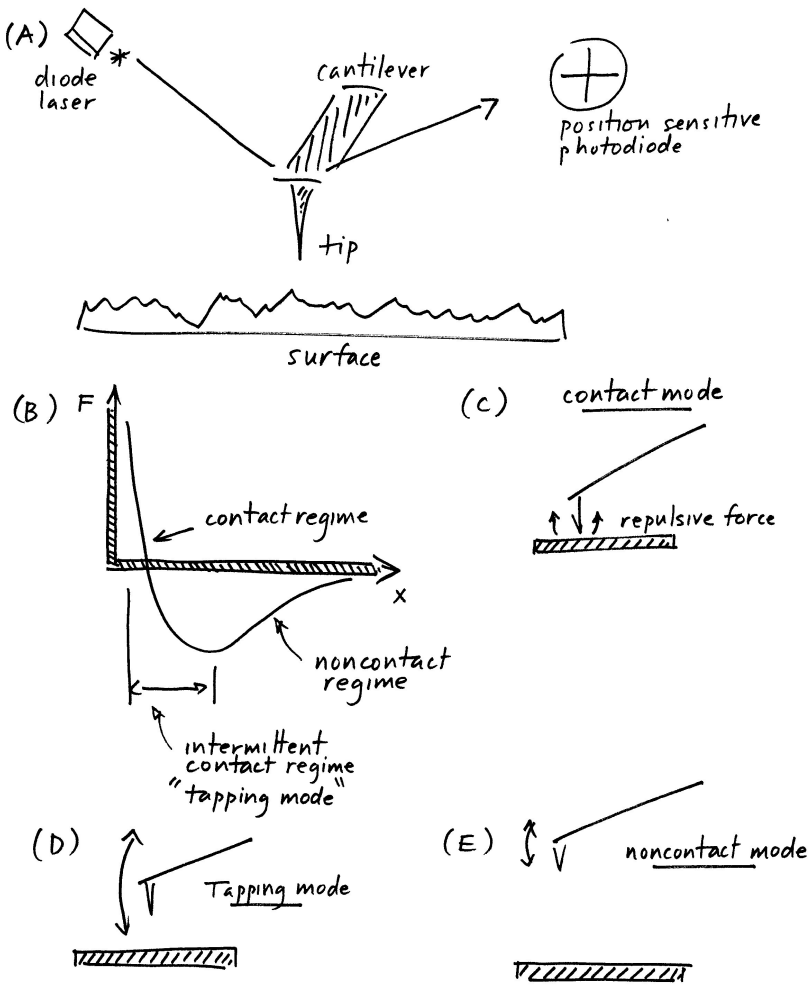

Figure 14.3: Cartoon showing the AFM technique. (A) General concept behind the technique. (B) Force distance curve. Parts of the curve below zero are in the attractive realm. Parts of the curve above zero are in the repulsive regime. (C) Contact mode AFM operating with tip very close to the sample, repulsive regime. (D) Tapping mode AFM. Tip is oscillated with large peak to peak amplitude resulting in brief forrays into the repulsive regime. Hence the name intermittent contact mode. Tapping mode is a Digital Instruments trademarked name. (E) Non-contact mode AFM. The tip is oscillated with small peak to peak amplitude. Operated exclusively in the attractive part of the potential.

Scanning tunneling microscopy

Scanning tunneling microscopy was the original probe microscopy. It was developed by Gerd Binnig and Heinrich Rohrer at IBM Zurich, ultimately leading to the Nobel Prize. The principle of operation is the tunneling of electron from a conductive tip to a conductive substrate or sample through a barrier. The tunneling current is found to be exponentially dependent upon the tip to sample separation allowing for very high sensitivity of sample height. STM has been used to investigate a number of nano related effects such as the discrete atomic like states of colloidal quantum dots and other systems. It has also been used to investigate the coulomb blockade and coulomb staircase phenomena. The STM has also been used to manipulate individual atoms ad described in recent work on quantum corrals. One disadvantage of the STM is that it requires conductive samples or relatively conductive samples on a conductive substrate. To circumvent this limitation, the AFM was subsequently developed.

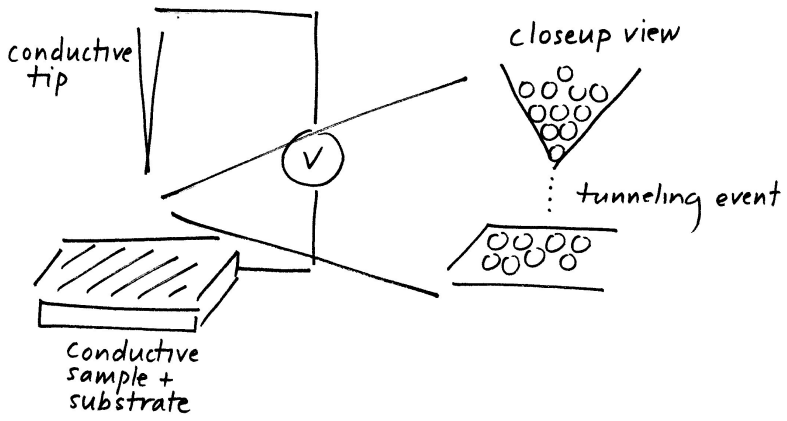

Figure 14.4: Cartoon showing the STM technique

Dip pen nanolithography

Dip-pen nanolithography is a recent atomic force microscopy based technique developed by Chad Mirkin at Northwestern university. The essential idea of the technique is to use the AFM tip as a quill pen. Dip or coat it with a molecular substance. Upon close approach to a substrate the molec-

ular "ink" rolls off the tip and comes into contact with the substrate. By scanning the tip one can pattern the substrate with a layer of molecules. Advantages of dip-pen over other patterning techniques is that it potentially has a very high resolution limited only by the AFM tip radius of curvature. The main disadvantage of the process is that it is serial in nature and hence patterning large areas may prove time consuming. A cartoon describing the technique is shown below.

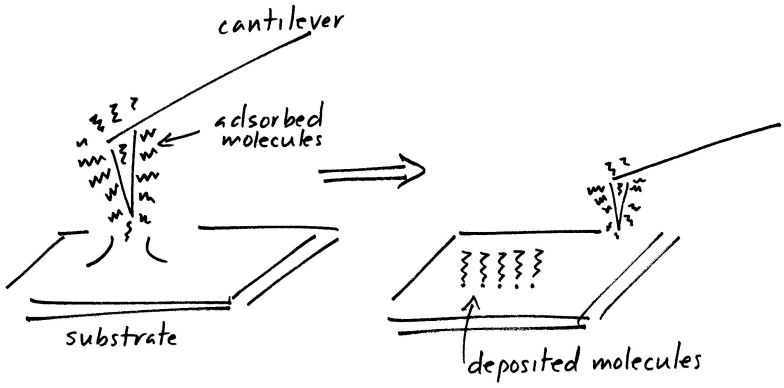

Figure 14.5: Cartoon showing the dip pen technique

Microcontact printing

Microcontact printing is a stamping technique developed by George Whitesides at Harvard University. The basis of the technique is to use a precursor of a polymer called polydimethylsiloxane (PDMS) which can be poured over a master pattern. This master pattern is created through standard photolithography and basically consists of raised features or islands in the desired pattern. The precursor can then be converted to PDMS and hardened to make a negative image of the original master. Then the PDMS "stamp" can be inked with molecular compounds and applied to a surface such as a thin film of gold. The molecular ink, thiols for example, are left behind on the substrate and reproduce the original master. The idea is much the same as with dip pen nanolithography, however, the microcontact printing is a serial process whereas dip-pen is a serial technique and is much slower. One of the disadvantages of microcontact printing, however,

is that it lacks the resolution of dip-pen which is ultimately limited only by the tip radius of curvature 1-10 nm. However, recent reports show that microcontact printing can be pushed to a resolution around 50 nm.

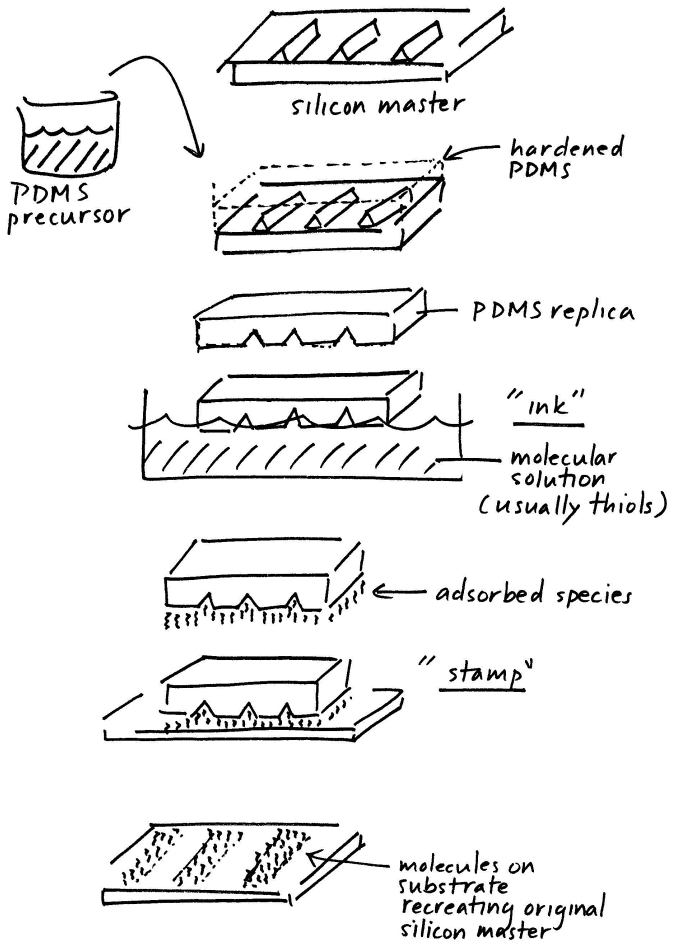

Figure 14.6: Cartoon showing the microcontact printing technique and general sequence of steps.

Exercises

1. Read any of the papers listed below or select a paper from the current literature and discuss it.

Relevant literature

The following papers are in no particular order

- "Directed assembly of one-dimensional nanostructures into functional networks"
  Y. Huang, X. Duan, Q. Wei, C. M. Lieber
  Science, 291, 630 (2001).

- "Submicrometer patterning of charge in thin-film electrets"
  H. O. Jacobs, G. M. Whitesides
  Science, 291, 1763 (2001).

- "Patterning self assembled monolayers: applications in materials science"
  A. Kumar, H. A. Biebuyck, G. M. Whitesides
  Langmuir, 10, 1498 (1994).

- "Generation of 30-50 nm structures using easily fabricated, composite PDMS masks"
  T. W. Odom, V. R. Thalladi, J. C. Love, G. M. Whitesides
  J. Am. Chem. Soc. 124, 12112 (2002).

- "Moving beyond moleucles: patterning solid-state features via dip-pen nanolithography with sol-based inks"
  M. Su, X. Liu, S-Y Li, V. P. Dravid, C. A. Mirkin
  J. Am. Chem. Soc. 124, 1560 (2002).

- "Direct patterning of modified oligonucleotides on metals and insulators by dip-pen nanolithography"
  L. M. Demers, D. S. Ginger, S-J. Park, Z. Li, S-W. Chung, C. A. Mirkin
  Science, 296, 1836 (2002).

- "The art of building small"
  G. M. Whitesides, C. J. Love
  Scientific American 285, 38 (2001).

Chapter 15

Applications

As described in the introduction, nanostructures, whether it be quantum dots, wires or wells, have interesting size dependent optical and electrical properties. The study of these intrinsic properties is the realm of nanoscience. However, at the end of the day, we expect that some of this acquired knowledge (funded largely through our tax dollars) will be put to good use for developing next generation consumer products. So how exactly are today's nanotechnologists trying to harness the potential of nano?

Since there are almost too many applications of nano to catalog here, this section is not meant to be comprehensive. However, we briefly touch upon some applications of quantum wells, quantum wires and quantum dots that are seen in the current literature.

Nanowires

We begin with a short discussion about applications of nanowires. Devices using these low dimensional materials have not been made to any great extent. This is because the historical development of nanostructures seems to have skipped nanowires, moving from wells to dots first. More recently, though, researchers have learned how to make asymetric nanowires using a number of approaches including vapor-liquid-solid (VLS) and solution-liquid-solid (SLS) growth. The move to applications has occured quickly with the key selling point being that, in addition to exhibiting quantum confinement effects, nanowires are at the same time (as their name implies) wires. This means that making electrical connections to the outside world and assembling actual devices may be a lot easier than with other nanostructures such as quantum dots.

Crossed nanowire junctions have been made, using p-type and n-type wires. These junctions, in turn, serve as diodes in one case, memory elements in another and even electroluminescent devices. A schematic of such a nanowire device is provided below. Ultimately, though, the trick is to learn how to assemble such nanowires into useful structures in a convenient and reproducible fashion.

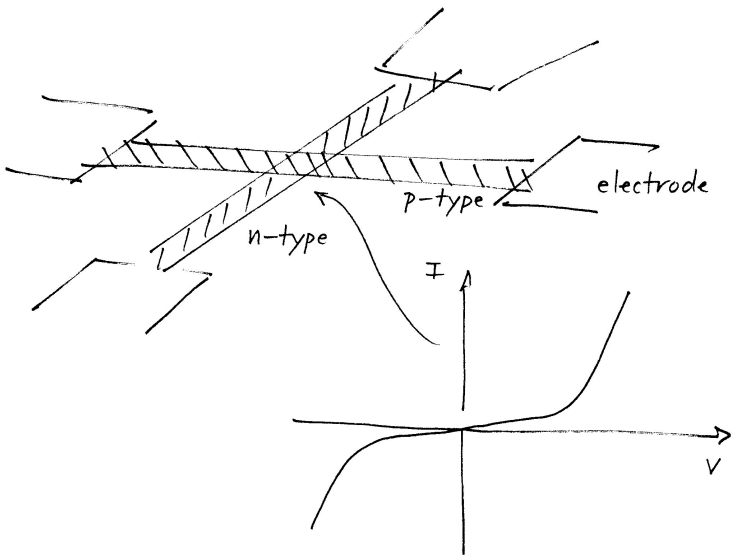

Figure 15.1: Cartoon of a crossed nanowire junction that has been used for proof of principle applications such as memory storage and electroluminescence.

Nanowires have also been used as sensors by monitoring changes in the conductance experienced when different compounds or gases are adsorbed to the wire's surface. In this respect, nanowires may one day be packaged as efficient sensors for minute amounts of toxic gases, chemical weapons, and explosives.

Quantum dots

In the realm of colloidal quantum dots the following applications have been proposed:

- Quantum dots for biological labeling

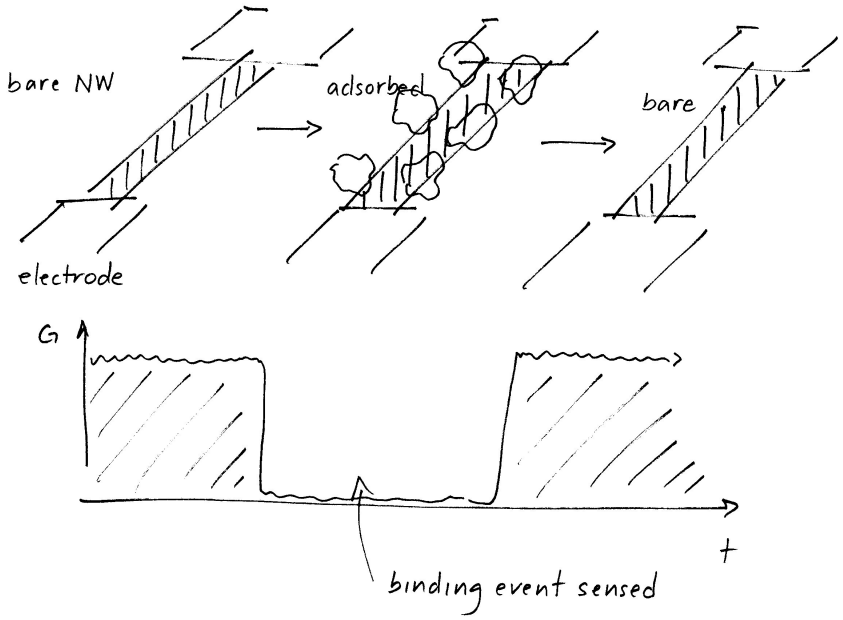

Figure 15.2: Cartoon of nanowire sensor based on changes in conductance.

- Quantum dots as lasing elements
- Quantum dots as sensitizers in photovoltaic applications
- Quantum dots for active layers in light emitting diodes
- Quantum dots as memory elements; single electron transistors

Brief descriptions of each application and reasons why quantum dots have distinct advantages over conventional solutions are presented below.

Medicine; Biological labeling

Conventional biological labeling is currently carried out using organic fluorescent molecules or in some cases radioactive sources. In the case of organic fluorophores such as tetramethylrhodamine (TMR), these molecules are covalently attached to a biological specimen of interest through specific linking chemistry. Organic fluorophores exhibit several disadvantages. Namely, organic dyes suffer from an effect called photobleaching where after exposure to incident light for a modest amount of time, they undergo some sort of photochemistry which ultimately renders them non-fluorescent. Basically the dyes "fade". This makes labeling and tracking experiments difficult because of the finite observation window one has before the fluorescent signal dissapears. As a general rule of thumb, organic dyes will absorb and/or emit approximately 10^6 photons before photobleaching. In addition, organic dyes typically have fairly discrete absorption spectra. So from dye to dye their absorption wavelength or energy will change dramatically. This makes multicolor experiments difficult because exciting each dye requires a different excitation color. Proper filtering of the desired emission signal becomes increasingly difficult in this evironment of multiple excitation frequencies. Finally, achieving different colors for these multicolor experiments may mean synthesizing different compounds, which, in itself, can be fairly involved.

Quantum dots, especially CdSe have narrow emission spectra ($\sim$ 30 nm FWHM). Furthermore, because of quantum confinement effects, different sized dots emit different colors (one material, many discrete colors). This eliminates the need for synthesizing many different organic fluorphores. As one progresses to higher energies in the dot absorption spectra, there are increasingly larger numbers of excited states present. This is analogous to solutions of the particle in a 3D box with progressively larger quantum numbers, n. So all dots whether they be "small" or "large" will absorb excitation wavelengths in the "blue". This makes multicolor experiments

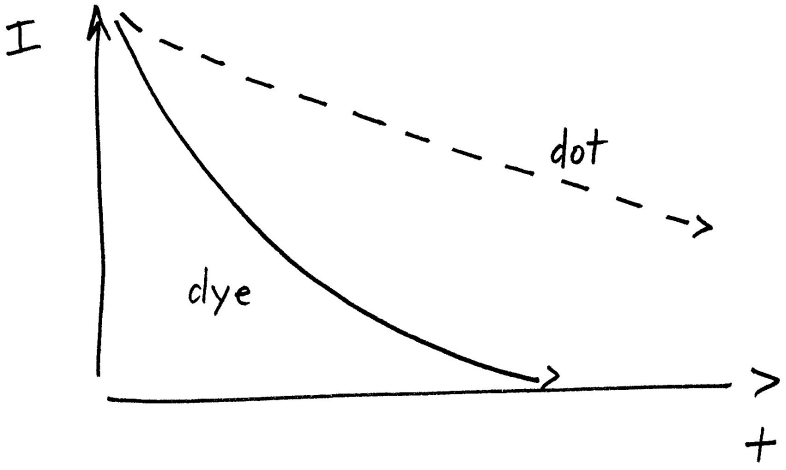

Figure 15.3: Comparison of a quantum dot to organic dye photobleaching rate.

easier since it eliminates the need for multiple excitation wavelengths. One laser, say the 488 nm line from an argon ion, can be used to excite all dots, giving emission anywhere in the visible. Filtering the 488 nm line is also much simpler than trying to simultaneously filter the 473 nm, 488 nm, 514 nm, 532 nm, and 543 nm lines of several lasers (argon ion lines plus YAG doubled line plus green HeNe line). Finally, semiconductor quantum dots are inorganic compounds. As such they are somewhat more robust that organic dyes when it comes to photobleaching. Dots have been seen to absorb and emit over 10^8 photons before experiencing irreversible photobleaching (two orders of magnitude more photons). Therefore, dots are much more resistant to fading. The accompanying figure is a depiction of this.

Ok, so what's the catch? Well, the surface chemistry of quantum dots is still in its infancy. There is still much that needs to be understood before we can begin to do specific chemistry, attaching dots to specific sites on proteins or cells or other biological specimens. This is an area where organic dyes still prevail. Furthermore, semiconductor quantum dots, although nanometer sized, may also be a little too big for some labeling experiments. There might be certain membranes or cellular regions that a dot cannot penetrate because of natural size restrictions (another area where organic dyes are better). Finally, labeling proteins or other specimens with relatively large

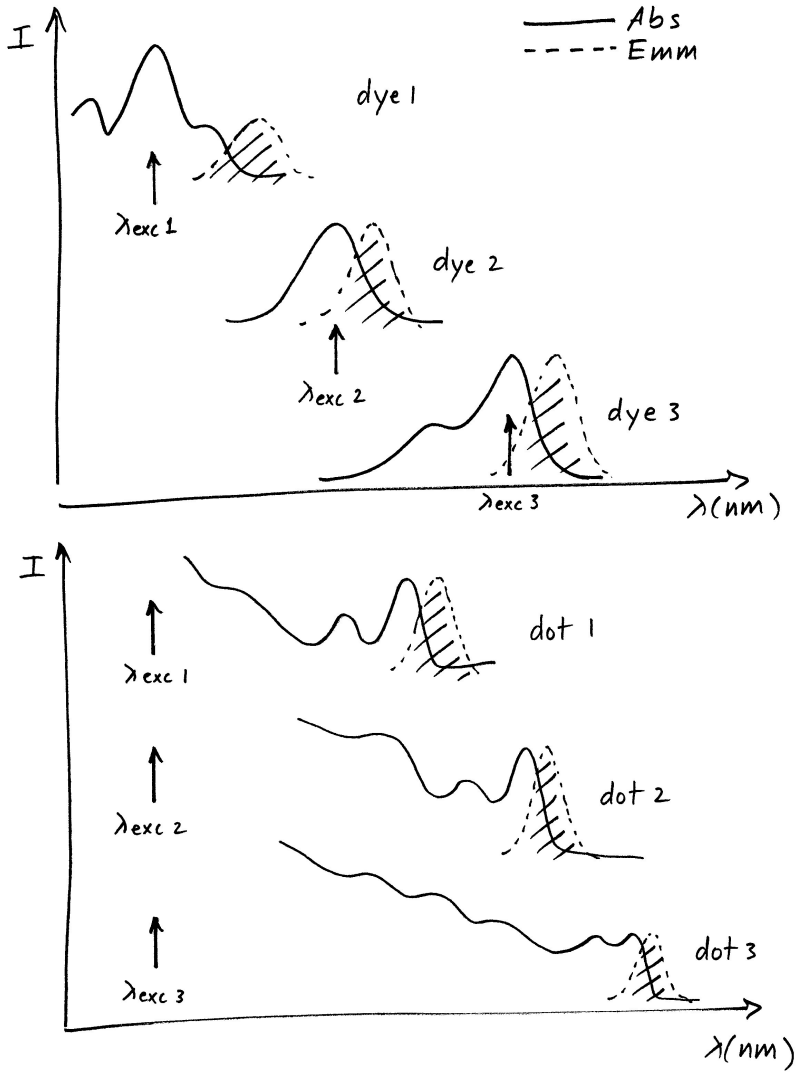

Figure 15.4: Comparison of quantum dot absorption/emission spectra to organic dye absorption emission spectra in light of multicolor labeling experiments.

quantum dots may also perturb the system in unintended ways. So for example if one is trying to watch protein folding in real time one needs to ask whether the dots attached to the protein are actually affecting the folding and unfolding pathways. Consider the size of a typical protein and the size of a typical quantum dot.

Lasing

Lasers are important devices used in everything from tomorrow's national missile defense system (Reagan Star Wars Version 2.0), the data reading element in your DVD or CD player, the red bar code scanner at the supermarket to an excitation source in the laboratory. Conventional lasing sources are based on gases, semiconductors and even organic dyes. With the general movement towards solid state lasers, semiconductors have received a lot of interest for diode laser applications. Further interest was generated with the realization of semiconductor nanostructures (also called low dimensional materials) since it was realized that these systems could potentially make even more efficient lasers than their bulk counterparts. This has to do with the density of states argument that we discussed in previous chapters. The density of states argument won't be repeated here but rather is briefly summarized in the accompanying figure. In this area, quantum well lasers have led the technology, producing some of the most efficient and tunable lasing systems to date. Nanowires have recently been made to lase but the technology in its infancy as with lasing in quantum dots. However, one can envision that the size dependent emission spectra of quantum dots, wires or wells make them attractive lasing elements. In the specific case of colloidal quantum dots, the emission from CdSe is shown to span the entire visible part of the spectrum. So, in principle, a single device could carry a CdSe blue laser, a CdSe green laser and a CdSe red laser. One potential drawback with this system though is a phenomenon called Auger ionization, which might ultimately limit the applicability of this material. However, we leave it to the reader to do some outside reading if they are interested in this subject.

Energy; Photovoltaics

Renewable energy has been an area of great interest since the 1973 OPEC oil embargo, in retaliation for our support of Israel in the 1973 Yom Kippur War The idea for alternative sources of energy is to eventually move away from coal or petroleum based sources of energy. Motivating this are economic,

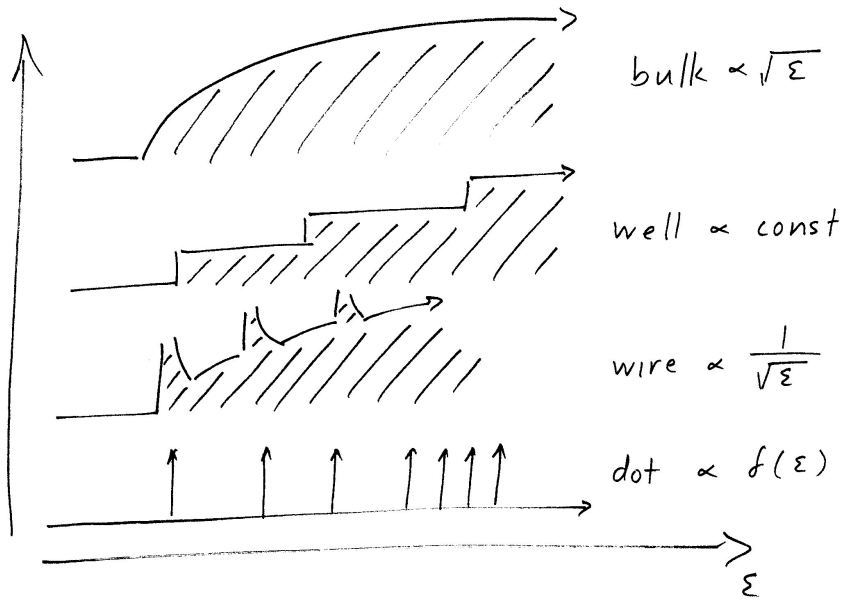

Figure 15.5: Comparison of the density of states for bulk versus a well versus a wire versus a dot.

political and environmental reasons. Solar energy is one facet of renewable energy with wind, methanol, and hydrogen being others. The idea here is to take advantage of the sun's abundant energy and convert it to usable energy much like how Nature has come up with photosynthesis in plants. What's needed, however, is an active material like chlorophyl that can absorb solar radiation and provide efficient charge separation to prevent radiative or nonradiative recombination in the material.

Commercial solar cells are currently made of silicon. Unfortunately, the efficiencies of these devices is typically on the order of 15%. So most of the solar energy collected by these devices is wasted. To make up for all of these losses, large tracts of land must be used for vast sprawling fields of solar cells (solar farms). Improved devices made of single crystal silicon have been shown to achieve conversion efficiencies of 30% but at the cost of being very expensive and impractical for commercial use. As a consequence solar energy has not broken through into mainstream use.

Quantum dots come into play for several reasons. They have tunable, size dependent, absorption and emission spectra. Different quantum dots can be made to absorb anywhere from the UV into the infrared. This tremendous dynamic range cannot be matched by organic dyes. Furthermore, there are few organic dyes that are efficient in the infrared. As a side note, one can imagine a quantum dot based solar cell that operates under cloudy conditions and rainy days where the overcast sky will block much of the visible yet still transmits most (if not all) of the infrared. In addition, the absorption cross section or exctinction coefficient of quantum dots is generally an order of magnitude greater than conventional organic dyes. This means it take fewer dots to absorb the same amount of light. Dots are also more photostable, meaning that they are more likely to reach the 10,000 hour threshold needed for practical commercial devices. Furthermore, nanoparticles when used as substrates or electrodes in dye based solar cells have much larger surface areas than conventional bulk substrates. As a consequence, one can adsorb a greater number of dye molecule per unit area in these hybrid devices than in conventional cells. The efficiencies of these hybrid devices is consequently higher, reaching that of conventional silicon cells. One of the first of such devices is referred to as the Gratzel cell after its inventor.

Lighting; Light emitting diodes

Lighting hasn't changed all that much since the light bulb was invented by Edison and others close to a hundred years ago. More efficient fluorescent

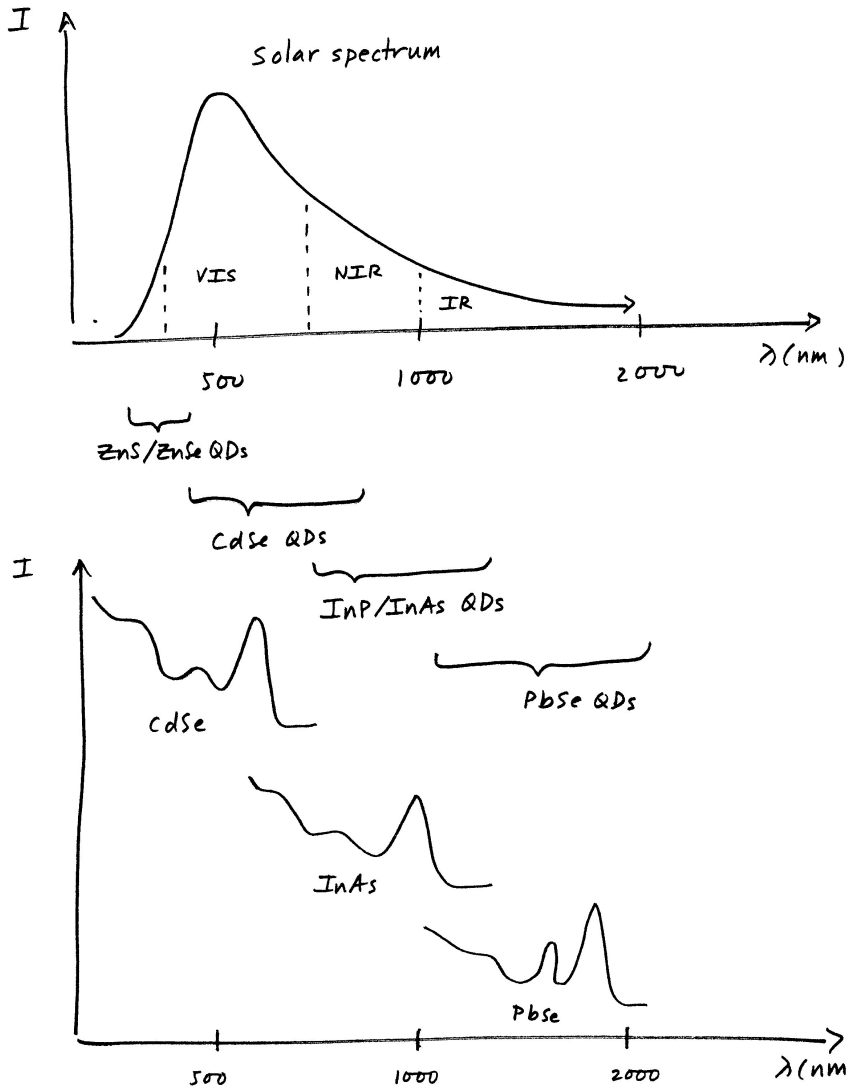

Figure 15.6: Comparison of the solar spectrum and representative quantum dot absorption spectra as well as achievable wavelength ranges.

lighting has since been developed but suffers from flicker and color purity issues. Recently solid state light emitting diodes (LED) have come on the market and are poised to revolutionalize the lighting industry. LED devices that exhibit tremendous brightness (look at some of the new red and green traffic lights), consume little power, come in different colors, and emit little or no heat (museum quality lighting for paintings) are now commercially available. In this regard, a major goal of the LED industry is to eventually achieve affordable white light by mixing red, green and blue LEDs. The idea is to one day replace *all* incandescent and fluorescent light bulbs in homes and offices. Furthermore, along these lines, brighter, more efficient, flat panel displays using this technology, rather than inefficient backlit liquid crystal displays, may come out of these developments. Along the same lines, cheaper high definition digital televisions may also emerge from this technology.

A current problem with LEDs, however, is that different active semiconductor elements must be manufactured via potentially expensive processes such as MOCVD to achieve multiple colors. For example, GaN is used for blue light, indium doped GaN can be used to get green and so forth. One way to circumvent this problem is to take advantage of quantum confinement as in the case of quantum dots. Different sized quantum dots will emit different colors so, in principle, one material can cover the entire visible spectrum. They can also be manufactured using the same process potentially lowering overall manufacturing costs. One disadvantage with current colloidal quantum dots is that the heterojunction between the dot and the outside world is imperfect. There are organic ligands present as well as many quantum dot surface defects that open up undesired states and recombination pathways in addition to creating large resistances to carrier transport.

Memory; the Coulomb staircase

What would a chapter on devices and applications be if we didn't touch on computers. Back in 1965, Gordon Moore, one of the founders of Intel made an empirical observation that has since become known as "Moore's law" (or sometimes referred to as Moore's first law). The number of transistors per unit area on an integrated circuit doubles each year. Since then, Moore's law has generally held with some minor modifications. It now doubles every 18 months. However, as you might suspect, this wild growth cannot continue forever and it was realized that with current photolithographic techniques that we would be in trouble by 2010. To consistently get more transistors per unit area means that their size decreases yearly. Currently the features

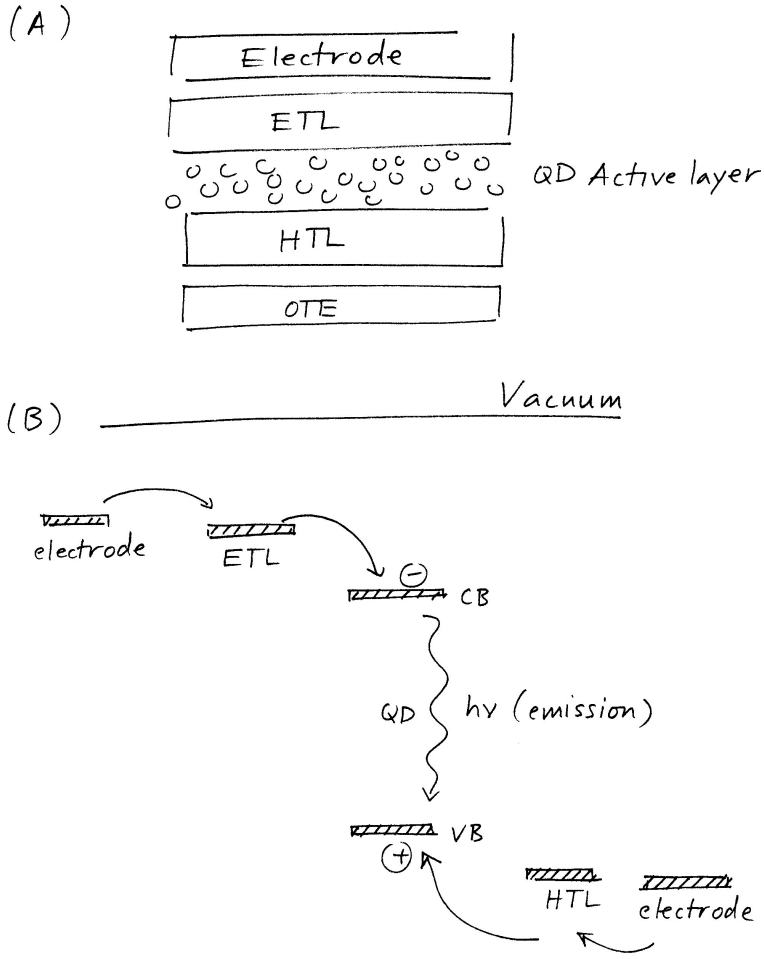

Figure 15.7: (A) Cartoon of a generic quantum dot light emitting diode. HTL (hole transport layer); ETL (electron transport layer); OTL (optically transparent electrode) (B) Ideal energy level diagram for injection of electrons and holes into a quantum dot device.

on a Pentium IV chip have spacings on the order of 0.11 microns (110 nm). Next generation chips will have features spaced by 0.09 microns (90 nm). How much lower can we go? Well, because of the diffaction limit we cannot continue to use existing techniques but are forced to invest in deep UV photolithography or x-ray lithography or even e-beam lithography if we are to get smaller transistors and stay on track with Moore's law. Such new technologies are very expensive and potentially too costly to scale up to the fab level (Moore's second law of costs). Because of this, researchers have looked to nano for a solution. Among the ideas people have come up with are what are refered to as single electron transistors.

Early on, researchers realized that if one has a very small metal nanoparticle, its capacitance might be large enough to store discrete charges. Lowering the temperature also helps. Both work because either raising the capacitance or lowering the temperature decreases the value of the thermal energy relative to the Coulomb energy between discrete charges. In turn, this allows one to store charges on the metal nanoparticle without having it thermally expelled. Alternatively, with semiconductor quantum dots, the discrete particle in a box-like energy levels with spacings large compared to kT also means discrete steps in the conductance of electrons through the dot and the additional possibility of storing charges just as with the metal nanoparticles. These effects could then form the basis of single electron electronics of which the single electron transistor is a member. We review the principles of what is knows as the Coulomb blockade and Coulomb staircase model below because of its potential importance.

In the orthodox model for single electron tunneling, a simple circuit model is considered as shown in the accompanying figure. Basically the circuit consists of a perfect voltage source and two capacitors that may or may not have equivalent capacitances. In the orthodox model, one of the two capacitors is generally considered to have a much higher capacitance than the other. The region in between the capacitors is the "island" where electrons can be stored. This region represents a quantum dot or metal nanoparticle in real life.

The total electrostatic energy of the system is

$$\boxed{E_s = \frac{q_1^2}{2C_1} + \frac{q_2^2}{2C_2}} \tag{15.1}$$

where C_1 is the gate capacitance. At the same time the potential drops

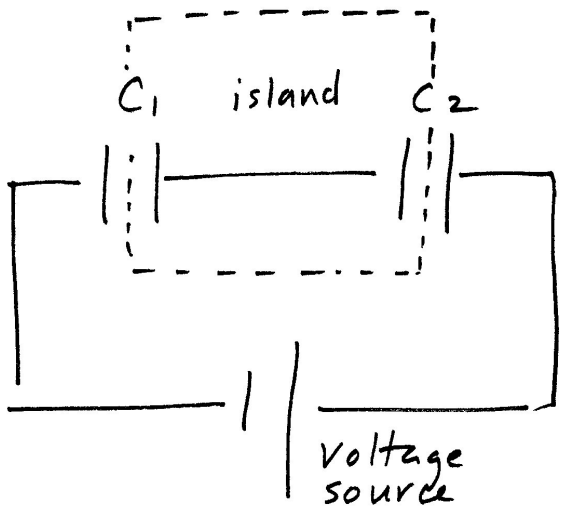

Figure 15.8: Orthodox model of single electron tunneling and Coulomb blockade/Coulomb staircase

across junctions 1 and 2 are

$$\begin{aligned} V_1 &= \left(\frac{C_2}{C_1+C_2}\right)V + \frac{ne}{C_1+C_2} \\ &= \frac{C_2V+ne}{C_1+C_2} \end{aligned} \tag{15.2}$$

$$\begin{aligned} V_2 &= \left(\frac{C_1}{C_1+C_2}\right)V - \frac{ne}{C_1+C_2} \\ &= \frac{C_1V-ne}{C_1+C_2} \end{aligned} \tag{15.3}$$

Therefore the total electrostatic energy of the system is

$$\begin{aligned} E_s &= \frac{q_1^2}{2C_1} + \frac{q_2^2}{2C_2} \\ &= \frac{C_1^2V_1^2}{2C_1} + \frac{C_2^2V_2^2}{2C_2} \end{aligned}$$

$$
\begin{aligned}
&= \frac{C_1V_1^2}{2} + \frac{C_2V_2^2}{2} \\
&= \frac{1}{2}\left(C_1V_1^2 + C_2V_2^2\right) \\
&= \frac{1}{2}\left(C_1\left(\frac{C_2V + ne}{C_1 + C_2}\right)^2 + C_2\left(\frac{C_1V - ne}{C_1 + C_2}\right)^2\right) \\
&= \frac{1}{2}\left(\frac{1}{C_1 + C_2}\right)^2\left(C_1(C_2V + ne)^2 + C_2(C_1V - ne)^2\right)
\end{aligned}
$$

The term in the last parenthesis can be expanded and reduced to give

$$
\begin{aligned}
E_s &= \frac{1}{2}\left(\frac{1}{C_1 + C_2}\right)^2\left(C_1C_2V^2(C_1 + C_2) + (ne)^2(C_1 + C_2)\right) \\
&= \frac{1}{2C_{tot}}(C_1C_2V^2 + (ne)^2) \qquad (15.4)
\end{aligned}
$$

where $C_{tot} = C_1 + C_2$.

Now the net energy of the system, (or free energy) is the difference in energy between the total electrostatic energy stored and the work needed to shove an electron onto the island.

$$E_{tot} = E_s - W \qquad (15.5)$$

where $W = \frac{C_1QV}{C_{tot}}$ is the work done by the system to load the island. This results in

$$
\begin{aligned}
E_{tot} &= \frac{1}{2C_{tot}}(C_1C_2V^2 + (ne)^2) - \frac{C_1QV}{C_{tot}} \\
&= \frac{(ne)^2}{2C_{tot}} - \frac{2C_1QV}{2C_{tot}} + \frac{C_1C_2V^2}{2C_{tot}} \\
&= \frac{(ne)^2 - 2C_1QV}{2C_{tot}} + \frac{(C_1V)^2}{2C_{tot}} - \frac{(C_1V)^2}{2C_{tot}} + \frac{C_1C_2V^2}{2C_{tot}}
\end{aligned}
$$

Notice the trick consisting of adding and subtracting the middle terms

$$
\begin{aligned}
&= \frac{(ne)^2 - 2C_1QV + (C_1V)^2}{2C_{tot}} - \frac{(C_1V)^2}{2C_{tot}} + \frac{C_1C_2V^2}{2C_{tot}} \\
&= \frac{(ne - C_1V)^2}{2C_{tot}} - \frac{1}{2C_{tot}}(C_1^2V^2 - C_1C_2V^2)
\end{aligned}
$$

where $C_2 = C_{tot} - C_1$

$$\begin{aligned}
&= \frac{(ne - C_1V)^2}{2C_{tot}} - \frac{1}{2C_{tot}}(C_1^2V^2 - C_1(C_{tot} - C_1)V^2) \\
&= \frac{(ne - C_1V)^2}{2C_{tot}} - \frac{1}{2C_{tot}}(C_1^2V^2 - C_1C_{tot}V^2 + C_1^2V^2) \\
&= \frac{(ne - C_1V)^2}{2C_{tot}} - \frac{1}{2C_{tot}}(2C_1^2V^2 - C_1C_{tot}V^2) \\
&= \frac{(ne - C_1V)^2}{2C_{tot}} - \frac{C_1V^2}{2C_{tot}}(2C_1 - C_{tot}) \\
&= \frac{(ne - C_1V)^2}{2C_{tot}} - \frac{C_1V^2}{2C_{tot}}(C_{tot}) \\
&= \frac{(ne - C_1V)^2}{2C_{tot}} - \frac{C_1V^2}{2}
\end{aligned}$$

This gives the total free energy of the system

$$\boxed{E_{tot} = \frac{(ne - C_1V)^2}{2C_{tot}} - \frac{C_1V^2}{2}} \tag{15.6}$$

Island occupation number

The average number of electrons on the island is given by

$$< n >= \frac{\sum_{-\infty}^{\infty} ne^{\frac{-E_n}{kT}}}{\sum_{-\infty}^{\infty} e^{\frac{-E_n}{kT}}}$$

where from before

$$E_n = \frac{(-ne + \bar{Q})^2}{2C_{tot}} - \frac{\bar{Q}^2}{2C_1}$$

Therefore

$$< n > = \frac{\sum_{-\infty}^{\infty} ne^{-\frac{(-ne+\bar{Q})^2}{2C_{tot}kT} + \frac{\bar{Q}^2}{2C_1kT}}}{\sum_{-\infty}^{\infty} e^{-\frac{(-ne+\bar{Q})^2}{2C_{tot}kT} + \frac{\bar{Q}^2}{2C_1kT}}}$$

$$
\begin{aligned}
&= \frac{e^{\frac{\bar{Q}^2}{2C_1kT}} \sum_{-\infty}^{\infty} ne^{-\frac{(-ne+\bar{Q})^2}{2C_{tot}kT}}}{e^{\frac{\bar{Q}^2}{2C_1kT}} \sum_{-\infty}^{\infty} e^{-\frac{(-ne+\bar{Q})^2}{2C_{tot}kT}}} \\
&= \frac{\sum_{-\infty}^{\infty} ne^{-\frac{(-ne+\bar{Q})^2}{2C_{tot}kT}}}{\sum_{-\infty}^{\infty} e^{-\frac{(-ne+\bar{Q})^2}{2C_{tot}kT}}} \\
&= \frac{\sum_{-\infty}^{\infty} ne^{-e^2\frac{\left(-n+\frac{\bar{Q}}{e}\right)^2}{2C_{tot}kT}}}{\sum_{-\infty}^{\infty} e^{-e^2\frac{\left(-n+\frac{\bar{Q}}{e}\right)^2}{2C_{tot}kT}}} \\
&= \frac{\sum_{-\infty}^{\infty} ne^{-\frac{\left(-n+\frac{\bar{Q}}{e}\right)^2}{2\Theta}}}{\sum_{-\infty}^{\infty} e^{-\frac{\left(-n+\frac{\bar{Q}}{e}\right)^2}{2\Theta}}}
\end{aligned}
$$

where $\Theta = \frac{C_{tot}kT}{e^2}$

Furthermore, let $x = (\frac{\bar{Q}}{e})$ to get our final expression for the average island occupation

$$
\boxed{< n >= \frac{\sum_{-\infty}^{\infty} ne^{-\frac{(x-n)^2}{2\Theta}}}{\sum_{-\infty}^{\infty} e^{-\frac{(x-n)^2}{2\Theta}}}} \tag{15.7}
$$

A plot of this below, shows the characteristic Coulomb staircase behavior.

Relevant literature

These are papers from the current literature in no particular order

- "Single-nanowire electrically driven lasers"
  X. Duan, Y. Huang, R. Agarwal, C. M. Lieber
  Nature, 421, 241 (2003).

- "Functional nanoscale electronic devices assembled using silicon nanowire building blocks"

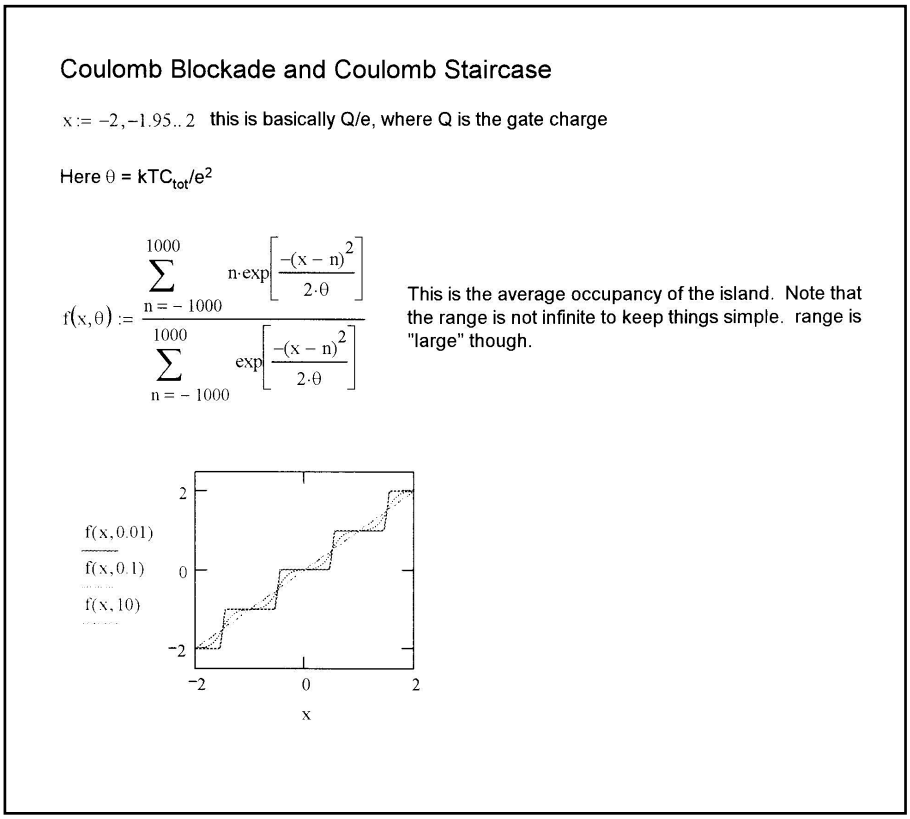

Figure 15.9: Coulomb staircase: Mathcad numerical solutions

Y. Cui, C. M. Lieber
Science, 291, 851 (2001).

- "Quantum dot bioconjugates for ultrasensitive nonisotopic detection"
  W. C. Chan, S. Nie
  Science, 281, 2016 (1998).

- "Semiconductor nanocrystals as fluorescent biological labels"
  M. Bruchez Jr, M. Moronne, P. Gin, S. Weiss, A. P. Alivisatos
  Science, 281, 2013 (1998).

- "Indium phosphide nanowires as building blocks for nanoscale electronic and optoelectronic devices"
  X. Duan, Y. Huang, Y. Cui, J. Wang, C. M. Lieber
  Nature, 409, 66 (2001).

- "Immunofluorescent labeling of cancer marker Her2 and other cellular targets with semiconductor quantum dots"
  X. Wu et al.
  Nature Biotechnology, 21, 41 (2003).

- "Nanowire nanosensors for highly sensitive and selective detection of biological and chemical species"
  Y. Cui, Q. Wei, H. Park, C. M. Lieber
  Science, 293, 1289 (2001).

- "Room-temperature ultraviolet nanowire nanolasers"
  M. H. Huang et al.
  Science, 292, 1897 (2001).

- "Hybrid nanorod-polymer solar cells"
  W. U. Huynh, J. J. Dittmer, A. P. Alivisatos
  Science, 295, 2425 (2002).

- "Quantum dot solar cells"
  A. J. Nozik
  Physica E. 12, 115 (2002).

- "Electroluminescence from single monolayers of nanocrystals in molecular organic devices"
  S. Coe, W-K Woo, M. Bawendi, V. Bulovic
  Nature, 420, 800 (2002).

- "A silicon nanowire with a coulomb blockade effect at room temperature"
  S. Hu, W-Z. Wong, S-S. Liu, Y-C. Wu, C-L. Sung, T-Y. Huang, T-J. Yang
  Adv. Mater. 14, 736 (2002).

- "Quantum dot solar cells"
  R. P. Raffaelle, S. L. Castro, A. F. Hepp, S. G. Bailey
  Progress in photovoltaics: research and applications, 10, 433 (2002).

- "A multiwavelength semiconductor laser"
  A. Tredicucci, C. Gmachl, F. Capasso, D. L. Sivco, A. L. Hutchinson, A. Y. Cho
  Nature, 396, 350 (1998).

- "Bidirectional semiconductor laser"
  C. Gmachl, A. Tredicucci, D. L. Sivco, A. L. Hutchinson, F. Capasso, A. Y. Cho
  Science, 286, 749 (1999).

- "Array-based electrical detection of DNA with nanoparticle probes"
  S-J. Park, T. A. Taton, C. A. Mirkin
  Science, 295, 1503 (2002)

- "Scanometric DNA array detection with nanoparticle probes"
  T. A. Taton, C. A. Mirkin, R. L. Letsinger
  Science, 289, 1757 (2000).

- "Efficient near-infrared polymer nanocrystal light-emitting diodes"
  N. Tessler, V. Medvedev, M. Kazes, S. Kan, U. Banin
  Science, 295, 1506 (2002).

- "Nanotube molecular wires as chemical sensors"
  J. Kong, N. R. Frankliin, C. Zhou, M. G. Chapline, S. Peng, K. Cho, H. Dai
  Science, 287, 622 (2000).

- "Carbon nanotube actuators"
  R. H. Baughman et. al.
  Science, 284, 1340 (1999).

- "Logic circuits with carbon nanotube transistors"
  A. Backtold, P. Hadley, T. Nakanishi, C. Dekker
  Science, 294, 1317 (2001).

- "Single-and multi-wall carbon nanotube field-effect transistors"
  R. Martel, T. Schmidt, H. R. Shea, T. Hertel, Ph. Avouris
  Appl. Phys. Lett. 73, 2447 (1998).

- "Carbon nanotube electron emitter with a gated structure using backside exposure processes"
  D-S. Chung et. al.
  Appl. Phys. Lett. 80, 4045 (2002).

- "Nano-particle transistors and energy-level spectroscopy in metals"
  D. C. Ralph, C. T. Black, M. Tinkham
  Superlattices and Microstructures, 20, 389 (1996).

- "A single-electron transistor made from a cadmium selenide nanocrystal"
  D. L. Klein, R. Roth, A. L. L. Lim, A. P. Alivisatos, P. L. McEuen
  Nature, 389, 699 (1997).

- "Gold nanoparticle single-electron transistor with carbon nanotube leads"
  C. Thelander, M. H. Magnusson, K. Deppert, L. Samuelson, P.R. Poulsen, J. Nygard, J. Borggreen
  Appl. Phys. Lett. 79, 2106 (2001).

- "Single-electron transistor made of two crossing multiwalled carbon nanotubes and its noise properties"
  M. Ahlskog, R. Tarkiainen, L. Roschier, P. Hakonen
  Appl. Phys. Lett. 77, 4037 (2000).

- "Single electron transistor using a molecularly linked gold colloidal particle chain"
  T. Sato, H. Ahmed, D. Brown, B. F. G. Johnson
  J. Appl. Phys. 82, 696 (1997).

- "Room temperature coulomb blockade and coulomb staircase from self assembled nanostructures"
  R. P. Anders et al.
  J. Vac. Sci. Technol. A 14, 1178 (1996).

- "Single electron tunneling through nano-sized cobalt particles"
  C. Petit, T. Cren, D. Roditchev, W. Sacks, J. Klein, M-P. Pileni
  Adv. Mater. 11, 1198 (1999).

- "Size-dependent tunneling and optical spectroscopy of CdSe quantum rods"
  D. Katz, T. Wizansky, O. Millo, E. Rothenberg, T. Mokari, U. Banin
  Phys. Rev. Lett. 89, 086801-1 (2002).

- "Scanning tunneling spectroscopy of InAs nanocrystal quantum dots"
  O. Millo, D. Katz, Y. Cao, U. Banin
  Phys. Rev. B 61, 16773 (2000).

- "A tunneling spectroscopy study on the single-particle energy levels and electron-electron interactions in CdSe quantum dots"
  E. P. A. M. Bakkers, Z. Hens, L. P. Kouwenhoven, L. Gurevich, D. Vanmaekelbergh
  Nanotechnology, 13, 258 (2002).

Acknowledgments

I'd like to take the opportunity to thank the Notre Dame Radiation Laboratory and the Department of Chemistry and Biochemistry for financial support over the spring and summer of 2003. I'd also like to thank Jean-Christophe Ducom in the chemistry department for figuring out how to insert a figure in a TEX coverpage as well as Matt Meineke for alerting me to the use (and power) of the TEX label command. Finally, I'd like to thank Fred Mikulec, currently at Innovalight, for putting up with all my e-mail questions and always being open to my crazy ideas/garage projects. This text was written and typeset using the TEX environment withing PCTex Ver 4.2.05.

Index